

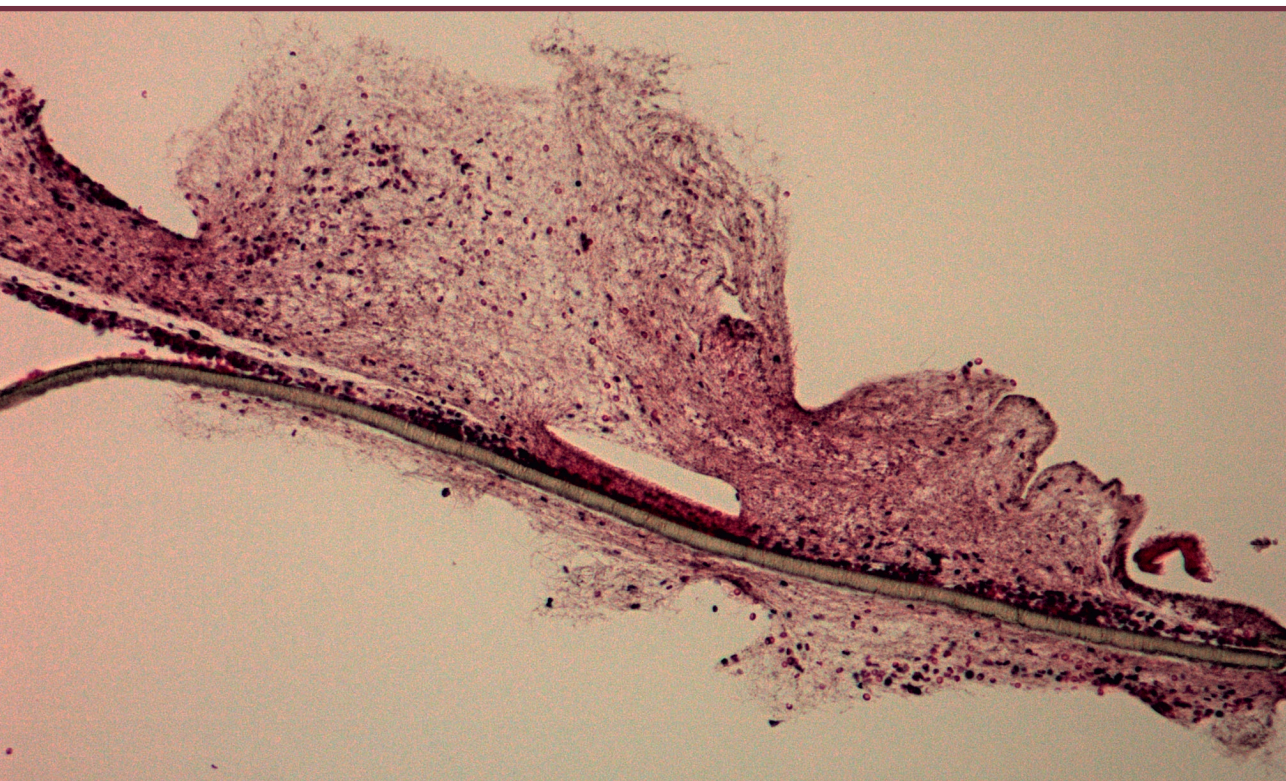
Karina Egle

**AUTOLOGU FIBRĪNA MATRICU IZSTRĀDE
MEDICĪNISKAM PIELIETOJUMAM**

Promocijas darbs

**DEVELOPMENT OF AUTOLOGOUS FIBRIN MATRICES
FOR MEDICAL APPLICATION**

Doctoral Thesis



RĪGAS TEHNISKĀ UNIVERSITĀTE

Dabazinātņu un tehnoloģiju fakultāte
Biomateriālu un bioinženierijas institūts

RIGA TECHNICAL UNIVERSITY

Faculty of Natural Sciences and Technology
Institute of Biomaterials and Bioengineering

Karina Egle

Doktorantūras studiju programmas “Ķīmija, materiālzinātne un tehnoloģijas” doktorante
Doctoral Student of the Study Programme “Chemistry, Materials Science and Engineering”

AUTOLOGU FIBRĪNA MATRICU IZSTRĀDE MEDICĪNISKAM PIELIETOJUMAM

Promocijas darbs

DEVELOPMENT OF AUTOLOGOUS FIBRIN MATRICES FOR MEDICAL APPLICATION

Doctoral Thesis

Zinātniskā vadītāja / Scientific supervisor
Docente / Assistant Professor. *Dr. sc. ing.*
ARITA DUBŅIKA

RTU Izdevniecība / RTU Press
Rīga 2024 / Riga 2024

Egle, K. Autologu fibrīna matricu izstrāde medicīniskam pielietojumam. Promocijas darba kopsavilkums. – Rīga: RTU Izdevniecība, 2024. – 136 lpp.

Egle, K. Development of Autologous Fibrin Matrices for Medical Application. Summary of the Doctoral Thesis. Riga: RTU Press, 2024. 136 p.

Iespiests saskaņā ar promocijas padomes “RTU P-02” 2024. gada 5. jūnija lēmumu, protokols Nr. 04030-9.2.2/7.

Published in accordance with the decision of the Promotion Council “P-02” of 5 June 2024, Minutes No. 04030-9.2.2/7.

Promocijas darba pētījumi izstrādāti, pateicoties Eiropas Savienības pētniecības un inovāciju programmai “Apvārsnis 2020” ar grantu līgumiem Nr. 857287 (BBCE) un Nr. 952347 (RISEus2). Šo promocijas darbu atbalstīja arī Latvijas Zinātnes padomes pētniecības projekts Nr. Izp-2020/1-0054 “Antibakteriālu autologu fibrīna matricu izstrāde mutes, sejas un žokļu ķirurģijai (MATRI-X)”.

The Doctoral Thesis research was supported by the European Union’s Horizon 2020 research and innovation programme under grant agreements No. 857287 (BBCE) and No. 952347 (RISEus2). This Thesis was also supported by the Latvian Council of Science research project No. Izp-2020/1-0054 “Development of antibacterial autologous fibrin matrices in maxillofacial surgery (MATRI-X).”



PATEICĪBAS

Liels paldies manai ģimenei – mammai Nataļjai, omei Tamārai, opim Vladimiram un pārējiem par ieguldījumu, uzmundrinājumu un centību šad un tad saprast, ar ko es vispār nodarbojos!

Paldies arī maniem draugiem – Ritai, Marinai, Oznur, Kristīnei, Agnesei, Karolinai, Esterei, Eleonorai, Signei, Annai – par atbalstu, idejām, uzmundrinājumu un tām reizēm, kurās es nedomāju par šī darba izstrādi!

Milzīgs paldies maniem projektu partneriem Ilzei Šalmai, Ingum Skadiņam, Lanai Mičko, Evai Dohlei, Verenai Hoffmann, Geraldine Guex par ieguldījumu šī darba tapšanā un paveikto kopīgu mērķu sasniegšanai! Paldies arī maniem kolēģiem par atbalstu un uzmundrinājumiem!

Visdziļākā pateicība manai darba vadītājai docentei *Dr.sc.ing.* Aritai Dubņikai par zinātniskajām idejām, izaicinājumiem un sniegtajām zināšanām!

ACKNOWLEDGEMENTS

A big thank you to my family- to my mom Natalia, grandmother Tamara, grandfather Vladimirs, and the rest of my family for their contribution, encouragement, and for occasionally trying to understand what I was doing!

I am thankful to my friends – Rita, Marina, Oznur, Kristīne, Agnese, Carolina, Estere, Eleonora, Signe and Anna – for their support, ideas, encouragement and for the special occasions where I was not thinking about this work!

My deepest gratitude to my project partners Ilze Šalma, Ingus Skadiņš, Lana Mičko, Eva Dohle, Verena Hoffmann, Geraldine Guex for their contribution to the development of the Thesis! Thanks also to my colleagues for their support and encouragement!

My profound appreciation to my supervisor Assistant Professor Dr. sc. ing. Arita Dubnika, for the scientific ideas, challenges, and knowledge that I have gained!

“Success is the sum of small efforts - repeated day in and day out.”

/Robert Collier/

PROMOCIJAS DARBS IZVIRZĪTS ZINĀTNES DOKTORA GRĀDA IEGŪŠANAI RĪGAS TEHNISKAJĀ UNIVERSITĀTĒ

Promocijas darbs zinātnes doktora (*Ph. D.*) grāda iegūšanai tiek publiski aizstāvēts 2024. gada 26. augustā Rīgas Tehniskās universitātes Dabaszinātņu un tehnoloģiju fakultātē, Paula Valdena ielā 3, 272. auditorijā.

OFICIĀLIE RECENZENTI

Profesors *Dr. sc. ing.* Remo Merijs-Meri,
Rīgas Tehniskā universitāte

Profesore *Dr. med.* Ilze Akota,
Rīgas Stradiņa universitāte, Latvija

Profesors *João F. Mano*,
Aveiro Universitāte, Portugāle

APSTIPRINĀJUMS

Apstiprinu, ka esmu izstrādājusi šo promocijas darbu, kas iesniegts izskatīšanai Rīgas Tehniskajā universitātē zinātnes doktora (*Ph. D.*) grāda iegūšanai. Promocijas darbs zinātniskā grāda iegūšanai nav iesniegts nevienā citā universitātē.

Karina Egle (paraksts)

Datums:

Promocijas darbs sagatavots kā tematiski vienotu zinātnisko publikāciju kopa ar kopsavilkumu latviešu un angļu valodā. Tajā ietvertas četras zinātniskas publikācijas. Publikācijas zinātniskajos žurnālos uzrakstītas angļu valodā, to kopējais apjoms, ieskaitot pielikumus, ir 76 lpp.

SATURS

PROMOCIJAS DARBA VISPĀRĒJS RAKSTUROJUMS.....	6
Tēmas aktualitāte.....	6
Mērķi un uzdevumi	9
Tēzes aizstāvēšanai	9
Zinātniskā novitāte un galvenie rezultāti	9
Praktiskā nozīme	9
Darba struktūra un apjoms	10
Darba aprobācija un publikācijas	10
PROMOCIJAS DARBA GALVENIE REZULTĀTI.....	13
Ceļš no pacienta asins paraugiem līdz injicējamam PRF.....	13
PRF potenciāls stimulēt CLP antibakteriālo jūtību	15
Ievadīto piegādes sistēmu īpašību ietekme uz zāļu izdalīšanos no PRF matricas	19
Nesējsistēmu ietekme uz PRF sastāvā esošo bioaktīvo molekulu izdalīšanos.....	23
SECINĀJUMI	29
LITERATŪRAS SARAKSTS	30
PIELIKUMI	64

- 1. pielikums** Egle, K., Salma, I., Dubnika, A. From Blood to Regenerative Tissue: How Autologous Platelet-Rich Fibrin Can Be Combined with Other Materials to Ensure Controlled Drug and Growth Factor Release. *Int. J. Mol. Sci.*, **2021**, 22 (21), 11553.
- 2. pielikums** Egle, K., Skadins, I., Grava, A., Micko, L., Dubniks, V., Salma, I., Dubnika, A. Injectable Platelet-Rich Fibrin as a Drug Carrier Increases the Antibacterial Susceptibility of Antibiotic – Clindamycin Phosphate. *Int. J. Mol. Sci.*, **2022**, 23 (13), 7407.
- 3. pielikums** Dubnika, A., Egle, K., Skrinda-Melne, M., Skadins, I., Rajadas, J., Salma, I. Development Development of Vancomycin Delivery Systems Based on Autologous 3D Platelet-Rich Fibrin Matrices for Bone Tissue Engineering. *Biomedicines*, **2021**, 9 (7), 814.
- 4. pielikums** Egle, K., Dohle, E., Hoffmann, V., Salma, I., Al-Maawi, S., Ghanaati, S., Dubnika, A. Fucoidan/Chitosan Hydrogels as Carrier for Sustained Delivery of Platelet-Rich Fibrin Containing Bioactive Molecules. *Int. J. Biol. Macromol.*, **2024**, 262 (1), 129651.

PROMOCIJAS DARBA VISPĀRĒJS RAKSTUROJUMS

Tēmas aktualitāte

Mūsdienās joprojām tiek diskutēts par to, vai trombocītus var uzskatīt par asins šūnu fragmentiem vai sīkām bez kodola asins šūnām [1], taču ir zināms, ka tie atbild par biomolekulu aktivēšanu un atbrīvošanu. Ar trombocītiem bagātināts fibrīns (*PRF*) ir autologs materiāls, ko centrifugēšanas ceļā var iegūt no cilvēka asinīm. *PRF* izmanto, lai veicinātu brūču dzīšanu un audu reģenerāciju, kā arī dažādās medicīnās jomās, tostarp zobārstniecībā un sejas žokļu ķirurģijā [2].

PRF sastāvā esošie leikocīti veicina brūču dzīšanu, un tas satur augšanas faktoros, kas izdalās laika gaitā. Mutes un sejas žokļu ķirurģijā, plastiskā ķirurģijā, sirds ķirurģijā un zobārstniecībā ir liela interese par *PRF* antimikrobiālo iedarbību [3]. *PRF* struktūras sarežģītība, neviendabīgais raksturs un recēšanas spēja apgrūtina tā antimikrobiālo iedarbības novērtēšanu. Jāņem vērā, ka lielākā daļa izmantoto testēšanas metožu antimikrobiālās iedarbības izvērtēšanai ir balstītas antibakteriālo līdzekļu spējā difundēt barotnē. *PRF* visbiežāk izmanto mutes un sejas žokļu reģionos, tāpēc tā antimikrobiālās aktivitātes novērtējums ir plašāk apskatīts mutes mikrobiomā. *PRF*, kas sagatavots saskaņā ar noteiktu protokolu (atkarībā no ķirurģiskās vietas), var nodrošināt antimikrobiālas un pretiekaisuma īpašības un var būt noderīgs līdzeklis klīniskajā praksē mutes un sejas žokļu ķirurģijā [4]. Pēdējo 10 gadu laikā veikti vairāki pētījumi, kuros antibiotikas kombinētas ar *PRF*, lai nodrošinātu antimikrobiālo efektu. Pamatojoties uz apkopoto literatūru par *PRF* antimikrobiālajām īpašībām, ir ieteicams tajā integrēt zāles, lai izveidotu vienotu sistēmu, nevis izmantotu zāles un *PRF* atsevišķi [5].

Mutes un sejas žokļu ķirurģijas pacientiem, kuriem ir alerģija pret penicilīnu, kā aizstājēju lieto klindamicīnu, līdz ar to palielinās nepieciešamība šo medikamentu izpētīt padziļināti. Ārsti min, ka papildus baktericīdajai iedarbībai klindamicīnam ir augstāka perorālā uzsūkšanās, ievērojams sadalījums audos (radot augstāku zāļu koncentrāciju kaulos) un zems rezistences līmenis [6]. Turklāt bieži vien priekšroka tiek dota zāļvielu prekursoriem, neaktīviem prekursoriem, kas organismā tiek pārveidoti par aktīvām vielām, nevis tiešai aktīvo vielu lietošanai farmācijā. Šī izvēle ir saistīta ar to spēju uzlabot zāļu stabilitāti, šķīdību un biopieejamību, uzlabojot terapeitiskos rezultātus. Klindamicīna fosfāts (*CLP*) ir klindamicīna zāļvielu prekursori, kam nav antimikrobiālas aktivitātes. Tiek ziņots, ka *CLP* asinīs ātri hidrolizējas par aktīvo bāzi (klindamicīnu) [2]. Promocijas darbā pētīta spēja pārveidot *CLP* aktīvajā formā, apvienojot to ar *PRF*. Turklāt pētīts arī vankomicīna hidroģēnhlorīds (*VANKA*), lai apskatītu plašākas aktīvo vielu izmantošanas iespējas kombinācijā ar *PRF*. *VANKA* ir ūdenī šķīstoša triciklisko glikopeptīdu antibiotika [7], kas novērš/iznīcina noteiktus grampozitīvus mikroorganismus, kas ir visizplatītākie patogēni. *VANKA*, tāpat kā klindamicīns, tiek lietots gadījumos, kad penicilīns ir neefektīvs vai izraisa alerģiskas reakcijas, kā arī tādu infekciju ārstēšanai, kurās citas antibiotikas ir rezistentas [8,9].

Zāļu pamata farmakoloģiskās īpašības var uzlabot, izmantojot piemērotu zāļu piegādes sistēmu, kas nodrošina to ievadīšanu kā brīvu molekulu [10]. Zāļu piegādes sistēma ir metode

vai tehnoloģiska pieeja, ko izmanto, lai sistemātiski un precīzi ievadītu terapeitiskās vielas (piemēram, zāles vai medikamentus) cilvēka organismā. Šis process ietver tādu sistēmu izveidi un ieviešanu, kas uzlabo ārstēšanas efektivitāti un drošību. Šo sistēmu galvenais mērķis ir precīzi kontrolēt zāļu piegādi konkrētiem audiem vai šūnām, vienlaikus cenšoties samazināt iespējamās blakusparādības [11, 12]. Piemēram, *VANKA* var iekapsulēt liposomās, unikālos zāļu nesējos, jo tās var pārvarēt perorāli vai intravenozi lietojamo zāļu trūkumus. Kā alternatīva *VANKA* iekapsulēšanai ir pētītas arī polipien-ko-glikolskābes (*PLGA*) polimēru mikro kapsulas. Gan liposomām, gan *PLGA* mikro kapsulām ir zema iekapsulēšanas efektivitāte, bet, neskatoties uz to, *VANKA* iekapsulēšana nesējā nodrošina augstus klīniskos ieguvumus ilgstošai antibiotiku lietošanai. Tāpēc ir būtiski pielāgot *VANKA* nesēja sastāvu un zāļu izdalīšanās ātrumu no autologajiem paraugiem. Pašreizējo pētījumu skaits par zāļu nesējiem, kas integrēti autologajos *PRF* paraugos, ir ierobežots [13].

Papildus *PRF* kombinācijai ar zāļu piegādes sistēmām, kas nodrošina kontrolētu zāļu piegādi, *PRF* ietver augšanas faktorus un citokīnus, ko var atbrīvot tieši ievadīšanas vietā. Vairāki autori aprakstījuši dažādu centrifugēšanas protokolu ietekmi uz augšanas faktoru un citokīnu izdalīšanos, apstiprinot pagatavošanas protokolu būtisko ietekmi uz *PRF* īpašībām. Ir pierādīts, ka augšanas faktoru un citokīnu izdalīšanās modeļu atšķirības pastāv ne tikai starp dažādiem trombocītu koncentrātiem, bet arī katra veida *PRF* [14]. Trombocītu koncentrāts galvenokārt satur trombocītus, savukārt *PRF* ir papildus sajaukts ar fibrīna šķiedru veidojošiem proteīniem, kas veicina audu dzīšanu. Esošajā literatūrā pētītas trombocītiem bagātinātas plazmas (*PRP*) vai *PRF* kombinācijas ar hitozāna/fukoidāna kompleksiem vai želatīna/hitozāna hidrogēliem [15, 16]. Šajos pētījumos abu veidu trombocītu koncentrāti tika iejaukti hitozāna šķīdumā, un iegūtajiem materiāliem novērtēts atbrīvoto olbaltumvielu daudzums. Jaunu metodoloģiju ieviešana, balstoties šajās publikācijās, sarežģītu medicīniskās procedūras, kas ietveru vairākus izstrādes posmus. Iepriekšējos pētījumos noteikta gan individuāla *PRF* ietekme uz kaulu veidošanos un reģenerāciju, gan integrējot to polimēru matricās [17]. *Xu et al.* iekļāva granulu-liofilizētu trombocītiem bagātinātu fibrīnu (*G-L-PRF*) polivinilspirta (*PVA*) hidrogēlos, panākot ilgstošu augšanas faktoru izdalīšanos no *G-L-PRF/PVA* pamatnēm līdz deviņām dienām [18]. Citā *ex vivo* pētījumā tika analizēta injicējamā *PRF* kombinācija ar piecām dažāda veida kolagēna bāzes membrānām un to spēja nodrošināt autologu augšanas faktoru piegādi. Tādējādi šis bija pirmais pētījums, kurā mēģināts izprast biomateriālu spēju un piemērotību iekļaut *PRF* [19].

Nesen kaulaudu inženierijas nolūkos izstrādāti vairāki fukoidānu (*FU*) saturoši kompozītmateriāli, jo *FU* palielina osteoblastiem līdzīgo šūnu proliferācijas spēju un uzlabo osteoblastu veidoto minerālu nogulsnešanos [20]. *FU* līdzība cilvēka ārpusšūnu matricai un plašās īpašības, piemēram, augsta bioloģiskā saderība un atjaunojība, ir ieinteresējušas pētniekus. Šīs īpašības ir nozīmīgas reģeneratīvās medicīnas materiālu izstrādē, īpaši brūču ārstēšanai [21]. *FU* ir heparīnam līdzīga molekula un tas uzlabo augšanas faktoru ietekmi uz šūnu proliferāciju, osteogēno diferenciāciju un mezenhimālo cilmes šūnu aktivitāti [22]. Vairākos pētījumos [23, 24] aprakstīts, ka *FU* var mijiedarboties ar augšanas faktoriem (piemēram, *bFGF* un *TGF-β*), lai kontrolētu to izdalīšanās ātrumu un aktivitāti, saistoties un

regulējot signāla vadīšanas ceļus. Signāla vadīšanas ceļi ir ļoti svarīgi autologos *PRF* paraugos, lai nodrošinātu augšanas faktoru izdalīšanos no matricām.

Kopumā hitozāna struktūra un īpašības ir līdzīgas glikozaminoglikānam (GAG), dabiskajam polisaharīdam un galvenajai ārpusšūnas matricas (*ECM*) sastāvdaļai [25]. Hitozāns ir dabisks katjonu kopolimērs, kas radījis ievērojamu interesi par tā potenciālu hidrogēlu izstrādē. Šī polimēra hidrofilā daba nodrošina tā noārdīšanos cilvēka fermentu darbības rezultātā, tādējādi veicinot bioloģisko saderību un bioloģisko noārdīšanos, kas ir divas būtiskas medicīnisko ierīču īpašības. Hitozānā balstīti hidrogēli varētu kalpot kā pamatnes audu atjaunošanai [26]. Hitozāns paātrina brūču dzīšanu, aktivējot un modulējot iekaisuma šūnas un veicinot granulāro audu veidošanos. Tā spēja saistīt negatīvi lādētas sarkanās asins šūnas uzlabo recēšanu, padarot to par būtisku brūču pārsēju sastāvdaļu [27].

Līdz šim kontrolētas augšanas faktoru piegādes metodes, kas balstītas *PRF* kombinācijā ar citiem biomateriāliem, nodrošinot ilgstošākas terapijas iespējas, nav pētītas. Šajā darbā tika izstrādāti hidrogēli, kas sastāv no fukoidāna (FU) un hitozāna (CS), ņemot vērā to bioloģisko saderību un spēju veidot polielektrolītu kompleksus pašsavienošanās ceļā [28]. Polielektrolītu kompleksu veidošanās starp pretēji lādētām hitozāna un fukoidāna aktīvajām grupām padara iespējamu *PRF* sastāvā esošo augšanas faktoru iekļaušanu FU un CS hidrogēlā elektrostatiskās mijiedarbības rezultātā [29]. Tādējādi promocijas darbā izstrādāti fukoidāna/hitozāna hidrogēli, pētīt to turpmākās izmantošanas iespējas kā materiālus, lai iekļautu un uzglabātu *PRF*.

Šajā promocijas darbā tika izvirzīti šādi mērķi: 1) izpētīt *PRF* potenciālu zāļvielu prekursoru pārveidošanā aktīvajā formā, izmantojot klindamicīna fosfātu kā vienu no zāļvielu prekursoriem piemēriem; 2) novērtēt *PRF* spēju palēnināt aktīvās vielas straujo sākotnējo izdalīšanos, iekļaujot aktīvo vielu *PLGA* mikrokapsulās vai liposomās, izmantojot *VANKA* kā vienu no aktīvās vielas piemēriem; 3) izpētīt *PRF* sastāvā esošo bioaktīvo molekulu kontrolētu izdalīšanos no *PRF* saturošām jūras polisaharīdu (fukoidāna un hitozāna) hidrogēlu piegādes sistēmām.

Mērķi un uzdevumi

Promocijas darba mērķis ir izstrādāt *PRF* balstītas matricas, kas var nodrošināt antimikrobiālās īpašības, pievienojot zāles vai to piegādes sistēmas, kā arī nodrošināt kontrolētu *PRF* sastāvā esošo bioaktīvo molekulu piegādi, izvērtējot dažādus *PRF* nesējus. Lai sasniegtu mērķi, tika definēti vairāki uzdevumi.

1. Izpētīt *PRF* ierosināšanas potenciālu klindamicīna fosfāta pārveidošanai par aktīvo zāļu formu klindamicīnu, nodrošinot efektīvākas antimikrobiālās īpašības.
2. Novērtēt *PRF* matricu mijiedarbību ar zāļu piegādes sistēmu nesējiem (*PLGA* mikrokapsulas vai liposomas) un to ietekmi uz antibiotiku (*VANKA*) izdalīšanās kinētiku.
3. Izstrādāt fukoidāna/hitozāna hidrogēlu iegūšanas tehnoloģijas metodiku to apvienošanai ar *PRF*, lai nodrošinātu *PRF* sastāvā esošo bioaktīvo molekulu aizkavētu izdalīšanos.

Tēzes aizstāvēšanai

1. *CLP* iekļaušana *PRF* kā nesējmatricā paaugstina tā antibakteriālās īpašības, nodrošinot zāļvielu prekursora pārveidošanos par tā bioloģiski aktīvo formu klindamicīnu.
2. *PRF* matricās iekļauto antibiotiku *VANKA* izdalīšanās kinētiku var modelēt no sešām līdz 10 dienām atkarībā no zāļu piegādei izmantotā nesēja (*PLGA* mikrokapsulas vai liposomas).
3. Balstoties fukoidāna spējā regulēt bioaktīvo molekulu izdalīšanos un aktivitāti, ilgstošu bioaktīvo molekulu izdalīšanos (no sešām stundām līdz septiņām dienām) no *PRF* var panākt, apvienojot *PRF* ar fukoidāna/hitozāna hidrogēliem.

Zinātniskā novitāte un galvenie rezultāti

Zinātniskā novitāte balstās uz perspektīvu duālu *PRF* lietojumu. Pirmkārt, inoatīva hidrogēla izstrāde ar spēju modulēt *PRF* sastāvā esošo bioaktīvo molekulu izdalīšanos, un, otrkārt, jaunu zāļu piegādes sistēmu izstrāde, ietverot kontrolētu antibiotiku vai daļiņu piegādi, kurā daļiņas iekļautas *PRF* un darbojas kā bioloģiski aktīvo molekulu nesēji.

Darbā izstrādāta jauna metode, lai nodrošinātu *PRF* sastāvā esošo bioaktīvo molekulu iekapsulēšanu jūras polisaharīdu fukoidāna un hitozāna hidrogēlos, tādējādi panākot to ilgstošu izdalīšanos. Šajā metodē izmantoti videi draudzīgi materiāli hitozāns un fukoidāns, kas polielektrolītu pašsavienošanās ceļā veido hidrogēlus. Atšķirībā no tradicionālajām zāļu piegādes sistēmu sagatavošanas metodēm šī hidrogēlu iegūšanas metode nav atkarīga no ķīmiskiem šķērssaistītājiem.

Paralēli izstrādāta arī jauna metodoloģija *PRF* izmantošanai kā bioaktīvo molekulu nesējam, lai uzlabotu zāļu antibakteriālās īpašības. *PRF* kā nesējs paplašina zāļvielu prekursoru (piemēram, klindamicīna fosfāta), kam ir mazāk blakusparādību nekā aktīvajai formai, izmantošanas iespējas. Iegūtā zāļu/*PRF* kombinācija uzrāda nepieciešamību pēc zemākas

zāļvielu prekursoru koncentrācijas, salīdzinot ar nepieciešamo zāļvielu prekursoru daudzumu bez *PRF*. Nākotnē šī metodoloģija tiks attīstīta plašākai zāļu antibakteriālo īpašību uzlabošanai.

Praktiskā nozīme

Darbā pētītas *PRF* īpašības un tā kombinācijas ar dažādām zāļu piegādes sistēmām un matricām. Atrasts *PRF* lietojums tālāk minēto inovatīvo kombināciju izstrādē.

1. *PRF* kā nesējmatrica zāļvielu prekursoram – *CLP* mutes, sejas un žokļu ķirurģijā, tādējādi iegūstot aktīvo zāļu formu, kas nodrošinātu antibakteriālu iedarbību pēcoperācijas periodā.
2. *PRF* kombinēšana ar dažādiem bioloģiski aktīvo vielu (piemēram, *VANKA*) nesējiem (*PLGA* mikrokapsulas vai liposomas), samazinot nepieciešamību pēc perorālas zāļu lietošanas un pielāgojot bioloģiski aktīvas vielas terapijas ilgumu.
3. Jauna un videi draudzīga metode fukoidāna/hitozāna hidroģēlu iegūšanai kombinācijā ar *PRF*, nodrošinot ilgstošu *PRF* sastāvā esošo bioaktīvo molekulu izdalīšanos.

Darba struktūra un apjoms

Promocijas darbs ir sagatavots kā tematiski vienotu zinātnisko publikāciju kopa, kas veltīta pētījumiem par autologo fibrīna matricu izstrādi medicīniskiem nolūkiem. Darbs ietver trīs oriģinālpublikācijas *SCI* žurnālos un vienu apskatrakstu.

Darba aprobācija un publikācijas

Promocijas darba galvenie rezultāti publicēti trīs zinātniskajos oriģinālrakstos. Promocijas darba izstrādes laikā sagatavots viens apskatraksts. Promocijas darba rezultāti prezentēti 14 zinātniskajās konferencēs.

Zinātniskās publikācijas

1. **Egle, K.**, Dohle, E., Hoffmann, V., Salma, I., Al-Maawi, S., Ghanaati, S., Dubnika, A. Fucoidan/Chitosan Hydrogels as Carrier for Sustained Delivery of Platelet-Rich Fibrin Containing Bioactive Molecules. *Int. J. Biol. Macromol.*, **2024**, 262 (1), 129651. doi: 10.1016/j.ijbiomac.2024.129651.
2. **Egle, K.**, Skadins, I., Grava, A., Micko, L., Dubniks, V., Salma, I., Dubnika, A. Injectable Platelet-Rich Fibrin as a Drug Carrier Increases the Antibacterial Susceptibility of Antibiotic – Clindamycin Phosphate. *International Journal of Molecular Sciences*, **2022**, 23 (13), 7407. doi: 10.3390/ijms23137407 (Scopus, Open Access).
3. Dubnika, A., **Egle, K.**, Skrinda-Melne, M., Skadins, I., Rajadas, J., Salma, I. Development of Vancomycin Delivery Systems Based on Autologous 3D Platelet-Rich Fibrin Matrices for Bone Tissue Engineering. *Biomedicines*, **2021**, 9 (7), 814. doi: 10.3390/biomedicines9070814 (Scopus, Open Access).

4. **Egle, K.**, I.Salma, A.Dubnika. From Blood to Regenerative Tissue: How Autologous Platelet-Rich Fibrin Can Be Combined with Other Materials to Ensure Controlled Drug and Growth Factor Release. *International Journal of Molecular Sciences*, **2021**, 22(21), 11553. doi: 10.3390/ijms222111553 (Scopus, Open Access).

Promocijas darba rezultāti ir prezentēti 14 zinātniskajās konferencēs.

1. **Egle, K.**, Dohle, E., Hoffmann, V., Salma, I., Al-Maawi, S., Ghanaati, S., Dubnika, A. Exploring Platelet-Rich Fibrin Microstructure and Histology: with and without Hydrogel Carriers. *64th International Scientific Conference of RTU: Materials Science and Applied Chemistry*, Riga, Latvia, October 6, **2023** (mutiskā prezentācija).
2. **Egle, K.**, Dohle, E., Hoffmann, V., Salma, I., Al-Maawi, S., Ghanaati, S., Dubnika, A. Fucoidan/Chitosan Hydrogels for Sustained Delivery of Platelet-Rich Fibrin Containing Growth Factors. *33rd Annual Conference of the European Society for Biomaterials*, Davos, Switzerland, 4th-8th September **2023** (stenda referāts).
3. Dubnika, A., **Egle, K.**, Skadins, I., Skrinda-Melne, M., Micko, L., Grava, A., Dubniks, V., Salma, I. Development Of Drug Delivery Systems Based On Autologous 3D Platelet-rich Fibrin Matrices, *TERMIS-AM 2023 Annual Conference*, Boston, MA, 11th -14th April **2023** (stenda referāts).
4. Micko, L., Salma, I., Skadins, I., Salms, G., Dubnika, A., **Egle, K.** Platelet-rich fibrin immunological testing methodology using Elisa assay, *RSU International Research Conference on Medical and Health Care Sciences: Knowledge for Use in Practice*, Riga, Latvia, 29th – 31st March **2023** (mutiskā prezentācija).
5. Micko, L., Skadins, I., Salma, I., Dubnika, A., **Egle, K.**, Salms G. Platelet-rich fibrin antibacterial activity against *Klebsiella pneumoniae*, *RSU International Research Conference on Medical and Health Care Sciences: Knowledge for Use in Practice*, Riga, Latvia, 29th – 31st March **2023** (mutiskā prezentācija).
6. **Egle, K.**, Skadins, I., Grava, A., Micko, L., Dubniks, V., Salma, I., Dubnika, A. Injectable platelet-rich fibrin as a drug carrier increases the antibacterial susceptibility of antibiotic-clindamycin phosphate. *16th Annual Meeting for Scandinavian Society for Biomaterials*, Roros, Norway, 21st – 24th March **2023** (stenda referāts).
7. Micko, L., **Egle, K.**, Grava, A., Skadins, I., Salma, I., Salms, G., Dubnika, A. Antimicrobial activity of platelet-rich fibrin. *26th Congress of the European Association for Cranio-Maxillo-Facial Surgery*, Madrid, Spain, 27th -30th September **2022** (stenda referāts).
8. **Egle, K.**, Dohle, E., Hoffmann, V., Salma, I., Al-Maawi, S., Ghanaati, S., Dubnika, A. Fucoidan/chitosan hydrogels as matrices for sustained delivery of platelet-rich fibrin containing bioactive molecules. *32nd Annual Conference of the European Society for Biomaterials*, Bordeaux, France, 4th-8th September **2022** (stenda referāts).
9. Salma, I., Micko, L., **Egle, K.**, Dubnika, A. Development of protocol for obtaining autologous liquid PRF for local drug delivery systems. *32nd Annual Conference of the European Society for Biomaterials*, Bordeaux, France, 4th-8th September **2022** (stenda referāts).

10. **Egle, K.**, Micko, L., Grava, A., Salma, I., Skadins, I., Dubnika, A. Study on the effect of fibrin matrice on the antibacterial activity of clindamycin phosphate. *Scandinavian Society for Biomaterials 2022 15th Annual Meeting*, Jurmala, Latvia, 13th – 15th June **2022** (stenda referāts).
11. **Egle, K.**, Salma, I., Dubnika, A. From blood to regenerative tissue: how autologous platelet-rich fibrin can be used as drug carrier system. *62nd International Scientific Conference of RTU: Materials Science and Applied Chemistry*, Riga, Latvia, October 22, **2021** (stenda referāts).
12. **Egle, K.**, Dubnika, A. Development of fibrin matrices for sustained drug delivery. *31st Conference of the European Society for Biomaterials*, Porto, Portugal, 5th-9th September **2021** (stenda referāts).
13. **Egle, K.**, Salma, I., Skadins, I., Dubnika, A. Study of autologous fibrin matrices for controlled drug delivery. *Scandinavian Society for Biomaterials*, Jurmala, Latvia, 14th June **2021** (stenda referāts).
14. Skadins, I., Micko, L., Salma, I., Dubnika, A., **Egle K.** Antibacterial properties of platelet-rich fibrin matrices saturated with vancomycin. *Scandinavian Society for Biomaterials*, Jurmala, Latvia, June 14 **2021** (stenda referāts).
15. Dubnika, A., **Egle, K.**, Skadins, I., Salma, I. Commercial vs autologous fibrin-handling from material point of view. *RSU International Research Conference on Medical and Health Care Sciences: Knowledge for Use in Practice*, Riga, Latvia, 24th – 26th March **2021** (mutiskā prezentācija tiešsaistē).
16. Skadins, I., Dubnika, A., **Egle, K.**, Dovbenko, A., I.Salma, L.Micko. Antibacterial effect of autologous matrices. *RSU International Research Conference on Medical and Health Care Sciences: Knowledge for Use in Practice*, Riga, Latvia, 24th – 26th March **2021** (stenda referāts).
17. **Egle, K.**, Dubnika, A. Development of fibrin matrices for controlled drug delivery. *61st International Scientific Conference of RTU: Materials Science and Applied Chemistry*, Riga, Latvia, October 23, **2020** (stenda referāts).
18. **Egle, K.** Development of autologous fibrin matrices for controlled drug delivery. *61st Riga Technical University Student Scientific and Technical Conference*, Riga, Latvia, May 22, **2020** (mutiskā prezentācija).

Citas zinātniskās publikācijas, kas publicētas promocijas darba izstrādes laikā

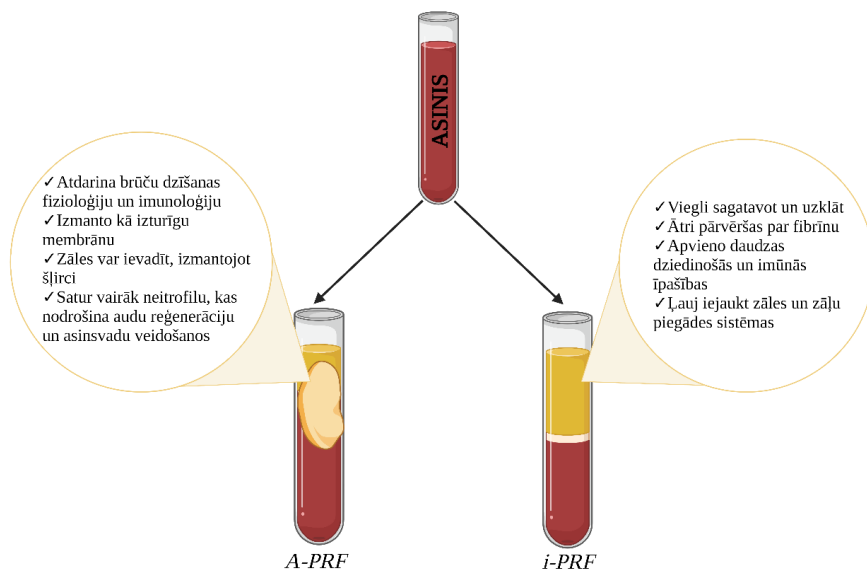
1. Micko, L., Salma, I., Skadins, I., **Egle, K.**, Salms, G., Dubnika, A. Can Our Blood Help Ensure Antimicrobial and Anti-Inflammatory Properties in Oral and Maxillofacial Surgery? *International Journal of Molecular Sciences*, **2023**, 24 (2), 1073.doi: 10.3390/ijms24021073 (Scopus, Open Access).
2. Grava, A., **Egle, K.**, Dubnika, A. Enzymatically Crosslinked In Situ Synthesized Silk/Gelatin/Calcium Phosphate Hydrogels for Drug Delivery. *Materials*, **2021**, 14 (23), 7191. doi: 10.3390/ma14237191 (Scopus, Open Access).

PROMOCIJAS DARBA GALVENIE REZULTĀTI

Ceļš no pacienta asins paraugiem līdz injicējamam *PRF*

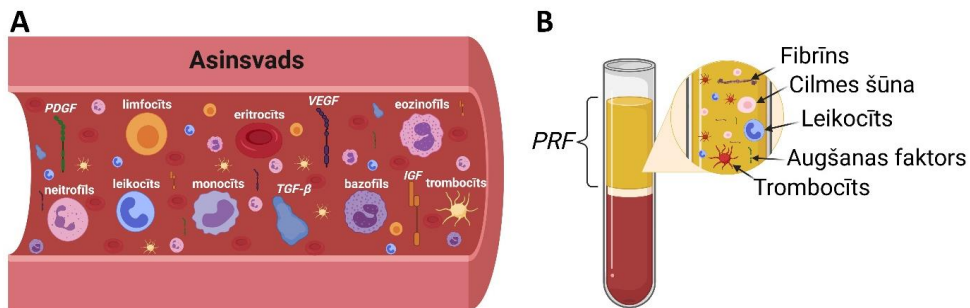
Asinis ir plazmas, trombocītu, sarkano un balto asins šūnu maisījums, kas cirkulē pa visu ķermeni. Pacienta asinis tiek savāktas, un, pakļaujot tās centrālās spēkam, sastāvā esošie komponenti, tostarp trombocīti un fibrīns, tiek dabiski atdalīti atkarībā no to blīvuma [30]. Līdz ar to *PRF* tiek iegūts no asinīm, izmantojot vienkāršu centrifugēšanas procesu. Mūsdienās *PRF* plaši izmanto, lai paātrinātu mīksto un cieto audu atjaunošanos. 2001. gadā Francijā pirmo reizi pētnieks *Choukroun et al.* aprakstīja *PRF*. *PRF* ir ar trombocītiem bagātinātas plazmas (*PRP*) modifikācija, autologa fibrīna matrica, ko medicīniski izmanto kaulu reģenerācijas uzlabošanai un mīksto audu paplašināšanai un stiprināšanai. Salīdzinot ar citiem trombocītu koncentrātiem, *PRF* ir ar trombocītiem bagātināts fibrīna receklis, kura iegūšanai nav nepieciešams izmantot trombinu (prokoagulantu, kas paātrinātu koagulāciju). To iegūst, centrifugējot asinis bez jebkādiem piemaisījumiem. *PRF* ir jauns biomateriāls, kas līdzinās autologai rētu matricai, bet tajā pašā laikā nav ne fibrīna līme, ne klasisks trombocītu koncentrāts. Turklāt *PRF* satur augstu saimniekorganismā esošo imūnšūnu koncentrāciju, kas nepieciešama brūču dzīšanai un infekciju samazināšanai [5].

Mūsdienās tiek izmantoti dažādi *PRF* atvasinājumi atkarībā no to lietojuma un vēlamajām īpašībām. Kā minēts *Wend et al.* pētījumos, papildus blīvajam *PRF* (*A-PRF*) pastāv klīniska nepieciešamība izstrādāt injicējamu *PRF* (*i-PRF*) dažādām medicīniskām procedūrām, kā arī, lai uzlabotu angiogēno potenciālu, balstoties iespējā kombinēt *i-PRF* ar dažādiem biomateriāliem [5, 31]. 1. attēlā parādītas *i-PRF* un *A-PRF* priekšrocības.



1. att. Divu autologo trombocītiem bagātināto koncentrātu *i-PRF* un *A-PRF* priekšrocību salīdzinājums. Attēls izveidots ar *Biorender.com* [5].

i-PRF ir šķidrums injicējams *PRF*, kas nodrošina iespēju iekļaut zāles un zāļu piegādes sistēmas pirms koagulācijas. *i-PRF* ir nesens klīnikā ieviests trombocītu koncentrāts, ko var viegli kombinēt ar dažādiem biomateriāliem, lai uzlabotu biomateriālu īpašības. *i-PRF* satur ne tikai asinīs esošos autologos augšanas faktorus, bet arī šūnas, kas iesaistītas brūču dzīšanas procesā (2. att.). 2. attēla B pusē redzams, ka ne visi elementi, kas ir asinīs, pēc centrifugēšanas nonāk *PRF* slānī.



2. att. Galvenie asins (A) un *PRF* (B) elementi. Attēls izveidots ar *Biorender.com* [5].

PRF piemīt antibakteriāla aktivitāte, taču tā ir salīdzinoši maz pētīta, un nav pietiekami daudz datu par to, kas to ietekmē. Antimikrobiālo aktivitāti var definēt kā mikroorganismu (baktēriju, sēnīšu un vīrusu) iznīcināšanu vai augšanas kavēšanu [32]. Cilvēka organismā ir apgrūtināta brūču dzīšana iespējamo infekciju dēļ, īpaši brūcēm, kas atrodas mutes dobumā. Tādējādi *PRF* izmantošanas panākumi varētu būt saistīti ar tā pretmikrobu īpašībām. Pilnībā autologs otrās paaudzes *PRF* bez piedevām, kas sagatavots, vienreiz centrifugējot, var visprecīzāk atspoguļot no asinīm iegūta materiāla pretmikrobu potenciālu. Vēl viena būtiska *PRF* īpašība ir tā spēja atbrīvot dažādus augšanas faktorus un citokīnus suprafizioloģiskās koncentrācijās, padarot to par nozīmīgu medicīnisko līdzekli, īpaši audu reģenerācijā [4]. Augšanas faktoriem ir īss bioloģiskais pussabrukšanas periods, tie ātri tiek izvadīti no asinsrites un darbojas galvenokārt lokāli. Tos kā neviendabīgu olbaltumvielu grupu izdala leikocīti un trombocīti. Trombocīti ir iesaistīti hemostāzē un aiztur augšanas faktorus alfa granulās, kas tiek aktivizētas, lai atbrīvotu šos faktorus traumas vietā [33].

Literatūrā minētie pētījumi liecina, ka *PRF* bieži lieto kombinācijā ar tādām zālēm kā metronidazols, klindamicīns, penicilīns [34], *VANKA*, teikoplanīns, gentamicīns vai amikacīns, lai izskaustu baktērijas un paātrinātu dzīšanas procesu [35]. Mūsdienās mutes, sejas un žokļu ķirurģijā novērota pastiprināta klindamicīna kā farmaceitiskā līdzekļa nepieciešamība. Klindamicīnu un *VANKA* parasti izskata kā alternatīvos līdzekļus pacientiem, kuriem ir alerģiska reakcija pret penicilīnu [36]. Pēdējā desmitgadē dažos pētījumos *PRF* apvieno ar antibiotikām antibakteriālā efekta nodrošināšanai. Pamatojoties uz apkopoto literatūru par *PRF* piemītošajām antibakteriālajām īpašībām, optimāla pieeja būtu *PRF* apvienošana ar zālēm pirms lietošanas klīniski, lai izveidotu vienotu sistēmu, nevis atsevišķu zāļu un *PRF* ievadīšanu [4]. Jāņem vērā arī tas, ka *PRF* var kalpot ne tikai kā zāļu piegādes sistēma, bet arī kā citu materiālu matrica. Zinātnieki ir pārbaudījuši iespējas apvienot *Bombyx mori* zīda fibroīna

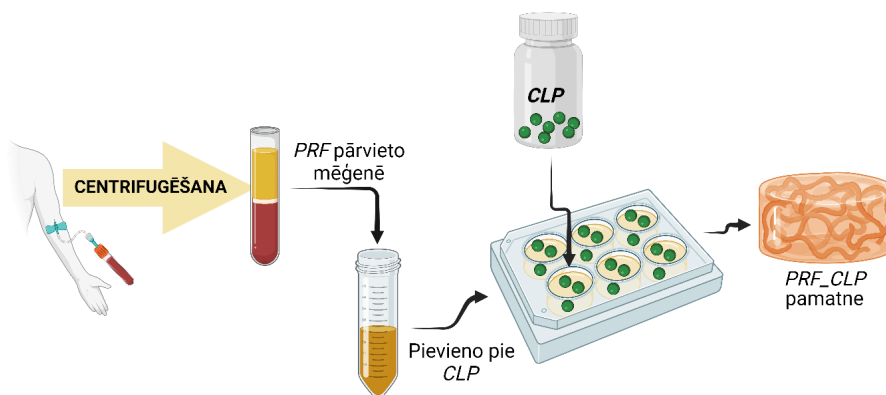
pulveri ar *PRF*, kas iegūts pēc Choukroun izstrādātās metodikas. Izstrādātais materiāls uzrādīja spēju novērst periimplanta audu defektus [37]. Izskatot literatūru par periodontīta ārstēšanu, tika konstatēts, ka *PRF* kombinācijās ar citiem materiāliem var izmantot arī intraalveolāru defektu ārstēšanai. Apkopojot visus pieejamos pētījumus, novērots, ka, izmantojot *PRF* kā matricas vai iekļaujot to citā nesēju sistēmā, nav nepieciešams papildus pievienot augšanas faktorus, jo pats *PRF* ietver noteiktus augšanas faktorus. Vienīgais, kas jāņem vērā, ir vēlamā medikamenta iekapsulēšanas process un tā mijiedarbība ar citiem nesējiem, kas tiks iekļauti *PRF*. Svarīgi ir arī izpētīt, vai izmantotā nesējsistēma spēs nodrošināt kontrolētu *PRF* sastāvā esošo augšanas faktoru izdalīšanos [5].

Šis promocijas darbs izceļ ar trombocītiem bagātinātā fibrīna (*PRF*) daudzpusīgo potenciālu biomedicīnas lietojumam. Nākamajās nodaļās padziļināti aplūkoti konkrēti aspekti, tostarp: 1) *PRF* spēja uzlabot klindamicīna fosfāta antibakteriālo jutību; 2) piegādes sistēmu ietekme uz zāļu izdalīšanos no *PRF* matricas; 3) nesējsistēmu ietekme uz *PRF* sastāvā esošo bioaktīvo molekulu izdalīšanos. Šo nodaļu mērķis ir sniegt visaptverošu izpratni par to, kā *PRF* var izmantot un optimizēt mērķtiecīgām un efektīvām ārstnieciskām manipulācijām.

***PRF* potenciāls stimulēt CLP antibakteriālo jutību**

Viens no visbiežāk sastopamajiem pēcoperāciju riskiem ir infekcijas, ko izraisa patogēnas un oportūnistiskas baktērijas. *S. aureus* un *S. epidermidis* ir grampozitīvas oportūnistiskas baktērijas, kas atrodas normālā cilvēka mikrobiomā [2]. Oportūnistiskās baktērijas parasti ir nekaitīgas, ja tās uzturas cilvēka vai dzīvnieka ķermenī, bet var izraisīt slimību vai infekciju, ja apstākļi to atļauj, piemēram, ja ir novājināta imūnsistēma [38].

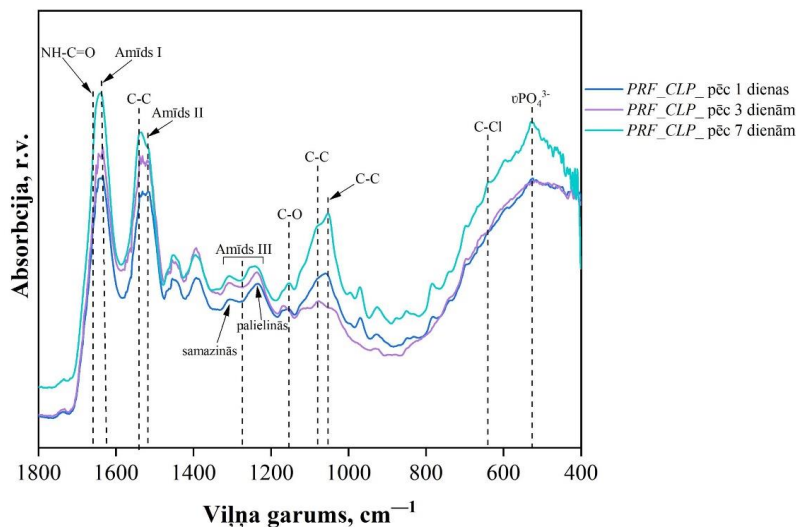
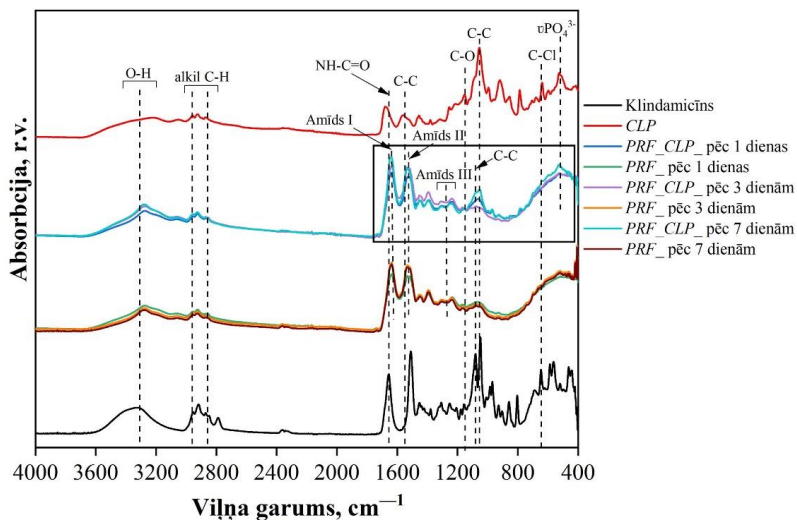
Klindamicīnu jau daudzus gadus iesaka, lai ārstētu sabiedrībā iegūtas, pret meticilīnu rezistentas un pret meticilīnu jutīgas *S. aureus* infekcijas, un tas var arī samazināt izturību pret meticilīnu rezistentu *S. aureus* klīnisko izolātu jutību [39, 40]. Patlaban pieaug nepieciešamība izmantot klindamicīnu mutēs, sejas un žokļu ķirurģijā, īpaši žokļa osteonekrozes profilaksei un ārstēšanai [41]. To plaši izskata kā alternatīvu pacientiem ar alerģisku reakciju pret penicilīnu [36]. Klindamicīna fosfāts (*CLP*) ir klindamicīna zāļvielu prekursors, kam nav antibakteriālas aktivitātes [42]. Literatūrā aprakstīts, ka *CLP* asinīs ātri hidrolizējas par aktīvo formu (klindamicīnu) [43]. Pētījuma mērķis bija izpētīt *CLP* antibakteriālo īpašību izmaiņas pret *S. aureus* un *S. epidermidis* references kultūrām un klīniskajiem izolātiem, izmantojot *PRF* kā nesēja matricu. Viens no galvenajiem veidiem, kā novērtēt antibakteriālās īpašības, ir minimālās inhibējošās koncentrācijas (MIK) un minimālās baktericīdās koncentrācijas (MBK) noteikšana. *PRF-CLP* paraugu sagatavošanas shēma parādīta 3. attēlā.



3. att. *PRF-CLP* paraugu sagatavošanas shēma. Attēls izveidots ar *Biorender.com*.

Furjē transformācijas infrasarkanā spektrometrija (*FTIR*) darbā izmantota, lai pētītu strukturālās izmaiņas pēc klindamicīna fosfāta (*CLP*) apvienošanas ar *PRF* (4. att.). *CLP* un *PRF* kombināciju antibakteriālā efekta noteikšanai izmantoti antibakteriālie testi, paralēli apstiprinot teoriju, ka *PRF* klātbūtnē nepieciešama zemāka *CLP* koncentrācija, lai izskaustu un novērstu baktēriju augšanu (5. att.).

FTIR spektros attēlota *CLP* mijiedarbība ar *PRF* septiņu dienu inkubācijas periodā, novērota daļēja hidrolīze un *CLP* pārvēršanās par klindamicīnu. Pēc septiņām inkubācijas dienām tika novērota jaunas saites veidošanās ($C-C$ pie 1080 cm^{-1}) un maksimālais fosfātu grupas absorbcijas pieaugums laika gaitā, liecinot par strukturālām izmaiņām, kas, iespējams, ir *CLP* pārvēršanās aktīvās zālēs – klindamicīnā.

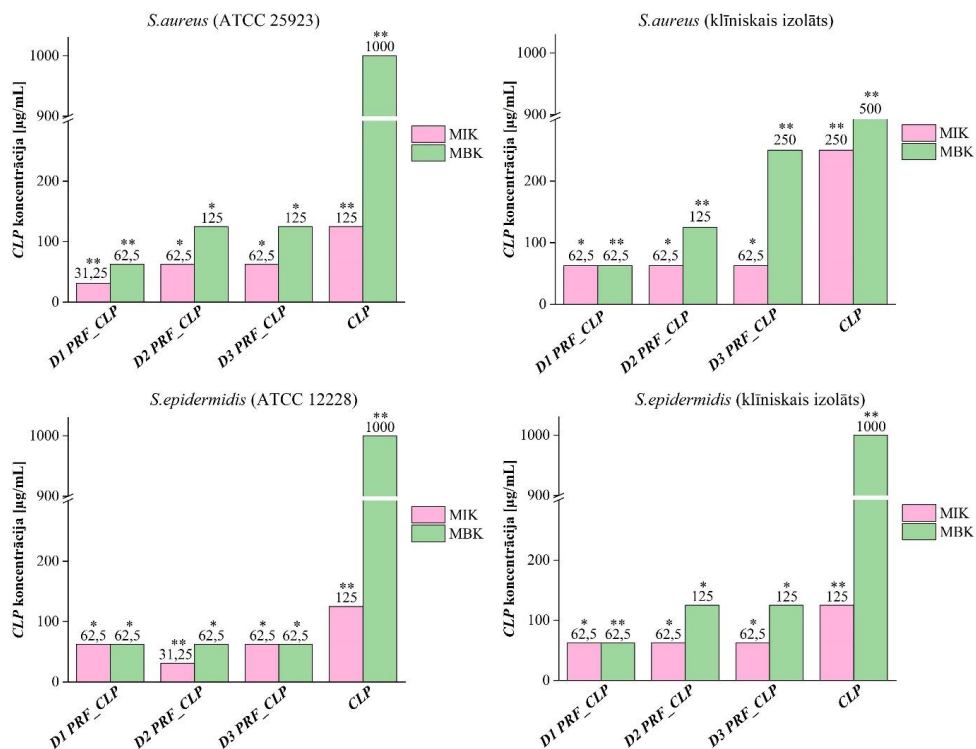


4. att. FTIR spektri: (A) PRF, PRF_CLP, CLP un klindamicīna paraugi pilnā spektra apgabalā; (B) PRF_CLP paraugi inkubācijas laika punktos 1800–400 cm^{-1} apgabalā [2].

Katra donora asins sastāvs ietekmē parauga antibakteriālās īpašības, specifiski – arī CLP daudzumu, kas nepieciešams, lai sasniegtu antibakteriālo aktivitāti.

Salīdzinot PRF_CLP paraugu MIK un MBK vērtības ar CLP paraugiem, novērota šo vērtību samazināšanās pret visiem analizētajiem baktēriju celmiem PRF_CLP paraugiem. Antibakteriālie testi parādīja, ka PRF pievienošana CLP uzlabo antibakteriālo aktivitāti ne tikai pret stafilokoku references kultūrām, bet arī pret klīniskajiem izolātiem, salīdzinot ar tīru CLP paraugu. Noteikts, ka pret *S. aureus* un *S. epidermidis* baktēriju klīniskajiem izolātiem PRF_CLP paraugos ir nepieciešama augstāka CLP koncentrācija, lai nodrošinātu zemāku MBK vērtību, salīdzinot ar abām baktēriju references kultūrām. Katram donoram asins īpašības ir

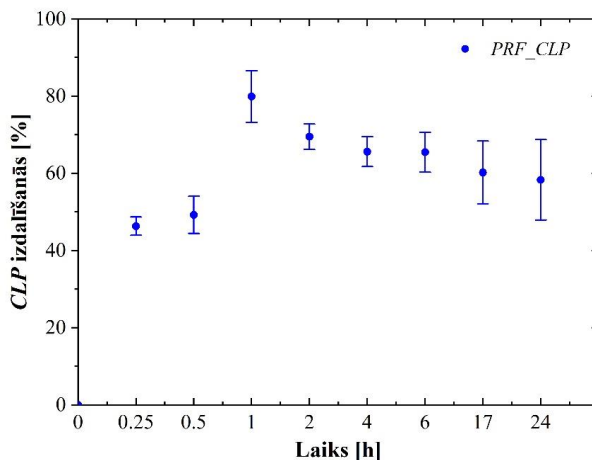
atšķirīgas (piemēram, atšķirīgs balto asins šūnu skaits vai D vitamīna līmenis), kas krasi var ietekmēt arī antibakteriālo iedarbību. Literatūrā aprakstītie *Schilcher* [44, 45] un Kuriyama [46] grupu pētījumi parādīja, ka tīra klindamicīna MIK vērtības klīniskajos izolātos pret meticilīnu rezistentu *S. aureus* (MRSA) var sasniegt > 256 µg/mL. Savukārt, apkopojot iegūtos datus, redzams, ka *CLP* ar *PRF* nodrošina labākas antibakteriālās īpašības nekā tīrs *CLP*, un, salīdzinot ar literatūru, ir iegūts materiāls, kas nodrošina zemākas MIK vērtības (svārstās no 62,5 µg/mL līdz 145,8 µg/mL atkarībā no baktēriju celma) nekā nepieciešams klindamicīnam (> 256 mg/mL). Atkarībā no baktēriju celma ir jāpielāgo izmantotā zāļu koncentrācija (5. att.).



5. att. MIK un MBK vērtību atšķirības starp *CLP* un *PRF_CLP* paraugiem pret četriem baktēriju celmiem (*S. aureus* (ATCC 25923), *S. epidermidis* (ATCC 12228), *S. aureus* (klīniskais izolāts), *S. epidermidis* (klīniskais izolāts) visiem trim donoriem. Paraugi sagatavoti no 1. donora asinīm (D1 *PRF_CLP*); paraugi sagatavoti no 2. donora asinīm (D2 *PRF_CLP*); paraugi sagatavoti no 3. donora asinīm (D3 *PRF_CLP*).

* $p > 0,05$; ** $p < 0,05$ [2].

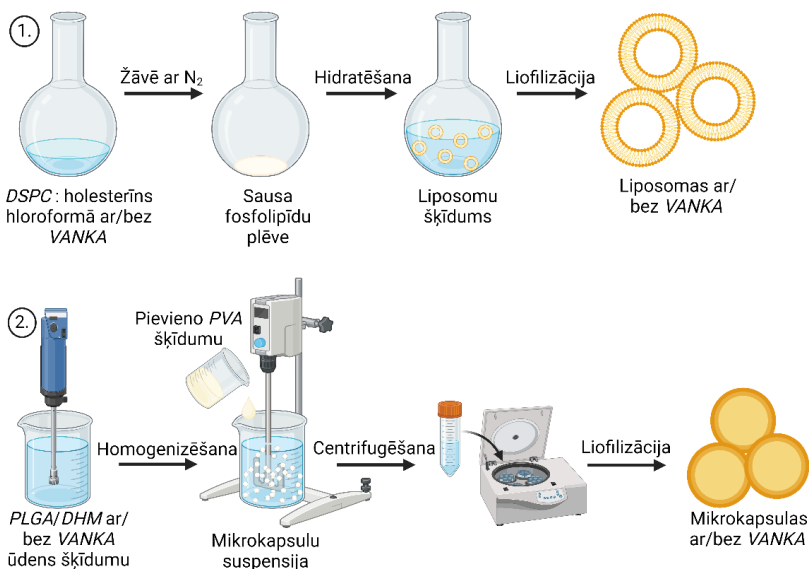
PRF spēja dabiski noārdīties tiek uzskatīta par priekšrocību, izmantojot to kā kontrolētu zāļu atbrīvošanas sistēmu “noliktavu”. *CLP* izdalīšanās dati liecina, ka *PRF_CLP* paraugu var izmantot vienas dienas lokālai terapijai, nodrošinot maksimālo *CLP* izdalīšanos (80 %) vienas stundas laikā (6. att.).



6. att. *CLP* izdalīšanās no *PRF* matricām Dulbeko modificētā Īgla vidē (*DMEM*); vidējie *CLP* izdalīšanās dati no trīs donoru *CLP-PRF* paraugiem [2].

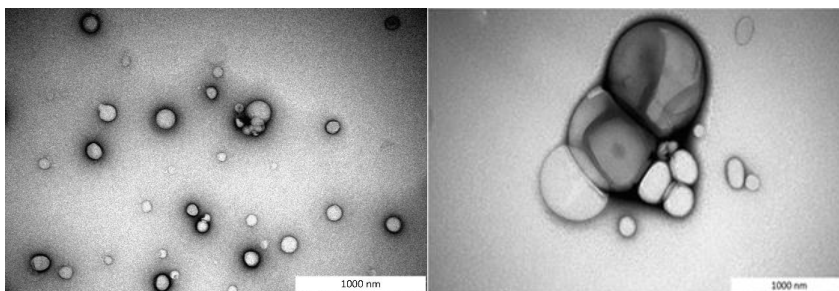
Ievadīto piegādes sistēmu īpašību ietekme uz zāļu izdalīšanos no *PRF* matricas

Sistemātiski lietojot zāles bez noteikta nesēja, tās izplatās pa visu organismu, un bieži vien zāļu noārdīšanās ātrums ir salīdzinoši īss. Tas nodrošina ne tikai pozitīvu ietekmi uz bojātajiem audiem, bet var izraisīt arī nelabvēlīgas blakusparādības veselajiem audiem [47]. Kā novērots iepriekš aprakstītajā pētījumā [2], iejaucot zāles *PRF*, tiek uzlabotas to antibakteriālās īpašības; tomēr zāles izdalās ļoti ātri. Zāļu piegādes sistēmu mērķis ir sasniegt augstāko terapeitisko efektu ar zemāko zāļu koncentrāciju [48]. Šajā pētījumā tika izmantotas antibiotikas *VANKA*, kas iekapsulētas *PLGA* mikroapsulās (*PLGA- μ C-VANKA*) un liposomās. 7. attēlā redzamas abu veidu piegādes sistēmu sagatavošanas shēmas. Abas izstrādātās *VANKA* piegādes metodes iekļautas *PRF* matricā, pārbaudot *PRF* spēju kontrolēti atbrīvot zāles no šādām zāļu piegādes sistēmām.



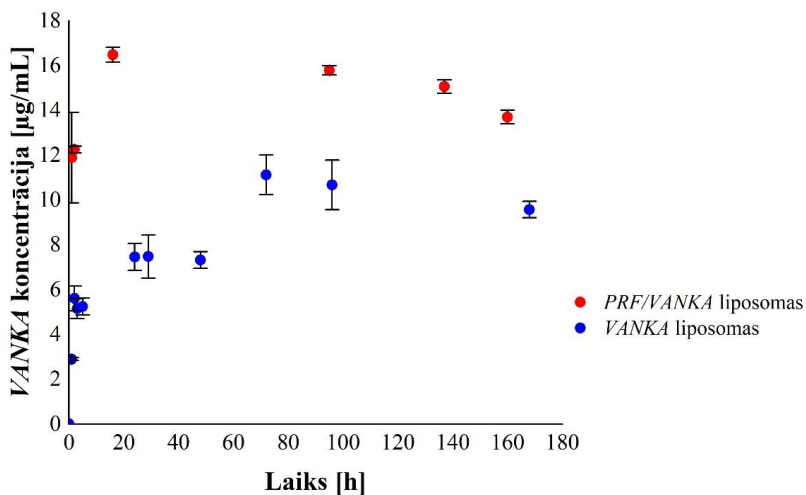
7. att. Paraugu sagatavošanas shēma: 1) liposomas ar/bez VANKA; 2) mikrokapulas ar/bez VANKA. Attēls izveidots ar *Biorender.com*.

Transmisijas elektronu mikroskopijas (TEM) analīze parādīja, ka sagatavotajām VANKA saturošajām liposomām ir nevienmīga izmēru variācija, turklāt novērojama liposomu divslāņu struktūra. Arī 8. attēlā redzams, ka lielākā daļa liposomu ir sfēriskas daļiņas.



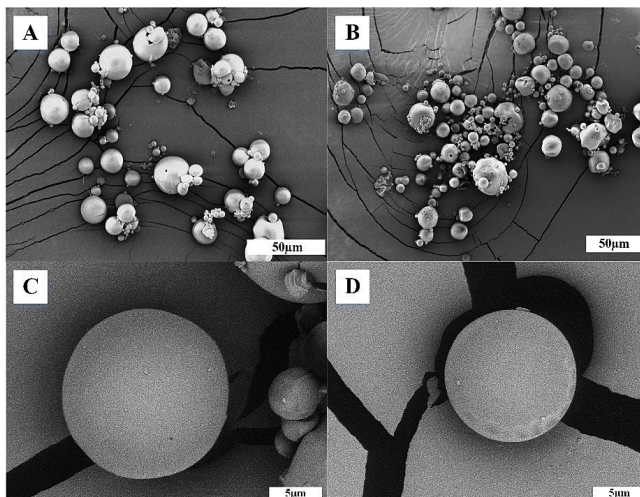
8. att. VANKA saturošu liposomu TEM attēli [13].

VANKA izdalīšanās kinētika no PRF/VANKA liposomām liecina par VANKA straujāku izdalīšanos, salīdzinot ar VANKA liposomām bez PRF matricas (9. att.). Paaugstināta VANKA koncentrācija ir skaidrojama ar to, ka PRF sastāvā esošie Ca²⁺ joni veido čaulu ap lipīdiem, tos saspiežot un tādējādi sagraujot liposomas [49, 50]. Pamatojoties uz iegūtajiem rezultātiem, var secināt, ka Ca²⁺ joni nelabvēlīgi ietekmē liposomas, tāpēc VANKA izdalās ātrāk un lielākā koncentrācijā.



9. att. Zāļu izdalīšanās kinētika no *PRF/VANKA* liposomām un *VANKA* liposomām [13].

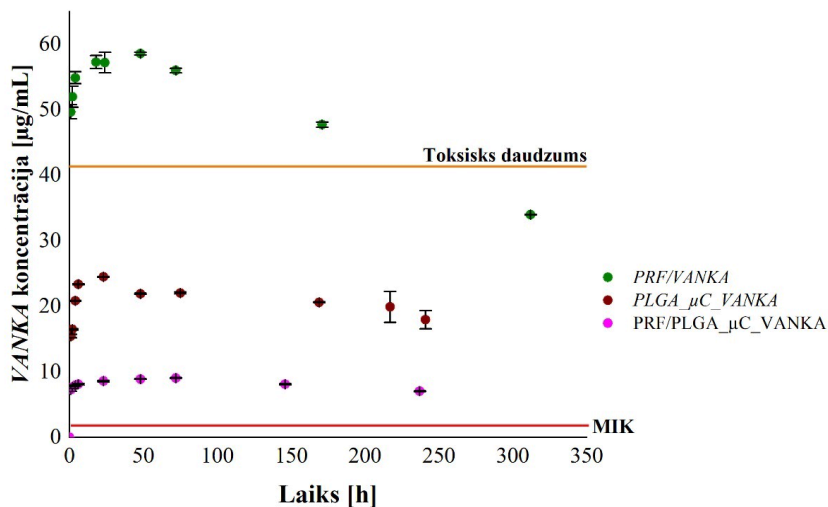
Savukārt *VANKA* saturošu *PLGA* mikro kapsulu skenējošās elektronu mikroskopijas (SEM) attēlos bija redzamas sfēriskas daļiņas ar gludu virsmu, kas liecināja par zāļu kristālu neesamību uz virsmas un apstiprināja vienmērīgu zāļu sadalījumu polimēru matricā (10. B att.).



10. att. *PLGA* mikro kapsulu virsmas SEM attēli bez (A, C) un ar (B, D) *VANKA* [13].

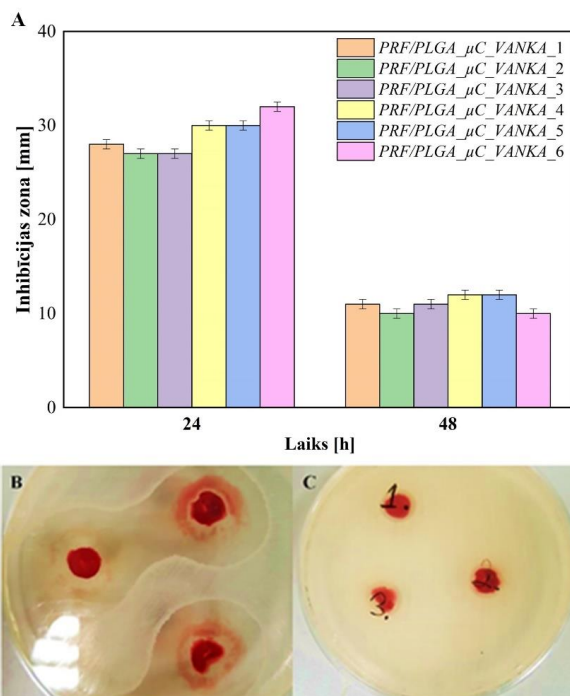
Pamatojoties uz *VANKA* izdalīšanās pētījumiem no *PLGA* mikro kapsulām (11. att.), *VANKA* izdalīšanās kinētika no *PRF* ar *VANKA* saturošām *PLGA* mikro kapsulām (*PRF/PLGA_µC_VANKA*) ir piecas reizes zemāka, salīdzinot ar *PRF*, kam *VANKA* pievienots neapstrādāta pulvera formā (*PRF/VANKA* paraugi), nodrošinot kontrolētu *VANKA* izdalīšanos (no sešām līdz 10 dienām) un novēršot strauju izdalīšanos. Savukārt, salīdzinot *PLGA_µC_VANKA* ar *PRF/PLGA_µC_VANKA* matricām, var novērot, ka *VANKA* izdalīšanās

koncentrācija samazinās divas reizes. Tas liecina par to, ka *PRF* matrica aizkavē *VANKA* strauju izdalīšanos. Turklāt, *PRF* matricās ienesot *VANKA* bez nesējsistēmas, netiek nodrošināta kontrolēta aktīvās *VANKA* formas piegāde terapeitiskā efekta līmenī.



11. att. Zāļu izdalīšanās no *PRF/VANKA*, *PLGA_µC_VANKA* un *PRF/PLGA_µC_VANKA* matricām [13].

Maksimālais antibakteriālās iedarbības ilgums paraugiem, kas satur *VANKA* (*PLGA_µC_VANKA*), tika novērots līdz 48 stundām. Pirmajās 24 stundās sterilās zonas vidējais diametrs ap paraugiem bija 30 mm. Nākamo 24 stundu laikā sterilās zonas diametrs samazinājās par 50 % (12. att.). Kā viena no risinājuma iespējām turpmākiem pētījumiem varētu būt iegūto paraugu ievietošana baktēriju suspensijā un inkubēšana, novēršot paraugu izžūšanu.

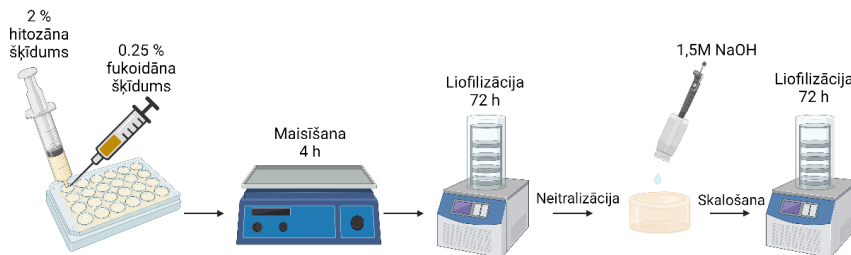


12. att. *PRF/PLGA_μC_VANKA* paraugu antibakteriālās īpašības: (A) inhibīcijas zonas mm; (B) sterilas zonas ap *PRF/PLGA_μC_VANKA* paraugiem pēc 24 stundu inkubācijas; (C) sterilas zonas ap *PRF/PLGA_μC_VANKA* paraugiem pēc 48 stundu inkubācijas. Petri trauciņu diametrs ir 8,5 cm [13].

Papildus spējai nodrošināt kontrolētu zāļu izdalīšanos *PRF* piemīt vēl viena būtiska īpašība – tā loma audu reģenerācijas veicināšanā, kas saistīta ar autologu augšanas faktoru un citokīnu esamību *PRF* sastāvā.

Nesējsistēmu ietekme uz *PRF* sastāvā esošo bioaktīvo molekulu izdalīšanos

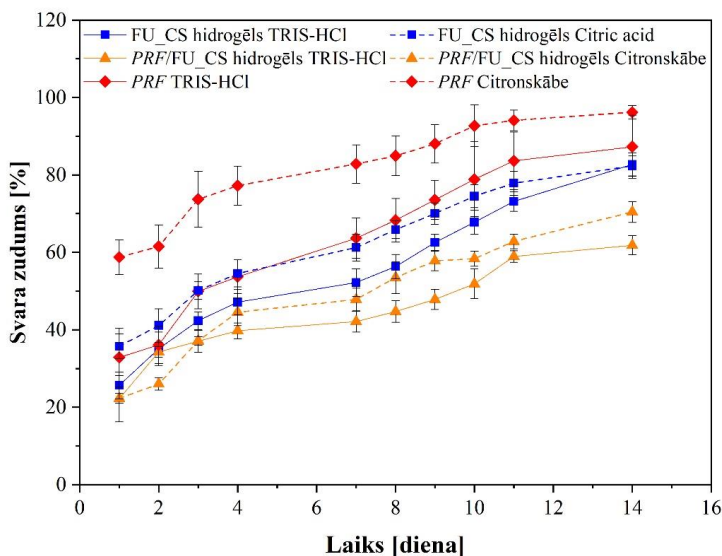
Turpmākajā pētījumā tika izstrādāti hidrogēli, kas sastāv no fukoidāna (FU) un hitozāna (CS), balstoties to bioloģiskajā saderībā un spējā veidot polielektrolītu kompleksus pašsavienšanās ceļā [28], kā arī fukoidāna spēju piesaistīt augšanas faktorus [24]. FU_CS hidrogēla sagatavošanas shēma redzama 13. attēlā. Lai noteiktu optimālo *PRF* daudzumu un tajā esošo bioaktīvo molekulu izdalīšanās kinētiku, hidrogēliem tika pētīti šādi parametri: 1) stabilitāte, deformācija un plūsmas īpašības; 2) bioaktīvo molekulu izdalīšanās kinētika.



13. att. FU_CS hidroģēlu sagatavošanas shēma. Attēls izveidots ar *Biorender.com* [51].

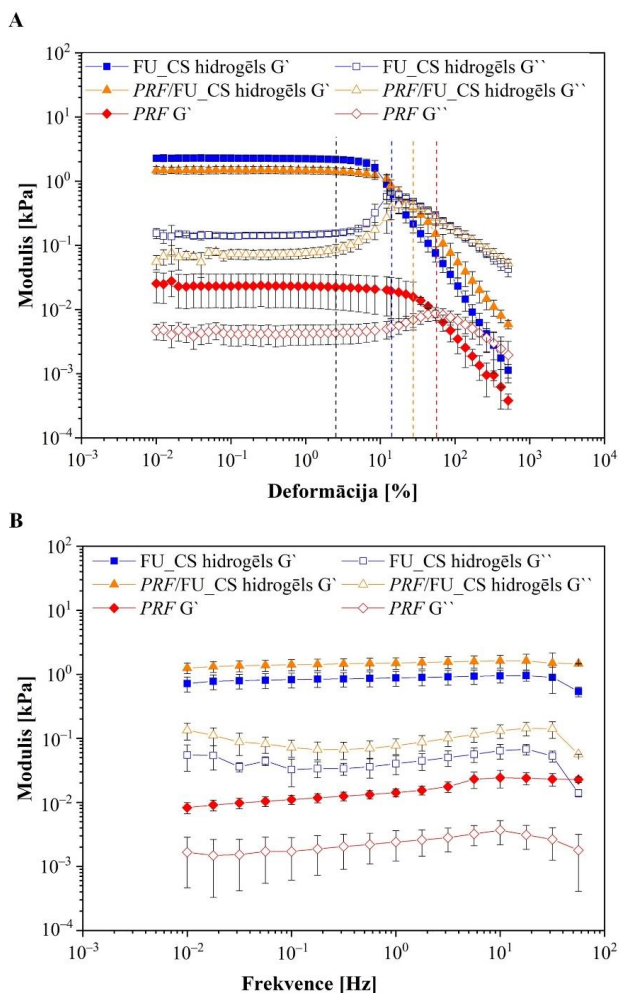
Hidroģēlu degradēšanās un reoloģiskās īpašības tika analizētas kā galvenie faktori, kas nosaka to mehānisko uzvedību un jutīgumu pret sadalīšanos, tādējādi noskaidrojot, vai *PRF* pievienošana spēj uzlabot izstrādāto hidroģēlu īpašības (14. un 15. att.). Kā nākamais solis bija izdalīto bioaktīvo molekulu (*TGF-1*, *PDGF-BB*, *VEGF*, *EGF* un *IL-8*) daudzuma noteikšana no nemodificētas *PRF* matricas un *PRF* apvienojumā ar hidroģēlu (16. att.).

Darbā noteikta FU_CS hidroģēlu ar/bez *PRF* un tūra *PRF* degradēšanās kinētika divu nedēļu laikā TRIS-HCl un citronskābē, un iegūtie dati redzami 14. attēlā. Pamatojoties uz rezultātiem, *PRF* pievienošana FU_CS hidroģēliem palēnināja izveidotā kompozīta hidroģēla degradēšanās ātrumu. Statistiskā analīze neatklāja būtisku atšķirību inkubācijas vides ietekmei uz FU_CS un *PRF*/FU_CS hidroģēlu paraugu degradēšanās kinētiku. Taču pastāv ievērojama atšķirība *PRF* degradācijas kinētikai – 14 dienu laikā *PRF* svara zudums novērots $87,26 \pm 8,21$ % TRIS-HCl un $96,21 \pm 1,71$ % citronskābes vidē.



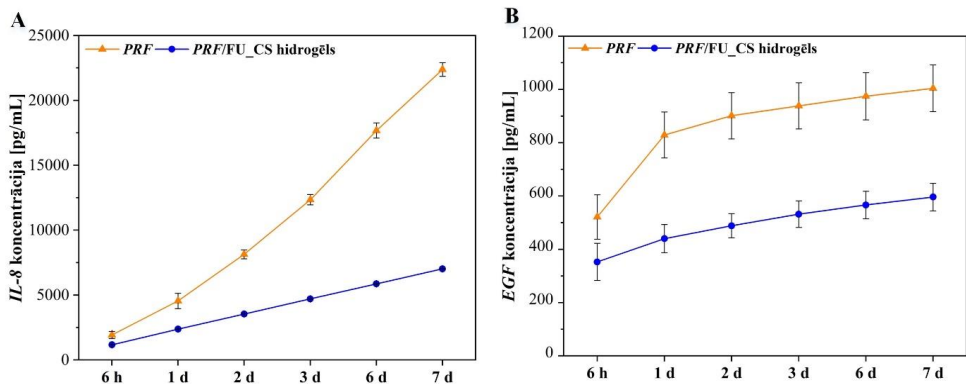
14. att. *PRF*, FU_CS un *PRF*/FU_CS hidroģēlu degradēšanās kinētika TRIS-HCl (ar nepārtrauktu līniju) un citronskābē (ar punktētu līniju) 37 °C temperatūrā. Visi dati ir attēloti kā vidējais \pm SD, $n = 3$ [51].

Reoloģiskie eksperimenti izmantoti, lai izpētītu *PRF*, *FU_CS* un *PRF/FU_CS* hidrogēlu deformācijas un plūsmas īpašības. Visiem paraugiem raksturīga želejveida uzvedība, krājuma modulim (G') ievērojami pārsniedzot zuduma moduli (G'') (15. att.). Izmantojot amplitūdas maiņas testu oscilācijas režīmā, tika noteikts konsekvents lineārais viskoelastiskais reģions (*LVER*) līdz $\epsilon \approx 2,5$ % visiem paraugiem (atzīmēts ar melnu līniju 15. A attēlā), G' - G'' krustošanās punkts novērots pie $\epsilon \approx 14$ % *FU_CS* hidrogēlam, $\epsilon \approx 28$ % *PRF/FU_CS* hidrogēlam un pie $\epsilon \approx 55$ % *PRF* (atzīmēts ar krāsainām līnijām). Reoloģijā “ ϵ ” apzīmē deformāciju, cik daudz materiāls ir deformējies noteikta sprieguma vai spēka ietekmē. Visos frekvenču diapazonos G' palika nemainīgs visiem paraugiem (15. B att.), liecinot par cietai struktūrai līdzīgu un stabilu iekšējo struktūru.



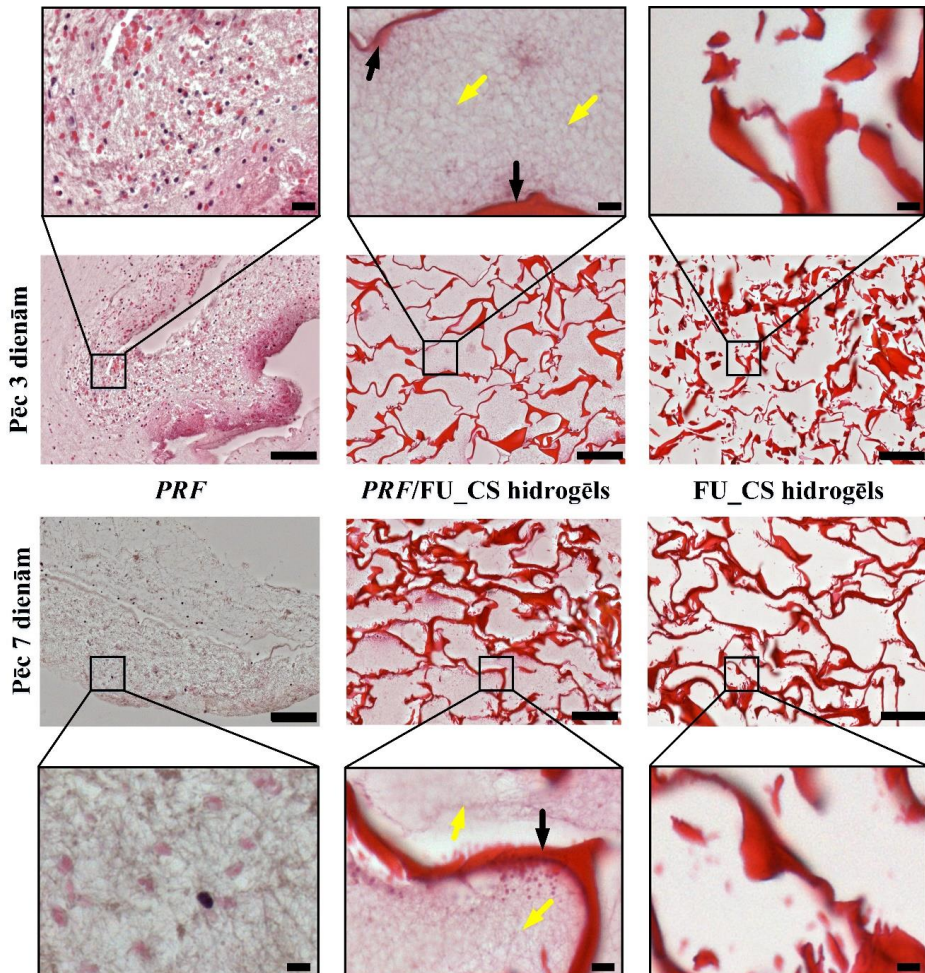
15. att. Hidrogēlu mehāniskās īpašības. **(A)** Amplitūdas maiņas tests oscilācijas režīmā FU_CS hidrogēliem ar/bez PRF pie frekvences 1 Hz; **(B)** frekvences izmaiņas tests FU_CS hidrogēlu ar/bez PRF pie deformācijas 0,2 %. Visi dati ir attēloti kā vidējais lielums \pm SD ($n = 3$) [51].

Iegūtie dati liecina, ka izstrādātais hidrogēls, kas iegūts elektrostātiskās mijiedarbības rezultātā, ļauj iekapsulēt PRF sastāvā esošos augšanas faktoros un nodrošina to pakāpenisku izdalīšanos. Novērots, ka visiem analizētajiem augšanas faktoriem un citokīniem (*TGF-1*, *PDGF-BB*, *VEGF*, *EGF* un *IL-8*) izdalīšanās koncentrācija no nemodificētiem PRF paraugiem ir augstāka nekā no PRF/FU_CS hidrogēlu matricām. Tas liecina par to, ka FU_CS hidrogēls var efektīvi iekļaut bioaktīvās molekulas hidrogēla matricā un ilgstoši tās izdalīt, nodrošinot to ilgtermiņa pieejamību audu inženierijas nolūkos.



16. att. Augšanas faktora un citokīna kumulatīva izdalīšanās. A–B parāda augšanas faktora un citokīna (attiecīgi *IL-8* un *EGF*) izdalīšanos katrā laika punktā [51].

Histoloģiskie pētījumi apstiprināja *PRF* iekļaušanos *FU_CS* hidrogēla matricā, attiecīgi ļaujot atbrīvot augšanas faktorus. Pēc trīs un septiņām dienām salīdzinājums starp nemodificētu *PRF* un *PRF/FU_CS* hidrogēlu atklāj šūnu skaita samazināšanos *PRF* matricā, tādējādi izskaidrojot bioaktīvo molekulu atbrīvošanos. Iegūtie dati arī apliecina, ka pēc septiņām dienām *PRF* joprojām ir iekļauts *FU_CS* hidrogēla struktūrā (17. att.).



17. att. Fibrīna morfoloģija pēc trīs un septiņu dienu inkubācijas. (Mērogs = 100 μm , palielinājumam ir mērogs – 20 μm ; dzeltenās bultiņas norāda *PRF* klātbūtni, melnās bultiņas – hidrogēla klātbūtni) [51].

Hidrogēlu izmantošana, lai modulētu *PRF* augšanas faktoru izdalīšanās kinētiku, īpaši kombinācijās ar zālēm (potenciāli zāļu vielu prekursoriem), piedāvātu daudzsoļu iespēju uzlabot materiālu antibakteriālo aktivitāti. Turpmākajos pētījumos būtu jākoncentrējas uz zāļu un hidrogēlu īpašību mijiedarbības optimizēšanu, ilgstošas izdalīšanās modeļu izpēti un citu zāļu spēju *PRF* klātbūtnē pārveidoties aktīvākā formā, sniedzot vērtīgu ieskatu uzlabotu terapeitisko materiālu izmantošanā.

SECINĀJUMI

1. *PRF* pievienošana ietekmē *CLP* antibakteriālo iedarbību pret *S. aureus* un *S. epidermidis* baktēriju celmiem (gan references kultūrām, gan klīniskajiem izolātiem), kā rezultātā iespējams nodrošināt zemākas MIK vērtības (no 62,5 µg/mL līdz 145,8 µg/mL atkarībā no baktērijas celms) nekā klindamicīnam (MIK > 256 µg/ml).
2. Fosfatidiholīnu liposomu kā zāļu piegādes sistēmu izmantošana *PRF* matricās nespēj nodrošināt kontrolētu *VANKA* izdalīšanos, jo to stabilitāti ietekmē *PRF* sastāvā esošie Ca^{2+} joni, tādējādi izdalot augstu zāļu koncentrāciju.
3. *PLGA* mikrokapsulu izmantošana kā zāļu piegādes sistēma *PRF* matricā var nodrošināt kontrolētu *VANKA* izdalīšanos no sešām līdz 10 dienām.
4. *FU_CS* hidrogēls, kas izveidots elektrostatiskās mijiedarbības rezultātā, ļauj iekapsulēt *PRF* bioaktīvās molekulas (*TGF-1*, *PDGF-BB*, *VEGF*, *EGF* un *IL-8*) un nodrošināt to pakāpenisku izdalīšanos septiņu dienu laikā.

LITERATŪRAS SARAKSTS

1. Garraud, O.; Cognasse, F. Are Platelets Cells? And if Yes, are They Immune Cells? *Front. Immunol.* **2015**, *6*, 1–8, doi:10.3389/fimmu.2015.00070.
2. Egle, K.; Skadins, I.; Grava, A.; Micko, L.; Dubniks, V.; Salma, I.; Dubnika, A. Injectable Platelet-Rich Fibrin as a Drug Carrier Increases the Antibacterial Susceptibility of Antibiotic – Clindamycin Phosphate. *Int. J. Mol. Sci.* **2022**, *23*, 7407, doi: 10.3390/ijms23137407.
3. Jasmine, S.; A., T.; Janarthanan, K.; Krishnamoorthy, R.; Alshatwi, A. A. Antimicrobial and antibiofilm potential of injectable platelet rich fibrin – a second-generation platelet concentrate – against biofilm producing oral staphylococcus isolates. *Saudi J. Biol. Sci.* **2020**, *27*, 41–46, doi: 10.1016/j.sjbs.2019.04.012.
4. Micko, L.; Salma, I.; Skadins, I.; Egle, K.; Salms, G.; Dubnika, A. Can Our Blood Help Ensure Antimicrobial and Anti-Inflammatory Properties in Oral and Maxillofacial Surgery? *Int. J. Mol. Sci.* **2023**, *24*, 1073, doi:10.3390/ijms24021073.
5. Egle, K.; Salma, I.; Dubnika, A. From Blood to Regenerative Tissue: How Autologous Platelet-Rich Fibrin Can Be Combined with Other Materials to Ensure Controlled Drug and Growth Factor Release. *Int. J. Mol. Sci.* **2021**, *22*, 11553, doi: 10.3390/ijms222111553.
6. Sancho-Puchades, M.; Herráez-Vilas, J.M.; Berini-Aytés, L.; Gay-Escoda, C. Antibiotic prophylaxis to prevent local infection in Oral Surgery: use or abuse? *Med. Oral Patol. Oral Cir. Bucal* **2009**, *14*, E28-33.
7. Yang, Z.; Liu, J.; Gao, J.; Chen, S.; Huang, G. Chitosan coated vancomycin hydrochloride liposomes: Characterizations and evaluation. *Int. J. Pharm.* **2015**, *495*, 508–515, doi:10.1016/j.ijpharm.2015.08.085.
8. Liu, J.; Wang, Z.; Li, F.; Gao, J.; Wang, L.; Huang, G. Liposomes for systematic delivery of vancomycin hydrochloride to decrease nephrotoxicity: Characterization and evaluation. *Asian J. Pharm. Sci.* **2015**, *10*, 212–222, doi:10.1016/j.ajps.2014.12.004.
9. Pumerantz, A.; Muppidi, K.; Agnihotri, S.; Guerra, C.; Venketaraman, V.; Wang, J.; Betageri, G. Preparation of liposomal vancomycin and intracellular killing of meticillin-resistant Staphylococcus aureus (MRSA). *Int. J. Antimicrob. Agents* **2011**, *37*, 140–144, doi:10.1016/j.ijantimicag.2010.10.011.
10. Upputuri, R. T. P.; Kulandaivelu, K.; Mandal, A. K. A. Nanotechnology-Based Approach for Enhanced Bioavailability and Stability of Tea Polyphenols – A Review. In *Studies in Natural Products Chemistry*; 2016; pp. 399–410.
11. Tyle, P. *Drug Delivery*; Hillery, A., Park, K., Eds.; CRC Press, 2016; Vol. 77; ISBN 9781482217728.
12. Saeed Jan, M.; Alam, W.; Shabnam, M. Fundamentals Applications of Controlled Release Drug Delivery. In *Drug Development and Safety [Working Title]*; IntechOpen, 2023.
13. Dubnika, A.; Egle, K.; Skrinda-Melne, M.; Skadins, I.; Rajadas, J.; Salma, I. Development of Vancomycin Delivery Systems Based on Autologous 3D Platelet-Rich Fibrin Matrices for Bone Tissue Engineering. *Biomedicines* **2021**, *9*, 814, doi: 10.3390/biomedicines9070814.

14. Micko, L.; Salma, I.; Skadins, I.; Egle, K.; Salms, G.; Dubnika, A. Can Our Blood Help Ensure Antimicrobial and Anti-Inflammatory Properties in Oral and Maxillofacial Surgery? *Int. J. Mol. Sci.* **2023**, *24*, 1073, doi: 10.3390/ijms24021073.
15. Mirjalili, F.; Mahmoodi, M. Controlled release of protein from gelatin/chitosan hydrogel containing platelet-rich fibrin encapsulated in chitosan nanoparticles for accelerated wound healing in an animal model. *Int. J. Biol. Macromol.* **2023**, *225*, 588–604, doi: 10.1016/j.ijbiomac.2022.11.117.
16. Rao, S.S.; Venkatesan, J.; Yuvarajan, S.; Rekha, P.D. Self-assembled polyelectrolyte complexes of chitosan and fucoidan for sustained growth factor release from PRP enhance proliferation and collagen deposition in diabetic mice. *Drug Deliv. Transl. Res.* **2022**, *12*, 2838–2855, doi: 10.1007/s13346-022-01144-3.
17. Rastegar, A.; Mahmoodi, M.; Mirjalili, M.; Nasirizadeh, N. Platelet-rich fibrin-loaded PCL/chitosan core-shell fibers scaffold for enhanced osteogenic differentiation of mesenchymal stem cells. *Carbohydr. Polym.* **2021**, *269*, 118351, doi: 10.1016/j.carbpol.2021.118351.
18. Xu, F.; Zou, D.; Dai, T.; Xu, H.; An, R.; Liu, Y.; Liu, B. Effects of incorporation of granule-lyophilised platelet-rich fibrin into polyvinyl alcohol hydrogel on wound healing. *Sci. Rep.* **2018**, *8*, 14042, doi: 10.1038/s41598-018-32208-5.
19. Al-Maawi, S.; Herrera-Vizcaino, C.; Orlowska, A.; Willershausen, I.; Sader, R.; Miron, R.J.; Choukroun, J.; Ghanaati, S. Biologization of Collagen-Based Biomaterials Using Liquid-Platelet-Rich Fibrin: New Insights into Clinically Applicable Tissue Engineering. *Materials (Basel)*. **2019**, *12*, 3993, doi: 10.3390/ma12233993.
20. Lu, H.-T.; Lu, T.-W.; Chen, C.-H.; Lu, K.-Y.; Mi, F.-L. Development of nanocomposite scaffolds based on biomineralization of N,O-carboxymethyl chitosan/fucoidan conjugates for bone tissue engineering. *Int. J. Biol. Macromol.* **2018**, *120*, 2335–2345, doi: 10.1016/j.ijbiomac.2018.08.179.
21. V. K., A. D.; Udduttula, A.; Jaiswal, A. K. Unveiling the secrets of marine – derived fucoidan for bone tissue engineering – A review. *Front. Bioeng. Biotechnol.* **2023**, *10*, 1100164, doi: 10.3389/fbioe.2022.1100164.
22. Park, S.; Lee, K.W.; Lim, D.-S.; Lee, S. The Sulfated Polysaccharide Fucoidan Stimulates Osteogenic Differentiation of Human Adipose-Derived Stem Cells. *Stem Cells Dev.* **2012**, *21*, 2204–2211, doi: 10.1089/scd.2011.0521.
23. Purnama, A.; Aid-Launais, R.; Haddad, O.; Maire, M.; Mantovani, D.; Letourneur, D.; Hlawaty, H.; Le Visage, C. Fucoidan in a 3D scaffold interacts with vascular endothelial growth factor and promotes neovascularization in mice. *Drug Deliv. Transl. Res.* **2015**, *5*, 187–197, doi: 10.1007/s13346-013-0177-4.
24. Zeng, H.-Y.; Huang, Y.-C. Basic fibroblast growth factor released from fucoidan-modified chitosan/alginate scaffolds for promoting fibroblasts migration. *J. Polym. Res.* **2018**, *25*, 83, doi: 10.1007/s10965-018-1476-8.
25. Domalik-Pyzik, P.; Chłopek, J.; Pielichowska, K. Chitosan-Based Hydrogels: Preparation, Properties, and Applications. *Int. J. Biol. Macromol.*; 2019; pp. 1665–1693.
26. Ahmadi, F.; Oveisi, Z.; Samani, S.M.; Amoozgar, Z. Chitosan based hydrogels:

- characteristics and pharmaceutical applications. *Res. Pharm. Sci.* **2015**, *10*, 1–16.
27. Levengood, S.K.L.; Zhang, M. Chitosan-based scaffolds for bone tissue engineering. *J. Mater. Chem. B* **2014**, *2*, 3161, doi: 10.1039/c4tb00027g.
 28. Venkatesan, J.; Singh, S.; Anil, S.; Kim, S.-K.; Shim, M. Preparation, Characterization and Biological Applications of Biosynthesized Silver Nanoparticles with Chitosan-Fucoidan Coating. *Molecules* **2018**, *23*, 1429, doi: 10.3390/molecules23061429.
 29. Chitosan-based polyelectrolyte complexes as pharmaceutical excipients. In *Controlled Drug Delivery*; M.A. Mateescu, P.I.-S. and E.A., Ed.; Elsevier, 2015; pp. 127–161.
 30. Theodoridis, T.; Kraemer, J. *Guyton and Hall Textbook of Medical Physiology*; 2020; ISBN 9783131450715.
 31. Wend, S.; Kubesch, A.; Orłowska, A.; Al-Maawi, S.; Zender, N.; Dias, A.; Miron, R.J.; Sader, R.; Booms, P.; Kirkpatrick, C.J.; et al. Reduction of the relative centrifugal force influences cell number and growth factor release within injectable PRF-based matrices. *J. Mater. Sci. Mater. Med.* **2017**, *28*, 188, doi: 10.1007/s10856-017-5992-6.
 32. No Title Available online: <https://medical-dictionary.thefreedictionary.com/antimicrobial>.
 33. Leong, D.K.C.; Benedict, B.C.T.; Chew, K.T.L. Autologous Growth Factors: A Biological Treatment in Sports Medicine. *Proc. Singapore Healthc.* **2010**, *19*, 229–236, doi: 10.1177/201010581001900309.
 34. Polak, D.; Clemer-Shamai, N.; Shapira, L. Incorporating antibiotics into platelet-rich fibrin: A novel antibiotics slow-release biological device. *J. Clin. Periodontol.* **2019**, *46*, 241–247, doi: 10.1111/jcpe.13063.
 35. Knafl, D.; Thalhammer, F.; Vossen, M. G. In-vitro release pharmacokinetics of amikacin, teicoplanin and polyhexanide in a platelet rich fibrin – layer (PRF) – a laboratory evaluation of a modern, autologous wound treatment. *PLoS One* **2017**, *12*, e0181090, doi: 10.1371/journal.pone.0181090.
 36. Maestre-Vera, J.R. Treatment options in odontogenic infection. *Med. Oral Patol. Oral Cir. Bucal* **2004**, *9 Suppl*, 25–31; 19–24.
 37. Jang, E.-S.; Park, J.-W.; Kweon, H.; Lee, K.-G.; Kang, S.-W.; Baek, D.-H.; Choi, J.-Y.; Kim, S.-G. Restoration of peri-implant defects in immediate implant installations by Choukroun platelet-rich fibrin and silk fibroin powder combination graft. *Oral Surgery, Oral Med. Oral Pathol. Oral Radiol. Endodontology* **2010**, *109*, 831–836, doi: 10.1016/j.tripleo.2009.10.038.
 38. Schmidt, T. *Encyclopedia of Microbiology 4th ed.*; Faculty Bookshelf. 260, 2019; ISBN 9780128117378.
 39. Martinez-Aguilar, G.; Hammerman, W. A.; Mason, E. O.; Kaplan, S. L. Clindamycin treatment of invasive infections caused by community-acquired, methicillin-resistant and methicillin-susceptible *Staphylococcus aureus* in children. *Pediatr. Infect. Dis. J.* **2003**, *22*, 593–599, doi: 10.1097/01.inf.0000073163.37519.ee.
 40. Mohamed, M. A.; Nasr, M.; Elkhatib, W. F.; Eltayeb, W. N.; Elshamy, A. A.; El-Sayyad, G. S. Nanobiotic formulations as promising advances for combating MRSA resistance: susceptibilities and post-antibiotic effects of clindamycin, doxycycline, and linezolid. *RSC Adv.* **2021**, *11*, 39696–39706, doi: 10.1039/D1RA08639A.

41. Fortunato, L.; Bennardo, F.; Buffone, C.; Giudice, A. Is the application of platelet concentrates effective in the prevention and treatment of medication-related osteonecrosis of the jaw? A systematic review. *J. Cranio-Maxillofacial Surg.* **2020**, *48*, 268–285, doi: 10.1016/j.jcms.2020.01.014.
42. Li, H.; Deng, J.; Yue, Z.; Zhang, Y.; Sun, H.; Ren, X. Clindamycin hydrochloride and clindamycin phosphate: two drugs or one? A retrospective analysis of a spontaneous reporting system. *Eur. J. Clin. Pharmacol.* **2017**, *73*, 251–253, doi: 10.1007/s00228-016-2161-7.
43. Borin, M. T.; Powley, G. W.; Tackwell, K. R.; Batts, D. H. Absorption of clindamycin after intravaginal application of clindamycin phosphate 2 % cream. *J. Antimicrob. Chemother.* **1995**, *35*, 833–841, doi: 10.1093/jac/35.6.833.
44. Schilcher, K.; Andreoni, F.; Uchiyama, S.; Ogawa, T.; Schuepbach, R. A.; Zinkernagel, A.S. Increased Neutrophil Extracellular Trap–Mediated Staphylococcus aureus Clearance Through Inhibition of Nuclease Activity by Clindamycin and Immunoglobulin. *J. Infect. Dis.* **2014**, *210*, 473–482, doi: 10.1093/infdis/jiu091.
45. Schilcher, K.; Andreoni, F.; Dengler Haunreiter, V.; Seidl, K.; Hasse, B.; Zinkernagel, A. S. Modulation of Staphylococcus aureus Biofilm Matrix by Subinhibitory Concentrations of Clindamycin. *Antimicrob. Agents Chemother.* **2016**, *60*, 5957–5967, doi: 10.1128/AAC.00463-16.
46. Kuriyama, T.; Karasawa, T.; Nakagawa, K.; Saiki, Y.; Yamamoto, E.; Nakamura, S. Bacteriologic features and antimicrobial susceptibility in isolates from orofacial odontogenic infections. *Oral Surgery, Oral Med. Oral Pathol. Oral Radiol. Endodontology* **2000**, *90*, 600–608, doi: 10.1067/moe.2000.109639.
47. Safari, J.; Zarnegar, Z. Advanced drug delivery systems: Nanotechnology of health design A review. *J. Saudi Chem. Soc.* **2014**, *18*, 85–99, doi: 10.1016/j.jscs.2012.12.009.
48. Li, J.; Wang, X.; Zhang, T.; Wang, C.; Huang, Z.; Luo, X.; Deng, Y. A review on phospholipids and their main applications in drug delivery systems. *Asian J. Pharm. Sci.* **2015**, *10*, 81–98, doi: 10.1016/j.ajps.2014.09.004.
49. Hincha, D. K. Effects of calcium-induced aggregation on the physical stability of liposomes containing plant glycolipids. *Biochim. Biophys. Acta – Biomembr.* **2003**, *1611*, 180–186, doi: 10.1016/S0005-2736(03)00053-1.
50. Melcrová, A.; Pokorna, S.; Pullanchery, S.; Kohagen, M.; Jurkiewicz, P.; Hof, M.; Jungwirth, P.; Cremer, P.S.; Cwiklik, L. The complex nature of calcium cation interactions with phospholipid bilayers. *Sci. Rep.* **2016**, *6*, 1–12, doi: 10.1038/srep38035.
51. Egle, K.; Dohle, E.; Hoffmann, V.; Salma, I.; Al-Maawi, S.; Ghanaati, S.; Dubnika, A. Fucoidan/chitosan hydrogels as carrier for sustained delivery of platelet-rich fibrin containing bioactive molecules. *Int. J. Biol. Macromol.* **2024**, *262*, 129651, doi: 10.1016/j.ijbiomac.2024.129651.

DOCTORAL THESIS PROPOSED TO RIGA TECHNICAL UNIVERSITY FOR PROMOTION TO THE SCIENTIFIC DEGREE OF DOCTOR OF SCIENCE

To be granted the scientific degree of Doctor of Science (Ph. D.), the present Doctoral Thesis has been submitted for defense at the open meeting of RTU Promotion Council on 26 August 2024, at 10.00 at the Faculty of Natural Sciences and Technology of Riga Technical University, 3 Paula Valdena Street, Room 272.

OFFICIAL REVIEWERS

Professor Dr. sc. ing. Remo Merijs-Meri
Riga Technical University

Professor Dr. Med. Ilze Akota
Riga Stradiņš University, Latvia

Professor João F. Mano
University of Aveiro, Portugal

DECLARATION OF ACADEMIC INTEGRITY

I hereby declare that the Doctoral Thesis submitted for review to Riga Technical University for promotion to the scientific degree of Doctor of Science (Ph. D.) is my own. I confirm that this Doctoral Thesis has not been submitted to any other university for promotion to a scientific degree.

Karina Egle (signature)

Date:

The Doctoral Thesis has been prepared as a collection of thematically related scientific publications completed by summaries in Latvian and English. The Doctoral Thesis unites four scientific publications. The scientific publications have been written in English, with a total volume of 76 pages, including supplementary data.

CONTENTS

GENERAL OVERVIEW OF THE THESIS	35
Introduction	36
Aim and Objectives	39
Thesis to Defend.....	39
Scientific Novelty and Main Results.....	39
Practical Significance	40
Structure and volume of the Thesis.....	40
Publications and approbation of the Thesis.....	40
MAIN RESULTS OF THE THESIS	43
Pathway from Patient Blood Samples to Injectable PRF.....	43
The Potential of PRF to Stimulate CLP Antibacterial Susceptibility	45
Impact of Delivery System on Drug Release from PRF Matrix	49
Effect of Carrier Systems on the Release of Bioactive Molecules within PRF	53
CONCLUSIONS.....	59
REFERENCES.....	60
APPENDICES.....	64

Appendix I: Egle, K., Salma, I., Dubnika, A. From Blood to Regenerative Tissue: How Autologous Platelet-Rich Fibrin Can Be Combined with Other Materials to Ensure Controlled Drug and Growth Factor Release. *Int. J. Mol. Sci.*, **2021**, 22(21), 11553.

Appendix II: Egle, K., Skadins, I., Grava, A., Micko, L., Dubniks, V., Salma, I., Dubnika, A. Injectable Platelet-Rich Fibrin as a Drug Carrier Increases the Antibacterial Susceptibility of Antibiotic – Clindamycin Phosphate. *Int. J. Mol. Sci.*, **2022**, 23(13), 7407.

Appendix III Dubnika, A., Egle, K., Skrinda-Melne, M., Skadins, I., Rajadas, J., Salma. I. Development of Vancomycin Delivery Systems Based on Autologous 3D Platelet-Rich Fibrin Matrices for Bone Tissue Engineering. *Biomedicines*, **2021**, 9(7), 814.

Appendix IV: Egle, K., Dohle, E., Hoffmann, V., Salma, I., Al-Maawi, S., Ghanaati, S., Dubnika, A. Fucoidan/Chitosan Hydrogels as Carrier for Sustained Delivery of Platelet-Rich Fibrin Containing Bioactive Molecules. *Int. J. Biol. Macromol.*, **2024**, 262 (1), 129651.

GENERAL OVERVIEW OF THE THESIS

Introduction

It is still debated whether platelets can be considered as cell fragments or small non-nucleated blood cells [1], but they are known to be responsible for the activation and release of biomolecules. Platelet-rich fibrin (PRF) is an autologous material that is easily produced. It can be derived from human blood by centrifugation and is used to promote wound healing and tissue regeneration. PRF can be used in various fields of medicine, including dentistry and maxillofacial surgery [2].

The leukocytes in the PRF promote wound healing, and PRF contains growth factors that are released over time. There is a great interest in PRF antimicrobial activity, such as oral and maxillofacial surgery, plastic surgery, cardiac surgery, and dentistry [3]. The structural complexity, inhomogeneous nature, and clotting ability of PRF make its antimicrobial effect evaluation complicated. Nevertheless, most antimicrobial testing methods used are based on antibacterial agent diffusion ability in culture media. Since the most common use of PRF is in the oral and maxillofacial region, its antimicrobial activity evaluation also prevails in the oral microbiome. PRF prepared according to a specific protocol (depending on the surgical site) can ensure antibacterial and anti-inflammatory properties, and it can be a beneficial clinical tool in oral and maxillofacial surgery [4]. In the last decade, there have been few studies that combine antibiotics with PRF to provide an antibacterial effect. Based on the gathered literature regarding the antibacterial properties of PRF, it appears advantageous to integrate it with drugs to create a unified system rather than employing separate drugs and PRF individually [5].

Currently, there is a growing need for clindamycin in oral and maxillofacial surgery, where it is commonly used as a substitute for patients allergic to penicillin. Doctors claim that in addition to the bactericidal power of clindamycin, it has increased oral absorption, significant distribution in tissues (achieving a high concentration of the drug in bones), and a low level of resistance [6]. Prodrugs, inactive precursors that transform into active substances in the body, are frequently favored over the direct use of active substances in pharmaceuticals. This preference arises from their ability to enhance drug stability, solubility, and bioavailability, improving therapeutic outcomes. Clindamycin phosphate (CLP) is a prodrug of clindamycin with no antibacterial activity. CLP is reported to be rapidly hydrolyzed to the active base (clindamycin) in the blood [2]. In this PhD Thesis, the ability to convert CLP into an active form by combining it with PRF is investigated. Additionally, to explore broader possibilities of using active substances in PRF, Vancomycin hydrochloride (VANKA) was also studied. VANKA is a water-soluble tricyclic glycopeptide antibiotic [7] that prevents/destroys several gram-positive microorganisms, which are the most common pathogens. VANKA, like clindamycin, is applied in cases when penicillin is ineffective or causes allergic reactions, as well as for treating infections where other antibiotics are resistant [8,9].

The drug's essential pharmacological characteristics can be enhanced by employing a suitable drug delivery system that allows their administration as a free molecule [10]. A drug delivery system is a technique or technological approach used to systematically and precisely

deliver therapeutic substances (such as drugs or medications) to the human body. This process entails creating and implementing systems that improve the effectiveness and safety of drug treatments. The primary objective of these systems is to finely tune the delivery of drugs to particular tissues or cells, with a concurrent effort to minimize any potential side effects [11,12]. For example, VANKA can be encapsulated into liposomes, unique medication carriers, because they overcome the disadvantages of the peroral or intravenously administered drugs. As an alternative, polymeric microparticles from poly lactic-co-glycolic acid (PLGA) have been studied to encapsulate VANKA. Both liposomes and PLGA microcapsules have drawbacks regarding encapsulation efficiency, but encapsulation of VANKA in carrier provides high clinical benefits for the long-term use of antibiotics. Therefore, adjusting VANKA carrier composition and the drug release rate in autologous samples is essential. Current studies on drug carriers within the autologous PRF samples are limited [13].

In addition to the PRF combination with drug delivery systems that provide controlled drug delivery, PRF incorporates growth factors and cytokines that can be released directly at the administration site. Several authors described the effect of different centrifugation protocols on growth factor and cytokine release and confirmed the substantial impact of the protocols. It has been demonstrated that variations in growth factors and cytokine release patterns exist not only among different platelet concentrates but also within each type of PRF [14]. Platelet concentrate mainly contains platelets, but PRF is additionally mixed with fibrin-forming proteins that promote tissue healing. Related research in existing literature explores the combination of PRP or PRF with chitosan/fucoidan complex or gelatin/chitosan hydrogel [15,16]. In these studies, both types of platelet concentrates are blended within a chitosan solution, and the quantity of proteins released is assessed for the resulting materials. Implementing the methodologies described in these publications would complicate medical procedures, involving multiple stages. Prior studies have explored the impact of PRF both independently and when integrated into polymer matrices, focusing on bone formation and regeneration [17]. Xu et al. incorporated granule-lyophilized platelet-rich fibrin (G-L-PRF) into polyvinyl alcohol (PVA) hydrogels, achieving sustained release of growth factors from G-L-PRF/PVA scaffolds for up to 9 days [18]. One *ex vivo* study analyzed the ability of the i-PRF matrix to be an autologous growth factor delivery system in combination with 5 collagen-based membranes. Thus, this was the first study that attempted to understand the ability and suitability of biomaterials to incorporate PRF [19].

Several fucoidan (FU) based composites have recently been established for bone tissue engineering purposes because FU increased the proliferation capacity of osteoblast-like cells and enhanced osteoblast-mediated mineral deposition [20]. FU's similarity to the human extracellular matrix and impressive qualities, like high biocompatibility and renewability, have recently intrigued researchers. It shows promise in developing regenerative medicine materials, particularly for wound treatment [21]. FU, a heparin-like molecule, enhances growth factor effects on cell proliferation, osteogenic differentiation, and mesenchymal stem cell activity [22]. Several studies [23,24] have reported that FU can interact with growth factors (such as bFGF and TGF- β) to control their release and activity by binding and regulating signaling pathways. These are highly important in autologous PRF samples to support the release of growth factors from the matrices.

In general, the structure and properties of chitosan are similar to glycosaminoglycan (GAG), a natural polysaccharide and the main component of the extracellular matrix (ECM) [25]. Chitosan, a natural cationic copolymer, has generated significant interest for its potential in hydrogel formations. This polymer's hydrophilic nature allows it to degrade using human enzymes, ensuring biocompatibility and biodegradability, two crucial properties for medical devices. Chitosan-based hydrogels could serve as scaffolds for tissue repair success [26]. Chitosan accelerates wound healing by activating and modulating inflammatory cells and promoting granulation tissue formation. Its ability to bind negatively charged red blood cells enhances clotting, making it a crucial component in wound dressings [27].

So far, a method for the controlled release of growth factors from PRF in combination with other biomaterials has not yet been investigated, providing the possibility for longer-lasting therapy. In this study, we developed a hydrogel composed of fucoidan (FU) and chitosan (CS) due to their biocompatibility and ability to form polyelectrolyte complexes via self-assembly [28]. The formation of polyelectrolyte complexes between oppositely charged groups of chitosan and fucoidan makes the incorporation of factors possible due to electrostatic interactions [29]. Thus, fucoidan/chitosan hydrogels were used in the Thesis, investigating their potential for further use as PRF storage material.

In this PhD Thesis, the following goals were set: 1) investigating the potential of PRF's role in converting prodrug to the active form, using clindamycin phosphate as a model drug; 2) assessing PRF's ability to decelerate the burst release of the active substance by incorporating it in PLGA microcapsules and liposomes, using VANKA as a model drug and 3) investigate the controlled release of bioactive molecules within PRF by incorporating them into carrier systems, using marine polysaccharide (fucoidan and chitosan) hydrogel as a model carrier systems.

Aim and Objectives

The aim of this Thesis was to develop PRF-based matrices that can provide antibacterial properties through the addition of drugs or their delivery systems, as well as ensure controlled delivery of bioactive molecules within PRF by evaluating different carriers. To achieve the goal, the following tasks were set:

1. To investigate the potential of PRF as an imitator for the conversion of the clindamycin phosphate (CLP) into the active drug form clindamycin, ensuring more effective antimicrobial properties.
2. To evaluate the influence of drug delivery carriers (PLGA microcapsules or liposomes) and their interaction with PRF matrices on the release kinetic of antibiotic drug VANKA.
3. To develop a methodology for obtaining fucoidan/chitosan hydrogel, combining it with PRF to ensure delayed release of bioactive molecules within PRF.

Theses to Defend

1. CLP incorporation in PRF as a carrier matrix upregulates its antibacterial properties as transformation to its active form – clindamycin is ensured.
2. The release of antibiotic drug VANKA can be modeled from six to ten days, depending on the carriers (PLGA microcapsules or liposomes) used in the PRF matrices.
3. Sustained release (from 6 h to 7 days) of bioactive molecules from PRF can be achieved by combining PRF with fucoidan/chitosan hydrogel, based on the ability of fucoidan to regulate the release and activity of bioactive molecules.

Scientific Novelty and Main Results

The scientific novelty of the Thesis lies in the dual perspective of PRF application: first, the development of an innovative hydrogel capable to modulating the release of bioactive molecules within PRF, and secondly, the development of a new drug delivery system involving controlled antibiotic or particle delivery, where the particles are incorporated into PRF and act as carriers of biologically active molecules.

A new method has been developed to encapsulate bioactive molecules within PRF in marine polysaccharide (fucoidan/chitosan) hydrogels, thereby achieving their sustained release. Environmentally friendly materials, chitosan and fucoidan, are used in this method, forming hydrogels through polyelectrolyte self-assembly. Unlike traditional drug delivery system preparation methods, this hydrogel production method does not rely on chemical crosslinkers.

Additionally, a new methodology for utilizing PRF as a carrier of biologically active molecules to enhance the antibacterial properties of drugs has been developed. PRF as a carrier extends the applications of prodrugs (e.g., clindamycin phosphate), which have fewer side effects than the active form. The obtained drug/PRF combination demonstrates the need for lower prodrug concentrations compared to the required prodrug amount without PRF. In the

future, this methodology will be further developed to enhance the antibacterial properties of drugs more broadly.

Practical Significance

PRF properties and its combinations with various drug delivery systems and matrices were investigated, and the application of its use was found in the development of the following combinations:

- 1) Clindamycin phosphate with PRF as a carrier matrix for maxillofacial surgery, thus obtaining an active drug form that would provide an antibacterial effect in the postoperative period.
- 2) Combining PRF with various carriers (PLGA microcapsules or liposomes) of biologically active substances (such as VANKA), reducing the need for oral drug administration and adjusting the duration of biologically active substance therapy.
- 3) A new and environmentally friendly method of obtaining fucoidan/chitosan hydrogels combined with PRF, thus ensuring the long-term release of bioactive molecules within PRF.

Structure and Volume of the Thesis

This Doctoral Thesis was prepared as a collection of thematically related scientific publications dedicated to the development of autologous fibrin matrices for medical applications. The Thesis unites three original publications in SCI journals and one review article.

Publications and Approbation of the Thesis

The Thesis results are reported in three original experimental publications. One review article has been published. The main results were presented at 14 conferences.

Scientific publications

1. **Egle, K.**, Dohle, E., Hoffmann, V., Salma, I., Al-Maawi, S., Ghanaati, S., Dubnika, A. Fucoidan/Chitosan Hydrogels as Carrier for Sustained Delivery of Platelet-Rich Fibrin Containing Bioactive Molecules. *Int. J. Biol. Macromol.*, **2024**, 262 (1), 129651. doi: 10.1016/j.ijbiomac.2024.129651.
2. **Egle, K.**, Skadins, I., Grava, A., Micko, L., Dubniks, V., Salma, I., Dubnika, A. Injectable Platelet-Rich Fibrin as a Drug Carrier Increases the Antibacterial Susceptibility of Antibiotic – Clindamycin Phosphate. *International Journal of Molecular Sciences*, **2022**, 23(13), 7407. doi: 10.3390/ijms23137407 (Scopus, Open Access).
3. Dubnika, A., **Egle, K.**, Skrinda-Melne, M., Skadins, I., Rajadas, J., Salma, I. Development of Vancomycin Delivery Systems Based on Autologous 3D Platelet-Rich

- Fibrin Matrices for Bone Tissue Engineering. *Biomedicines*, **2021**, 9(7), 814. doi: 10.3390/biomedicines9070814 (Scopus, Open Access).
4. **Egle, K.**, Salma, I., Dubnika, A. From Blood to Regenerative Tissue: How Autologous Platelet-Rich Fibrin Can Be Combined with Other Materials to Ensure Controlled Drug and Growth Factor Release. *International Journal of Molecular Sciences*, **2021**, 22(21), 11553. doi: 10.3390/ijms222111553 (Scopus, Open Access).

The results of the Thesis were presented at the following conferences

1. **Egle, K.**, Dohle, E., Hoffmann, V., Salma, I., Al-Maawi, S., Ghanaati, S., Dubnika, A. Exploring Platelet-Rich Fibrin Microstructure and Histology: with and without Hydrogel Carriers. *64th International Scientific Conference of RTU: Materials Science and Applied Chemistry*, Riga, Latvia, October 6, **2023** (oral presentation).
2. **Egle, K.**, Dohle, E., Hoffmann, V., Salma, I., Al-Maawi, S., Ghanaati, S., Dubnika, A. Fucoidan/Chitosan Hydrogels for Sustained Delivery of Platelet-Rich Fibrin Containing Growth Factors. *33rd Annual Conference of the European Society for Biomaterials*, Davos, Switzerland, 4–8 September **2023** (poster).
3. Dubnika, A., **Egle, K.**, Skadins, I., Skrinda-Melne, M., Micko, L., Grava, A., Dubniks, V., Salma, I. Development of Drug Delivery Systems Based On Autologous 3D Platelet-rich Fibrin Matrices, *TERMIS-AM 2023 Annual Conference*, Boston, MA, 11–14 April **2023** (poster).
4. Micko, L., Salma, I., Skadins, I., Salms, G., Dubnika, A., **Egle, K.** Platelet-rich fibrin immunological testing methodology using Elisa assay, *RSU International Research Conference on Medical and Health Care Sciences: Knowledge for Use in Practice*, Riga, Latvia, 29–31 March **2023** (oral presentation).
5. Micko, L., Skadins, I., Salma, I., Dubnika, A., **Egle, K.**, Salms G. Platelet-rich fibrin antibacterial activity against *Klebsiella pneumoniae*, *RSU International Research Conference on Medical and Health Care Sciences: Knowledge for Use in Practice*, Riga, Latvia, 29–31 March **2023** (oral presentation).
6. **Egle, K.**, Skadins, I., Grava, A., Micko, L., Dubniks, V., Salma, I., Dubnika, A. Injectable platelet-rich fibrin as a drug carrier increases the antibacterial susceptibility of antibiotic-clindamycin phosphate. *16th Annual Meeting for Scandinavian Society for Biomaterials*, Roros, Norway, 21–24 March **2023** (poster).
7. Micko, L., **Egle, K.**, Grava, A., Skadins, I., Salma, I., Salms, G., Dubnika, A. Antimicrobial activity of platelet-rich fibrin. *26th Congress of the European Association for Cranio-Maxillo-Facial Surgery*, Madrid, Spain, 27–30 September **2022** (poster).
8. **Egle, K.**, Dohle, E., Hoffmann, V., Salma, I., Al-Maawi, S., Ghanaati, S., Dubnika, A. Fucoidan/chitosan hydrogels as matrices for sustained delivery of platelet-rich fibrin containing bioactive molecules. *32nd Annual Conference of the European Society for Biomaterials*, Bordeaux, France, 4–8 September **2022** (poster).
9. Salma, I., Micko, L., **Egle, K.**, Dubnika, A. Development of protocol for obtaining autologous liquid PRF for local drug delivery systems. *32nd Annual Conference of the European Society for Biomaterials*, Bordeaux, France, 4–8 September **2022** (poster).

10. **Egle, K.**, Micko, L., Grava, A., Salma, I., Skadins, I., Dubnika, A. Study on the effect of fibrin matrice on the antibacterial activity of clindamycin phosphate. *Scandinavian Society for Biomaterials 2022. 15th Annual Meeting*, Jurmala, Latvia, 13–15 June **2022** (poster).
11. **Egle, K.**, Salma, I., Dubnika, A. From blood to regenerative tissue: how autologous platelet-rich fibrin can be used as drug carrier system. *62nd International Scientific Conference of RTU: Materials Science and Applied Chemistry*, Riga, Latvia, October 22, **2021** (poster).
12. **Egle, K.** Dubnika, A. Development of fibrin matrices for sustained drug delivery. *31st Conference of the European Society for Biomaterials*, Porto, Portugal, 5–9 September **2021** (poster).
13. **Egle, K.**, Salma, I., Skadins, I., Dubnika, A. Study of autologous fibrin matrices for controlled drug delivery. *Scandinavian Society for Biomaterials*, Jurmala, Latvia, 14 June **2021** (poster).
14. Skadins, I., Micko, L., Salma, I., Dubnika, A., **Egle K.** Antibacterial properties of platelet-rich fibrin matrices saturated with vancomycin. *Scandinavian Society for Biomaterials*, Jurmala, Latvia, June 14, **2021** (poster).
15. Dubnika, A., **Egle, K.**, Skadins, I., Salma, I. Commercial vs autologous fibrin-handling from the material point of view. *RSU International Research Conference on Medical and Health Care Sciences: Knowledge for Use in Practice*, Riga, Latvia, 24–26 March **2021** (oral presentation online).
16. Skadins, I., Dubnika, A., **Egle, K.**, Dovbenko, A., Salma, I., Micko, L. Antibacterial effect of autologous matrices. *RSU International Research Conference on Medical and Health Care Sciences: Knowledge for Use in Practice*, Riga, Latvia, 24–26 March **2021** (poster).
17. **Egle, K.**, Dubnika, A. Development of fibrin matrices for controlled drug delivery. *61st International Scientific Conference of RTU: Materials Science and Applied Chemistry*, Riga, Latvia, October 23, **2020** (poster).
18. **Egle, K.** Development of autologous fibrin matrices for controlled drug delivery. *61st Riga Technical University Student Scientific and Technical Conference*, Riga, Latvia, May 22, **2020** (oral presentation).

Other scientific publications published during the research for Ph.D Thesis

1. Micko, L., Salma, I., Skadins, I., **Egle, K.**, Salms, G., Dubnika, A. Can Our Blood Help Ensure Antimicrobial and Anti-Inflammatory Properties in Oral and Maxillofacial Surgery? *International Journal of Molecular Sciences*, **2023**, 24(2), 1073.doi: 10.3390/ijms24021073 (Scopus, Open Access).
2. Grava, A., **Egle, K.**, Dubnika, A. Enzymatically Crosslinked in situ Synthesized Silk/Gelatin/Calcium Phosphate Hydrogels for Drug Delivery. *Materials*, **2021**, 14(23), 7191. doi: 10.3390/ma14237191 (Scopus, Open Access).

MAIN RESULTS OF THE THESIS

Pathway from Patient Blood Samples to Injectable PRF

Blood is a mixture of plasma, platelets, and red and white blood cells that flow throughout the body. Blood is drawn from the patient, and by subjecting it to centrifugal force, the different components, including platelets and fibrin, naturally separate based on their densities [30]. PRF is derived from blood through a simple centrifugation process. It is widely used to accelerate soft and hard tissue regeneration. This was first described by Choukroun and his group in 2001 in France. PRF is a modification of platelet-rich plasma (PRP) and, at the same time, an autologous fibrin matrix used to improve bone regeneration and clinically used for soft tissue augmentation. Compared to other platelet concentrates, PRF is a platelet-rich fibrin clot that does not require the use of thrombin (procoagulant is used to accelerate gelation) but only centrifuged blood without any impurities. It is a new biomaterial that resembles an autologous cicatricial matrix but, at the same time, is neither a fibrin glue nor a classic platelet concentrate. In addition, PRF contains a high concentration of host immune cells, which are needed to heal wounds and reduce infections [5].

Different PRF derivatives are used today depending on the application and the desired properties. As mentioned by Wend et al., in addition to solid PRF (A-PRF), there is a clinical need to develop injectable PRF (i-PRF) matrices for various clinical procedures and to improve angiogenic potential through the ability to combine i-PRF with various biomaterials [5,31]. Figure 1 shows the advantages of i-PRF and A-PRF.

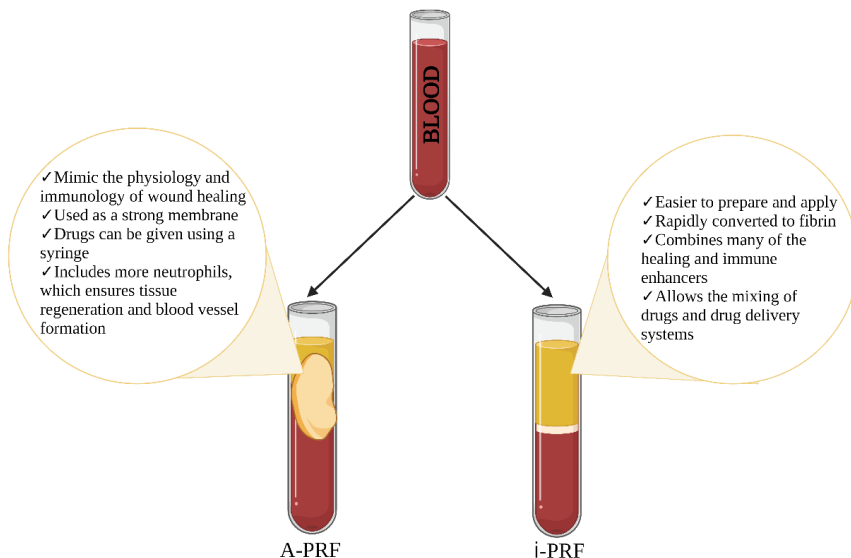


Fig. 1. Comparison of the advantages of two autologous platelet-rich concentrates i-PRF and A-PRF. Figure created with Biorender.com [5].

i-PRF is liquid injectable PRF and allows the incorporation of drugs and drug delivery systems prior to coagulation. i-PRF is a recently introduced platelet concentrate that can be easily combined with various biomaterials to improve the properties of the biomaterial. i-PRF contains not only autologous growth factors found in the blood, but also cells involved in the wound healing process (Fig. 2). Panel B shows that not all elements in the blood enter the PRF layer after centrifugation.

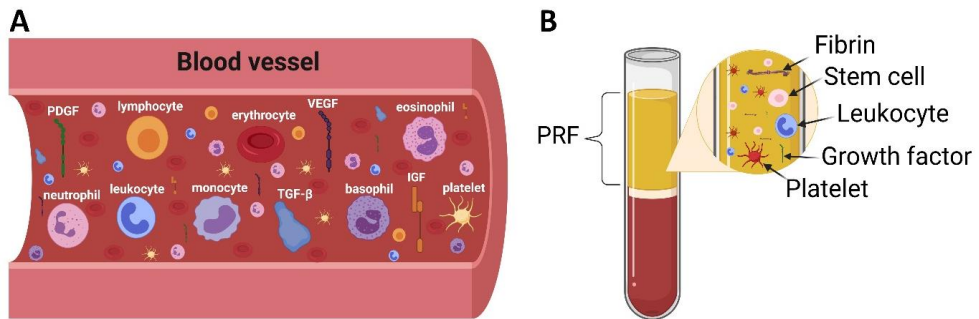


Fig. 2. Main elements of blood (A) and PRF (B). Figure created with Biorender.com [5].

PRF itself may demonstrate antibacterial activity, but it has not been relatively well studied, and there is insufficient data on what affects it. Antimicrobial activity can be defined as the destruction or inhibition of the growth of microorganisms (bacteria, fungi, and viruses) [32]. In the human body, wound healing is compromised by possible infection, especially in wounds in the oral region. Thus, the success of the use of PRF may be connected with its antimicrobial properties. Fully autologous second-generation PRF with no additives as prepared using one centrifugation may most directly reflect the antimicrobial potential of blood-derived material. Another critical and fundamental property of PRF is its ability to release various growth factors and cytokines at supraphysiologic concentrations, rendering it a significant agent in medical applications, particularly in tissue regeneration [4]. Growth factors are a heterogeneous group of proteins secreted by leukocytes and platelets with a short biological half-life rapidly eliminated from the bloodstream; they act mainly locally. Platelets are involved in hemostasis and store growth factors in alpha granules, which are activated to release these factors at the injury site [33].

Studies in the literature have shown that PRF is frequently used in combination with medications like metronidazole, clindamycin, penicillin [34], VANKA, teicoplanin, gentamicin, or amikacin to eradicate bacteria and expedite the healing process [35]. In contemporary oral and maxillofacial surgery, there is a growing requirement for clindamycin as a pharmaceutical agent. Clindamycin and VANKA are commonly considered an alternative for patients who exhibit allergic reactions to penicillin [36]. In the last decade, few studies have combined antibiotics with PRF to provide an antibacterial effect. Based on the gathered literature regarding PRF's antibacterial characteristics, an optimal approach would involve

amalgamating PRF with drugs to create a unified system rather than employing distinct drugs and PRF independently [4]. It should also be mentioned that the PRF can serve not only as a drug delivery system but also as a matrix of other materials. Scientists have tried to combine silk fibroin powder from *Bombyx mori* with Choukroun PRF, which showed the ability to prevent peri-implant defects [37]. While searching for articles on the treatment of periodontitis, it was found that PRF, in combination with other materials, can also be used to treat intrabony defects. Summarizing all available studies, it is observed that when using PRF as matrices or including it in another carrier system, there is no need to add growth factors, as PRF itself includes certain growth factors. The only thing to consider is the encapsulation of the desired drug and its interaction with other carriers that will be included in the PRF. It is also important to investigate whether the used carrier system will be able to ensure the controlled release of the growth factors in the PRF [5].

This PhD Thesis highlights the multifaceted potential of platelet-rich fibrin (PRF) in biomedical applications. The subsequent chapters will delve into specific aspects, including 1) the capacity of PRF to enhance the antibacterial sensitivity of clindamycin phosphate, 2) the influence of delivery systems on drug release from the PRF matrix, and 3) the impact of carrier systems on the release of bioactive molecules within PRF. These chapters aim to provide a comprehensive understanding of how PRF can be harnessed and optimized for targeted and effective medical interventions.

The Potential of PRF to Stimulate CLP Antibacterial Susceptibility

Infections are one of the most common postoperative risks caused by pathogenic and opportunistic bacteria. *S. aureus* and *S. epidermidis* are gram-positive opportunistic bacteria, present in the normal human microbiome [2]. Opportunistic bacteria are usually harmless when residing in the human or animal body, but can cause illness or infection when conditions allow, such as a weakened immune system [38].

For the treatment of community-acquired, methicillin-resistant, and methicillin-susceptible *S. aureus* infections, clindamycin has been recommended for many years, and it can also reduce the susceptibility of methicillin-resistant *S. aureus* clinical isolates [39,40]. Currently, there is a growing need for clindamycin in oral and maxillofacial surgery, particularly for preventing and treating jaw osteonecrosis [41]. It is widely considered an alternative for patients with an allergic reaction to penicillin [36]. Clindamycin phosphate (CLP) is a prodrug of clindamycin that has no antibacterial activity [42]. It is reported that CLP is rapidly hydrolyzed to the active base (clindamycin) in the blood [43]. The aim was to investigate the change in CLP antibacterial properties against reference culture and clinical isolates of *S. aureus* and *S. epidermidis* using PRF as a carrier matrix. Determination of minimal inhibitory concentration (MIC) and minimal bactericidal concentration (MBC) is one of the main ways to assess this. See the PRF_CLP sample preparation scheme in Fig. 3.

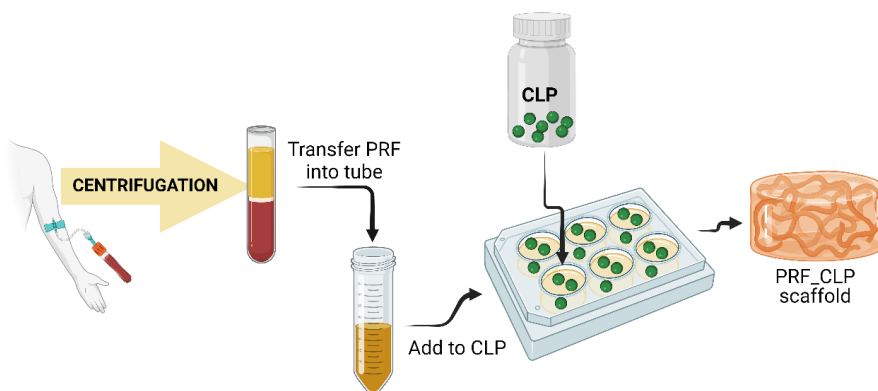


Fig. 3. CLP sample preparation scheme. Figure created with Biorender.com.

Fourier transform infrared spectrometry (FTIR) was used to examine the structural changes after combining clindamycin phosphate (CLP) with PRF (Fig. 4). Antibacterial tests were used to verify whether the combination of CLP with PRF shows an antibacterial effect and confirms the theory that in the presence of PRF, a lower concentration of CLP is required to kill and prevent bacterial growth (Fig. 5).

FTIR spectra show the interaction of CLP with PRF during the seven-day incubation period. Partial hydrolysis and conversion of CLP to clindamycin were observed. After seven days of incubation, a new bond formation ($C-C$ at 1080 cm^{-1}) and a maximal increase in phosphate group absorbance over time were observed, indicating structural changes, possibly suggesting the conversion of CLP into the active drug – clindamycin.

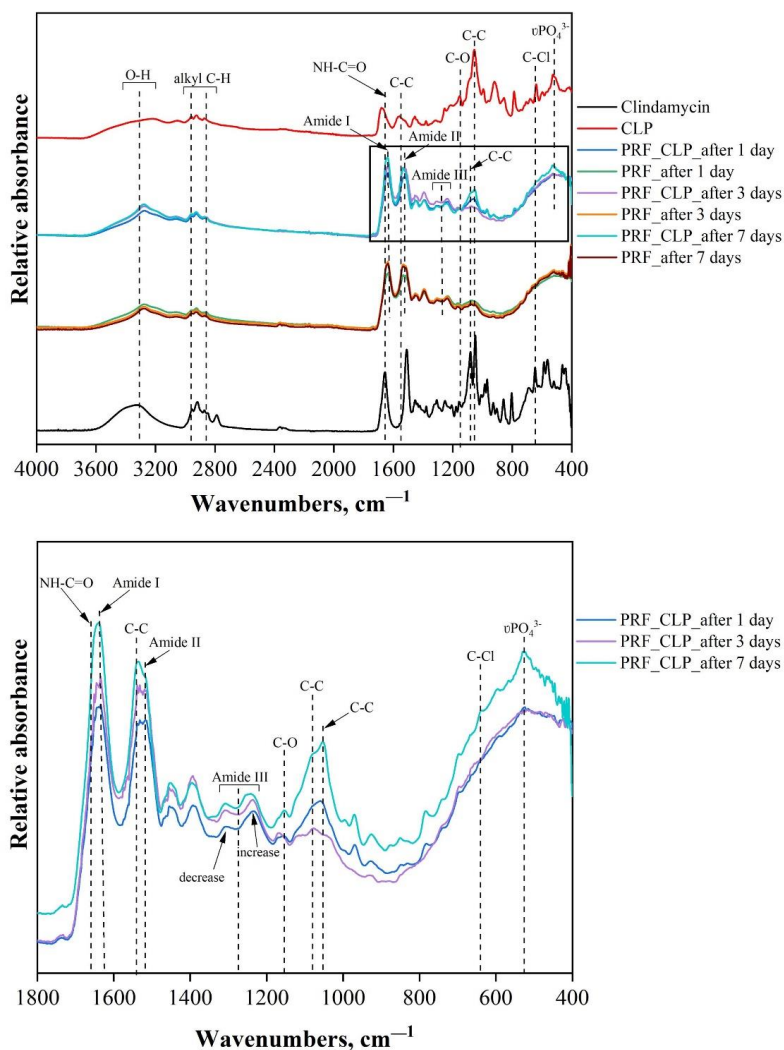


Fig. 4. FTIR spectra: **A** – PRF, PRF_CLP samples, CLP and clindamycin samples in the full spectral range; **B** – PRF_CLP samples at incubation time points in the range of 1800–400 cm^{-1} [2].

The composition of the blood from each donor affects the antibacterial properties of the sample, specifically, the amount of CLP required to achieve the antibacterial activity.

Comparing the MIC and MBC values of the PRF_CLP samples with pure CLP samples for all bacteria strains, a decrease in these values is observed by adding PRF to the CLP. Antibacterial tests showed that the addition of PRF enhances the antibacterial activity of CLP not only against staphylococcal reference cultures but also against clinical isolates. It can be seen that against the clinical isolates of *S. aureus* and *S. epidermidis*, higher CLP concentrations are required in PRF_CLP samples to provide a lower MBC value compared to both bacteria

reference cultures. Each donor has different blood properties (such as different white blood cell counts or vitamin D levels) that drastically affect the antibacterial effect. Studies by Schilcher et al. [44,45] and Kuriyama et al. [46] showed that the MIC of pure clindamycin in clinical isolates against methicillin-resistant *S. aureus* (MRSA) can reach > 256 mg/L. Summarizing all the data, it can be seen that CLP with PRF is a better antibacterial material than pure CLP; and compared to the literature, we have obtained lower MIC values (ranging from 62.5 µg/mL to 145.8 µg/mL depending on the bacterial strain) than required for clindamycin (> 256 µg/mL). Depending on the bacterial strain, the concentration of the drug has to be adjusted (Fig. 5).

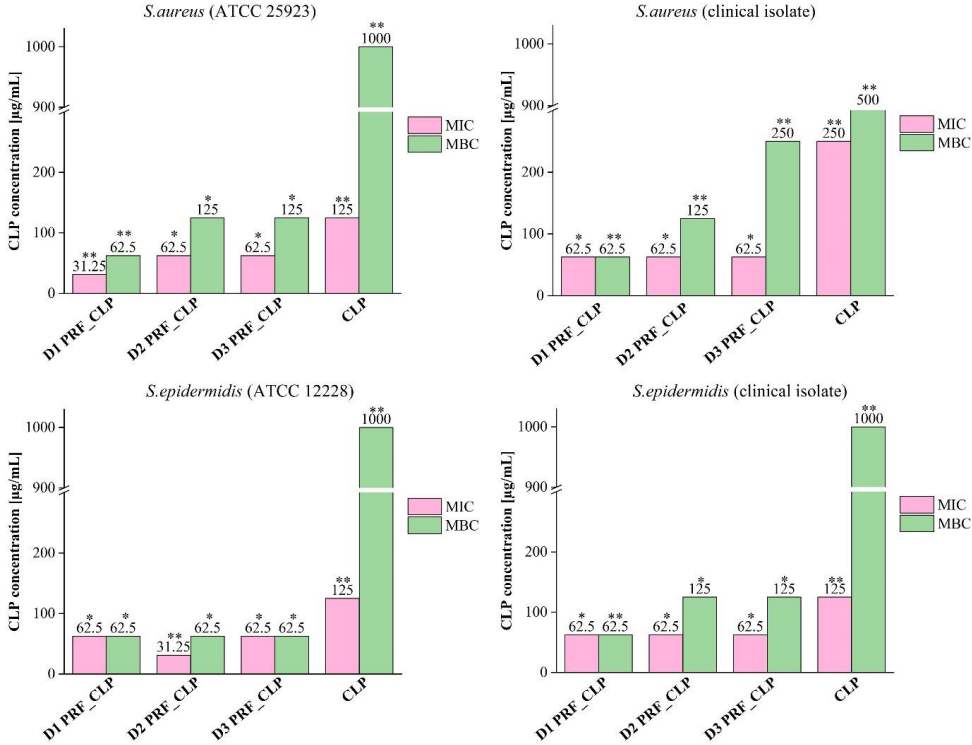


Fig. 5. MIC and MBC value differences between CLP and PRF_CLP samples against four bacteria stains (*S. aureus* (ATCC 25923), *S. epidermidis* (ATCC 12228), *S. aureus* (clinical isolate), *S. epidermidis* (clinical isolate) for all three donors. Samples were prepared from Donor 1 blood (D1 PRF_CLP); samples were prepared from Donor 2 (D2 PRF_CLP); samples were prepared from Donor 3 (D3 PRF_CLP). * $p > 0.05$; ** $p < 0.05$ [2].

The ability of PRF to degrade naturally is considered an advantage for its use as a “warehouse” of controlled drug release systems. The release data indicated that the PRF_CLP sample can be used for a one-day local therapy, ensuring maximum CLP release (80 %) within 1 h (Fig. 6).

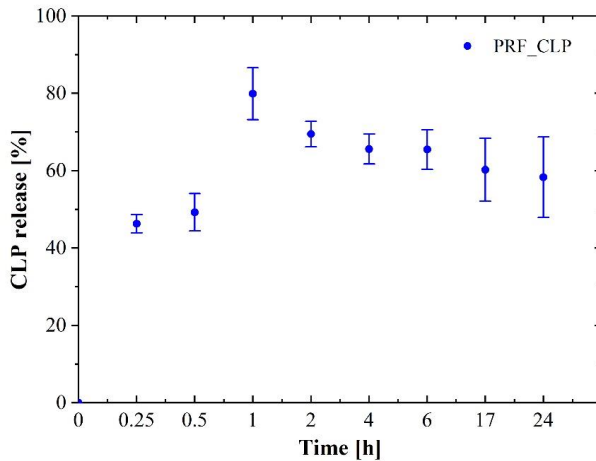


Fig. 6. CLP release from PRF matrices in Dulbecco's modified Eagle medium (DMEM); an average of the three donors' release data [2].

Impact of Delivery System on Drug Release from PRF Matrix

Systematically used drugs, without a specific carrier, spread throughout the body, and often, the drug degradation rate is relatively short. It ensures not only a positive effect on the damaged tissue but may also induce adverse side effects on healthy tissues [47]. As observed in the previous study [2], simply mixing the drug into PRF enhances its antibacterial properties; however, the drug is released very rapidly. The aim of drug delivery systems is to achieve the highest therapeutic effect with the lowest drug concentration [48]. In this study, antibiotics VANKA encapsulated in PLGA microcapsules (PLGA_μC_VANKA) and liposomes were used. Figure 7 shows the preparation schemes of both types of delivery systems. Both developed VANKA delivery methods were incorporated into PRF matrices, testing the ability of PRF to release drugs uniformly.

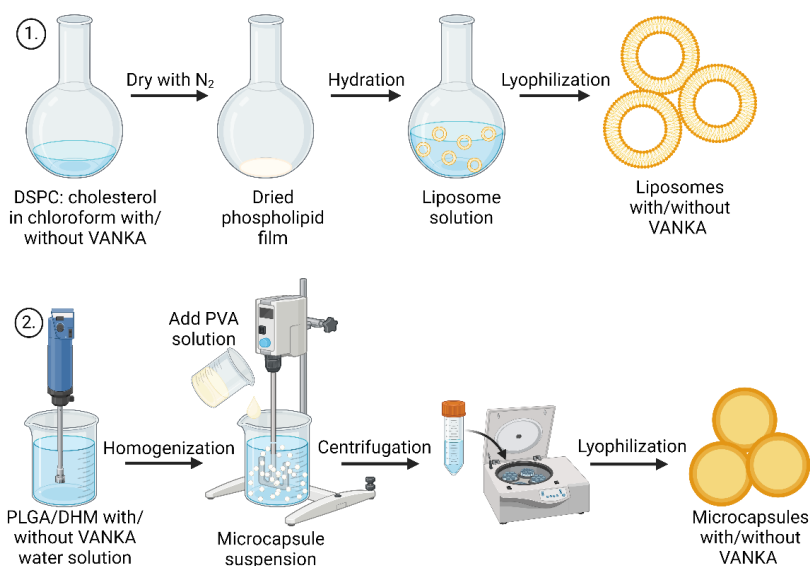


Fig. 7. Sample preparation scheme: 1) liposomes with/without VANKA; 2) microcapsules with/without VANKA. Figure created with Biorender.com.

Transmission electron microscopy (TEM) analysis showed that prepared VANKA-loaded liposomes have a heterogeneous population in which it is possible to observe a close presence of two-layer structures. Also, Fig. 8 shows that the majority of liposomes are spherical particles.

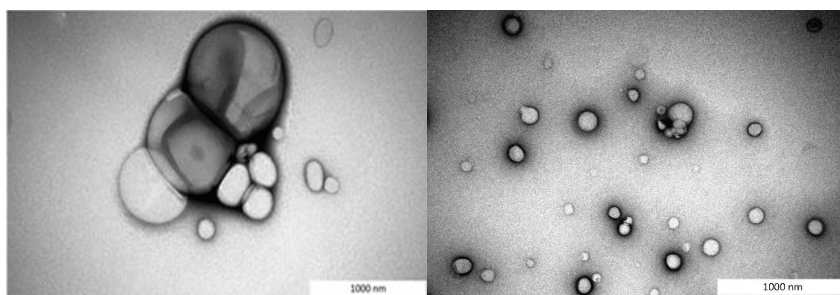


Fig. 8. TEM pictures of VANKA-loaded liposomes [13].

The release kinetics of VANKA from PRF/VANKA liposomes is higher than from VANKA liposomes without PRF matrix (Fig. 9). The increased concentration of VANKA can be explained by the fact that the Ca^{2+} ions in PRF form a shell around the lipids, compressing them and thus destroying the liposomes [49,50]. Based on the results, it can be concluded that Ca^{2+} ions adversely affect the liposomes; therefore, VANKA is released faster and in higher concentrations.

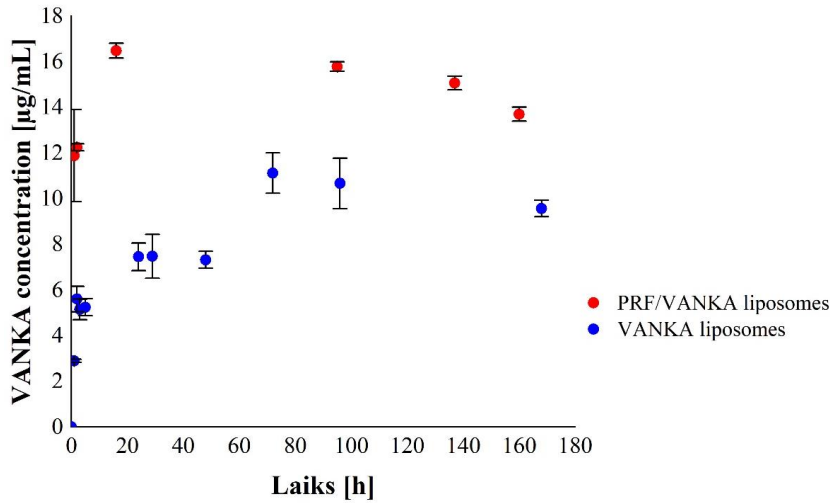


Fig. 9. Drug release from PRF/VANKA liposomes and VANKA liposomes [13].

On the other hand, scanning electron microscopy (SEM) photographs of PLGA microcapsules showed spherical particles with smooth surfaces, which indicated the absence of any drug crystal on the surface and confirmed the even distribution of the drug in the polymeric matrix (Fig. 10 B).

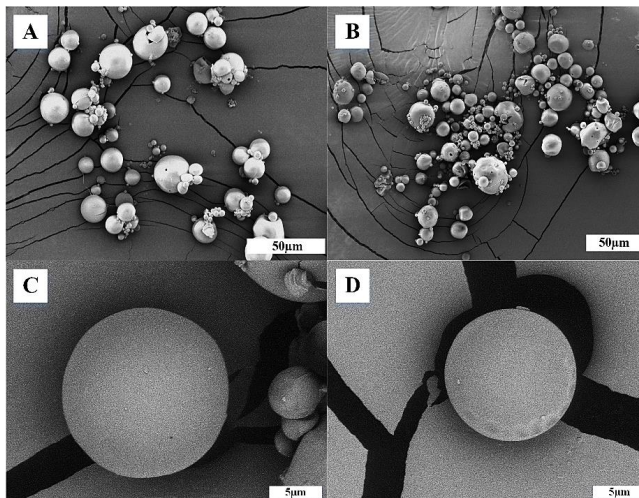


Fig. 10. SEM pictures of the surface of PLGA microcapsules without (A and C) and with (B and D) VANKA [13].

Based on the VANKA release studies from PLGA microcapsules (Fig. 11), the kinetics of VANKA release from PRF with VANKA-loaded PLGA microcapsules (PRF/PLGA_µC_VANKA) scaffolds are reduced fivefold compared to PRF with VANKA-added as free drug powder, non-encapsulated (PRF/VANKA) samples, ensuring controlled

VANKA release (from 6 to 10 days) and preventing burst release. In contrast, comparing PLGA_μC_VANKA with PRF/PLGA_μC_VANKA scaffolds, it can be observed that the VANKA release concentration is reduced twofold. This suggests that the PRF scaffold inhibits the rapid release of VANKA. Also, VANKA in PRF scaffolds without a carrier system does not ensure controlled delivery of active VANKA form at the therapeutic effect level.

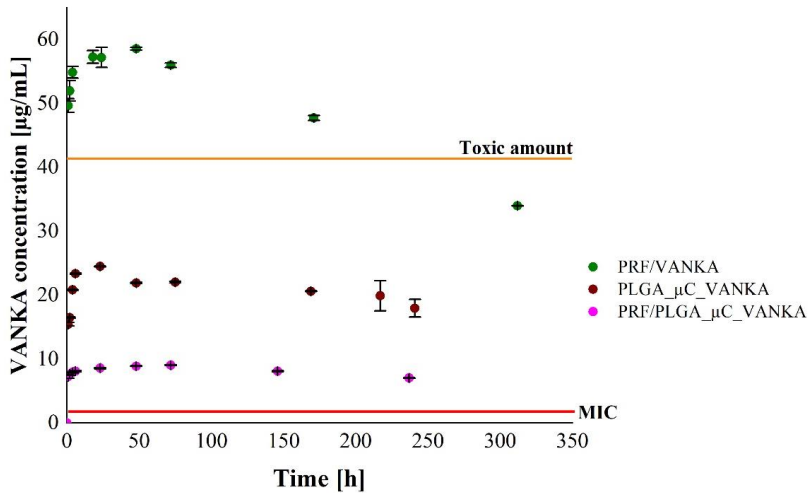


Fig. 11. Drug release from PRF/VANKA, PLGA_μC_VANKA, and PRF/ PLGA_μC_VANKA scaffolds [13].

The maximum duration of antibacterial effect for VANKA-containing samples (PLGA_μC_VANKA) was observed for 48 hours. For the first 24 hours, the mean diameter of the sterile area around the samples was 30 mm. For the next 24 hours, the diameter of the sterile area was reduced by 50 % (Fig. 12). As one of the possible solutions for further research, obtained samples could be placed in a bacterial suspension and incubated, preventing sample drying.

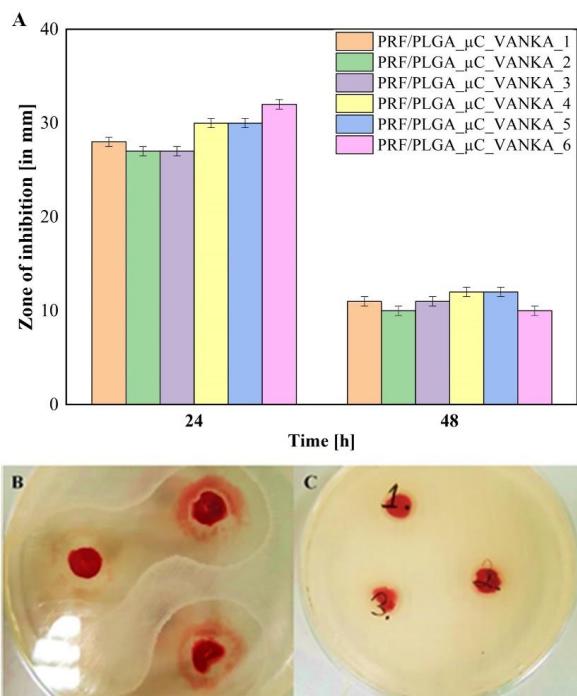


Fig. 12. Antibacterial properties of PRF/PLGA_μC_VANKA samples: (A) inhibition zones in mm; (B) sterile areas around the PRF/PLGA_μC_VANKA samples after 24 h incubation; (C) sterile areas around the PRF/PLGA_μC_VANKA samples after 48 h incubation. The diameter of the petri dishes is 8.5 cm [13].

Beyond its capacity for controlled drug release, PRF possesses another vital characteristic: its role in promoting healing and tissue regeneration, which is made possible by the presence of growth factors and cytokines within PRF.

Effect of Carrier Systems on the Release of Bioactive Molecules within PRF

In this study, we developed a hydrogel composed of fucoidan (FU) and chitosan (CS) due to their biocompatibility and ability to form polyelectrolyte complexes via self-assembly [28], as well as the ability of fucoidan to bind growth factors [24]. See the FU_CS hydrogel preparation scheme in Fig. 13. To determine the optimal amount of PRF and the release kinetics of the bioactive molecules it contains, the following parameters were investigated for the hydrogels: 1) stability, deformation and flow behavior and 2) release kinetics of the bioactive molecules.

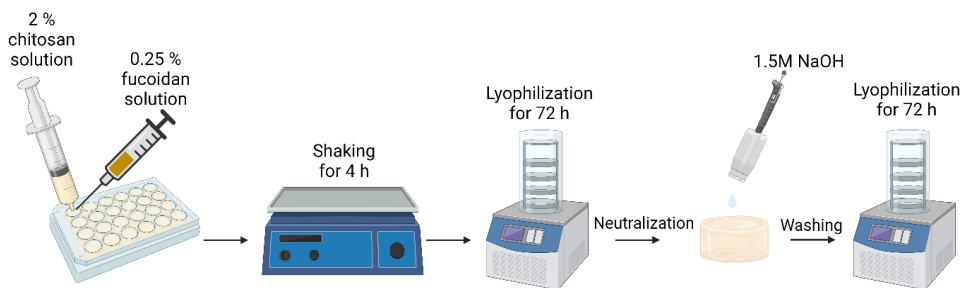


Fig. 13. FU_CS hydrogel preparation scheme. Figure created with Biorender.com [51].

Hydrogels` degradation and rheological properties were analyzed as key determinants of their mechanical behavior and susceptibility to breaking down. Thus, finding out whether the addition of PRF will be able to improve the properties of the hydrogel (Figs. 14 and 15). Then, the released amount of bioactive molecules (TGF-1, PDGF-BB, VEGF, EGF, and IL-8) from pure PRF matrix and combined with hydrogel was determined (Fig. 16).

The degradation of FU_CS hydrogels with/without PRF and pure PRF during two weeks in TRIS-HCl and citric acid was determined, and it is illustrated in Fig. 12. Based on the results, the addition of PRF to FU_CS hydrogels slowed down the degradation rates of both PRF and FU_CS hydrogels. Statistical analysis reveals no significant difference in media between FU_CS and PRF/FU_CS hydrogel samples. There is a notable gap in PRF degradation, with 87.26 ± 8.21 % in TRIS-HCl and 96.21 ± 1.71 % in citric acid within 14 days.

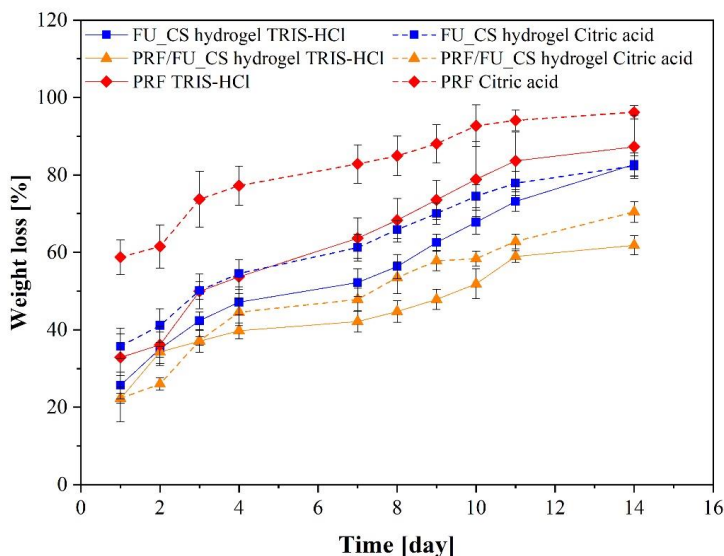


Fig. 14. Degradation degree of PRF, FU_CS and PRF/FU_CS hydrogels in TRIS-HCl (with a solid line) and citric acid (with dashed line) at 37 °C. All data is represented as average \pm SD, $n = 3$ [51].

Rheological experiments were used to explore the deformation and flow behaviors of PRF, FU_CS and PRF/FU_CS hydrogels. All samples exhibited characteristic gel-like behavior, with the storage modulus (G') substantially exceeding the loss modulus (G'') (Fig. 15). The amplitude sweep test identified a consistent linear viscoelastic region (LVER) down to $\varepsilon \approx 2.5\%$ for all samples (marked with a black line in Fig. 15 A), and $G'-G''$ crossing point was observed at $\varepsilon \approx 14\%$ for FU_CS hydrogel, $\varepsilon \approx 28\%$ for PRF/FU_CS hydrogel, and at $\varepsilon \approx 55\%$ for PRF (marked with colored lines). In rheology, " ε " typically represents strain, how much a material has deformed under a certain amount of stress or force. In all frequency ranges, G' remained constant for all samples (Fig. 15 B), indicating a solid-like and stable internal structure.

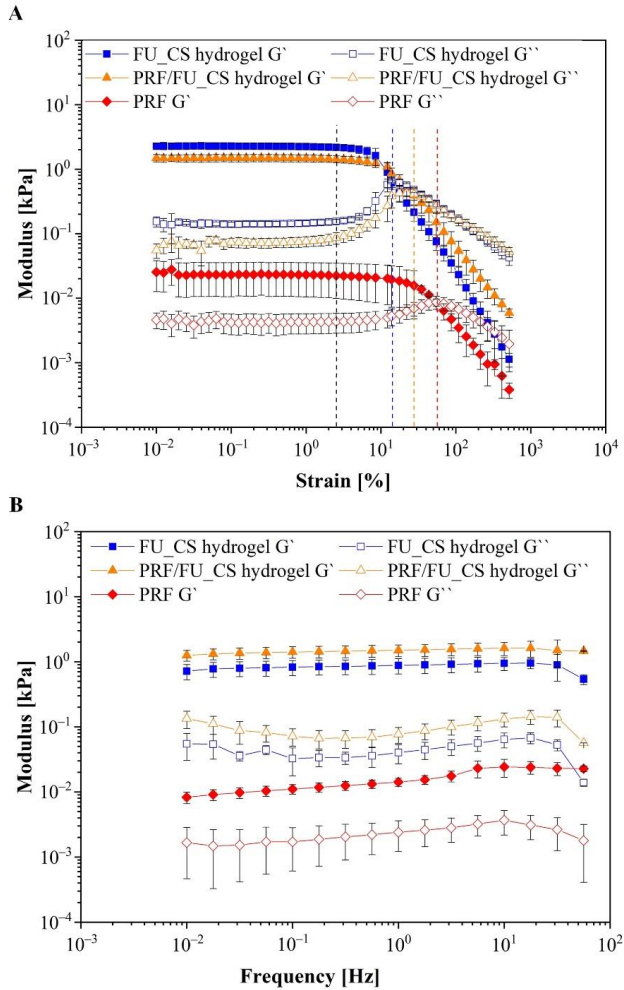


Fig. 15. Mechanical properties of scaffolds: **A** –amplitude sweep test of hydrogels with/without PRF was obtained at 1 Hz frequency; **B** – frequency sweep test of FU_CS hydrogels with/without PRF was obtained at 0.2 % strain. All data is represented as average \pm SD ($n = 3$) [51].

The data obtained show that the hydrogel, as a result of electrostatic interaction, allows the growth factors contained in PRF to be encapsulated and ensures their gradual release. For all analyzed growth factors and cytokines (TGF-1, PDGF-BB, VEGF, EGF, and IL-8), a general trend of higher released concentrations from pure PRF matrices than from PRF/FU_CS hydrogel matrices was observed. This indicates that the FU_CS hydrogel can effectively sustain the release of bioactive molecules and incorporate them into the hydrogel matrix, ensuring their long-term availability for tissue engineering purposes.

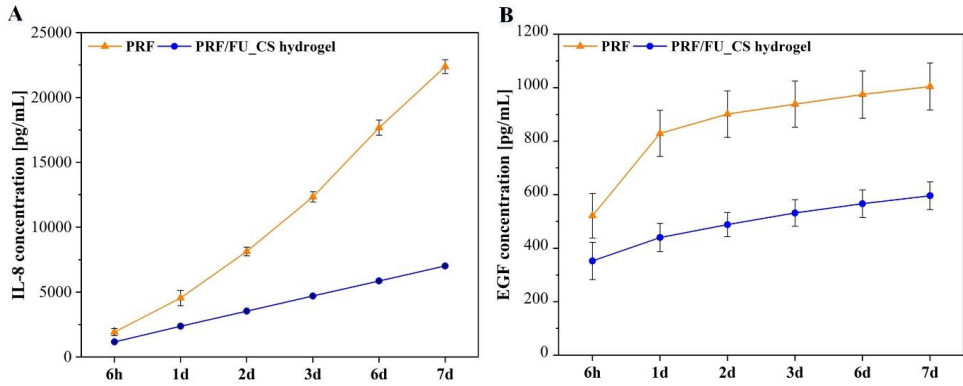


Fig. 16. Cumulative release of growth factor and cytokine. A and B show growth factor and cytokine release (IL-8 and EGF, respectively) at each time [51].

Histological studies have also shown that PRF penetrates the FU_CS hydrogel matrix, enabling the release of growth factors. After three and seven days, the comparison between unmodified PRF and PRF/FU_CS hydrogel reveals a reduction in cell count within the PRF matrix, indicating the release of bioactive molecules. The obtained data also confirm that after seven days, PRF is still incorporated into the FU_CS hydrogel structure (Fig. 17).

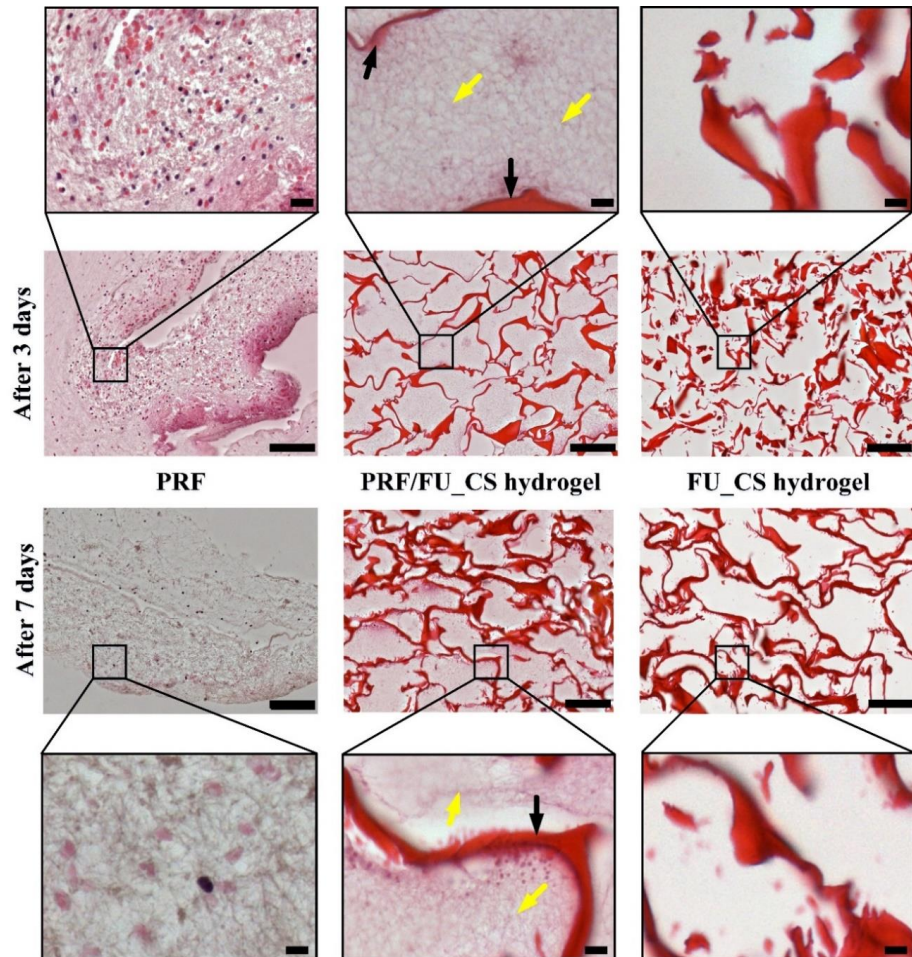


Fig. 17. Fibrin morphology after three and seven days of incubation. (Scale bar: 100 μm , increases have scale bar = 20 μm ; yellow arrows show the presence of PRF and black arrows the presence of hydrogel) [51].

The use of hydrogels to modulate PRF growth factor release schedules, particularly in combination with drugs (potentially prodrugs), would offer a promising opportunity to enhance antibacterial activity. Future research should focus on optimizing drug-hydrogel interactions, exploring sustained release patterns, and assessing the capability of other drugs to convert into active forms in the presence of PRF, providing valuable insights for advanced therapeutic applications.

CONCLUSIONS

1. The addition of PRF affects the antibacterial activity of CLP against *S. aureus* and *S. epidermidis* bacterial strains (both reference cultures and clinical isolates), resulting in lower MIC values (ranging from 62.5 $\mu\text{g/mL}$ to 145.8 $\mu\text{g/mL}$ depending on the bacterial strain) compared to clindamycin (MIC > 256 $\mu\text{g/mL}$).
2. The use of phosphatidylcholine liposomes as drug delivery systems in PRF matrices fails to provide a controlled release of VANKA, as their stability is influenced by the Ca^{2+} ions present in the PRF, thereby releasing a high concentration of the drug.
3. The use of PLGA microcapsules as a drug delivery system in PRF matrices can ensure the controlled release of VANKA for six to ten days.
4. The FU_CS hydrogel, created through electrostatic interactions, enables the encapsulation of PRF bioactive molecules (TGF-1, PDGF-BB, VEGF, EGF, and IL-8) and ensures their gradual release over seven days.

REFERENCES

1. Garraud, O.; Cognasse, F. Are Platelets Cells? And if Yes, are They Immune Cells? *Front. Immunol.* **2015**, *6*, 1–8, doi:10.3389/fimmu.2015.00070.
2. Egle, K.; Skadins, I.; Grava, A.; Micko, L.; Dubniks, V.; Salma, I.; Dubnika, A. Injectable Platelet-Rich Fibrin as a Drug Carrier Increases the Antibacterial Susceptibility of Antibiotic – Clindamycin Phosphate. *Int. J. Mol. Sci.* **2022**, *23*, 7407, doi:10.3390/ijms23137407.
3. Jasmine, S.; A., T.; Janarthanan, K.; Krishnamoorthy, R.; Alshatwi, A.A. Antimicrobial and antibiofilm potential of injectable platelet rich fibrin—a second-generation platelet concentrate – against biofilm producing oral staphylococcus isolates. *Saudi J. Biol. Sci.* **2020**, *27*, 41–46, doi:10.1016/j.sjbs.2019.04.012.
4. Micko, L.; Salma, I.; Skadins, I.; Egle, K.; Salms, G.; Dubnika, A. Can Our Blood Help Ensure Antimicrobial and Anti-Inflammatory Properties in Oral and Maxillofacial Surgery? *Int. J. Mol. Sci.* **2023**, *24*, 1073, doi:10.3390/ijms24021073.
5. Egle, K.; Salma, I.; Dubnika, A. From Blood to Regenerative Tissue: How Autologous Platelet-Rich Fibrin Can Be Combined with Other Materials to Ensure Controlled Drug and Growth Factor Release. *Int. J. Mol. Sci.* **2021**, *22*, 11553, doi:10.3390/ijms22111553.
6. Sancho-Puchades, M.; Herráez-Vilas, J.M.; Berini-Aytés, L.; Gay-Escoda, C. Antibiotic prophylaxis to prevent local infection in Oral Surgery: use or abuse? *Med. Oral Patol. Oral Cir. Bucal* **2009**, *14*, E28–33.
7. Yang, Z.; Liu, J.; Gao, J.; Chen, S.; Huang, G. Chitosan coated vancomycin hydrochloride liposomes: Characterizations and evaluation. *Int. J. Pharm.* **2015**, *495*, 508–515, doi:10.1016/j.ijpharm.2015.08.085.
8. Liu, J.; Wang, Z.; Li, F.; Gao, J.; Wang, L.; Huang, G. Liposomes for systematic delivery of vancomycin hydrochloride to decrease nephrotoxicity: Characterization and evaluation. *Asian J. Pharm. Sci.* **2015**, *10*, 212–222, doi:10.1016/j.ajps.2014.12.004.
9. Pumerantz, A.; Muppidi, K.; Agnihotri, S.; Guerra, C.; Venketaraman, V.; Wang, J.; Betageri, G. Preparation of liposomal vancomycin and intracellular killing of meticillin-resistant Staphylococcus aureus (MRSA). *Int. J. Antimicrob. Agents* **2011**, *37*, 140–144, doi:10.1016/j.ijantimicag.2010.10.011.
10. Upputuri, R. T. P.; Kulandaivelu, K.; Mandal, A. K. A. Nanotechnology-Based Approach for Enhanced Bioavailability and Stability of Tea Polyphenols – A Review. In *Studies in Natural Products Chemistry*; 2016; pp. 399–410.
11. Tyle, P. *Drug Delivery*; Hillery, A., Park, K., Eds.; CRC Press, 2016; Vol. 77; ISBN 9781482217728.
12. Saeed Jan, M.; Alam, W.; Shabnam, M. Fundamentals Applications of Controlled Release Drug Delivery. In *Drug Development and Safety [Working Title]*; IntechOpen, 2023.
13. Dubnika, A.; Egle, K.; Skrinda-Melne, M.; Skadins, I.; Rajadas, J.; Salma, I. Development of Vancomycin Delivery Systems Based on Autologous 3D Platelet-Rich Fibrin Matrices for Bone Tissue Engineering. *Biomedicines* **2021**, *9*, 814, doi:10.3390/biomedicines9070814.

14. Micko, L.; Salma, I.; Skadins, I.; Egle, K.; Salms, G.; Dubnika, A. Can Our Blood Help Ensure Antimicrobial and Anti-Inflammatory Properties in Oral and Maxillofacial Surgery? *Int. J. Mol. Sci.* **2023**, *24*, 1073, doi:10.3390/ijms24021073.
15. Mirjalili, F.; Mahmoodi, M. Controlled release of protein from gelatin/chitosan hydrogel containing platelet-rich fibrin encapsulated in chitosan nanoparticles for accelerated wound healing in an animal model. *Int. J. Biol. Macromol.* **2023**, *225*, 588–604, doi:10.1016/j.ijbiomac.2022.11.117.
16. Rao, S. S.; Venkatesan, J.; Yuvarajan, S.; Rekha, P. D. Self-assembled polyelectrolyte complexes of chitosan and fucoidan for sustained growth factor release from PRP enhance proliferation and collagen deposition in diabetic mice. *Drug Deliv. Transl. Res.* **2022**, *12*, 2838–2855, doi:10.1007/s13346-022-01144-3.
17. Rastegar, A.; Mahmoodi, M.; Mirjalili, M.; Nasirizadeh, N. Platelet-rich fibrin-loaded PCL/chitosan core-shell fibers scaffold for enhanced osteogenic differentiation of mesenchymal stem cells. *Carbohydr. Polym.* **2021**, *269*, 118351, doi:10.1016/j.carbpol.2021.118351.
18. Xu, F.; Zou, D.; Dai, T.; Xu, H.; An, R.; Liu, Y.; Liu, B. Effects of incorporation of granule-lyophilised platelet-rich fibrin into polyvinyl alcohol hydrogel on wound healing. *Sci. Rep.* **2018**, *8*, 14042, doi:10.1038/s41598-018-32208-5.
19. Al-Maawi, S.; Herrera-Vizcaino, C.; Orlowska, A.; Willershausen, I.; Sader, R.; Miron, R.J.; Choukroun, J.; Ghanaati, S. Biologization of Collagen-Based Biomaterials Using Liquid-Platelet-Rich Fibrin: New Insights into Clinically Applicable Tissue Engineering. *Materials (Basel)*. **2019**, *12*, 3993, doi:10.3390/ma12233993.
20. Lu, H.-T.; Lu, T.-W.; Chen, C.-H.; Lu, K.-Y.; Mi, F.-L. Development of nanocomposite scaffolds based on biomineralization of N,O-carboxymethyl chitosan/fucoidan conjugates for bone tissue engineering. *Int. J. Biol. Macromol.* **2018**, *120*, 2335–2345, doi:10.1016/j.ijbiomac.2018.08.179.
21. V. K., A.D.; Udduttula, A.; Jaiswal, A.K. Unveiling the secrets of marine—derived fucoidan for bone tissue engineering – A review. *Front. Bioeng. Biotechnol.* **2023**, *10*, 1100164, doi:10.3389/fbioe.2022.1100164.
22. Park, S.; Lee, K.W.; Lim, D.-S.; Lee, S. The Sulfated Polysaccharide Fucoidan Stimulates Osteogenic Differentiation of Human Adipose-Derived Stem Cells. *Stem Cells Dev.* **2012**, *21*, 2204–2211, doi:10.1089/scd.2011.0521.
23. Purnama, A.; Aid-Launais, R.; Haddad, O.; Maire, M.; Mantovani, D.; Letourneur, D.; Hlawaty, H.; Le Visage, C. Fucoidan in a 3D scaffold interacts with vascular endothelial growth factor and promotes neovascularization in mice. *Drug Deliv. Transl. Res.* **2015**, *5*, 187–197, doi:10.1007/s13346-013-0177-4.
24. Zeng, H.-Y.; Huang, Y.-C. Basic fibroblast growth factor released from fucoidan-modified chitosan/alginate scaffolds for promoting fibroblasts migration. *J. Polym. Res.* **2018**, *25*, 83, doi:10.1007/s10965-018-1476-8.
25. Domalik-Pyzik, P.; Chłopek, J.; Pielichowska, K. Chitosan-Based Hydrogels: Preparation, Properties, and Applications. *Int. J. Biol. Macromol.*; 2019; pp. 1665–1693.
26. Ahmadi, F.; Oveisi, Z.; Samani, S.M.; Amoozgar, Z. Chitosan based hydrogels:

- characteristics and pharmaceutical applications. *Res. Pharm. Sci.* **2015**, *10*, 1–16.
27. Levengood, S.K.L.; Zhang, M. Chitosan-based scaffolds for bone tissue engineering. *J. Mater. Chem. B* **2014**, *2*, 3161, doi:10.1039/c4tb00027g.
 28. Venkatesan, J.; Singh, S.; Anil, S.; Kim, S.-K.; Shim, M. Preparation, Characterization and Biological Applications of Biosynthesized Silver Nanoparticles with Chitosan-Fucoidan Coating. *Molecules* **2018**, *23*, 1429, doi:10.3390/molecules23061429.
 29. Chitosan-based polyelectrolyte complexes as pharmaceutical excipients. In *Controlled Drug Delivery*; M.A. Mateescu, P.I.-S. and E.A., Ed.; Elsevier, 2015; pp. 127–161.
 30. Theodoridis, T.; Kraemer, J. *Guyton and Hall Textbook of Medical Physiology*; 2020; ISBN 9783131450715.
 31. Wend, S.; Kubesch, A.; Orłowska, A.; Al-Maawi, S.; Zender, N.; Dias, A.; Miron, R.J.; Sader, R.; Booms, P.; Kirkpatrick, C.J.; et al. Reduction of the relative centrifugal force influences cell number and growth factor release within injectable PRF-based matrices. *J. Mater. Sci. Mater. Med.* **2017**, *28*, 188, doi:10.1007/s10856-017-5992-6.
 32. The Free Dictionary: <https://medical-dictionary.thefreedictionary.com/antimicrobial>.
 33. Leong, D. K. C.; Benedict, B. C. T.; Chew, K. T. L. Autologous Growth Factors: A Biological Treatment in Sports Medicine. *Proc. Singapore Healthc.* **2010**, *19*, 229–236, doi:10.1177/201010581001900309.
 34. Polak, D.; Clemer-Shamai, N.; Shapira, L. Incorporating antibiotics into platelet-rich fibrin: A novel antibiotics slow-release biological device. *J. Clin. Periodontol.* **2019**, *46*, 241–247, doi:10.1111/jcpe.13063.
 35. Knafl, D.; Thalhammer, F.; Vossen, M.G. In-vitro release pharmacokinetics of amikacin, teicoplanin and polyhexanide in a platelet rich fibrin – layer (PRF) – a laboratory evaluation of a modern, autologous wound treatment. *PLoS One* **2017**, *12*, e0181090, doi:10.1371/journal.pone.0181090.
 36. Maestre-Vera, J.R. Treatment options in odontogenic infection. *Med. Oral Patol. Oral Cir. Bucal* **2004**, *9 Suppl*, 25–31; 19–24.
 37. Jang, E.-S.; Park, J.-W.; Kweon, H.; Lee, K.-G.; Kang, S.-W.; Baek, D.-H.; Choi, J.-Y.; Kim, S.-G. Restoration of peri-implant defects in immediate implant installations by Choukroun platelet-rich fibrin and silk fibroin powder combination graft. *Oral Surgery, Oral Med. Oral Pathol. Oral Radiol. Endodontology* **2010**, *109*, 831–836, doi:10.1016/j.tripleo.2009.10.038.
 38. Schmidt, T. *Encyclopedia of Microbiology 4th ed.*; Faculty Bookshelf. 260, 2019; ISBN 9780128117378.
 39. Martinez-Aguilar, G.; Hammerman, W. A.; Mason, E. O.; Kaplan, S. L. Clindamycin treatment of invasive infections caused by community-acquired, methicillin-resistant and methicillin-susceptible *Staphylococcus aureus* in children. *Pediatr. Infect. Dis. J.* **2003**, *22*, 593–599, doi:10.1097/01.inf.0000073163.37519.ee.
 40. Mohamed, M. A.; Nasr, M.; Elkhatib, W. F.; Eltayeb, W. N.; Elshamy, A. A.; El-Sayyad, G. S. Nanobiotic formulations as promising advances for combating MRSA resistance: susceptibilities and post-antibiotic effects of clindamycin, doxycycline, and linezolid. *RSC Adv.* **2021**, *11*, 39696–39706, doi:10.1039/D1RA08639A.

41. Fortunato, L.; Bennardo, F.; Buffone, C.; Giudice, A. Is the application of platelet concentrates effective in the prevention and treatment of medication-related osteonecrosis of the jaw? A systematic review. *J. Cranio-Maxillofacial Surg.* **2020**, *48*, 268–285, doi:10.1016/j.jcms.2020.01.014.
42. Li, H.; Deng, J.; Yue, Z.; Zhang, Y.; Sun, H.; Ren, X. Clindamycin hydrochloride and clindamycin phosphate: two drugs or one? A retrospective analysis of a spontaneous reporting system. *Eur. J. Clin. Pharmacol.* **2017**, *73*, 251–253, doi:10.1007/s00228-016-2161-7.
43. Borin, M.T.; Powley, G.W.; Tackwell, K.R.; Batts, D.H. Absorption of clindamycin after intravaginal application of clindamycin phosphate 2% cream. *J. Antimicrob. Chemother.* **1995**, *35*, 833–841, doi:10.1093/jac/35.6.833.
44. Schilcher, K.; Andreoni, F.; Uchiyama, S.; Ogawa, T.; Schuepbach, R.A.; Zinkernagel, A.S. Increased Neutrophil Extracellular Trap-Mediated Staphylococcus aureus Clearance Through Inhibition of Nuclease Activity by Clindamycin and Immunoglobulin. *J. Infect. Dis.* **2014**, *210*, 473–482, doi:10.1093/infdis/jiu091.
45. Schilcher, K.; Andreoni, F.; Dengler Haunreiter, V.; Seidl, K.; Hasse, B.; Zinkernagel, A.S. Modulation of Staphylococcus aureus Biofilm Matrix by Subinhibitory Concentrations of Clindamycin. *Antimicrob. Agents Chemother.* **2016**, *60*, 5957–5967, doi:10.1128/AAC.00463-16.
46. Kuriyama, T.; Karasawa, T.; Nakagawa, K.; Saiki, Y.; Yamamoto, E.; Nakamura, S. Bacteriologic features and antimicrobial susceptibility in isolates from orofacial odontogenic infections. *Oral Surgery, Oral Med. Oral Pathol. Oral Radiol. Endodontology* **2000**, *90*, 600–608, doi:10.1067/moe.2000.109639.
47. Safari, J.; Zarnegar, Z. Advanced drug delivery systems: Nanotechnology of health design A review. *J. Saudi Chem. Soc.* **2014**, *18*, 85–99, doi:10.1016/j.jscs.2012.12.009.
48. Li, J.; Wang, X.; Zhang, T.; Wang, C.; Huang, Z.; Luo, X.; Deng, Y. A review on phospholipids and their main applications in drug delivery systems. *Asian J. Pharm. Sci.* **2015**, *10*, 81–98, doi:10.1016/j.ajps.2014.09.004.
49. Hincha, D. K. Effects of calcium-induced aggregation on the physical stability of liposomes containing plant glycolipids. *Biochim. Biophys. Acta – Biomembr.* **2003**, *1611*, 180–186, doi:10.1016/S0005-2736(03)00053-1.
50. Melcrová, A.; Pokorna, S.; Pullanchery, S.; Kohagen, M.; Jurkiewicz, P.; Hof, M.; Jungwirth, P.; Cremer, P. S.; Cwiklik, L. The complex nature of calcium cation interactions with phospholipid bilayers. *Sci. Rep.* **2016**, *6*, 1–12, doi:10.1038/srep38035.
51. Egle, K.; Dohle, E.; Hoffmann, V.; Salma, I.; Al-Maawi, S.; Ghanaati, S.; Dubnika, A. Fucoidan/chitosan hydrogels as carrier for sustained delivery of platelet-rich fibrin containing bioactive molecules. *Int. J. Biol. Macromol.* **2024**, *262*, 129651, doi:10.1016/j.ijbiomac.2024.129651.

PIELIKUMI / APPENDICES

From Blood to Regenerative Tissue: How Autologous Platelet-Rich Fibrin Can Be Combined with Other Materials to Ensure Controlled Drug and Growth Factor Release


Karina Egle, Ilze Salma, Arita Dubnika

Int. J. Mol. Sci., **2021**, *22*(21), 11553



Review

From Blood to Regenerative Tissue: How Autologous Platelet-Rich Fibrin Can Be Combined with Other Materials to Ensure Controlled Drug and Growth Factor Release

Karina Egle^{1,2}, Ilze Salma^{2,3} and Arita Dubnika^{1,2,*} 

¹ Rudolfs Cimdinš Riga Biomaterials Innovations and Development Centre, Institute of General Chemical Engineering, Riga Technical University, LV-1658 Riga, Latvia; karina.egle@rtu.lv

² Baltic Biomaterials Centre of Excellence, Headquarters at Riga Technical University, LV-1658 Riga, Latvia; ilze.salma@rsu.lv

³ Institute of Stomatology, Riga Stradiņš University, LV-1007 Riga, Latvia

* Correspondence: arita.dubnika@rtu.lv; Tel.: +371-67089605

Abstract: The purpose of this review is to examine the latest literature on the use of autologous platelet-rich fibrin (PRF) as a drug and growth factor carrier system in maxillofacial surgery. Autologous platelet-rich fibrin (PRF) is a unique system that combines properties such as biocompatibility and biodegradability, in addition to containing growth factors and peptides that provide tissue regeneration. This opens up new horizons for the use of all beneficial ingredients in the blood sample for biomedical purposes. By itself, PRF has an unstable effect on osteogenesis: therefore, advanced approaches, including the combination of PRF with materials or drugs, are of great interest in clinics. The main advantage of drug delivery systems is that by controlling drug release, high drug concentrations locally and fewer side effects within other tissue can be achieved. This is especially important in tissues with limited blood supply, such as bone tissue compared to soft tissue. The ability of PRF to degrade naturally is considered an advantage for its use as a “warehouse” of controlled drug release systems. We are focusing on this concentrate, as it is easy to use in manipulations and can be delivered directly to the surgical site. The target audience for this review are researchers and medical doctors who are involved in the development and research of PRFs further studies. Likewise, surgeons who use PRF in their work to treat patients and who advice patients to take the medicine orally.

Keywords: platelet-rich fibrin; endogenous growth factors; carrier systems; drug delivery; platelet concentrates; tissue engineering; autologous growth factors



Citation: Egle, K.; Salma, I.; Dubnika, A. From Blood to Regenerative Tissue: How Autologous Platelet-Rich Fibrin Can Be Combined with Other Materials to Ensure Controlled Drug and Growth Factor Release. *Int. J. Mol. Sci.* **2021**, *22*, 11553. <https://doi.org/10.3390/ijms222111553>

Academic Editors: Tomoyuki Kawase and Monica Montesi

Received: 6 September 2021

Accepted: 18 October 2021

Published: 26 October 2021

Publisher's Note: MDPI stays neutral with regard to jurisdictional claims in published maps and institutional affiliations.



Copyright: © 2021 by the authors. Licensee MDPI, Basel, Switzerland. This article is an open access article distributed under the terms and conditions of the Creative Commons Attribution (CC BY) license (<https://creativecommons.org/licenses/by/4.0/>).

1. Introduction

Although many approaches to bone tissue engineering have traditionally focused on synthetic materials (such as polymers or hydrogels), nowadays new emerging methods involve the use of natural materials due to their biological properties, such as autologous bone grafting. It is still debated whether platelets can be considered as cell fragments or whole cells [1], but they are known to be responsible for the activation and release of biomolecules. The growth factors that accelerate the wound healing process. Due to this, the use of platelet concentrates has been known for more than four decades [2]. Platelet-rich fibrin (PRF) is an autologous material that is easily produced; it can be derived from a person's own blood and is used to promote wound healing and tissue regeneration. PRF can be used in various fields of medicine, including dentistry and maxillofacial surgery [3]. PRF is expected to have a direct effect on enhancing tissue regeneration by saturating these tissues with growth factors from the blood. The autologous nature of PRF makes it the preferred choice for a variety of biomaterials in use today.

In this review, we considered 4 types of platelet concentrates as a possible drug delivery systems listed in Table 1.

Table 1. Abbreviation of different platelet concentrates.

Abbreviation	Platelet Concentrate	Explanation
PRP	Platelet-rich plasma	First-generation platelet concentrate with high platelet concentrations [4]
PRF	Platelet-rich fibrin	Second-generation platelet concentrate [5]
i-PRF	Injectable platelet-rich fibrin	Advanced version of PRF in liquid form which can be injected and contains stem cells with high regenerative potential [6]
A-PRF	Advanced platelet-rich fibrin	An autogenous blood product with applications in dento-alveolar surgery [7]

Several studies have reported that these platelet concentrates are most commonly used in medicine. There are also articles on other platelet concentrates, such as pure platelet-rich plasma (P-PRP), leukocyte-platelet-rich plasma (L-PRP), pure platelet-rich fibrin (P-PRF), and leukocyte- and platelet-rich fibrin (L-PRF). These concentrates are used alone or in combination with bone grafts. To promote tissue regeneration the platelet concentrates should contain not only platelets, but also substances in our blood, such as growth factors and host immune cells. Various growth factors are known to promote wound healing, with PRF being able to release them slowly. In addition, when combined with drugs, they can provide faster recovery and reduce the risk of infections. Platelet-rich plasma contains large amounts of platelets and is injectable, while not as easy to prepare and use it [8].

The second type of platelets, platelet-rich fibrin (PRF), plays an important role in modern medicine and is used as one of the components in the production of biomaterials. As mentioned in several sources, PRF is a second-generation platelet concentrate derived from centrifuged blood [5] and, in addition to platelets, also contains white blood cells, serum and concentrated growth factors [9], such as platelet-derived growth factor (PDGF), transforming growth factor- β (TGF- β) and insulin-like growth factor 1 (IGF-I) [10]. The properties of growth factors and cytokines within the PRF are shown in Table 2.

Table 2. Description of growth factors and cytokines within the PRF.

Abbreviation	Growth Factor/Cytokine	Properties
PDGF	Platelet-derived growth factor	Provides fibroblast chemotaxis [11], extracellular matrix modification [12], and increases TGF- β release from macrophages [13]. Its addition ensures the growth of cultured cells [14] and improves bone cell proliferation [15]
TGF- β	Transforming growth factor β	A multifunctional cytokine [16] and one of 30 members of the superfamily [5] that has been shown to promote extracellular matrix formation [15]. The most common of the three isoforms [13] of TGF- β is TGF- β 1, which has the ability to stimulate the production of collagen and fibronectin in cells [17]
IGF-I	Insulin-like growth factor I	A growth hormone-dependent polypeptide that stimulates skeletal growth in vivo [18], has an effect on the behavior of cells, thus providing tissue regeneration [19]
VEGF	Vascular endothelial growth factor	Promotes the proliferation [20] of endothelial cells and stimulates their migration [21]. It plays an important role in the cardiovascular system, increasing blood flow and enriching the injury site with nutrients [22]. In addition, it plays a role in bone formation and wound healing [23]
IL-1 β	Interleukin-1 β	Plays an important role in protection against infections and injuries [24], it is also involved in the activation of monocytes [25]

Table 2. Cont.

Abbreviation	Growth Factor/Cytokine	Properties
IL-6	Interleukin-6	Able to respond to infections and tissue injuries by stimulating hematopoiesis [26]. The main signal enhancement pathway [20] upon exposure to epithelium and immune cells [27]
IL-4	Interleukin-4	Acts as a powerful immune regulator [28] that inhibits the proliferation of osteoblast-like cells in vitro [29] and modulates the regeneration of macrophage cells [30]. It is also able to stimulate the accumulation of extracellular matrix macromolecules [31]
TNF- α	Tumor necrosis factor- α	Provides growth and differentiation of different cell types [32]. Stimulates the ability of fibroblasts to transform [20], and regulates the activity of vascular endothelial cells and keratinocytes. Determines the synthesis of extracellular matrix proteins [33]; it plays a key role in healing inflammation and wounds [34]

PRF is widely used to accelerate soft and hard tissue regeneration [17]. This was first described by Choukroun and his group in 2001 in France [35]. The PRF production protocol originally developed by his group used 10 mL of anticoagulant-free blood sample that was centrifugated at 2700 rpm for 12 min [16]. PRF is a modification of platelet rich plasma (PRP) and at the same time an autologous fibrin matrix used to improve bone regeneration and clinically used for soft tissue augmentation [10]. Compared to other platelet concentrates, PRF is a platelet-rich fibrin clot that does not require the use of thrombin (anticoagulants which used to accelerate gelation), but only centrifuged blood without any impurities [36,37]. It is a new biomaterial that resembles an autologous cicatricial matrix, but at the same time is neither a fibrin glue or a classic platelet concentrate [38]. The absence of anticoagulants does not delay the cascade of wound healing allowing natural blood clots to form. In addition, PRF contains a high concentration of host immune cells, which are needed to heal wounds and reduce infections [39].

Compared to platelet-rich plasma (PRP) (it requires multi-stage centrifugation in combination with the addition of non-autologous anticoagulants and the additional use of bovine thrombin or calcium chloride [16]), PRF does not dissolve for following hours after application, on the contrary it is slowly destroyed in the same way as a natural blood clot [40]. As mentioned above, bovine thrombin or anticoagulant is not required to obtain PRF, thus PRF provides lower costs and fewer disadvantages of biochemical modifications [8]. After centrifugation, PRF still combines many of the healing and immune enhancers found in the initial blood [17]. After injection, unlike PRP, liquid PRF (i-PRF) is rapidly converted to fibrin and, similarly to PRP, i-PRF is used for the local delivery of autologous angiogenic and regenerative growth factors [2,41].

Different platelet-rich fibrin (PRF) derivatives are used today depending on the application and the desired properties. Efficacy of autologous platelet concentrates in promoting wound healing and tissue regeneration is at the center of a recent academic debate [42]. In this review, we will consider few of the PRFs mentioned above that have attracted the most attention as drug delivery systems, and will try to understand which type of PRF is better and more suitable for development of controlled drug delivery systems.

2. Materials and Methods

Articles were searched for keywords such as “platelet-rich fibrin”, “growth factors PRF”, “drug delivery systems PRF”, “platelet-rich fibrin”, “antibiotics PRF”, “drug PRF”, and “drug fibrin”. In case it was necessary to find other articles with the PRF that included the specified drug, then the name of the drug was used as a keyword. Emphasis on the literature related to PRF clinical trials and studies investigating drug incorporation, growth factor secretion was placed. Antibacterial studies to understand whether drugs can provide antibacterial efficacy by being included in the PRF matrices were also reviewed in relation to drug studies. Databases such as PubMed/MEDLINE, ScienceDirect, Scopus were used

for search. In total, 200 studies were found for the above keywords, from which 121 articles were selected for further analysis in this review.

3. From Blood to Injectable or Solid System

i-PRF is liquid injectable PRF and allows the incorporation of drugs and drug delivery systems prior to coagulation. i-PRF is a recently introduced platelet concentrate [43] that can be easily combined with various biomaterials [44] to improve the properties of the biomaterial. i-PRF contains not only autologous growth factors found in the blood, but also cells involved in the wound healing process [45] (Figure 1). The functions of cells found in the PRF are shown in Table 3.

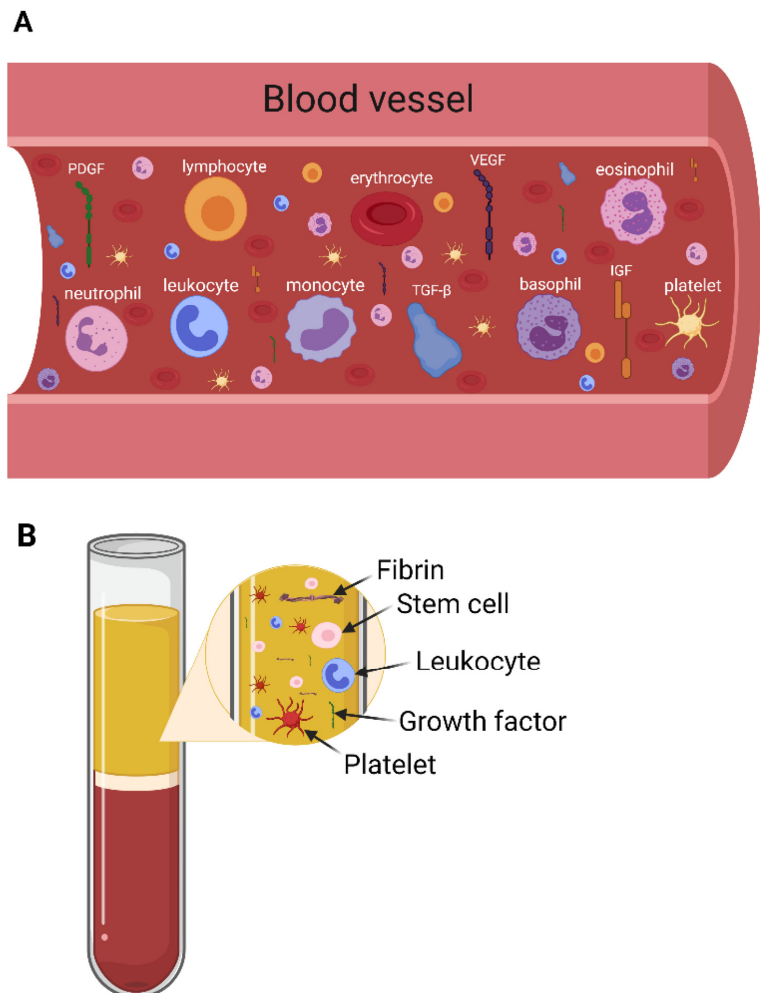


Figure 1. Main elements of blood (A) and PRF (B). Panel B shows that not all elements in the blood enter the PRF layer after centrifugation. Both figures created with Biorender.com.

Table 3. Description of cells within the PRF.

Cell Type	Functions
Platelets	Involved in primary wound closure and able to release several growth factors to attract inflammatory cells to the site of injury [46,47]
Leukocytes	Essential for tissue regeneration as they direct and attract different types of cells in the wound healing process [44]
Red blood cells	Physical and chemical interactions between platelets and the blood surface may be provided [48]. Induces an increase in platelet concentrations at the site of action and in vitro coordination [49]
Neutrophils	Play an important role in healing processes [50]. Serves as the first signals for the activation of local fibroblasts and keratinocytes [51]
Lymphocytes	It affects the osteogenic differentiation of mesenchymal stromal cells [52] and releases a wide range of cytokines [53]
Monocytes	A key role in supporting tissue homeostasis by disseminating immune responses to convenience [54]
Stem cells	Play an important role in regenerative medicines [55], also have the opportunity to regenerate and differentiate in different types of cells [56]. PRF is a unique source of hematopoietic stem cells (HSCs) [57]

After about 20 min fibrin is polymerized (the liquid state of PRF depends on the speed, G-force and time of centrifugation), during which fibrin changes from a liquid state to a solid, forming a three-dimensional fibrin network. This network contains cellular components that are distributed in the network and ensure the slow and steady release of growth factors over a period of time. In addition, a controlled release system maintains bioactivity throughout healing [4]. As mentioned by Bennardo et. al., liquid PRF can also be used as an injection to treat lichens [58].

A-PRF, on the other hand, is a solid system (in the form of a clot) that can be compressed and used as a strong membrane. Modification of PRF preparation procedures at lower centrifugation rates with lower G-forces results in A-PRF with higher levels of growth factors [9]. This is indicated by a Caruana et.al group study on the variability of TGF- β 1 and VEGF growth factor concentrations depending on the change in the PRF preparation protocol. At high relative centrifugal force (RCF), they obtained PRF with TGF- β 1 less than 2000 pg/mL and VEGF equal to 0 pg/mL. The use of a moderate RCF protocol increases the concentration of growth factors, resulting in TGF- β 1 greater than 2000 pg/mL and VEGF greater than 10 pg/mL. On the other hand, when RCF was reduced to low, a 2-fold increase in growth factors was observed, resulting in TGF- β 1 > 4000 pg/mL and VEGF > 20 pg/mL [59]. Due to the high concentration of growth factors, A-PRF has the potential to mimic the physiology and immunology of wound healing [60]. During the production of A-PRF, it is important to maintain platelets, leukocytes, circulating stem cells and endothelial cells in the fibrin clot [9]. In the A-PRF obtained by the Choukroun et al. group method, the white blood cell count includes more neutrophils, which ensures tissue regeneration and vessel formation [61] due to its ability to promote the anti-inflammatory state of macrophages [60]. As mentioned by Wend et al., in addition to solid PRF, there is a clinical need to develop injectable PRF matrices for various clinical procedures and to improve angiogenic potential through the ability to combine i-PRF with various biomaterials [52]. Figure 2 shows the advantages of i-PRF and A-PRF. The idea of the review is to show that these 2 types of PRFs can be used as candidates for the development of drug delivery systems. That they are the ones that contain more growth factors that can ensure wound healing.

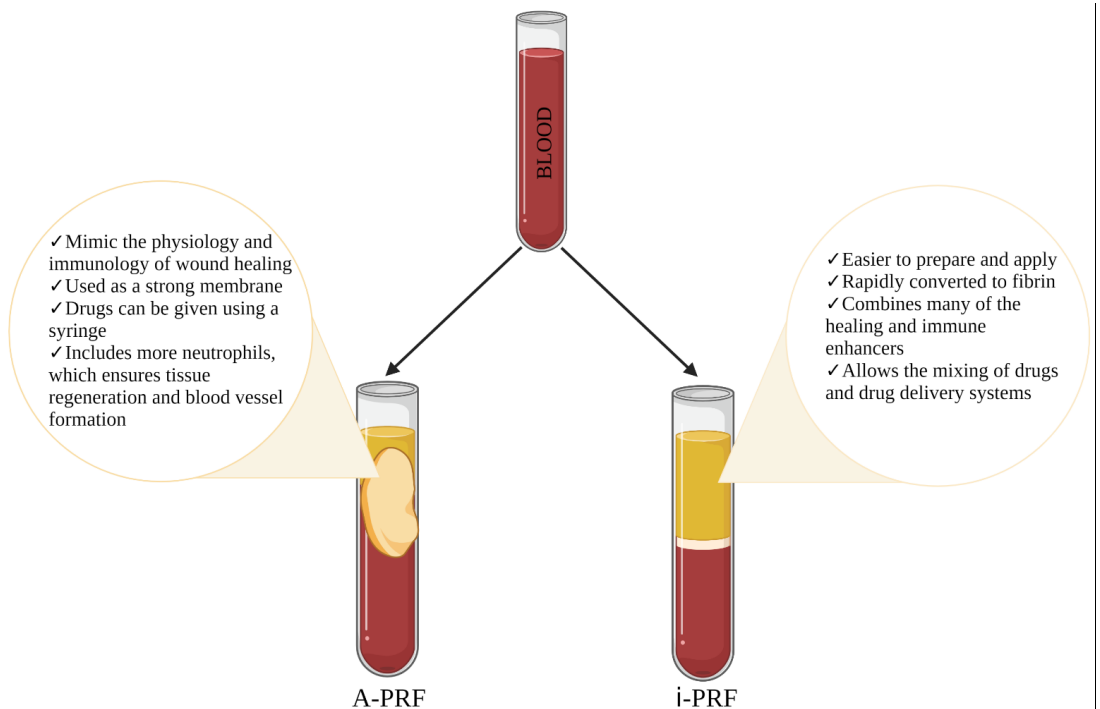


Figure 2. Comparison of the advantages for two concentrates i-PRF and A-PRF. Figure created with Biorender.com.

4. Therapeutic Enhancement of PRF

The most common postoperative risk of minor surgeries is infection caused by membrane exposure and colonization of wound bacteria [62,63]. PRF itself may show antibacterial activity, but it has not been relatively well studied and there are insufficient data on what affects it. The main unanswered questions are: 1. Does it depend on the concentration or on the characteristics of the patient's blood? 2. If derived from a patient, then what properties are crucial to obtain a PRF antibacterial? There are also no data against which bacteria PRF itself may be antibacterial and which certain antibiotics must be added. In an attempt to delve into this issue, studies were found describing the antibacterial activity of L-PRF (leukocyte- and platelet-rich fibrin) [64,65] and H-PRF (PRF prepared by horizontal centrifugation) samples [65]. Another study looked at the antimicrobial properties of i-PRF against biofilm formation produced by certain *Staphylococcal* isolates, indicating the need to further investigate the antimicrobial properties of i-PRF based on an *in vivo* model [66]. This is also confirmed by other studies indicating that PRF has only mild antibacterial activity against some bacterial agents, including *S. aureus*, and does not show efficacy against resistant bacteria [67,68]. In turn, it is known that there are other bacterial isolates against which i-PRF would need to be antibacterial.

Oral administration of drugs is sometimes ineffective because absorption is irregular and incomplete in the most cases. Changes in drug solubility can occur as a result of reaction with other materials in the gastrointestinal tract. It is not suitable for emergencies where the medication must be taken as soon as possible, since the onset of action of the oral medication is relatively slow (long process from intake to destination) [69]. In addition, a significant advantage of local drug delivery is the ability to achieve high and stable local drug concentrations without high systemic doses, thereby reducing systemic toxicity [70]. Based on the collected literature on the antibacterial properties of PRF, we believe that it

would be ideal to combine it with drugs to form a single system, rather than using separate drugs and PRF. In the last decade, there are few studies that combine antibiotics with PRF to provide an antibacterial effect.

The literature has reported that PRF is often combined with drugs, such as metronidazole, clindamycin, penicillin [71], vancomycin, teicoplanin, gentamicin, or amikacin to kill bacteria and speed up the healing process [72]. Today, in oral and maxillofacial surgery (including the prevention and treatment of osteonecrosis of the jaw [73]), there is an increasing demand for clindamycin as a drug. It is widely regarded as an alternative for patients who have an allergic reaction to penicillin [74]. Below we have shown the possible applications of PRF with drugs, the studies are systematized by drug classes.

The studies related to the combination of PRF with the drugs are shown in the Table 4.

Table 4. Various drugs for inclusion in platelet-rich fibrin system (summary of the drugs in platelet-rich fibrin system).

Drug	Incorporation Method	Time of the Study	Reference
Clindamycin	Drug mixing in a blood sample, use of PRF clot	4 days	[71]
Lincomycin	Drug mixing in a blood sample, use of PRF clot	10 days antibacterial activity	[75,76]
Amikacin, teicoplanin or polyhexanide or	PRF mixing with drug, using co-delivery applicator	168 h for amikacin, 120 h for teicoplanin and 24 h for polyhexanide antimicrobial effect	[72]
1% Alendronate gel	PRF combined with drugs	9 months	[77,78]
1.2% Atorvastatin	Drug combination with PRF and open flap debridement (OFD)	9 months	[79]
1.2% Rosuvastatin gel	Drug gel adding into PRF membrane	9 months	[80]
1% Metformin	Drug combination with PRF and OFD	9 months	[81–83]
Diclofenac sodium	Drugs injected in PRF using needle	7 days	[84]
Triple antibiotic mixture (MET + CIP + MINO)	Antibiotic mixture mixing with i-PRF, i-PRF scaffold prepare	28 days	[85]
0.5% Metronidazole	Metronidazole added to the PRF membrane combined with freeze-dried bone allograft	10 weeks	[86]
Amoxicillin	Drugs used orally 1 h before blood collection	48 h	[64]

4.1. Antibiotics

Antibiotics are considered to be an effective treatment for various types of infections caused by bacteria (gram-positive and gram-negative). In turn, their misuse can lead to antibiotic resistance [87]. Wound healing is a normal biological process in the human body, but in the postoperative period there is a high risk that there may be factors that will affect this process. It is important to ensure a proper healing process and reduce the risk of infections [88]. For wound healing, PRF can also be used as a drug carrier in another system. Therefore, we collected the literature in which PRF is used in combination with antibiotics to determine if PRF can provide antibiotic therapy at wound sites. One of the discovered studies described a method in which PRF together with one of 3 different drugs

(amikacin, teicoplanin, and polyhexanide (a group of drugs used to treat wounds)) was sprayed onto a patch and tested for antimicrobial activity for 7 days. The results showed that for amikacin antimicrobial activity was observed up to 120 h, for teicoplanin—168 h, while for polyhexanide it can be observed only for 24 h [72]. This study indicates that it is possible to obtain a system in which certain drugs are dispensed at a specific time, providing the necessary therapy.

Lincosamides

This class of drugs is obtained from *Streptomyces spp.* [89]. Lincosamides are mainly used to treat anaerobic infections caused by gram-positive organisms, including infections developed by methicillin resistant *Staphylococcus aureus* [90]. Originally this class of antibiotics comes from natural product lincomycin, but derivatives also include clindamycin and pirlimycin, from which clindamycin is the most clinically relevant lincosamide [90,91]. Drugs such as lincomycin and clindamycin are bacteriostatic and inhibit protein synthesis. In the same way, both drugs are used in clinical practice and at higher concentrations in vivo, they will become bactericide [92]. Clindamycin has been shown to be more effective than lincomycin in treating bacterial infections. In turn, doctors choose it for the treatment of odontogenic infections. The choice of doctors can be explained by the fact that clindamycin has not only bactericidal activity, but also significant tissue distribution and low resistance [93].

Summarizing the literature on current in vitro studies, it was found that there was one study in which lincosamide, a clindamycin, was included in the A-PRF. There is direct mixing of the drug in the blood sample and afterwards A-PRF clot was used. This system is relatively easy to obtain and can provide drug release for up to 4 days. However, in order to be used for further studies, it would have to be processed if a non-cylindrical sample was required. Additionally, this sample is not injectable, so it can be used as a ready-made clot, without the possibility to use to fill the defect site. In addition, this study lacks data on the effectiveness of drug encapsulation, which cannot predict what percentage of added drugs are encapsulated [71]. The effect of lincomycin form and volume on the antibacterial activity of PRF after 24 h, 48 h, 120 h, and 240 h was also studied using the drug in 3 forms (ampoule, capsule-mixed with saline and powder). The results showed that greater antibacterial activity was obtained by adding ampoule-type lincomycin to a blood sample [75,76].

4.2. Bisphosphonates

It is a group of medicines that are used in osteoporosis (a systemic skeletal disease that results in increased bone fragility and susceptibility to fractures [94]) and when the bone is not formed properly [95]. The most common condition that causes bone defects is periodontitis (an inflammatory disease of the supporting tissues of the teeth caused by certain microorganisms or groups of certain microorganisms [96]). It is believed that intrabony defects are less prevalent than horizontal bone loss. Intrabony defects pose a risk of disease progression and need to be treated. Looking at the literature, one gets the impression that not all intrabony defects can be cured. Due to the development of new biomaterials by scientists, it is likely that dental prognosis will be improved [97]. An interesting fact is that the combination of PRF with drugs can be used to treat this disease. Some studies [77,78] have described that PRF is used in combination with drugs, such as alendronate (ALN) to treat this disease. In the first study, combining 1% ALN gel with A-PRF, the researchers tried to prove the effectiveness of a combination of the two in treating grade II mandibular furcation defects compared to PRF. The PRF/1% ALN gel composition allowed to fill a higher percentage of defects ($56.01 \pm 2.64\%$), where simply for PRF therapy ($49.43 \pm 3.70\%$), indicating that the PRF/1% ALN combination has a recovery potential [77]. In the second study, the PRF/1% ALN combination is already being studied for the treatment of intrabony defect in chronic periodontitis. As in the previous study, the PRF/1% ALN combination was able to provide a greater reduction in defect depth

(54.05 ± 2.88%) compared to PRF (46 ± 1.89%) [78]. As can be seen, both studies have similar results, confirming the reliability of the results of the PRF/1% ALN combination. This study indicates that the use of PRF in combination with a bisphosphonate drug can be used to reduce the size of the defect.

4.3. Statins

It is a class of drugs that is effectively used to lower cholesterol and also to reduce the risk of cardiovascular morbidity and mortality [98]. At the time of writing this report, studies were found where a representative of this class of drugs is used in the treatment of intrabony defects. Martande et al. in their study used 1.2% atorvastatin gel in combination with A-PRF and open flap debridement (OFD) to achieve the desired outcome [79]. Scientists have concluded that additional studies related to the use of PRF in the treatment of intrabony defects may reduce the number of patients with periodontitis. Another study also looked at the effect of the combination of the drugs and the PRF on clinical parameters. In this study alone, rosuvastatin (RSV) was selected as a drug, and the effects of open-flap debridement (OFD) with or without PRF and PRF/RSV were further investigated. In the present study, Pradeep et al. study results showed that combining RSV with PRF provided greater periodontal benefits compared to OFD alone or OFD/PRF [80]. The results of this study are similar to those of Pradeep et al. studies where RSV gel was used in combination with PRF and hydroxyapatite bone graft [99]. Both of the above studies indicate that statin drugs can be used not only for the treatment of blood and vascular diseases, but also for the treatment of other, no less common diseases, thus expanding the use of the drug.

4.4. Biguanides

Biguanides are a class of herbal drugs [100] classified as non-sulfonylureas that act directly against insulin resistance [101]. In addition to one of the drugs in the class of statins, biguanide drugs can be used to treat intrabony defects. As one of these drugs, Pradeep et al. used 1% metformin (MTF) in combination with A-PRF and OFD in their study [83]. As with statins, metformin has been shown to reduce periodontitis. A similar study was performed Taneja et.al, comparing the differences between PRF/MFT and PRF at 6 and 9 months [82]. A study was also found evaluating the possible use of OFD/PRF/MFT in the treatment of grade II mandibular furcation defects [81]. It has been shown that biguanide drugs in combination with PRF is widely used in periodontal therapy, which indicates the ability of PRF to be a drug delivery vehicle.

4.5. Non-Steroidal Anti-Inflammatory Drugs

This class of drugs is one of the most widely used therapeutic classes in clinical medicine [102]. Additionally, drugs in PRF can be incorporated not only by mixing in the blood or by mixing with i-PRF, they can be injected with a needle into the A-PRF clot obtained after centrifugation. This method was used by Pillai et al. in their study to administer diclofenac to test whether the PRF as a carrier would be able to deliver the drugs locally. Their study was more based on comparing pure PRF with PRF/diclofenac on the basis of clinical parameters (postoperative pain, swelling, soft tissue healing, and infection risk, etc.). The obtained results confirmed the hypothesis that PRF/diclofenac gel improves the clinical parameters, thus indicating that such a method of drug administration can improve the wound healing process and promote bone regeneration [84].

4.6. PRF Combination with Several Drugs

Another interesting fact is that PRF can combine not only one type of drugs, but also a mixture of several drugs. In the study where i-PRF was mixed with the triple drug mixture (metronidazole (MET), ciprofloxacin (CIP), minocycline (MINO)), release was observed for up to 28 days, but burst release was already observed within the first 24 h [85]. If a high concentration one of these drugs is included in the i-PRF with a view to prolonged therapy, it is likely that a toxic drug concentration will be released within the first 24 h and

the required controlled drug therapy will not be achieved. The study also says that the simultaneous release of all three drugs takes only 14 days, followed by the release of only MINO and MET, resulting in the loss of i-PRF from its initial use.

4.7. PRF Combination with Materials and Drugs

Another way to restore diseased or damaged bones is bone grafting. Nowadays, it receives a lot of attention today due to the slow and difficult integration of the grafted material. Platelet concentrates are used to improve this integration process, which also accelerates bone and mucosal healing. PRF is no exception, which, regardless of the way it is used (membranes or fragments), can be used to protect a surgical site after surgery. To protect the bone graft from anaerobic bacterial infections, the Simonpieri team added metronidazole to the PRF membrane combined with freeze-dried bone allograft. In addition, the combination of these two excipients improved the histological quality of bone tissue in the graft [86].

In most cases, the drugs are mixed into the PRF, creating the necessary material to treat a specific problem. In contrast, there is a study in which the drug is first taken orally, indicating that administration of the drug to a previously acquired PRF system is not the only way to improve antibacterial efficacy. This time, an attempt was made to determine whether L-PRF, prepared after a single dose of oral antibiotic, was able to produce significant antimicrobial activity within 48 h. After 48 h, no sterile area was observed, indicating that 1 dose of oral antibiotic was insufficient to provide 48 h of antimicrobial activity. The data suggest that most antibiotics are concentrated in plasma and that only a small proportion of them end up in the PRF [64]. The drug concentration in the PRF after an oral drug consumption should be determined. The calculated amount could be used as ground for further use of the drugs. Additionally, it has to be investigated, is the calculated amount of the drug is safe to use in medical practice.

Looking at all of the studies described above, there is a tendency to combine PRF with drugs. However, several of these studies show insufficient analysis and lack of data (drug release time and amount).

5. PRF as a Bioactive Agent in Different Matrices

One of the main requirements for carrier systems is the controlled release of the drugs and growth factors they contain (the bioactive molecule is delivered locally or systemically at a specific rate over a period of time). There are studies describing the successful combination of cells and growth factors or biomolecules with non-autologous fibrin. In turn, the autologous liquid i-PRF offers additional advantages as a carrier system for cells and growth factors [45] (Figure 3).

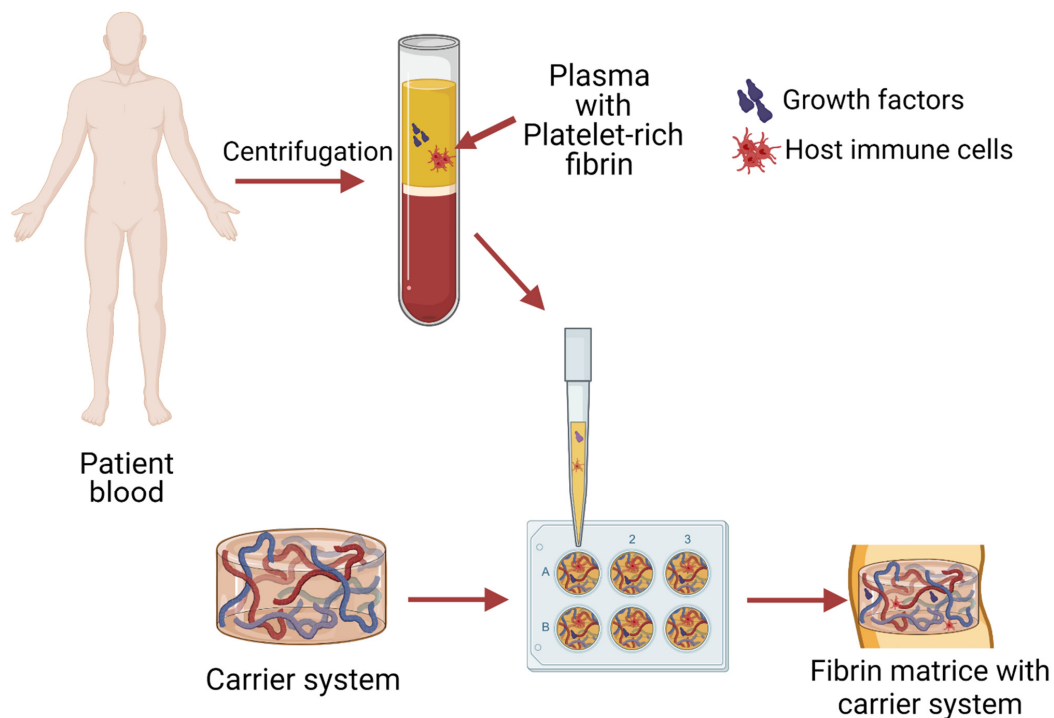


Figure 3. Principle scheme of platelet-rich fibrin as a carrier system preparation. Human blood is centrifuged by separating the PRF with a plasma layer. Obtained PRF is added it to pre-prepared carrier systems to obtain a PRF/drug carrier matrices. Figure created with Biorender.com.

In this section, we have summarized the studies in which the PRF serves as a carrier system of bioactive molecules or was included in one of the carrier systems (Table 5).

Table 5. Carrier systems incorporated in injectable platelet-rich fibrin.

Carrier System	Target	Incorporation Method	Time of the Study	Reference
G-L-PRF	Accelerate wound healing	Fresh lyophilized PRF added to PVA hydrogels (simple physical method)	9 days	[103]
PRF granules	Improve periodontal healing	PDLSC cultivated with PRF membrane	7 days	[104]
PRF membrane	Improve wound healing	TGF β -1, PDGF-AB, VEGF and TSP-1 included in PRF	7 days	[105]
Fibrin glue	Enrich the microenvironment with growth factors	Adding PRF into DBC/fibrin glue	36 weeks	[106]
Gelatin nanoparticles	Get mechanically tough and bioactive hydrogel	Mixing i-PRF with GNPs by repetitive extrusion	3 weeks	[107]
Collagen membrane	Enhance the bioactivity of collagen-based biomaterials	Liquid-PRF is applied to collagen membrane	24 h	[108]

Table 5. Cont.

Carrier System	Target	Incorporation Method	Time of the Study	Reference
PRF	Prevent peri-implant defect	Silk fibroin mixing with PRF in vivo	8 weeks	[109]
PRF membrane	Treatment of furcation defect	β -TCP granules insertion at the defect site and sealing with a PRF membrane	9 months	[110]
PRF membrane	Treatment of intrabony defects	ABBM mixed with PRF	6 months	[111]
PRF membrane	Treatment for periodontal intrabony defects	BPBM mixed with PRF	6 months	[112]

PRF could not only serve as a carrier, but also be placed in another material. Xu et al. group described a study in which fresh granule-lyophilized platelet-rich fibrin (G-L-PRF) was incorporated into polyvinyl alcohol (PVA) hydrogels to improve wound healing. The results showed that increasing the G-L-PRF concentration could improve the mechanical strength and degradation rate of the scaffolds, but the concentration did not affect the flexibility and biocompatibility of the scaffolds. Regarding growth factors, the incorporation of G-L-PRF into PVA hydrogels provided a sustained and controlled release of growth factors from G-L-PRF/PVA scaffolds for up to 9 days [103]. Summarizing the literature, it was found that using PRF it is possible to develop a cell transplantation method. Such a method was developed in vitro by Zhao and his team using periodontal ligament stem cell (PDLSC) cell sheet fragments and PRF granules. The aim of this study was to improve periodontal healing in avulsed dental re-implantation. The results of the study showed that PRF induces significant and continuous stimulation of proliferation in human PDLSC throughout the 7-day incubation period, suggesting that the PDLSC/PRF construct may improve clinical outcomes in subsequent dental re-implantations. However, before using this method in patients, additional studies on the molecular mechanisms of the PDLSC/PRF interaction are required to ensure reliable results [104].

Returning to wound healing, growth factors are worth mentioning as they play an important role in the healing stages. Platelets are the main cell type in the inflammatory phase as they release PDGF and TGF- β . Both are growth factors that attract macrophages and neutrophils [113]. Therefore, it cannot be forgotten that PRF itself can serve as a matrices for the growth factors that are in every person's blood. In their study, Ehrenfest et al. described three growth factors (TGF β -1, PDGF-AB, VEGF) and coagulation matrix cellular protein, thrombospondin-1, (TSP-1), and the ability to release them in large amounts from the PRF membrane within 7 days. The results showed that comparing the amount of growth factors initially released to the end, it can be concluded that the leukocytes in PRF provide high TGF β -1 and VEGF release throughout the experiment [105]. It turns out that PRF can be combined with other related materials to improve recovery. More specifically, this is described in a study by Yang et al., in which dental bud cells (DBC) were suspended in fibrin glue (used as one of the most effective scaffold materials) and then A-PRF was added. Thus, the restoration of dental tissue was achieved [106].

One of the studies is a double network (DN) hydrogel of i-PRF and gelatin nanoparticles (GHPs), with the aim to obtain a mechanically strong and bioactive hydrogel that can adapt to the irregular shape of the defect and withstand the required pressure. During this study, the release of growth factors (VEGF, platelet derived growth factor-BB (PDGF-BB), TGF- β and IGF-1) was observed for more than 3 weeks. This is higher compared to other studies [44,52] where in vitro release from pure i-PRF gel occurred in 2 weeks. In addition, DN hydrogels prevent the burst release of growth factors during the first hours [107]. The in vivo studies, described above, have shown that PRF matrices can be perceived as carrier systems due to their ability to release growth factors.

It should also be mentioned that the PRF can serve not only as a drug delivery system but also as a matrices of other materials. One *ex vivo* study analyzed the ability of the i-PRF matrix to be a autologous growth factor delivery system in combination with 5 collagen-based membranes. Thus, this was the first study that attempted to understand the ability and suitability of biomaterials to incorporate PRF. The assay was performed by separating leukocytes and platelets across the collagen membrane and determining the interaction between the collagen membrane and i-PRF. The obtained results showed differences in the structural composition of collagen membranes and differences in the interaction of collagen-based biomaterials with liquid PRF [108]. The obtained data confirmed the previous results that the interaction of the cell with the biomaterial is partially determined by the structural properties of the biomaterial [114,115]. Scientists have also tried to combine silk fibroin powder from *Bombyx mori* with Choukroun PRF. The results showed that the combination of these two materials can successfully prevent peri-implant defect [109]. Regarding the inclusion of other materials in PRF, a new approach to the use of PRF for the treatment of periodontitis defect has been explored. The approach is based on the placement of beta-tricalcium phosphate (β -TCP) granules at the furcation defect site, followed by the application of a PRF membrane covering both the defect site and the bone graft. Despite the successful results, this method requires additional research to ensure its suitability [110]. While searching for articles on the treatment of periodontitis, we found that PRF in combination with other materials can also be used to treat intrabony defects. In one such study, researchers combined PRF with an anorganic bovine bone (material for transplantation into alveolar cavities after human extraction [116]) mineral (ABBM), indicating that it is effective in treating these defects and may increase the rate of clinical attachment [111]. A similar study was carried out by the Lekovic group, where A-PRF was combined with bovine porous bone mineral (BPBM) instead of ABBM. Combining BPBM with A-PRF resulted in significantly greater reductions in pocket depth, increased clinical attachment, and defect filling than PRF used alone [112].

Summarizing all the above studies, it is observed that when using PRF as a matrices or including it in another carrier system, there is no need to add growth factors, as PRF itself includes certain growth factors. The only thing to consider, then, is the encapsulation of the desired drug and its interaction with other carriers that will be included in the PRF. It is also important to investigate whether the used carrier system will be able to ensure the controlled release of the growth factors that are in the PRF.

6. Conclusions and Future Perspectives

Summarizing the literature on the possible application of PRF, it has been observed that nowadays there is a growing demand for its application in operations. Several pieces of clinical research shows that PRF can be used in different surgeries, such as open-heart surgery, cranial surgery, endodontic surgeries, and periodontitis [117]. This allows surgeons to use the beneficial properties of PRF to solve a given problem, such as closing a defect and improving recovery. PRF is also widely studied as a drug delivery system to reduce the risk of postoperative infections.

Although platelet-rich fibrin is autologous and contains growth factors and cells, its antibacterial properties are not specifically expressed. In addition, analgesics, anticancer, and other therapies that would otherwise be administered intravenously or orally may be added to the PRF. For optimal drug use, it is necessary to study the effect of interaction between PRF and drug on controlled release of the drug and the ability of the sample to retain properties, such as biocompatibility, biodegradability, mechanical strength, and shape retention. Already additional biomaterials are being added to the PRF to provide these properties. However, there is a need to further explore the ability of this biomaterial to be a drug delivery system, combining the ability of PRF to retain growth factors and incorporate drugs.

Current research shows that most drug or drug delivery systems are mixed with the A-PRF clot or its membrane, and the amount of growth factors or the antibacterial activity

of the material is studied. It seems that studies of the kinetics of drug release from the investigated samples are insufficient. Therefore, we propose to continue the study of i-PRF as a matrix for drug delivery systems, including liquid i-PRF before coagulation, and to test the ability of the material to provide controlled drug delivery. Only an understanding of the ability of these materials to be combined with other biomaterials and drugs will allow us to obtain new biomaterials with the necessary properties for use not only in maxillofacial surgery, but also in healing burns, neurosurgery, cartilage and tendon repair, and other fields.

Author Contributions: Conceptualization, writing—original draft preparation, visualization, K.E.; review and editing, I.S.; review, supervision and funding acquisition, A.D. All authors have read and agreed to the published version of the manuscript.

Funding: This research was funded by the Latvian Council of Science research project No. Izp-2020/1-0054 “Development of antibacterial autologous fibrin matrices in maxillofacial surgery (MATRI-X)”.

Institutional Review Board Statement: No applicable.

Informed Consent Statement: No applicable.

Data Availability Statement: No applicable.

Acknowledgments: This work was also supported by the European Union’s Horizon 2020 research and innovation program under the grant agreement No 857287.

Conflicts of Interest: The authors declare no conflict of interest.

References

- Garraud, O.; Cognasse, F. Are Platelets Cells? And if Yes, are They Immune Cells? *Front. Immunol.* **2015**, *6*, 70. [[CrossRef](#)]
- Miron, R.J.; Fujioka-Kobayashi, M.; Bishara, M.; Zhang, Y.; Hernandez, M.; Choukroun, J. Platelet-Rich Fibrin and Soft Tissue Wound Healing: A Systematic Review. *Tissue Eng. Part B Rev.* **2017**, *23*, 83–99. [[CrossRef](#)] [[PubMed](#)]
- Anitua, E.; Sánchez, M.; Nurdén, A.T.; Nurdén, P.; Orive, G.; Andía, I. New insights into and novel applications for platelet-rich fibrin therapies. *Trends Biotechnol.* **2006**, *24*, 227–234. [[CrossRef](#)] [[PubMed](#)]
- Shashank, B.; Bhushan, M. Injectable Platelet-Rich Fibrin (PRF): The newest biomaterial and its use in various dermatological conditions in our practice: A case series. *J. Cosmet. Dermatol.* **2021**, *20*, 1421–1426. [[CrossRef](#)]
- Dohan, D.M.; Choukroun, J.; Diss, A.; Dohan, S.L.; Dohan, A.J.J.; Mouhyi, J.; Gogly, B. Platelet-rich fibrin (PRF): A second-generation platelet concentrate. Part II: Platelet-related biologic features. *Oral Surg. Oral Med. Oral Pathol. Endodontol.* **2006**, *101*, e45–e50. [[CrossRef](#)]
- Arora, R.; Shukla, S. Injectable-platelet-rich fibrin-smart blood with stem cells for the treatment of alopecia: A report of three patients. *Int. J. Trichol.* **2019**, *11*, 128. [[CrossRef](#)]
- Clark, D.; Rajendran, Y.; Paydar, S.; Ho, S.; Cox, D.; Ryder, M.; Dollard, J.; Kao, R.T. Advanced platelet-rich fibrin and freeze-dried bone allograft for ridge preservation: A randomized controlled clinical trial. *J. Periodontol.* **2018**, *89*, 379–387. [[CrossRef](#)] [[PubMed](#)]
- Toffler, M.; Toscano, N.; Holtzclaw, D.; Corso, M.D.; Ehrenfest, D.D. Introducing Choukroun’s Platelet Rich Fibrin (PRF) to the Reconstructive Surgery Milieu. *J. Implant Adv. Clin. Dent.* **2009**, *1*, 21–32.
- Ravi, S.; Santhanakrishnan, M. Mechanical, chemical, structural analysis and comparative release of PDGF-AA from L-PRF, A-PRF and T-PRF—An in vitro study. *Biomater. Res.* **2020**, *24*, 16. [[CrossRef](#)] [[PubMed](#)]
- Lee, J.-W.; Kim, S.-G.; Kim, J.-Y.; Lee, Y.-C.; Choi, J.-Y.; Dragos, R.; Rotaru, H. Restoration of a peri-implant defect by platelet-rich fibrin. *Oral Surg. Oral Med. Oral Pathol. Oral Radiol.* **2012**, *113*, 459–463. [[CrossRef](#)]
- Marques, L.F.; Stessuk, T.; Camargo, I.C.C.; Sabeh Junior, N.; Santos, L.D.; Ribeiro-Paes, J.T. Platelet-rich plasma (PRP): Methodological aspects and clinical applications. *Platelets* **2015**, *26*, 101–113. [[CrossRef](#)] [[PubMed](#)]
- Antoniades, H.N.; Galanopoulos, T.; Neville-Golden, J.; Kiritsy, C.P.; Lynch, S.E. Injury induces in vivo expression of platelet-derived growth factor (PDGF) and PDGF receptor mRNAs in skin epithelial cells and PDGF mRNA in connective tissue fibroblasts. *Proc. Natl. Acad. Sci. USA* **1991**, *88*, 565–569. [[CrossRef](#)]
- Pavlovic, V.; Ciric, M.; Jovanovic, V.; Stojanovic, P. Platelet Rich Plasma: A short overview of certain bioactive components. *Open Med.* **2016**, *11*, 242–247. [[CrossRef](#)] [[PubMed](#)]
- Antoniades, H.N. Human platelet-derived growth factor (PDGF): Purification of PDGF-I and PDGF-II and separation of their reduced subunits. *Proc. Natl. Acad. Sci. USA* **1981**, *78*, 7314–7317. [[CrossRef](#)] [[PubMed](#)]
- Nikolidakis, D.; Jansen, J.A. The Biology of Platelet-Rich Plasma and Its Application in Oral Surgery: Literature Review. *Tissue Eng. Part B Rev.* **2008**, *14*, 249–258. [[CrossRef](#)] [[PubMed](#)]
- Pavlovic, V.; Ciric, M.; Jovanovic, V.; Trandafilovic, M.; Stojanovic, P. Platelet-rich fibrin: Basics of biological actions and protocol modifications. *Open Med.* **2021**, *16*, 446–454. [[CrossRef](#)] [[PubMed](#)]

17. Vinaya Kumar, R.; Shubhashini, N. Platelet rich fibrin: A new paradigm in periodontal regeneration. *Cell Tissue Bank.* **2013**, *14*, 453–463. [[CrossRef](#)] [[PubMed](#)]
18. Hock, J.M.; Centrella, M.; Canalis, E. Insulin-Like Growth Factor I Has Independent Effects on Bone Matrix Formation and Cell Replication. *Endocrinology* **1988**, *122*, 254–260. [[CrossRef](#)] [[PubMed](#)]
19. Provenzano, P.P.; Alejandro-Osorio, A.L.; Grorud, K.W.; Martinez, D.A.; Vailas, A.C.; Grindeland, R.E.; Vanderby, R. Systemic administration of IGF-I enhances healing in collagenous extracellular matrices: Evaluation of loaded and unloaded ligaments. *BMC Physiol.* **2007**, *7*, 2. [[CrossRef](#)] [[PubMed](#)]
20. Dohan, D.M.; Choukroun, J.; Diss, A.; Dohan, S.L.; Dohan, A.J.J.; Mouhyi, J.; Gogly, B. Platelet-rich fibrin (PRF): A second-generation platelet concentrate. Part III: Leucocyte activation: A new feature for platelet concentrates? *Oral Surg. Oral Med. Oral Pathol. Oral Radiol. Endodontol.* **2006**, *101*, e51–e55. [[CrossRef](#)] [[PubMed](#)]
21. Ruhrberg, C. Growing and shaping the vascular tree: Multiple roles for VEGF. *BioEssays* **2003**, *25*, 1052–1060. [[CrossRef](#)] [[PubMed](#)]
22. Dhillon, R.S.; Schwarz, E.M.; Maloney, M.D. Platelet-rich plasma therapy—Future or trend? *Arthritis Res. Ther.* **2012**, *14*, 219. [[CrossRef](#)] [[PubMed](#)]
23. Duffy, A.M.; Bouchier-Hayes, D.J.; Harmey, J.H. Vascular Endothelial Growth Factor (VEGF) and Its Role in Non-Endothelial Cells: Autocrine Signalling by VEGF. In *VEGF and Cancer*; Springer: Boston, MA, USA, 2004; pp. 133–144.
24. Lopez-Castejon, G.; Brough, D. Understanding the mechanism of IL-1 β secretion. *Cytokine Growth Factor Rev.* **2011**, *22*, 189–195. [[CrossRef](#)] [[PubMed](#)]
25. Hwang, D.H. Dietary Modulation of Inflammation. In *Encyclopedia of Human Nutrition*; Elsevier: Amsterdam, The Netherlands, 2013; pp. 74–78.
26. Tanaka, T.; Narazaki, M.; Kishimoto, T. IL-6 in Inflammation, Immunity, and Disease. *Cold Spring Harb. Perspect. Biol.* **2014**, *6*, a016295. [[CrossRef](#)] [[PubMed](#)]
27. Xue, X.; Falcon, D.M. The Role of Immune Cells and Cytokines in Intestinal Wound Healing. *Int. J. Mol. Sci.* **2019**, *20*, 6097. [[CrossRef](#)]
28. Gadani, S.P.; Cronk, J.C.; Norris, G.T.; Kipnis, J. IL-4 in the Brain: A Cytokine To Remember. *J. Immunol.* **2012**, *189*, 4213–4219. [[CrossRef](#)] [[PubMed](#)]
29. Melissa, A.; Guise, T.A.; David, R.G. Cytokine Regulation of Bone Cell Differentiation. In *Vitamins and Hormones*; Elsevier Masson SAS: Issy-les-Moulineaux, France, 1996; Volume 52, pp. 63–98.
30. Rossi, C.; Cusimano, M.; Zambito, M.; Finardi, A.; Capotondo, A.; Garcia-Manteiga, J.M.; Comi, G.; Furlan, R.; Martino, G.; Muzio, L. Interleukin 4 modulates microglia homeostasis and attenuates the early slowly progressive phase of amyotrophic lateral sclerosis. *Cell Death Dis.* **2018**, *9*, 250. [[CrossRef](#)]
31. Salmon-Ehr, V.; Ramont, L.; Godeau, G.; Birembaut, P.; Guenounou, M.; Bernard, P.; Maquart, F.-X. Implication of Interleukin-4 in Wound Healing. *Lab. Invest.* **2000**, *80*, 1337–1343. [[CrossRef](#)] [[PubMed](#)]
32. Fitzgerald, K.A.; O'Neill, L.A.J.; Gearing, A.J.H.; Callard, R.E. TNF α . In *The Cytokine FactsBook and Webfacts*; Elsevier: Amsterdam, The Netherlands, 2001; pp. 474–480.
33. Ritsu, M.; Kawakami, K.; Kanno, E.; Tanno, H.; Ishii, K.; Imai, Y.; Maruyama, R.; Tachi, M. Critical role of tumor necrosis factor- α in the early process of wound healing in skin. *J. Dermatol. Dermatol. Surg.* **2017**, *21*, 14–19. [[CrossRef](#)]
34. Brockmann, L.; Giannou, A.; Gagliani, N.; Huber, S. Regulation of TH17 Cells and Associated Cytokines in Wound Healing, Tissue Regeneration, and Carcinogenesis. *Int. J. Mol. Sci.* **2017**, *18*, 1033. [[CrossRef](#)] [[PubMed](#)]
35. Choukroun, J.; Adda, F.; Schoeffler, C.; Vervelle, A. An opportunity in paro-implantology: PRF. *Implantodontie* **2001**, *42*, 55–62.
36. He, L.; Lin, Y.; Hu, X.; Zhang, Y.; Wu, H. A comparative study of platelet-rich fibrin (PRF) and platelet-rich plasma (PRP) on the effect of proliferation and differentiation of rat osteoblasts in vitro. *Oral Surg. Oral Med. Oral Pathol. Oral Radiol. Endodontol.* **2009**, *108*, 707–713. [[CrossRef](#)] [[PubMed](#)]
37. Jayadev, M.; Marshal, V.; Naik, B.; Karunakar, P. Role of Platelet rich fibrin in wound healing: A critical review. *J. Conserv. Dent.* **2013**, *16*, 284. [[CrossRef](#)] [[PubMed](#)]
38. Dohan, D.M.; Choukroun, J.; Diss, A.; Dohan, S.L.; Dohan, A.J.J.; Mouhyi, J.; Gogly, B. Platelet-rich fibrin (PRF): A second-generation platelet concentrate. Part I: Technological concepts and evolution. *Oral Surg. Oral Med. Oral Pathol. Oral Radiol. Endodontol.* **2006**, *101*, e37–e44. [[CrossRef](#)] [[PubMed](#)]
39. Owen, C.A.; Campbell, E.J. The cell biology of leukocyte-mediated proteolysis. *J. Leukoc. Biol.* **1999**, *65*, 137–150. [[CrossRef](#)]
40. Choukroun, J.; Diss, A.; Simonpieri, A.; Girard, M.-O.; Schoeffler, C.; Dohan, S.L.; Dohan, A.J.J.; Mouhyi, J.; Dohan, D.M. Platelet-rich fibrin (PRF): A second-generation platelet concentrate. Part IV: Clinical effects on tissue healing. *Oral Surg. Oral Med. Oral Pathol. Oral Radiol. Endodontol.* **2006**, *101*, e56–e60. [[CrossRef](#)] [[PubMed](#)]
41. Bielecki, T.; Dohan Ehrenfest, D.M. Platelet-Rich Plasma (PRP) and Platelet-Rich Fibrin (PRF): Surgical Adjuvants, Preparations for In Situ Regenerative Medicine and Tools for Tissue Engineering. *Curr. Pharm. Biotechnol.* **2012**, *13*, 1121–1130. [[CrossRef](#)] [[PubMed](#)]
42. Bennardo, F.; Bennardo, L.; Del Duca, E.; Patruno, C.; Fortunato, L.; Giudice, A.; Nisticò, S.P. Autologous platelet-rich fibrin injections in the management of facial cutaneous sinus tracts secondary to medication-related osteonecrosis of the jaw. *Dermatol. Ther.* **2020**, *33*, e13334. [[CrossRef](#)] [[PubMed](#)]

43. Kour, P.; Pudukalkatti, P.S.; Vas, A.M.; Swetalin, D.; Padmanabhan, S. Comparative Evaluation of Antimicrobial Efficacy of Platelet-rich Plasma, Platelet-rich Fibrin, and Injectable Platelet—Rich Fibrin on the Standard Strains of *Porphyromonas gingivalis* and *Aggregatibacter actinomycetemcomitans*. *Contemp. Clin. Dent.* **2018**, *9*, S325–S330. [[CrossRef](#)]
44. Miron, R.J.; Fujioka-Kobayashi, M.; Hernandez, M.; Kandalam, U.; Zhang, Y.; Ghanaati, S.; Choukroun, J. Injectable platelet rich fibrin (i-PRF): Opportunities in regenerative dentistry? *Clin. Oral Investig.* **2017**, *21*, 2619–2627. [[CrossRef](#)]
45. Miron, R.J.; Zhang, Y. Autologous liquid platelet rich fibrin: A novel drug delivery system. *Acta Biomater.* **2018**, *75*, 35–51. [[CrossRef](#)] [[PubMed](#)]
46. Jenne, C.N.; Urrutia, R.; Kubes, P. Platelets: Bridging hemostasis, inflammation, and immunity. *Int. J. Lab. Hematol.* **2013**, *35*, 254–261. [[CrossRef](#)]
47. Nurden, A. Platelets, inflammation and tissue regeneration. *Thromb. Haemost.* **2011**, *105*, S13–S33. [[CrossRef](#)]
48. Turiitto, V.; Weiss, H. Red blood cells: Their dual role in thrombus formation. *Science* **1980**, *207*, 541–543. [[CrossRef](#)] [[PubMed](#)]
49. Vinholt, P.J. The role of platelets in bleeding in patients with thrombocytopenia and hematological disease. *Clin. Chem. Lab. Med.* **2019**, *57*, 1808–1817. [[CrossRef](#)]
50. Bielecki, T.; Dohan Ehrenfest, D.M.; Everts, P.A.; Wiczkowski, A. The Role of Leukocytes from L-PRP/L-PRF in Wound Healing and Immune Defense: New Perspectives. *Curr. Pharm. Biotechnol.* **2012**, *13*, 1153–1162. [[CrossRef](#)] [[PubMed](#)]
51. Martin, P. Wound Healing—Aiming for Perfect Skin Regeneration. *Science* **1997**, *276*, 75–81. [[CrossRef](#)]
52. Wend, S.; Kubesch, A.; Orłowska, A.; Al-Maawi, S.; Zender, N.; Dias, A.; Miron, R.J.; Sader, R.; Booms, P.; Kirkpatrick, C.J.; et al. Reduction of the relative centrifugal force influences cell number and growth factor release within injectable PRF-based matrices. *J. Mater. Sci. Mater. Med.* **2017**, *28*, 188. [[CrossRef](#)] [[PubMed](#)]
53. Boyce, D.E. The role of lymphocytes in human dermal wound healing. *Br. J. Dermatol.* **2000**, *143*, 59. [[CrossRef](#)] [[PubMed](#)]
54. Ożańska, A.; Szymczak, D.; Rybka, J. Pattern of human monocyte subpopulations in health and disease. *Scand. J. Immunol.* **2020**, *92*, 1–13. [[CrossRef](#)] [[PubMed](#)]
55. Loya, K. Stem Cells. In *Handbook of Pharmacogenomics and Stratified Medicine*; Elsevier: Amsterdam, The Netherlands, 2014; pp. 207–231.
56. Lin, S.C.; Talbot, P. Stem Cells. In *Encyclopedia of Toxicology*; Elsevier: Amsterdam, The Netherlands, 2014; pp. 390–394.
57. Ghanaati, S.; Booms, P.; Orłowska, A.; Kubesch, A.; Lorenz, J.; Rutkowski, J.; Landes, C.; Sader, R.; Kirkpatrick, C.; Choukroun, J. Advanced Platelet-Rich Fibrin: A New Concept for Cell-Based Tissue Engineering by Means of Inflammatory Cells. *J. Oral Implantol.* **2014**, *40*, 679–689. [[CrossRef](#)] [[PubMed](#)]
58. Bannardo, F.; Liborio, F.; Barone, S.; Antonelli, A.; Buffone, C.; Fortunato, L.; Giudice, A. Efficacy of platelet-rich fibrin compared with triamcinolone acetonide as injective therapy in the treatment of symptomatic oral lichen planus: A pilot study. *Clin. Oral Investig.* **2021**, *25*, 3747–3755. [[CrossRef](#)]
59. Ghanaati, S.; Mourão, C.; Adam, E.; Sader, R.; Zadeh, H.; Al-Maawi, S. The role of centrifugation process in the preparation of therapeutic blood concentrates: Standardization of the protocols to improve reproducibility. *Int. J. Growth Factors Stem Cells Dent.* **2019**, *2*, 41. [[CrossRef](#)]
60. Caruana, A.; Savina, D.; Macedo, J.P.; Soares, S.C. From Platelet-Rich Plasma to Advanced Platelet-Rich Fibrin: Biological Achievements and Clinical Advances in Modern Surgery. *Eur. J. Dent.* **2019**, *13*, 280–286. [[CrossRef](#)]
61. Cabaro, S.; D’Esposito, V.; Gasparro, R.; Borriello, F.; Granata, F.; Mosca, G.; Passaretti, F.; Sammartino, J.C.; Beguinot, F.; Sammartino, G.; et al. White cell and platelet content affects the release of bioactive factors in different blood-derived scaffolds. *Platelets* **2018**, *29*, 463–467. [[CrossRef](#)]
62. Heal, C.; Buettner, P.; Browning, S. Risk factors for wound infection after minor surgery in general practice. *Med. J. Aust.* **2006**, *185*, 255–258. [[CrossRef](#)]
63. Zhang, J.; Xu, Q.; Huang, C.; Mo, A.; Li, J.; Zuo, Y. Biological properties of an anti-bacterial membrane for guided bone regeneration: An experimental study in rats. *Clin. Oral Implants Res.* **2010**, *21*, 321–327. [[CrossRef](#)] [[PubMed](#)]
64. Peck, M.; Hiss, D.; Stephen, L.; Maboza, E. Antibiotic release from leukocyte-and platelet-rich fibrin (L-PRF)—An observational study. *S. Afr. Dent. J.* **2018**, *73*, 268–270.
65. Feng, M.; Wang, Y.; Zhang, P.; Zhao, Q.; Yu, S.; Shen, K.; Miron, R.J.; Zhang, Y. Antibacterial effects of platelet-rich fibrin produced by horizontal centrifugation. *Int. J. Oral Sci.* **2020**, *12*, 32. [[CrossRef](#)] [[PubMed](#)]
66. Jasmine, S.; Thangavelu, A.; Janarthanan, K.; Krishnamoorthy, R.; Alshatwi, A.A. Antimicrobial and antibiofilm potential of injectable platelet rich fibrin—A second-generation platelet concentrate—Against biofilm producing oral staphylococcus isolates. *Saudi J. Biol. Sci.* **2020**, *27*, 41–46. [[CrossRef](#)] [[PubMed](#)]
67. Moojen, D.J.F.; Everts, P.A.M.; Schure, R.-M.; Overvest, E.P.; van Zundert, A.; Knape, J.T.A.; Castelein, R.M.; Creemers, L.B.; Dhert, W.J.A. Antimicrobial activity of platelet-leukocyte gel against *Staphylococcus aureus*. *J. Orthop. Res.* **2008**, *26*, 404–410. [[CrossRef](#)] [[PubMed](#)]
68. Bielecki, T.M.; Gazdzik, T.S.; Arendt, J.; Szczepanski, T.; Król, W.; Wielkoszynski, T. Antibacterial effect of autologous platelet gel enriched with growth factors and other active substances. *J. Bone Joint Surg. Br.* **2007**, *89-B*, 417–420. [[CrossRef](#)]
69. Homayun, B.; Lin, X.; Choi, H.-J. Challenges and Recent Progress in Oral Drug Delivery Systems for Biopharmaceuticals. *Pharmaceutics* **2019**, *11*, 129. [[CrossRef](#)]
70. Greenstein, G.; Polson, A. The Role of Local Drug Delivery in the Management of Periodontal Diseases: A Comprehensive Review. *J. Periodontol.* **1998**, *69*, 507–520. [[CrossRef](#)] [[PubMed](#)]

71. Polak, D.; Clemer-Shamai, N.; Shapira, L. Incorporating antibiotics into platelet-rich fibrin: A novel antibiotics slow-release biological device. *J. Clin. Periodontol.* **2019**, *46*, 241–247. [[CrossRef](#)] [[PubMed](#)]
72. Knafl, D.; Thalhammer, F.; Vossen, M.G. In-vitro release pharmacokinetics of amikacin, teicoplanin and polyhexanide in a platelet rich fibrin—layer (PRF)—A laboratory evaluation of a modern, autologous wound treatment. *PLoS ONE* **2017**, *12*, e0181090. [[CrossRef](#)]
73. Fortunato, L.; Bennardo, F.; Buffone, C.; Giudice, A. Is the application of platelet concentrates effective in the prevention and treatment of medication-related osteonecrosis of the jaw? A systematic review. *J. Cranio-Maxillofac. Surg.* **2020**, *48*, 268–285. [[CrossRef](#)]
74. Maestre-Vera, J.R. Treatment options in odontogenic infection. *Med. Oral Patol. Oral Cir. Bucal.* **2004**, *9*, 19–24.
75. Bahaa, M.H.D.; Alhaffar, A. New Protocol to Improve the Antibacterial Activity of Platelet Rich Fibrin—In Vitro Study. *Res. Sq.* **2021**, 1–17. [[CrossRef](#)]
76. Bahaa, M.H.D.; Alhaffar, A. Modi ed Protocol to Use Platelet Rich Fibrin (PRF) as a local antibiotic delivery system—In Vitro study. *Res. Sq.* **2021**, 1–16. [[CrossRef](#)]
77. Kanoriya, D.; Pradeep, A.R.; Garg, V.; Singhal, S. Mandibular Degree II Furcation Defects Treatment With Platelet-Rich Fibrin and 1% Alendronate Gel Combination: A Randomized Controlled Clinical Trial. *J. Periodontol.* **2017**, *88*, 250–258. [[CrossRef](#)]
78. Kanoriya, D.; Pradeep, A.R.; Singhal, S.; Garg, V.; Guruprasad, C.N. Synergistic Approach Using Platelet-Rich Fibrin and 1% Alendronate for Intraony Defect Treatment in Chronic Periodontitis: A Randomized Clinical Trial. *J. Periodontol.* **2016**, *87*, 1427–1435. [[CrossRef](#)] [[PubMed](#)]
79. Martande, S.S.; Kumari, M.; Pradeep, A.R.; Singh, S.P.; Suke, D.K.; Guruprasad, C.N. Platelet-Rich Fibrin Combined with 1.2% Atorvastatin for Treatment of Intraony Defects in Chronic Periodontitis: A Randomized Controlled Clinical Trial. *J. Periodontol.* **2016**, *87*, 1039–1046. [[CrossRef](#)]
80. Pradeep, A.R.; Garg, V.; Kanoriya, D.; Singhal, S. Platelet-Rich Fibrin with 1.2% Rosuvastatin for Treatment of Intraony Defects in Chronic Periodontitis: A Randomized Controlled Clinical Trial. *J. Periodontol.* **2016**, *87*, 1468–1473. [[CrossRef](#)] [[PubMed](#)]
81. Sharma, P.; Grover, H.; Masamatti, S.; Saksena, N. A clinicoradiographic assessment of 1% metformin gel with platelet-rich fibrin in the treatment of mandibular grade II furcation defects. *J. Indian Soc. Periodontol.* **2018**. [[CrossRef](#)]
82. Shah, M.; Patel, J.; Dave, D.; Shah, S. Comparative evaluation of platelet-rich fibrin with demineralized freeze-dried bone allograft in periodontal intraony defects: A randomized controlled clinical study. *J. Indian Soc. Periodontol.* **2015**, *19*, 56. [[CrossRef](#)]
83. Pradeep, A.R.; Nagpal, K.; Karvekar, S.; Patnaik, K.; Naik, S.B.; Guruprasad, C.N. Platelet-Rich Fibrin With 1% Metformin for the Treatment of Intraony Defects in Chronic Periodontitis: A Randomized Controlled Clinical Trial. *J. Periodontol.* **2015**, *86*, 729–737. [[CrossRef](#)]
84. Pillai, A.K.; Thomas, S.; Seth, S.; Jain, N.; Chobey, A. Platelet Rich Fibrin (PRF) Gel as Efficient Vehicle for Local Drug Delivery in Minor Oral Surgical Defects. *SVOA Dent.* **2021**, *2*, 185–191.
85. Rafiee, A.; Memarpour, M.; Taghvamanesh, S.; Karami, F.; Karami, S.; Morowvat, M.H. Drug Delivery Assessment of a Novel Triple Antibiotic-Eluting Injectable Platelet-Rich Fibrin Scaffold: An In Vitro Study. *Curr. Pharm. Biotechnol.* **2021**, *22*, 380–388. [[CrossRef](#)]
86. Simonpieri, A.; Del Corso, M.; Sammartino, G.; Dohan Ehrenfest, D.M. The Relevance of Choukroun’s Platelet-Rich Fibrin and Metronidazole During Complex Maxillary Rehabilitations Using Bone Allograft. Part I: A New Grafting Protocol. *Implant Dent.* **2009**, *18*, 102–111. [[CrossRef](#)]
87. Riaz, L.; Anjum, M.; Yang, Q.; Safeer, R.; Sikandar, A.; Ullah, H.; Shahab, A.; Yuan, W.; Wang, Q. Treatment technologies and management options of antibiotics and AMR/ ARGs. In *Antibiotics and Antimicrobial Resistance Genes in the Environment*; Elsevier: Amsterdam, The Netherlands, 2020; pp. 369–393. ISBN 9780128188828.
88. Guo, S.; DiPietro, L.A. Factors Affecting Wound Healing. *J. Dent. Res.* **2010**, *89*, 219–229. [[CrossRef](#)]
89. Sauberman, J.B.; Bradley, J.S. Antimicrobial Agents. In *Principles and Practice of Pediatric Infectious Diseases*; Elsevier: Amsterdam, The Netherlands, 2018; pp. 1499.e3–1531.e3. ISBN 9780323401814.
90. Morar, M.; Bhullar, K.; Hughes, D.W.; Junop, M.; Wright, G.D. Structure and Mechanism of the Lincosamide Antibiotic Adenylyltransferase LinB. *Structure* **2009**, *17*, 1649–1659. [[CrossRef](#)]
91. Deane, J.; Rea, M.C.; Fouhy, F.; Stanton, C.; Ross, R.P.; Plant, B.J. Long-Term Implications of Antibiotic Use on Gut Health and Microbiota in Populations Including Patients With Cystic Fibrosis. In *The Gut-Brain Axis*; Elsevier: Amsterdam, The Netherlands, 2016; pp. 223–259. ISBN 9780128025444.
92. Spížek, J.; Řezanka, T. Lincomycin, clindamycin and their applications. *Appl. Microbiol. Biotechnol.* **2004**, *64*, 455–464. [[CrossRef](#)]
93. Sancho-Puchades, M.; Herráez-Vilas, J.M.; Berini-Aytés, L.; Gay-Escoda, C. Antibiotic prophylaxis to prevent local infection in Oral Surgery: Use or abuse? *Med. Oral Patol. Oral Cir. Bucal.* **2009**, *14*, E28–E33.
94. Blanchard, R.; Thomas, C.D.L.; Hardiman, R.; Clement, J.G.; Cooper, D.C.; Pivonka, P. Structural and Material Changes of Human Cortical Bone With Age: Lessons from the Melbourne Femur Research Collection. In *Encyclopedia of Biomedical Engineering*; Elsevier: Amsterdam, The Netherlands, 2019; Volume 1–3, pp. 246–264. ISBN 9780128051443.
95. Chang, C.; Greenspan, A.; Gershwin, M.E. Osteonecrosis. In *Kelley’s Textbook of Rheumatology*; Elsevier: Amsterdam, The Netherlands, 2013; pp. 1692–1711.e5.
96. Saini, R.; Marawar, P.; Shete, S.; Saini, S. Periodontitis, a true infection. *J. Glob. Infect. Dis.* **2009**, *1*, 149. [[CrossRef](#)]

97. Shukla, S.; Chug, A.; Mahesh, L.; Singh, S.; Singh, K. Optimal management of intrabony defects: Current insights. *Clin. Cosmet. Investig. Dent.* **2019**, *11*, 19–25. [CrossRef]
98. Zhao, W.; Xiao, Z.-J.; Zhao, S.-P. The Benefits and Risks of Statin Therapy in Ischemic Stroke: A Review of the Literature. *Neurol. India* **2019**, *67*, 983. [CrossRef]
99. Pradeep, A.R.; Karvekar, S.; Nagpal, K.; Patnaik, K.; Raju, A.; Singh, P. Rosuvastatin 1.2 mg In Situ Gel Combined With 1:1 Mixture of Autologous Platelet-Rich Fibrin and Porous Hydroxyapatite Bone Graft in Surgical Treatment of Mandibular Class II Furcation Defects: A Randomized Clinical Control Trial. *J. Periodontol.* **2016**, *87*, 5–13. [CrossRef]
100. Flory, J.; Lipska, K. Metformin in 2019. *JAMA* **2019**, *321*, 1926. [CrossRef]
101. Tupas, G.D.; Otero, M.C.B.; Ebhohimen, I.E.; Egbuna, C.; Aslam, M. Antidiabetic lead compounds and targets for drug development. In *Phytochemicals as Lead Compounds for New Drug Discovery*; Elsevier: Amsterdam, The Netherlands, 2020; pp. 127–141. ISBN 9780128178911.
102. Radi, Z.A.; Khan, K.N. Cardio-renal safety of non-steroidal anti-inflammatory drugs. *J. Toxicol. Sci.* **2019**, *44*, 373–391. [CrossRef]
103. Xu, F.; Zou, D.; Dai, T.; Xu, H.; An, R.; Liu, Y.; Liu, B. Effects of incorporation of granule-lyophilised platelet-rich fibrin into polyvinyl alcohol hydrogel on wound healing. *Sci. Rep.* **2018**, *8*, 14042. [CrossRef]
104. Zhao, Y.-H.; Zhang, M.; Liu, N.-X.; Lv, X.; Zhang, J.; Chen, F.-M.; Chen, Y.-J. The combined use of cell sheet fragments of periodontal ligament stem cells and platelet-rich fibrin granules for avulsed tooth reimplantation. *Biomaterials* **2013**, *34*, 5506–5520. [CrossRef]
105. Dohan Ehrenfest, D.M.; de Peppo, G.M.; Doglioli, P.; Sammartino, G. Slow release of growth factors and thrombospondin-1 in Choukroun's platelet-rich fibrin (PRF): A gold standard to achieve for all surgical platelet concentrates technologies. *Growth Factors* **2009**, *27*, 63–69. [CrossRef]
106. Yang, K.-C.; Wang, C.-H.; Chang, H.-H.; Chan, W.P.; Chi, C.-H.; Kuo, T.-F. Fibrin glue mixed with platelet-rich fibrin as a scaffold seeded with dental bud cells for tooth regeneration. *J. Tissue Eng. Regen. Med.* **2012**, *6*, 777–785. [CrossRef]
107. Mu, Z.; Chen, K.; Yuan, S.; Li, Y.; Huang, Y.; Wang, C.; Zhang, Y.; Liu, W.; Luo, W.; Liang, P.; et al. Gelatin Nanoparticle-Injectable Platelet-Rich Fibrin Double Network Hydrogels with Local Adaptability and Bioactivity for Enhanced Osteogenesis. *Adv. Healthc. Mater.* **2020**, *9*, 1901469. [CrossRef]
108. Al-Maawi, S.; Herrera-Vizcaíno, C.; Orłowska, A.; Willershausen, I.; Sader, R.; Miron, R.J.; Choukroun, J.; Ghanaati, S. Biologization of Collagen-Based Biomaterials Using Liquid-Platelet-Rich Fibrin: New Insights into Clinically Applicable Tissue Engineering. *Materials* **2019**, *12*, 3993. [CrossRef]
109. Jang, E.-S.; Park, J.-W.; Kweon, H.; Lee, K.-G.; Kang, S.-W.; Baek, D.-H.; Choi, J.-Y.; Kim, S.-G. Restoration of peri-implant defects in immediate implant installations by Choukroun platelet-rich fibrin and silk fibroin powder combination graft. *Oral Surg. Oral Med. Oral Pathol. Oral Radiol. Endodontol.* **2010**, *109*, 831–836. [CrossRef] [PubMed]
110. Sambhav, J.; Rohit, R.; Ranjana, M.; Shalabh, M. Platelet rich fibrin (PRF) and β -Tricalcium phosphate with coronally advanced flap for the management of grade-II furcation defect. *Ethiop. J. Health Sci.* **2014**, *24*, 269. [CrossRef]
111. Sezgin, Y.; Uraz, A.; Taner, I.L.; Çulhaoğlu, R. Effects of platelet-rich fibrin on healing of intra-bony defects treated with anorganic bovine bone mineral. *Braz. Oral Res.* **2017**, *31*, e15. [CrossRef] [PubMed]
112. Lekovic, V.; Milinkovic, I.; Aleksic, Z.; Jankovic, S.; Stankovic, P.; Kenney, E.B.; Camargo, P.M. Platelet-rich fibrin and bovine porous bone mineral vs. platelet-rich fibrin in the treatment of intrabony periodontal defects. *J. Periodontol. Res.* **2012**, *47*, 409–417. [CrossRef]
113. Stone, W.L.; Leavitt, L.; Varacallo, M. *Physiology, Growth Factor*; StatPearls Publishing LLC.: Treasure Island, FL, USA, 2021.
114. Chia-Lai, P.; Orłowska, A.; Al-Maawi, S.; Dias, A.; Zhang, Y.; Wang, X.; Zender, N.; Sader, R.; Kirkpatrick, C.J.; Ghanaati, S. Sugar-based collagen membrane cross-linking increases barrier capacity of membranes. *Clin. Oral Investig.* **2018**, *22*, 1851–1863. [CrossRef]
115. Al-Maawi, S.; Vorakulpipat, C.; Orłowska, A.; Zrnc, T.A.; Sader, R.A.; Kirkpatrick, C.J.; Ghanaati, S. In vivo Implantation of a Bovine-Derived Collagen Membrane Leads to Changes in the Physiological Cellular Pattern of Wound Healing by the Induction of Multinucleated Giant Cells: An Adverse Reaction? *Front. Bioeng. Biotechnol.* **2018**, *6*, 104. [CrossRef]
116. Gonshor, A.; Tye, C.L. Evaluation of an anorganic bovine bone mineral in post-extraction alveolar sockets: A case series. *J. Osseointegration* **2010**, *2*, 25–30. [CrossRef]
117. U.S. National Library of Medicine. Available online: <https://clinicaltrials.gov/ct2/results?cond=platelet-rich+fibrin+surgery&term=&cntry=&state=&city=&dist=> (accessed on 3 October 2021).

**Injectable Platelet-Rich Fibrin as a Drug Carrier Increases the Antibacterial Susceptibility
of Antibiotic— Clindamycin Phosphate**

Karina Egle, Ingus Skadins, Andra Grava, Lana Micko, Viktors Dubniks, Ilze Salma and Arita
Dubnika

Int. J. Mol. Sci., **2022**, *23*(13), 7407



Article

Injectable Platelet-Rich Fibrin as a Drug Carrier Increases the Antibacterial Susceptibility of Antibiotic—Clindamycin Phosphate

Karina Egle ^{1,2} , Ingus Skadins ^{2,3} , Andra Grava ^{1,2} , Lana Micko ^{2,4,5} , Viktors Dubniks ^{1,2} , Ilze Salma ^{2,4,5} and Arita Dubnika ^{1,2,*}

- ¹ Rudolfs Cimdins Riga Biomaterials Innovations and Development Centre, Institute of General Chemical Engineering, Faculty of Materials Science and Applied Chemistry, Riga Technical University, LV-1007 Riga, Latvia; karina.egle@rtu.lv (K.E.); andra.grava@rtu.lv (A.G.); viktors.dubniks@rtu.lv (V.D.)
- ² Baltic Biomaterials Centre of Excellence, Headquarters at Riga Technical University, LV-1048 Riga, Latvia; ingus.skadins@rsu.lv (I.S.); lana.micko@gmail.com (L.M.); ilze.salma@rsu.lv (I.S.)
- ³ Department of Biology and Microbiology, Riga Stradins University, LV-1007 Riga, Latvia
- ⁴ Institute of Stomatology, Riga Stradins University, LV-1007 Riga, Latvia
- ⁵ Department of Oral and Maxillofacial Surgery, Riga Stradins University, LV-1007 Riga, Latvia
- * Correspondence: arita.dubnika@rtu.lv; Tel.: +371-67089605

Abstract: The aim of this study was to investigate the change in clindamycin phosphate antibacterial properties against Gram-positive bacteria using the platelet-rich fibrin as a carrier matrix, and evaluate the changes in the antibiotic within the matrix. The antibacterial properties of CLP and its combination with PRF were tested in a microdilution test against reference cultures and clinical isolates of *Staphylococcus aureus* (*S. aureus*) or *Staphylococcus epidermidis* (*S. epidermidis*). Fourier-transform infrared spectroscopy (FTIR) and scanning electron microscope (SEM) analysis was done to evaluate the changes in the PRF_CLP matrix. Release kinetics of CLP was defined with ultra-performance liquid chromatography (UPLC). According to FTIR data, the use of PRF as a carrier for CLP ensured the structural changes in the CLP toward a more active form of clindamycin. A significant decrease in minimal bactericidal concentration values (from 1000 µg/mL to 62 µg/mL) against reference cultures and clinical isolates of *S. aureus* and *S. epidermidis* was observed for the CLP and PRF samples if compared to pure CLP solution. In vitro cell viability tests showed that PRF and PRF with CLP have higher cell viability than 70% after 24 h and 48 h time points. This article indicates that CLP in combination with PRF showed higher antibacterial activity against *S. aureus* and *S. epidermidis* compared to pure CLP solution. This modified PRF could be used as a novel method to increase drug delivery and efficacy, and to reduce the risk of postoperative infection.

Keywords: platelet-rich fibrin; antibacterial properties; antibiotic resistance; drug release; CLP



Citation: Egle, K.; Skadins, I.; Grava, A.; Micko, L.; Dubniks, V.; Salma, I.; Dubnika, A. Injectable Platelet-Rich Fibrin as a Drug Carrier Increases the Antibacterial Susceptibility of Antibiotic—Clindamycin Phosphate. *Int. J. Mol. Sci.* **2022**, *23*, 7407. <https://doi.org/10.3390/ijms23137407>

Academic Editor: Helena Felgueiras

Received: 7 June 2022

Accepted: 29 June 2022

Published: 3 July 2022

Publisher's Note: MDPI stays neutral with regard to jurisdictional claims in published maps and institutional affiliations.



Copyright: © 2022 by the authors. Licensee MDPI, Basel, Switzerland. This article is an open access article distributed under the terms and conditions of the Creative Commons Attribution (CC BY) license (<https://creativecommons.org/licenses/by/4.0/>).

1. Introduction

Platelet-rich fibrin (PRF) is an autogenous material derived from human blood and is widely used to promote wound healing and tissue regeneration [1]. The leukocytes in the PRF promote wound healing and PRF contains growth factors that are released over time [2]. In several applications, such as oral and maxillofacial surgery, plastic surgery, cardiac surgery and dentistry, there is a great interest in PRF antimicrobial activity. Until now, most clinical studies have been conducted in dentistry and oral and maxillofacial surgery. Platelet concentrates are used in maxillary sinus floor augmentation, as the filling of teeth extraction sockets, in dental implant surgery, in regenerative endodontic treatment, in peri-implantitis and periodontitis treatment.

During the last decade, the antimicrobial properties of PRF have been described in various studies and different testing methods and bacteria have been used. Not only is injectable platelet-rich fibrin (I-PRF) anti-microbial, but anti-biofilm activity against human

oral abscess pathogens has also been described. It was found that I-PRF decreases biofilm production at the minimal inhibitory concentration (MIC) and no biofilm production at the minimal bactericidal concentration (MBC) [3]. Using the disk diffusion method, I-PRF showed notable zones of inhibition, which varied depending on different bacterial species [4]. I-PRF also shows the superiority of antimicrobials against bacteria from the supragingival plate over PRF and PRP [4].

Infections are one of the most common postoperative risks caused by pathogenic and opportunistic bacteria [5,6]. *S. aureus* and *S. epidermidis* are Gram-positive opportunistic bacteria, which are present in the normal human microbiome. With the ability to produce biofilms, these bacteria can evade the host immune system and can cause various local and systemic infections, such as bacteremia, skin and soft tissue infections, osteomyelitis, and implant and device-related infections [7–9]. A lot of these infections can be prevented with antibiotics, especially those where the portals of entry for the bacteria are wounds due to surgery in the hospital environment. For treatment of community-acquired, methicillin-resistant and methicillin-susceptible *S. aureus* infections, clindamycin has been recommended for many years, and it also can increase the susceptibility of methicillin-resistant *S. aureus* clinical isolates [10,11]. The virulence of clinical isolates and their virulence factors, such as surface proteins, determine their ability to cause disease and the severity of the disease [12]. Nowadays, the demand for clindamycin as a medicine is increasing in oral and maxillofacial surgery (including for the prevention and treatment of osteonecrosis of the jaw [13]). It is widely considered as an alternative for patients with an allergic reaction to penicillin [14].

Clindamycin phosphate (CLP) is a prodrug of clindamycin that has no antibacterial activity [15]. As mentioned in the literature, prodrugs can offer many advantages over the parent drug (in our case clindamycin). These benefits include increased solubility, improved stability, reduced side effects, improved bioavailability and better selectivity [16]. CLP can be converted to clindamycin by in vitro hydrolysis of phosphatase esters [15,17]. Rapid in vivo hydrolysis also converts the CLP compound to the antibacterial clindamycin. Hydrolysis of the phosphatase ester is a relatively difficult mechanism (Figure 1). It has been reported that after hydrolysis using alkaline phosphatase, clindamycin phosphate is determined as clindamycin. Following topical, as well as upon intravaginal administration, clindamycin phosphate is slowly hydrolyzed to clindamycin due to limited hydrolysis of the prodrug by the phosphatase enzymes on the surface and within the skin. This prevents the incidence of antibiotic-induced GI side effects [18].

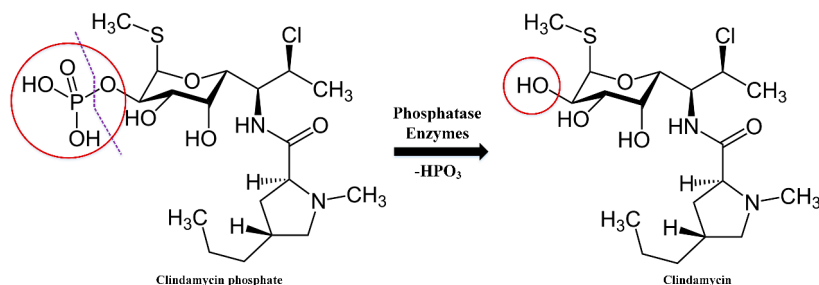


Figure 1. Clindamycin phosphate hydrolysis mechanism.

Clindamycin is known to be obtained by the chemical modification of lincomycin, so the potential impurities are analogs of lincomycin [19]. It is reported that the conversion of clindamycin phosphate to clindamycin in the blood is significantly lower than with oral administration of clindamycin hydrochloride [20,21]. CLP is absorbed as an inactive ester for parenteral use and is rapidly hydrolyzed to the active base in the blood.

CLP has not been widely studied in terms of antibacterial properties. Until now there are only a few studies on CLP's individual antibacterial properties, which show that the

MIC of CLP (w/v %) on *Staphylococcus aureus* is $0.02 \pm 0.005\%$ [22]. Nevertheless, it has a broad range of applications in biomaterials: for example, it is used in eye implants [23], periodontal films [24], and particles [25].

The aim of this study was to investigate the change in CLP antibacterial properties against reference culture and clinical isolates of *S. aureus* and *S. epidermidis* using platelet-rich fibrin as a carrier matrix, and evaluate the CLP structural changes, release kinetics and in vitro cytotoxicity within the PRF matrix.

2. Results

2.1. Structural Changes in PRF and PRF_CLP Samples at 37 °C

The FTIR spectrum of PRF and PRF_CLP is shown in Figure 2. The FTIR spectra of the samples in Figure 2A,B show the absorption peaks indicating the fibrin phase: peak at 1641 cm^{-1} —amide I (C=O), maximum at 1535 cm^{-1} —amide II (N-H) and amide III (C-N) (decreases at 1310 cm^{-1} and increases at 1236 cm^{-1}) (Figure 2B). Characteristic changes in the FTIR spectra are due to rearrangements in the secondary structure of the protein. According to other studies [26,27], the absorption of different proteins at higher wavelengths ($1633\text{--}1645\text{ cm}^{-1}$, $1531\text{--}1539\text{ cm}^{-1}$ and 1240 cm^{-1}) occurs mainly due to α -helical structures, whereas the lower wavenumbers (1651 cm^{-1} , 1539 cm^{-1}) are mostly characteristic of β -structures [28]. Thus, the α -structure is more pronounced in the studied sample. A pronounced absorption maximum at 3281 cm^{-1} indicates the presence of an OH group in the fibrin structure.

CLP and clindamycin have a similar molecular structure, except for the phosphate group. The absorption maximum, specific for both CLP and clindamycin, was observed in PRF_CLP samples incubated for 1, 3, and 7 days at 37 °C. The main structural components of clindamycin molecules are characterized by the vibrations of the pyrrole and saccharide rings, which form skeletal vibrations between 1600 and 600 cm^{-1} . The band group indicated in this region is mainly related to C double bond tensile vibrations. Large changes are observed at about 1047 cm^{-1} , which corresponds to the C-C stretching of the pyrrolidine group. It can be seen that as the incubation time of the PRF_CLP samples increases (from 1 to 7 days), the intensity of the C-C bond also increases. The tensile vibrations of the C-O groups bound to the saccharide ring are observed at 1157 cm^{-1} [23]. The band at 640 cm^{-1} corresponds to the tensile vibrations of the C-Cl groups. In the spectra of the PRF_CLP samples, a wide band with a maximum of 3350 cm^{-1} can also be observed, which corresponds to the vibrations of the O-H groups of aromatic alcohols [29].

It is also observed that the intensity of the phosphate group (PO_4^{3-} at 531 cm^{-1}) from CLP increases in the PRF_CLP sample after 7 days of incubation compared to the PRF_CLP sample after 1 day of incubation (Figure 2B). This may be due to the formation of other CLP degradation products or potential contaminants except clindamycin. Wang et al. [30] state that in addition to clindamycin, two other substances are formed: lincomycin-2-phosphate and clindamycin B-2-phosphate. Brown [19], on the other hand, mentioned the formation of three substances—clindamycin 3-phosphate, clindamycin 4-phosphate and clindamycin 2-phosphate. It can be concluded that the possible degradation products increased the intensity of the PO_4^{3-} absorption peak with increasing degradation time.

It has also been observed that the bands characteristic of clindamycin and CLP at 1673 cm^{-1} (NH-C=O) and at 1568 cm^{-1} (C-C) shift to the right in the presence of PRF. The spectra of the PRF_CLP samples show an increase in the absorption peaks of the above bands, which may have been influenced by the interaction of PRF with CLP. The development of additional intensity at 1080 cm^{-1} C-O cyclic ester galactose sugar elongation [31] was also observed for the PRF_CLP sample after 7 days of incubation. Looking at the CLP and clindamycin spectra, this absorption peak is most indicative of clindamycin. Based on the literature [15,17], CLP induces hydrolysis in the presence of blood and converts to clindamycin. It is possible that this hydrolysis and partial conversion to clindamycin is observed in the spectra of PRF_CLP samples.

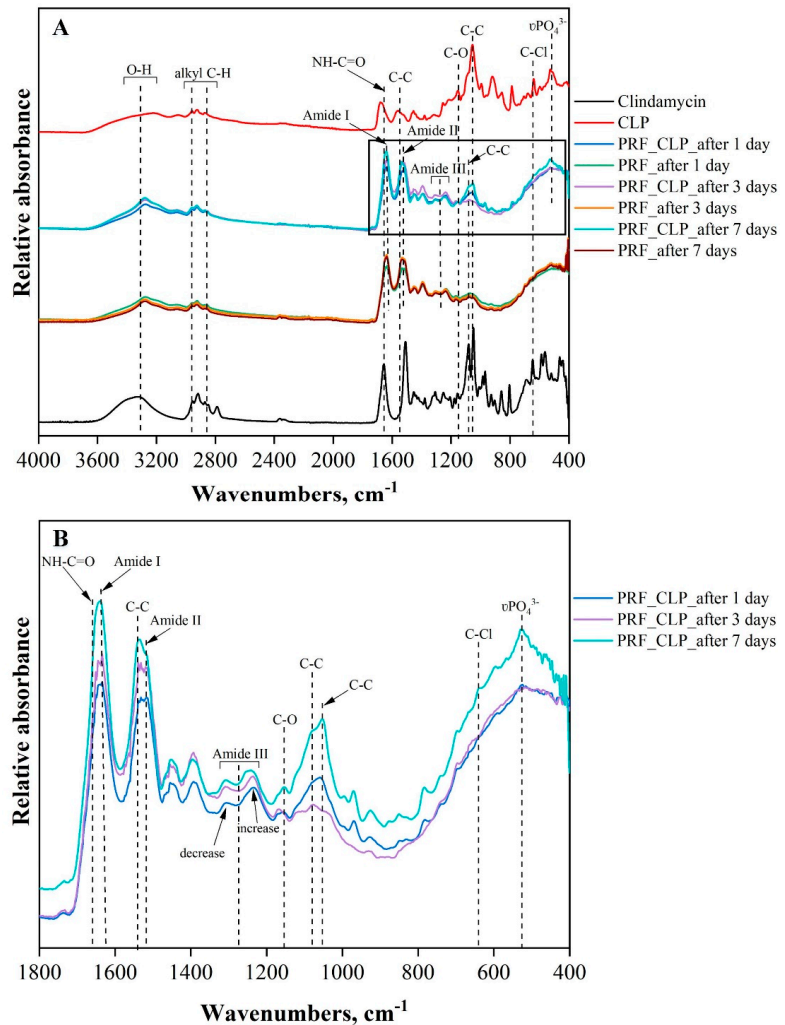


Figure 2. FTIR spectrum: (A) Full spectrum of absorption peaks PRF, PRF_CLP samples, CLP and clindamycin; (B) FTIR spectrum of PRF_CLP samples at incubation time points.

SEM images of the PRF matrices with and without CLP after incubation and lyophilization are shown in Figure 3. Examining PRF samples with SEM, it can be seen that their surface morphology is irregular with a porous microstructure. There are no visible differences in the structure of the PRF samples depending on the incubation time (1, 3 and 7 days at 37 °C). For PRF_CLP samples after 1-day incubation, crystalline structure formations can be seen on the surface of the sample (marked in the images with a red line), these are also observed after 3 and 7 days.

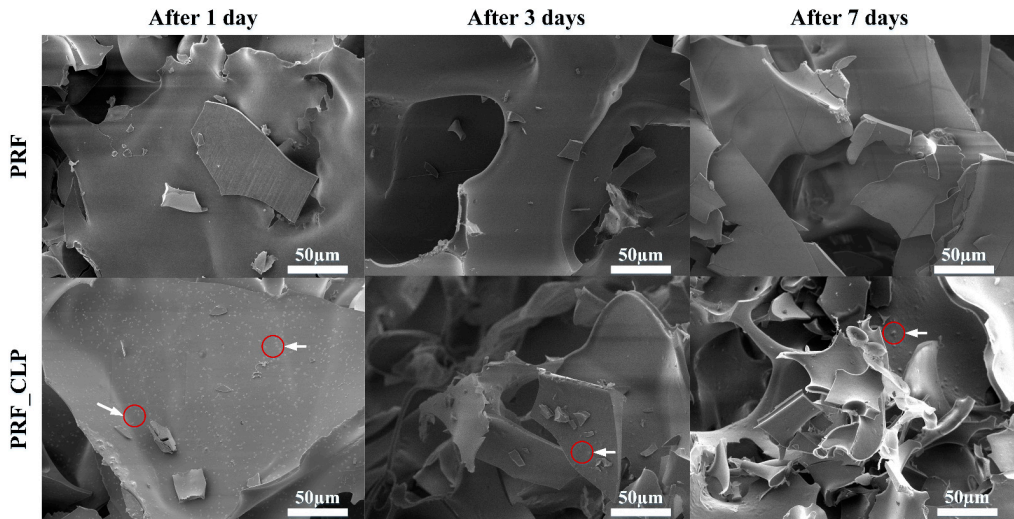


Figure 3. SEM pictures of PRF and PRF_CLP matrix surface; red circles with white arrows indicate the existence of NaCl in the PRF samples.

Comparing the PRF and PRF_CLP samples, it can be seen that the addition of CLP did not significantly affect the structure of the PRF after 1 and 3 days of incubation. In turn, after 7 days of incubation, small network formations are observed on the surface of the PRF_CLP sample. This could be related to the degradation of CLP, thus changing the structure of the PRF.

According to the SEM-EDX data, the crystalline structures present in the PRF_CLP sample contain a large amount of NaCl. PRF contains Na ions and according to Pradid et al., the Cl peaks indicate the presence of clindamycin phosphate [32].

2.2. Drug Release Kinetics

CLP release from PRF matrices was determined by incubating PRF matrices for 0.25, 0.5, 1, 2, 4, 6, 17 and 24 h (Figure 4).

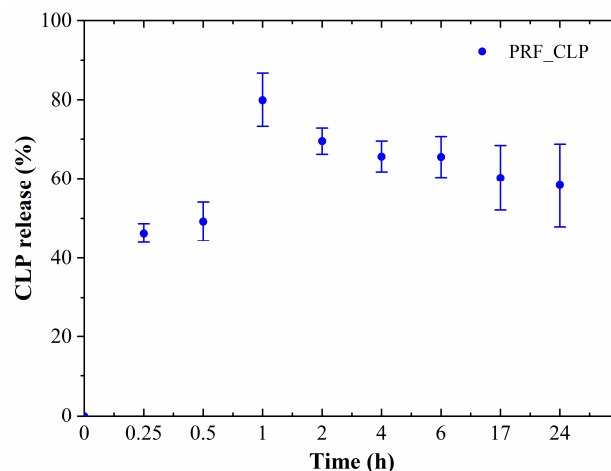


Figure 4. CLP release from PRF matrices in DMEM; average of 3 donor release data.

Burst release of CLP was observed for all PRF_CLP samples in the first incubation hour, when 80% of the encapsulated CLP was released. Based on the obtained data, it is possible to provide local antibacterial activity in a certain place in the first hours, thus reducing the risk of infection during the postoperative period. For long-term treatment, drug delivery systems should be used to prevent burst release during the first hours. ANOVA tests show that at $p < 0.05$, there is no significant difference between drug release from different donor samples.

2.3. Effect of PRF_CLP on Antibacterial Properties

Four Gram-positive bacterial cultures and three donors were used to evaluate and compare the antibacterial properties between CLP, PRF and PRF_CLP samples (Figures 5 and 6).

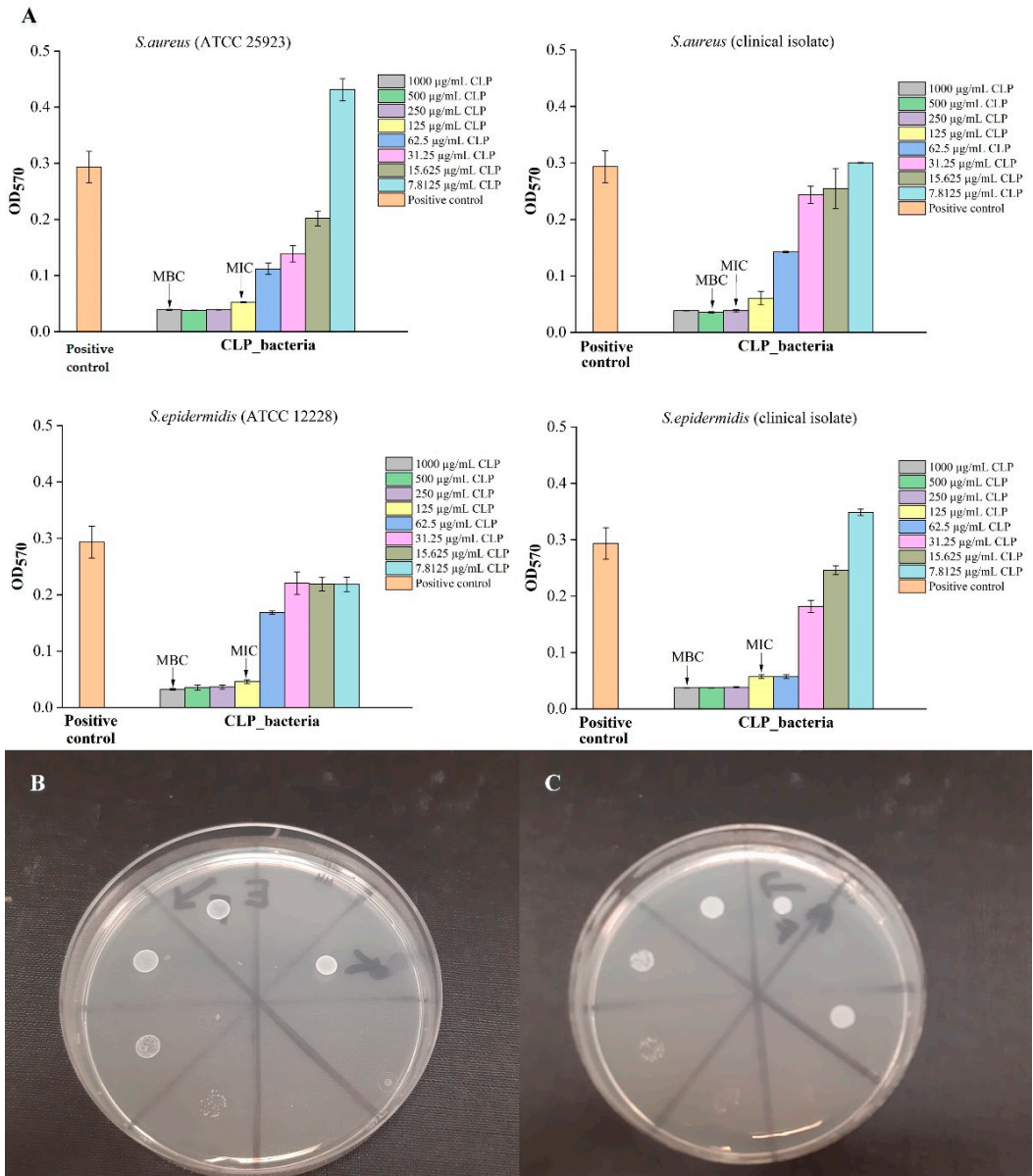
As shown in Figure 5, the MIC and MBC values for pure CLP solution were first determined to test the ability of the substance to provide an antibacterial effect against selected bacterial cultures. The data showed that against *S. aureus* (ATCC 25923), *S. epidermidis* (ATCC 12228) and *S. epidermidis* (clinical isolate), higher CLP concentrations (1000 µg/mL) were required if compared to *S. aureus* (clinical isolate)—500 µg/mL. In general, high CLP concentrations (1000 µg/mL) are required for maximal effect.

Obtained results showed that negative control (PRF_CLP_broth solution) has an increased level of absorption in the higher concentrations, due to the autologous PRF sample. This is because the PRF has a color that comes from the blood sample. According to the obtained results for each donor's antibacterial properties, MIC and MBC levels for PRF_CLP samples depend on the donor and the bacteria strain. In general, we observed that the incorporation of CLP within the PRF leads to lower MIC and MBC values for all donors and all bacteria strains (Figure 6).

The mean donor MIC values for PRF_CLP samples ranged from 52.1 to 62.5 µg/mL, which are lower than the MIC values for pure CLP samples (ranging from 125 to 250 µg/mL). In turn, the mean MBC values range from 62.5 to 145.8 µg/mL, while for pure CLP samples they are at 500–1000 µg/mL. Differences in MIC and MBC values are affected by the bacteria selected for testing (Figures S1 and S2).

As shown in Figure 6, there is a difference in the MIC value of the donor 1 PRF_CLP samples against *S. aureus* (ATCC 25923). It is lower (31.25 µg/mL) than against three other bacterial cultures (62.5 µg/mL). For donor 2 PRF_CLP samples, lower MIC (31.25 µg/mL) and MBC (62.5 µg/mL) values were observed against *S. epidermidis* (ATCC 12228) than for other donor samples. Finally, for donor 3 PRF_CLP samples, there is a difference in MIC values against *S. epidermidis* (clinical isolate); it is higher (125 µg/mL) than against *S. aureus* (ATCC 25923), *S. aureus* (clinical isolate), *S. epidermidis* (ATCC 12228)—62.5 µg/mL. A higher MBC value (250 µg/mL) is observed for clinical isolates of both bacteria. In turn, for the bacteria reference cultures, a lower MBC value (62.5 µg/mL) is observed against *S. epidermidis* than against *S. aureus* (125 µg/mL).

A U-shaped histogram is displayed in the test sections (see Figure 7). This is well observed in the negative control (PRF_CLP_broth), where the absorption capacity gradually decreases with increasing control dilution. The antibacterial data of all prepared PRF_CLP samples showed differences between the donors and the related MIC and MBC values of the samples (Figure 7). For PRF_CLP samples from donor 2 and donor 3 blood, all antibacterial data can be found in an additional file (Figure S3).



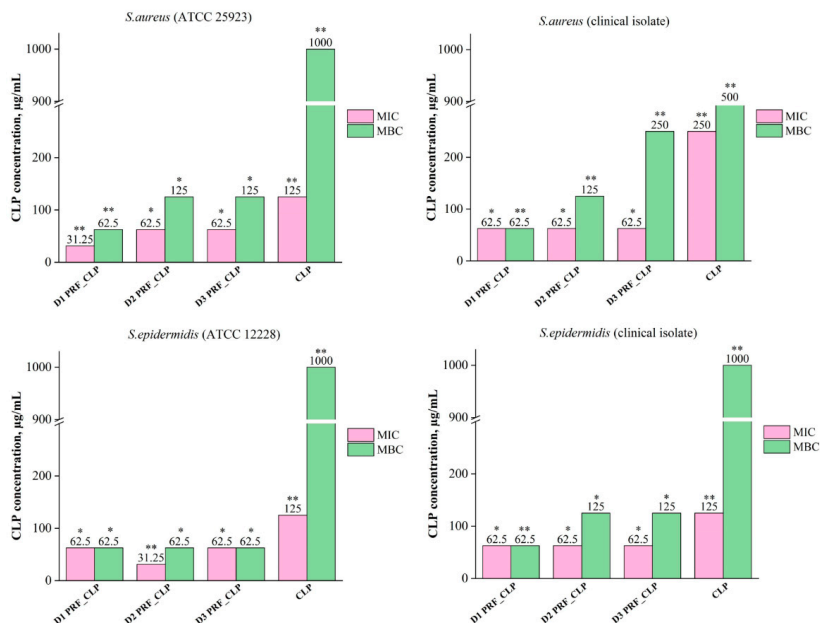


Figure 6. MIC and MBC value differences between CLP and PRF_CLP samples against four bacteria stains (*S. aureus* (ATCC 25923), *S. epidermidis* (ATCC 12228), *S. aureus* (clinical isolate) and *S. epidermidis* (clinical isolate) for all three donors. Samples prepared from donor 1 blood (D1 PRF_CLP); samples prepared from donor 2 (D2 PRF_CLP); samples prepared from donor 3 (D3 PRF_CLP). * $p > 0.05$; ** $p < 0.05$.

Comparing the results of PRF_CLP samples between *S. aureus* reference cultures and clinical isolates, it is observed that only for the donor 3 PRF_CLP samples require a higher CLP concentration (250 µg/mL) against the clinical isolate than against the reference culture (125 µg/mL) (Figure 7). Regarding MIC values, it was observed that only the donor 1 PRF_CLP samples against the clinical isolates required a higher CLP concentration (62.5 µg/mL) than against the reference culture (31.25 µg/mL).

From the results of PRF_CLP samples against the *S. epidermidis* reference culture and clinical isolate (Figure 7), we observed that there is a difference in MIC values for donor 2 PRF_CLP samples, with a higher CLP concentration to the clinical isolate (62.5 µg/mL) than to the reference cultures (31.25 µg/mL) being required to ensure antibacterial activity. MBC values required to provide antibacterial activity against both types of *S. epidermidis* bacteria differ from the *S. aureus* results described above. Looking at the results for donor 2 and donor 3 PRF_CLP samples, it was shown that a higher CLP concentration (125 µg/mL) was required against the *S. epidermidis* clinical isolate and a lower concentration against the *S. epidermidis* reference culture.

Differences in MIC and MBC values against a particular bacterial strain for all three donors are shown in Figure 6. Significantly, a higher MBC value—1000 µg/mL—was observed for CLP samples compared to all donor PRF_CLP samples against each bacterial strain. MBC value against *S. epidermidis* (ATCC 12228) decreased 16-fold for all donor PRF_CLP samples compared to the CLP samples, but decreased 8–16-fold against *S. epidermidis* (clinical isolate) and *S. aureus* (ATCC 25923). The efficacy of PRF_CLP samples against *S. aureus* (clinical isolate) is seen as a 4–16-fold reduction in the MBC value. Thus, indicating that the addition of the required CLP concentration to provide an antibacterial effect against the same bacteria varies greatly depending on the donor PRF. The average

MIC and MBC values of all antibacterial data for all PRF_CLP samples can be found in an additional file (Figures S1 and S2).

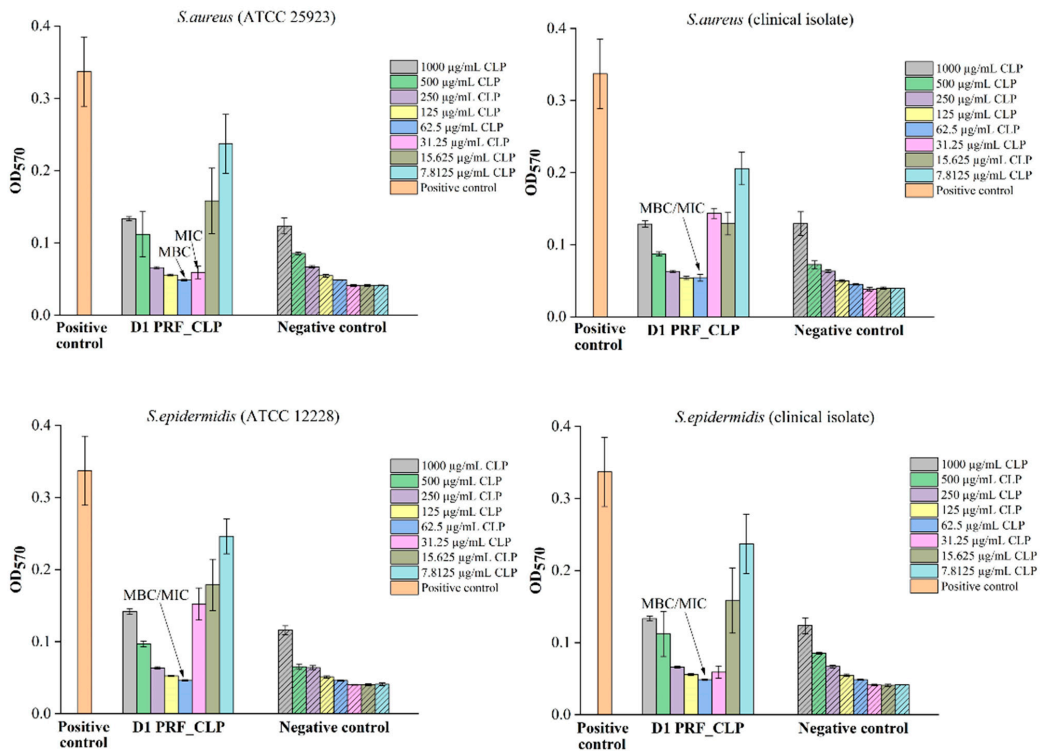


Figure 7. Antibacterial properties of PRF_CLP samples at various concentrations of CLP solution for 4 bacteria strains (*S. aureus* (ATCC 25923), *S. epidermidis* (ATCC 12228), *S. aureus* (clinical isolate) and *S. epidermidis* (clinical isolate) for PRF_CLP samples prepared from donor 1 blood. Pure bacterial suspension (10^6 CFU/mL) as a positive control and pure sterile Mueller–Hinton broth as a negative control were used.

2.4. Cell Viability

The obtained cell cytotoxicity results for PRF and PRF_CLP are shown in Figure 8. Fibroblasts are used for material testing because they have a wide range of functions in the human body, one of them being as part of connective tissue. As PRF has contact with fibroblasts in the body, it is important to test the biomaterial effect on them.

Precise results could be obtained after 24 h and 48 h. The reason for the vague results after 1 h, 2 h and 4 h is that PRF contains many cells, for example, leukocytes, monocytes, red blood cell platelets, neutrophils and lymphocytes [33], which affected cell staining (Figure 9). It should be noted that no difference was observed between PRF samples containing CLP and those not. The experiment had three controls—pure 10 mg/mL CLP solution, untreated cells (positive control) and cells treated with 5% DMSO (negative control).

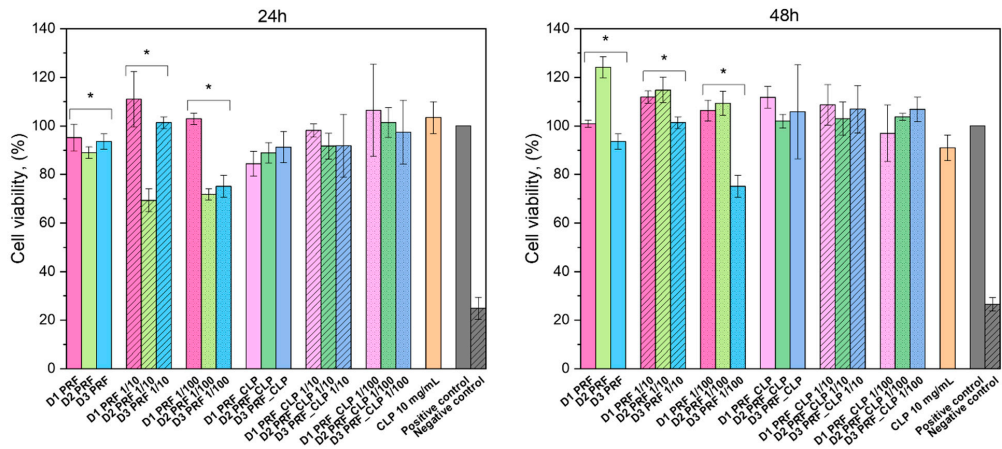


Figure 8. Cytotoxicity of PRF and PRF-CLP extracts and dilutions (significant statistical difference (* $p < 0.05$)).

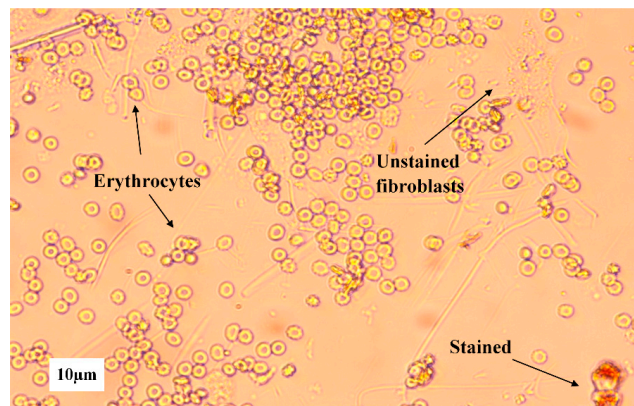


Figure 9. Different blood cells on 3T3 fibroblast cells from D2 PRF sample extract taken after 1 h.

Cell viability was above 70% for both PRF and PRF_CLP extracts and their dilutions were taken after 24 h and 48 h. According to ISO 10993-5:2009, a cytotoxicity effect is considered if the cell viability is decreased by more than 30% [34]. Dilutions did not show significant differences with extracts; however, PRF samples from different donors did have significant statistical differences (* $p < 0.05$). With PRF_CLP samples, there is a small trend of cell viability increasing with dilution, but there is no trend visible with pure PRF samples, which indicates that dilution does not have a significant effect on cell viability.

3. Discussion

This study examined the ability of CLP to convert to clindamycin in the presence of PRF, to provide higher antibacterial activity than PRF and CLP alone. To date, no one has studied the hydrolysis of CLP in the blood without a specific chemical reaction, nor the ability of CLP to enhance the antibacterial properties of PRF. The structure, surface properties, antibacterial properties and drug release kinetics of PRF_CLP were tested.

As observed in the FTIR spectra, CLP interacts with PRF during the incubation for 7 days to provide partial hydrolysis and conversion to clindamycin. After seven days of

incubation, a new bond formation and a phosphate group absorption maximum increase over time were observed, indicating structural changes that are likely to be a CLP switch to clindamycin. In addition, other impurities or degradation products than clindamycin can be formed during the degradation of clindamycin phosphate. Brown [19] mentions that in addition to free clindamycin, clindamycin 3-phosphate, clindamycin 4-phosphate and clindamycin 2-phosphate are formed during conversion. In contrast, Wang et al. [30] described the clindamycin phosphate degradation experiment, indicating that in addition to clindamycin, lincomycin-2-phosphate and a small amount of clindamycin B-2-phosphate are formed. Based on the obtained SEM results, we can conclude that the addition of CLP does not significantly affect the structure of PRF. Minor changes are observed during CLP degradation.

Release data suggest that the PRF_CLP sample can be used for one day local therapy, ensuring maximum CLP release within 1 h. Wang et al., 2020, combined clindamycin (2 µg/mL) with PRP, indicating that 90% of the administered dose was excreted within 10 min [35]. As we can see, our material is able to provide longer release kinetics. In the same way, the release time of the drug could be adjusted according to the required therapy by administering drug delivery systems.

The composition of the blood from each of the donors affects the antibacterial properties of the sample, specifically the amount of CLP required to achieve antibacterial activity. Comparing the MIC and MBC values of the PRF_CLP samples with pure CLP samples for all bacteria strains, a decrease in these values is observed with the addition of PRF to the CLP. The widespread increase in staphylococcal resistance to most antimicrobials, especially in resistant strains, points to the need for new effective treatments for staphylococcal infections [36]. Our antibacterial tests showed that the addition of PRF enhances the antibacterial activity of CLP not only against staphylococcal reference cultures but also against clinical isolates. It can be seen that against the clinical isolates of *S. aureus* and *S. epidermidis*, higher CLP concentrations are required in PRF_CLP samples to provide a lower MBC value compared to both bacteria reference cultures. Each donor has different blood properties (such as different white blood cell counts or vitamin D levels) that drastically affect the antibacterial effect and that is why we have such high error limits. All microbiological input data for all three donor PRF_CLP samples are shown in the supplement (Figure S2). The spread of the *S. aureus* strains that are resistant to certain antibiotics has been reported [37]. According to the Daum [38] and Naimi [39] studies, methicillin-resistant *S. aureus* (MRSA) isolates tend to be sensitive to clindamycin and are less likely to be resistant to antibiotics other than the β-lactam class. The same may be for the *S. epidermidis* clinical isolate. Studies from Schilcher et al. [40,41] and Kuriyama et al. [42] showed that the MIC of pure clindamycin in clinical isolates against MRSA can reach > 256 mg/L. Based on the review of the literature, studies have been performed to test the activity of CLP and clindamycin against dermally important microorganisms. The results showed that CLP had antimicrobial activity against the same organisms as clindamycin, with only a 3 to 44 times higher concentration dose [22]. Summarizing all the data, it can be seen that CLP with PRF is a better antibacterial material than pure CLP, and compared to the literature; we have obtained lower MIC values (ranging from 62.5 to 145.8 µg/mL depending on the bacterial strain) than required for clindamycin (>256 µg/mL) [40–42]. Depending on the bacterial strain, the concentration of the drug has to be adjusted.

To ensure that the obtained PRF_CLP matrices can be used for medical applications, *in vitro* cell viability tests were performed. The highest cell viability can be observed for 48 h extract and dilutions, where it increases above 100% for most of the samples. An increase in viability indicates that PRF increases cell proliferation [43]. PRF is known to be rich in transforming growth factor-β (TGF-β), platelet-derived growth factor (PDGF), vascular endothelial growth factor (VEGF) and epidermal growth factor (EGF) [44], which all have a significant role in new cell formation. Overall, CLP has a favorable effect on cell viability. By adding the antibiotic to PRF, the viability does not go below 80% in the extracts for the prepared time points. Navarro et al. [45] tested periodontal ligament (PDL) cell viability in

PRF and concluded that PRF increases cell viability after PDL is exposed to PRF for 30 min, 1 h and 2 h. In this case, it can be noted that all the PRF ingredients have a favorable effect on PDL cells. The positive effect of PRF was also noticed in a Bucur et al. [46] study on the blood clot effect on fibroblast proliferation and migration. The samples were tested for 24 h and 48 h and in both cases, PRF positively affected cell viability; the same can be observed in our experiment. An interesting difference between the studies is that Bucur et al. filtered the testing solution before applying it to cells to remove blood cells. This should be taken into account for future experiments.

4. Materials and Methods

4.1. Materials

Clindamycin phosphate (CLP, Sigma Aldrich, St. Louis, MO 63103, USA), acetonitrile ($\geq 99.9\%$, Sigma-Aldrich, St. Louis, MI, USA), phosphoric acid (H_3PO_4 ; C = 75% w/w, Latvijas ķīmija, Riga, Latvia), potassium dihydrogen phosphate (KH_2PO_4 , Sigma Aldrich, $\geq 99\%$), methanol ($\geq 99.9\%$, Sigma-Aldrich, St. Louis, MI, USA), Dulbecco's Modified Eagle's Medium (DMEM, Sigma Aldrich, St. Louis, MO, USA), bovine calf serum (CS, Sigma-Aldrich, St. Louis, MO, USA), Penicillin/Streptomycin (P/S, Sigma-Aldrich, St. Louis, MO, USA), dimethylsulfoxide (DMSO, Sigma-Aldrich, St. Louis, MO, USA), neutral red (NR, Sigma Aldrich, St. Louis, MO, USA), Phosphate Buffer Saline (PBS, Sigma-Aldrich, St. Louis, MO, USA), acetic acid (Sigma-Aldrich, St. Louis, MO, USA), ethanol (96%, Latvian Chemistry, Riga, Latvia).

4.2. Blood Collection and Platelet-Rich Fibrin Production

Blood of 3 healthy volunteers with vitamin D levels > 30 ng/mL was collected in 13 mL i-PRF+ tubes (PROCESS FOR PRF, 06000 Nice, France) and immediately placed in a centrifuge ("PRF DUO Quattro"). PRF was obtained by centrifugation at 700 rpm for 5 min (for women) or 6 min (for men). After the centrifugation, the upper layer of liquid PRF (1 mL) from one donor of each tube was transferred into a 50 mL tube, and mixed together for further use.

An amount of 0.5 mL of liquid PRF was used to obtain one PRF sample. To prepare PRF samples with CLP (PRF_CLP), 0.5 mL PRF was added to pre-weighed 0.5 mg CLP with an automatic pipette and mixed well with a spatula. Samples for FTIR and SEM analysis were prepared by incubation (Environmental Shaker-Incubator ES-20, Biosan, Riga, Latvia) at 37°C for 1, 3 and 7 days and then lyophilized for 72 h. For drug release and cell experiments, coagulated PRF and PRF_CLP samples were used.

Written consent from all of the volunteers for use of their samples in the research studies was obtained. All donors were free of any infectious disease and had no abnormal nicotine or alcohol use. None of the subjects used any anticoagulant drugs. Permission No. 6-2/10/53 of the Research Ethics Committee of Riga Stradins University was obtained for the study.

4.3. Characterization of Prepared Samples

4.3.1. Chemical Structure

The lyophilized PRF and PRF with CLP (PRF_CLP) samples after 1, 3 and 7 days of incubation were investigated with Fourier-transform infrared spectroscopy (FTIR) attenuated total reflection (ATR) method, to identify functional groups in PRF matrix. ATR spectroscopy spectra were taken with Thermo Fisher Scientific Nicolet iS5 with a diamond crystal. Spectra were recorded from 500 to 4000 cm^{-1} with 64 scans and with a resolution of 4 cm^{-1} , optical velocity 0.4747 , and aperture 100% .

4.3.2. Morphology

Scanning electron microscope Tescan Mira/LMU (Tescan, Brno, Czech Republic) was used to visualize the microstructure and morphology of obtained PRF and PRF_CLP samples. Prior to examination, samples were fixed to aluminum pin stubs with conductive

carbon tape and sputter coated with thin layer of gold at 25 mA for 3 min using Emitech K550X (Quorum Technologies, Ashford, Kent, UK). Secondary electrons created at 5 kV were used.

4.3.3. Evaluation of CLP Kinetics

Evaluation of CLP release kinetics was analyzed using ultra-performance liquid chromatography. The chromatographic method was adapted based on other studies [47,48]. A chromatograph “Waters Acquity UPLC H-class” with a UV/VIS detector “Waters Acquity TUV” at 195 nm and column “Waters Acquity UPLC BEH C18, 1.7 μm , 2.1 \times 150 mm” was used for data acquisition. The mobile phase consisted of 0.02M KH_2PO_4 buffer (PH = 2.5 ± 0.02): acetonitrile in ratio 79:21, respectively, and at a flow rate of 0.3 mL/min. The total analysis time for one sample was 7 min. During the analysis, the column temperature was maintained at $40 \text{ }^\circ\text{C} \pm 5 \text{ }^\circ\text{C}$ and the sample temperature at $10 \text{ }^\circ\text{C} \pm 5 \text{ }^\circ\text{C}$. The limit of quantification and the limit of detection for the developed method were found to be 1.157 $\mu\text{g}/\text{mL}$ and 0.382 $\mu\text{g}/\text{mL}$.

Samples for CLP release studies were immersed in 20 mL of DMEM and placed in an incubator at $37 \text{ }^\circ\text{C} \pm 5 \text{ }^\circ\text{C}$. At the first 2 time points (15 min and 30 min), the solution was completely removed, and at the other time points (1 h, 1.5 h, 2 h, 4 h, 6 h, 17 h, 24 h), 2 mL aliquots of the solution were used. Finally, 2 mL of DMEM was returned after each sample to ensure a constant volume during the release experiment.

4.4. Preparation of Bacterial Suspension

Four bacterial strains were used in the study, reference culture of *S. aureus* (ATCC 25923) and *S. epidermidis* (ATCC 12228), and clinical isolates of *S. aureus* and *S. epidermidis*, which previously were isolated from the pure sample and identified with VITEK2 system (bioMérieux, Marcy l’Etoile, France). Before the antibacterial tests, bacterial susceptibility against clindamycin was tested with the disc diffusion method. All bacterial suspensions were prepared according to EUCAST (European Committee on Antimicrobial Susceptibility Testing) standards in optic density of 0.5 according to McFarland standard with optic densitometer (Biosan, Riga, Latvia). All bacterial strains showed sensitivity against clindamycin (2 μg) discs (Liofilchem S.r.l., Roseto degli Abruzzi, Italy).

4.5. Determination of Antibacterial Properties

The antibacterial tests were investigated with EUCAST (European Committee on Antimicrobial Susceptibility Testing) standard laboratory antibacterial susceptibility testing method—broth microdilution (Figure 10) [49,50].

4.5.1. Determination of Minimal Inhibitory Concentration

Three different test sample solutions were used: pure PRF, PRF_CLP and pure CLP. Samples with PRF were diluted 1:5, accordingly 2 mL PRF and 8 mL Mueller–Hinton broth (MHB) (Oxoid, UK) to obtain 2 mg/mL stock solution of CLP. A 96-well plate (SARSTEDT, Nümbrecht, Germany) was used in the quantitative assay. Twofold serial dilutions of the pure CLP and PRF_CLP stock solutions (ranging between 2000 and 7.8125 $\mu\text{g}/\text{mL}$) were performed in a 100 μL volume. Each well was seeded with 100 μL of bacterial suspension (10^6 CFU/mL, 0.5 McFarland density), where 200 μL of pure bacterial suspension (10^6 CFU/mL) served as positive control while pure sterile MHB served as negative controls. To detect the MIC and MBC values we used PRF_CLP controls in broth with and without bacteria. After 2-fold dilution, instead of adding bacterial suspension, sterile MHB was added. Then, 96-well plates were incubated in a thermostat (Memmert GmbH, Schwabach, Germany) for 18 h at $37 \text{ }^\circ\text{C}$. MIC values were considered as the lowest concentration of the tested solution that inhibits bacterial growth in microdilution wells as visually detected. After incubation, the values of absorbance were measured with microplate reader at 570 nm (Tecan Infinite F50, Männedorf, Switzerland).

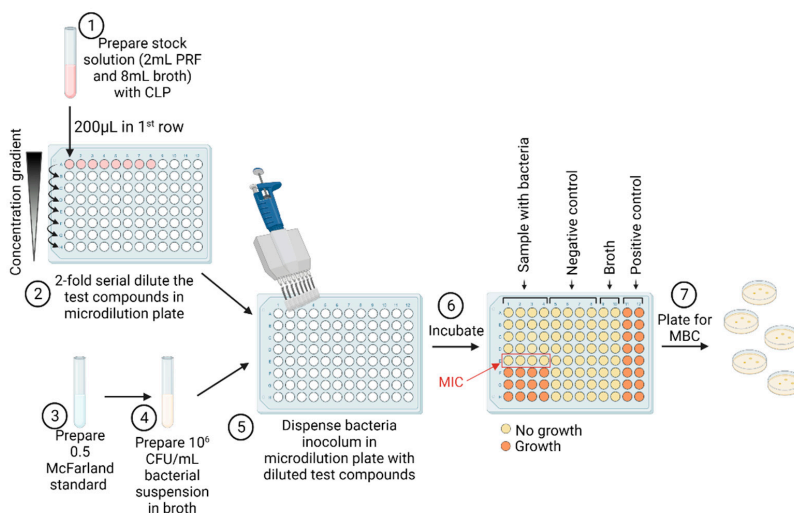


Figure 10. The MIC/MBC assay of CLP, PRF and PRF_CLP samples. Figure created with Biorender.com.

4.5.2. Determination of Minimal Bactericidal Concentration

The lowest concentration at which bacterial growth was completely inhibited by the additional culture method on non-selective media was taken as the MBC value. To determine MBC, extra cultivation of 10 μ L samples from the wells (prepared according to the methodology specified in Section 4.5.1) were inoculated on non-selective agar plates (Oxoid, UK); one sample from the well above the MIC value and all remaining below MIC value (MIC values based on data from methodology 4.5.1 were used). Agar plates were incubated in a thermostat (Memmert GmbH, Schwabach, Germany) for 18 h at 37 $^{\circ}$ C.

4.6. Cell Viability Experiments

PRF with and without CLP was tested on 3T3 mouse fibroblasts. Overall PRFs from 3 different donors were tested.

Prior to cell viability tests, 5000 cells were seeded in a 96-well plate in 200 μ L of full cell medium. To prevent the plates from drying out, PBS was added to the outer wells. After seeding the cells, the plates were incubated overnight (37 $^{\circ}$ C, 5%) (New Brunswick™ S41i CO₂ Incubator Shaker, Eppendorf, Hamburg, Germany).

The following day each PRF sample with and without CLP was submerged in 2 mL of full cell medium. The medium consisted of 89% DMEM, 10% CS and 1% P/S. After 1, 2, 4, 24 and 48 h, all the solution was removed from the testing sample and replaced with a fresh 2 mL cell medium. Extract and 2 types of dilutions—1:10 and 1:100—were directly put onto the cells. Before adding the analyzing solution to the cells, the old medium was removed. The experiment had two types of controls. The positive control consisted of untreated cells with medium; on the other hand, for the negative control, 5% DMSO solution in cell medium was applied to cells to analyze their viability. Each treatment had 6 replicates.

To analyze the PRF extract and its dilutions effect on cell viability, Natural Red (NR) test was used. The tests included PBS, NR and solubilization solution (1% acetic acid, 50% ethanol, 49% water).

After 24 h of each time point, the testing solutions were discarded and cells were washed with 200 μ L PBS solution. Subsequently, cells were treated with 150 μ L NR solution, after which plates were left to incubate for 2 h. Afterward, the solution with dye was taken off, and cells were washed again with 250 μ L PBS solution. Finally, cells were solubilized, which was done with a 150 μ L solubilization solution. Then, a 540 nm wavelength was used

to measure optical density with a microplate reader (Tecan Infinite M Nano, Switzerland). Every plate was analyzed appropriately with the method just described.

4.7. Statistical Evaluation

All results are expressed as the mean \pm standard deviation (SD) of at least three independent samples. The reliability of the results was assessed using the unpaired Student's t-test with a significance level of $p < 0.05$. One—and two-way analysis of variance (ANOVA) was performed to assess the differences between the results.

5. Conclusions

The results of the present study show the structure, surface properties, antibacterial properties, drug release kinetics, and cell viability of the PRF_CLP samples. Burst release (80% of CLP after 1 h) was observed for the PRF_CLP samples; thus, the development of more advanced drug delivery systems could be an area for future research. The antibacterial effect of CLP was affected by the addition of PRF, thus providing a reduction in MIC and MBC concentrations compared to pure CLP and pure PRF samples. Cell viability for the PRF_CLP samples increased indicating the ability of PRF to alter cell proliferation. Structural studies have also shown that clindamycin phosphate is converted to clindamycin within the PRF matrix at 37 °C.

This study proves that the presence of PRF in the resulting PRF_CLP samples improves the antibacterial efficacy and may be suitable for medical applications. The results are the first step in finding alternative solutions that can enhance the antibacterial properties of CLP to prevent postoperative infections and could lead to a new method to be developed, which may increase the efficiency of drug delivery and activity. Further clinical trials with larger patient groups are needed to introduce this method for reducing the risk of post-operative infections.

Supplementary Materials: The following supporting information can be downloaded at: <https://www.mdpi.com/article/10.3390/ijms23137407/s1>.

Author Contributions: Conceptualization, writing—original draft preparation, writing—review and editing, methodology, formal analysis, visualization, K.E.; conceptualization, writing—review and editing, methodology, I.S. (Ingus Skadins); writing, methodology, formal analysis, A.G.; writing, methodology, L.M.; assistance in the development of the UPLC method V.D.; conceptualization, writing—review and editing, methodology, I.S. (Ilze Salma); writing—review and editing, supervision, funding acquisition, project administration, conceptualization, A.D. All authors have read and agreed to the published version of the manuscript.

Funding: This research was funded by the Latvian Council of Science research project No. Izp-2020/1-0054 “Development of antibacterial autologous fibrin matrices in maxillofacial surgery” (MATRI-X).

Institutional Review Board Statement: The study was conducted according to the guidelines of the Declaration of Helsinki, and approved by the Research Ethics Committee at Riga Stradins University, Latvia, Permission No. 6-2/10/53, 28 November 2019.

Informed Consent Statement: Written informed consent has been obtained from the patients to publish this paper.

Data Availability Statement: The data presented in this study are available on request from the corresponding author.

Acknowledgments: The authors acknowledge financial support from the Latvian Council of Science research project “Development of antibacterial autologous fibrin matrices in maxillofacial surgery” (MATRI-X) under agreement No. Izp-2020/1-0054. This work was also supported by the European Union's Horizon 2020 research and innovation programme under the grant agreement No 857287 (BBCE). The authors thank Agnese Brangule for her help with FTIR analysis.

Conflicts of Interest: The authors declare no conflict of interest related to this study.

References

1. Chou, T.; Chang, H.; Wang, J. Autologous platelet concentrates in maxillofacial regenerative therapy. *Kaohsiung J. Med. Sci.* **2020**, *36*, 305–310. [[CrossRef](#)] [[PubMed](#)]
2. Fan, Y.; Perez, K.; Dym, H. Clinical Uses of Platelet-Rich Fibrin in Oral and Maxillofacial Surgery. *Dent. Clin. N. Am.* **2020**, *64*, 291–303. [[CrossRef](#)] [[PubMed](#)]
3. Jasmine, S.; Thangavelu, A.; Janarthanan, K.; Krishnamoorthy, R.; Alshatwi, A.A. Antimicrobial and antibiofilm potential of injectable platelet rich fibrin—a second-generation platelet concentrate—against biofilm producing oral *staphylococcus* isolates. *Saudi J. Biol. Sci.* **2020**, *27*, 41–46. [[CrossRef](#)] [[PubMed](#)]
4. Kour, P.; Pudukalkatti, P.; Vas, A.; Das, S.; Padmanabhan, S. Comparative evaluation of antimicrobial efficacy of platelet-rich plasma, platelet-rich fibrin, and injectable platelet-rich fibrin on the standard strains of *Porphyromonas gingivalis* and *Aggregatibacter actinomycetemcomitans*. *Contemp. Clin. Dent.* **2018**, *9*, S325. [[CrossRef](#)]
5. Heal, C.; Buettner, P.; Browning, S. Risk factors for wound infection after minor surgery in general practice. *Med. J. Aust.* **2006**, *185*, 255–258. [[CrossRef](#)]
6. Zhang, J.; Xu, Q.; Huang, C.; Mo, A.; Li, J.; Zuo, Y. Biological properties of an anti-bacterial membrane for guided bone regeneration: An experimental study in rats. *Clin. Oral Implant. Res.* **2010**, *21*, 321–327. [[CrossRef](#)]
7. Tong, S.Y.C.; Davis, J.S.; Eichenberger, E.; Holland, T.L.; Fowler, V.G. *Staphylococcus aureus* Infections: Epidemiology, Pathophysiology, Clinical Manifestations, and Management. *Clin. Microbiol. Rev.* **2015**, *28*, 603–661. [[CrossRef](#)]
8. Pollitt, E.J.G.; Szkuta, P.T.; Burns, N.; Foster, S.J. *Staphylococcus aureus* infection dynamics. *PLoS Pathog.* **2018**, *14*, e1007112. [[CrossRef](#)]
9. DeLeo, F.R.; Diep, B.A.; Otto, M. Host Defense and Pathogenesis in *Staphylococcus aureus* Infections. *Infect. Dis. Clin. N. Am.* **2009**, *23*, 17–34. [[CrossRef](#)]
10. Martinez-Aguilar, G.; Hammerman, W.A.; Mason, E.O.; Kaplan, S.L. Clindamycin treatment of invasive infections caused by community-acquired, methicillin-resistant and methicillin-susceptible *Staphylococcus aureus* in children. *Pediatr. Infect. Dis. J.* **2003**, *22*, 593–599. [[CrossRef](#)]
11. Mohamed, M.A.; Nasr, M.; Elkhatib, W.F.; Eltayeb, W.N.; Elshamy, A.A.; El-Sayyad, G.S. Nanobiotic formulations as promising advances for combating MRSA resistance: Susceptibilities and post-antibiotic effects of clindamycin, doxycycline, and linezolid. *RSC Adv.* **2021**, *11*, 39696–39706. [[CrossRef](#)] [[PubMed](#)]
12. Foster, T.J.; Geoghegan, J.A.; Ganesh, V.K.; Höök, M. Adhesion, invasion and evasion: The many functions of the surface proteins of *Staphylococcus aureus*. *Nat. Rev. Microbiol.* **2014**, *12*, 49–62. [[CrossRef](#)] [[PubMed](#)]
13. Fortunato, L.; Bennardo, F.; Buffone, C.; Giudice, A. Is the application of platelet concentrates effective in the prevention and treatment of medication-related osteonecrosis of the jaw? A systematic review. *J. Cranio-Maxillofac. Surg.* **2020**, *48*, 268–285. [[CrossRef](#)] [[PubMed](#)]
14. Maestre-Vera, J.R. Treatment options in odontogenic infection. *Med. Oral Patol. Oral Cir. Bucal* **2004**, *9* (Suppl. S25–S31), 19–24.
15. Li, H.; Deng, J.; Yue, Z.; Zhang, Y.; Sun, H.; Ren, X. Clindamycin hydrochloride and clindamycin phosphate: Two drugs or one? A retrospective analysis of a spontaneous reporting system. *Eur. J. Clin. Pharmacol.* **2017**, *73*, 251–253. [[CrossRef](#)] [[PubMed](#)]
16. Yang, Y.; Aloysius, H.; Inoyama, D.; Chen, Y.; Hu, L. Enzyme-mediated hydrolytic activation of prodrugs. *Acta Pharm. Sin. B* **2011**, *1*, 143–159. [[CrossRef](#)]
17. Stanković, M.; Savić, V.; Marinković, V. Determination of Clindamycin Phosphate in Different Vaginal Gel Formulations by Reverse Phase High Performance Liquid Chromatography. *Acta Fac. Med. Naissensis* **2013**, *30*, 63–71. [[CrossRef](#)]
18. Morozowich, W.; Karnes, H.A. Case Study: Clindamycin 2-Phosphate, A Prodrug of Clindamycin. In *Prodrugs*; Springer: New York, NY, USA, 2007; pp. 1207–1219.
19. Brown, L.W. High-Pressure Liquid Chromatographic Assays for Clindamycin, Clindamycin Phosphate, and Clindamycin Palmitate. *J. Pharm. Sci.* **1978**, *67*, 1254–1257. [[CrossRef](#)]
20. Borin, M.T.; Ryan, K.K.; Hopkins, N.K. Systemic Absorption of Clindamycin after Intravaginal Administration of Clindamycin Phosphate Ovule or Cream. *J. Clin. Pharmacol.* **1999**, *39*, 805–810. [[CrossRef](#)]
21. Borin, M.T.; Powley, G.W.; Tackwell, K.R.; Batts, D.H. Absorption of clindamycin after intravaginal application of clindamycin phosphate 2% cream. *J. Antimicrob. Chemother.* **1995**, *35*, 833–841. [[CrossRef](#)]
22. Amr, S.; Brown, M.B.; Martin, G.P.; Forbes, B. Activation of clindamycin phosphate by human skin. *J. Appl. Microbiol.* **2001**, *90*, 550–554. [[CrossRef](#)]
23. Mostafavi, S.; Karkhane, R.; Riazi-Esfahani, M.; Dorkoosh, F.; Rafiee-Tehrani, M.; Tamaddon, L. Thermoanalytical characterization of clindamycin-loaded intravitreal implants prepared by hot melt extrusion. *Adv. Biomed. Res.* **2015**, *4*, 147. [[CrossRef](#)] [[PubMed](#)]
24. Kilicarslan, M.; Ilhan, M.; Inal, O.; Orhan, K. Preparation and evaluation of clindamycin phosphate loaded chitosan/alginate polyelectrolyte complex film as mucoadhesive drug delivery system for periodontal therapy. *Eur. J. Pharm. Sci.* **2018**, *123*, 441–451. [[CrossRef](#)] [[PubMed](#)]
25. Uskoković, V.; Desai, T.A. Simultaneous bactericidal and osteogenic effect of nanoparticulate calcium phosphate powders loaded with clindamycin on osteoblasts infected with *Staphylococcus aureus*. *Mater. Sci. Eng. C* **2014**, *37*, 210–222. [[CrossRef](#)] [[PubMed](#)]
26. Cai, S.; Singh, B.R. A Distinct Utility of the Amide III Infrared Band for Secondary Structure Estimation of Aqueous Protein Solutions Using Partial Least Squares Methods. *Biochemistry* **2004**, *43*, 2541–2549. [[CrossRef](#)]

27. Jackson, M.; Mantsch, H.H. The Use and Misuse of FTIR Spectroscopy in the Determination of Protein Structure. *Crit. Rev. Biochem. Mol. Biol.* **1995**, *30*, 95–120. [[CrossRef](#)]
28. Litvinov, R.I.; Faizullin, D.A.; Zuev, Y.F.; Weisel, J.W. The α -Helix to β -Sheet Transition in Stretched and Compressed Hydrated Fibrin Clots. *Biophys. J.* **2012**, *103*, 1020–1027. [[CrossRef](#)]
29. Vukomanović, M.; Zavašnik-Bergant, T.; Bračko, I.; Škapin, S.D.; Ignjatović, N.; Radmilović, V.; Uskoković, D. Poly(d,l-lactide-co-glycolide)/hydroxyapatite core-shell nanospheres. Part 3: Properties of hydroxyapatite nano-rods and investigation of a distribution of the drug within the composite. *Colloids Surf. B Biointerfaces* **2011**, *87*, 226–235. [[CrossRef](#)]
30. Wang, S.-M.; Bu, S.-S.; Liu, H.-M.; Li, H.-Y.; Liu, W.; Wang, Y.-D. Separation and characterization of clindamycin phosphate and related impurities in injection by liquid chromatography/electrospray ionization mass spectrometry. *Rapid Commun. Mass Spectrom.* **2009**, *23*, 899–906. [[CrossRef](#)]
31. Mohamed, A.; Abd-Motagaly, A.; Ahmed, O.; Amin, S.; Mohamed Ali, A. Investigation of Drug–Polymer Compatibility Using Chemometric-Assisted UV-Spectrophotometry. *Pharmaceutics* **2017**, *9*, 7. [[CrossRef](#)]
32. Pradid, J.; Keawwatana, W.; Boonyang, U.; Tangbunsuk, S. Biological properties and enzymatic degradation studies of clindamycin-loaded PLA/HAP microspheres prepared from crocodile bones. *Polym. Bull.* **2017**, *74*, 5181–5194. [[CrossRef](#)]
33. Miron, R.J.; Chai, J.; Fujioka-Kobayashi, M.; Sculean, A.; Zhang, Y. Evaluation of 24 protocols for the production of platelet-rich fibrin. *BMC Oral Health* **2020**, *20*, 310. [[CrossRef](#)] [[PubMed](#)]
34. Mardashev, S.R.; Nikolaev Ya, A.; Sokolov, N.N. Isolation and properties of a homogenous L asparaginase preparation from *Pseudomonas fluorescens* AG (Russian). *Biokhimiya* **1975**, *40*, 984–989.
35. Wang, S.; Li, Y.; Li, S.; Yang, J.; Tang, R.; Li, X.; Li, L.; Fei, J. Platelet-rich plasma loaded with antibiotics as an affiliated treatment for infected bone defect by combining wound healing property and antibacterial activity. *Platelets* **2021**, *32*, 479–491. [[CrossRef](#)]
36. Aleksandra, A.; Misić, M.; Mira, Z.; Violeta, N.; Dragana, I.; Zoran, B.; Dejan, V.; Milanko, S.; Dejan, B. Prevalence of inducible clindamycin resistance among community-associated *staphylococcal* isolates in central Serbia. *Indian J. Med. Microbiol.* **2014**, *32*, 49–52. [[CrossRef](#)]
37. Indrawattana, N.; Sungkhachat, O.; Sookrung, N.; Chongsa-nguan, M.; Tungtrongchitr, A.; Voravuthikunchai, S.P.; Kong-ngoen, T.; Kurazono, H.; Chaicumpa, W. *Staphylococcus aureus* Clinical Isolates: Antibiotic Susceptibility, Molecular Characteristics, and Ability to Form Biofilm. *Biomed Res. Int.* **2013**, *2013*, 1–11. [[CrossRef](#)]
38. Daum, R.S. Skin and Soft-Tissue Infections Caused by Methicillin-Resistant *Staphylococcus aureus*. *N. Engl. J. Med.* **2007**, *357*, 380–390. [[CrossRef](#)]
39. Naimi, T.S. Comparison of Community- and Health Care–Associated Methicillin-Resistant *Staphylococcus aureus* Infection. *JAMA* **2003**, *290*, 2976–2984. [[CrossRef](#)]
40. Schilcher, K.; Andreoni, F.; Dengler Haunreiter, V.; Seidl, K.; Hasse, B.; Zinkernagel, A.S. Modulation of *Staphylococcus aureus* Biofilm Matrix by Subinhibitory Concentrations of Clindamycin. *Antimicrob. Agents Chemother.* **2016**, *60*, 5957–5967. [[CrossRef](#)]
41. Schilcher, K.; Andreoni, F.; Uchiyama, S.; Ogawa, T.; Schuepbach, R.A.; Zinkernagel, A.S. Increased Neutrophil Extracellular Trap-Mediated *Staphylococcus aureus* Clearance Through Inhibition of Nuclease Activity by Clindamycin and Immunoglobulin. *J. Infect. Dis.* **2014**, *210*, 473–482. [[CrossRef](#)]
42. Kuriyama, T.; Karasawa, T.; Nakagawa, K.; Saiki, Y.; Yamamoto, E.; Nakamura, S. Bacteriologic features and antimicrobial susceptibility in isolates from orofacial odontogenic infections. *Oral Surg. Oral Med. Oral Pathol. Endodontology* **2000**, *90*, 600–608. [[CrossRef](#)] [[PubMed](#)]
43. Strauss, F.-J.; Nasirzade, J.; Kargarpoor, Z.; Stähli, A.; Gruber, R. Effect of platelet-rich fibrin on cell proliferation, migration, differentiation, inflammation, and osteoclastogenesis: A systematic review of in vitro studies. *Clin. Oral Investig.* **2020**, *24*, 569–584. [[CrossRef](#)] [[PubMed](#)]
44. Pavlovic, V.; Ciric, M.; Jovanovic, V.; Trandafilovic, M.; Stojanovic, P. Platelet-rich fibrin: Basics of biological actions and protocol modifications. *Open Med.* **2021**, *16*, 446–454. [[CrossRef](#)]
45. Navarro, L.B.; Barchiki, F.; Navarro Junior, W.; Carneiro, E.; da Silva Neto, U.X.; Westphalen, V.P.D. Assessment of platelet-rich fibrin in the maintenance and recovery of cell viability of the periodontal ligament. *Sci. Rep.* **2019**, *9*, 19476. [[CrossRef](#)] [[PubMed](#)]
46. Bucur, M.; Constantin, C.; Neagu, M.; Zurac, S.; Dinca, O.; Vladan, C.; Cioplea, M.; Popp, C.; Nichita, L.; Ionescu, E. Alveolar blood clots and platelet-rich fibrin induce in vitro fibroblast proliferation and migration. *Exp. Ther. Med.* **2018**, *17*, 982–989. [[CrossRef](#)] [[PubMed](#)]
47. Vella, J.; Busuttill, F.; Bartolo, N.S.; Sammut, C.; Ferrito, V.; Serracino-Ingloft, A.; Azzopardi, L.M.; LaFerla, G. A simple HPLC-UV method for the determination of ciprofloxacin in human plasma. *J. Chromatogr. B Anal. Technol. Biomed. Life Sci.* **2015**, *989*, 80–85. [[CrossRef](#)]
48. Liu, C.; Chen, Y.; Yang, T.; Hsieh, S.; Hung, M.; Lin, E.T. High-performance liquid chromatographic determination of clindamycin in human plasma or serum: Application to the bioequivalency study of clindamycin phosphate injections. *J. Chromatogr. B Biomed. Sci. Appl.* **1997**, *696*, 298–302. [[CrossRef](#)] [[PubMed](#)]
49. Balouiri, M.; Sadiki, M.; Ibsouda, S.K. Methods for in vitro evaluating antimicrobial activity: A review. *J. Pharm. Anal.* **2016**, *6*, 71–79. [[CrossRef](#)]
50. Gajic, I.; Kabic, J.; Kekic, D.; Jovicevic, M.; Milenkovic, M.; Mitic Culafic, D.; Trudic, A.; Ranin, L.; Opavski, N. Antimicrobial Susceptibility Testing: A Comprehensive Review of Currently Used Methods. *Antibiotics* **2022**, *11*, 427. [[CrossRef](#)]

Development of Vancomycin Delivery Systems Based on Autologous 3D Platelet-Rich Fibrin Matrices for Bone Tissue Engineering



Arita Dubnika, Karina Egle, Marite Skrinda-Melne, Ingus Skadins, Jayakumar Rajadas and Ilze Salma

Biomedicines, **2021**, *9*(7), 814



Article

Development of Vancomycin Delivery Systems Based on Autologous 3D Platelet-Rich Fibrin Matrices for Bone Tissue Engineering

Arita Dubnika ^{1,2,*} , Karina Egle ^{1,2}, Marite Skrinda-Melne ^{1,2}, Ingus Skadins ³ , Jayakumar Rajadas ⁴ and Ilze Salma ^{2,5}

¹ Rudolfs Cimdins Riga Biomaterials Innovations and Development Centre, Institute of General Chemical Engineering, Riga Technical University, LV-1658 Riga, Latvia; karina.egle@rtu.lv (K.E.); marite.skrinda@rtu.lv (M.S.-M.)

² Baltic Biomaterials Centre of Excellence, Headquarters at Riga Technical University, LV-1658 Riga, Latvia; salma.ilze@rsu.lv

³ Department of Biology and Microbiology, Riga Stradiņš University, LV-1007 Riga, Latvia; ingus.skadins@rsu.lv

⁴ Department of Medicine and Advanced Drug Delivery and Regenerative Biomaterials Laboratory of Cardiovascular Institute, Stanford University School of Medicine, Palo Alto, CA 94304, USA; jayraja@stanford.edu

⁵ Institute of Stomatology, Riga Stradiņš University, LV-1007 Riga, Latvia

* Correspondence: arita.dubnika@rtu.lv; Tel.: +371-67089605



Citation: Dubnika, A.; Egle, K.; Skrinda-Melne, M.; Skadins, I.; Rajadas, J.; Salma, I. Development of Vancomycin Delivery Systems Based on Autologous 3D Platelet-Rich Fibrin Matrices for Bone Tissue Engineering. *Biomedicines* **2021**, *9*, 814. <https://doi.org/10.3390/biomedicines9070814>

Academic Editor: Toni Ibrahim

Received: 26 May 2021

Accepted: 5 July 2021

Published: 13 July 2021

Publisher's Note: MDPI stays neutral with regard to jurisdictional claims in published maps and institutional affiliations.



Copyright: © 2021 by the authors. Licensee MDPI, Basel, Switzerland. This article is an open access article distributed under the terms and conditions of the Creative Commons Attribution (CC BY) license (<https://creativecommons.org/licenses/by/4.0/>).

Abstract: Autologous platelet-rich fibrin (PRF) is derived from the blood and its use in the bone tissue engineering has emerged as an effective strategy for novel drug and growth factor delivery systems. Studies have approved that combined therapy with PRF ensures higher biological outcomes, but patients still undergo additional treatment with antibiotic drugs before, during, and even after the implantation of biomaterials with PRF. These systematically used drugs spread throughout the blood and lead not only to positive effects but may also induce adverse side effects on healthy tissues. Vancomycin hydrochloride (VANKA) is used to treat severe *Staphylococcal* infections but its absorption in the target tissue after oral administration is low; therefore, in this study, we have developed and analyzed two kinds of VANKA carriers—liposomes and microparticles in 3D PRF matrices. The adjustment, characterization, and analysis of VANKA carriers in 3D PRF scaffolds is carried out in terms of encapsulation efficiency, drug release kinetics and antibacterial activity; furthermore, we have studied the micro- and macrostructure of the scaffolds with microtomography.

Keywords: platelet-rich fibrin; drug delivery; liposomes; microcapsules; vancomycin; phospholipids; PLGA; drug release; microtomography

1. Introduction

The use of platelet-rich fibrin (PRF) in tissue engineering has emerged as an effective strategy for novel drug delivery systems [1]. Autologous PRF is derived from the blood by centrifugation and contains growth factors and cells (leucocytes and platelets). With an adjusted PRF preparation method, it can be stable in liquid phase for up to 30 min before coagulation, thus allowing to prepare a scaffold for the drug delivery system and use it as an injectable system [2,3]. The use of autologous PRF can improve the biological outcomes of the bone and tissue regeneration procedures, especially in maxillofacial surgeries [4–6]. Previous clinical studies have approved that for patients receiving therapy combined with PRF, the biological outcomes and healing were better [7–10].

Systematically used drugs, without a specific carrier, spread throughout the body and often drug degradation rate is relatively short. It ensures not only a positive effect on the damaged tissue, but may also induce adverse side effects on healthy tissues [11]. The

aim of drug delivery systems is to achieve the highest therapeutic effect with the lowest drug concentration [12]. Vancomycin hydrochloride (VANKA) is a water-soluble tricyclic glycopeptide antibiotic [13] that prevents/destroys several Gram-positive microorganisms, which are the most common pathogens. It is used to treat severe *Staphylococcal* infections, in particular methicillin-resistant *S. aureus* (MRSA) and is included in anti-cancer medicines. VANKA is applied in cases when penicillin is ineffective or causes allergic reactions, as well as for the treatment of infections where other antibiotics are resistant [14,15]. VANKA is administered intravenously by injections or infusions, as well as perorally in the form of capsules. A lack of oral administration explains the low VANKA absorption. Within 24 h, 80 to 90% of the orally administered VANKA is excreted unchanged in the urine. The average duration of VANKA therapy is 7 to 10 days [16]. According to clinical studies, VANKA microbiologic inhibitory activity (MIC) to the strains of MRSA ranges from 0.125 µg/mL to 2 µg/mL [17–19]. Additionally, over time, VANKA degrades into crystalline degradation products—chiral stationary phase, CDP-1; thus, the concentration of the VANKA active form decreases and, while monitoring the drug concentration, an appropriate method has to be selected [20–22].

VANKA can be encapsulated into the liposomes, which are unique medication carriers, because they overcome the disadvantages of the peroral or intravenously administered drugs. The most important liposomal properties are their biocompatibility, the ability to encapsulate a large amount of the substance, the ability to increase the stability of the encapsulated substance, controlled drug delivery and limited circulation time in the human body [23]. The main materials for liposome preparation are phospholipids and cholesterol [24]. Phospholipids are lipids composed of a polar and non-polar part that contain phosphorus and provide a spherical liposome formation process [12]. Cholesterol is added to the liposome composition to reduce the permeability of fluids through the membrane and increase liposome stability as well as promote the increase of phospholipid bilayer viscosity [24–26]. Nevertheless, the encapsulation efficiency of VANKA in liposomes depends on the preparation method and lipid composition, but it is usually below 20% [14,27]; higher encapsulation efficiency (33%) could be achieved by freezing/thawing [28]. As an alternative, polymeric microparticles from poly lactic-co-glycolic acid (PLGA) have been studied to encapsulate VANKA [25,27,28]. PLGA is a biodegradable copolymer that has been FDA approved and is used as a drug carrier. Drug release kinetics can be controlled by the polymerization rate of lactide and glycolide as well as molecular weight of PLGA [27,29]. Both liposomes and PLGA microcapsules have drawbacks in terms of encapsulation efficiency, but encapsulation of VANKA in carrier provides high clinical benefits for the long-term use of antibiotics. Therefore, the adjustment of VANKA carrier composition and the drug release rate in autologous samples is essential. Current studies on drug carriers within the autologous PRF samples are limited. Wang et al. studied platelet poor plasma-based fibrin gel containing liposomes/chitosan scaffold for hydrophilic drug delivery. The crosslinking process with glutaraldehyde ensured the drug delivery up to 18 days [30]. Micro- and nanoparticles and fibrin are studied in terms of their interaction to activate coagulation cascade [31], as well as to create double networks/hydrogels consisting of gelatin and PRF for bone healing [32]. Furthermore, PRF compositions are studied to develop three-dimensional networks with calcium phosphate granules [33], collagen membranes [34], and other materials [1], but these strategies are targeted towards delivery of autologous growth factors and cells that are within the PRF.

In this study, we aimed to develop controlled VANKA delivery systems based on PRF scaffold, combining antibacterial properties of VANKA against MRSA with autologous PRF scaffold containing living cells and growth factors.

2. Materials and Methods

2.1. Materials

VANKA hydrochloride (Sigma-Aldrich, St. Louis, MI, USA), polylactic-co-glycolic acid (PLGA; Resomer RG 502, Evonik Nutrition & Care GmbH, Essen, Germany), chole-

terol ($\geq 99\%$, M = 386.65 g/mol, Sigma-Aldrich, St. Louis, MI, USA), 1,2-distearoyl-sn-glycero-3-phosphocholine (DSPC; $>99\%$, M = 790.145 g/mol, Avanti Polar Lipids, Alabaster, Alabama), chloroform ($\geq 99\%$, M = 119.38 g/mol, Sigma-Aldrich, St. Louis, MI, USA), acetonitrile ($\geq 99.9\%$, Sigma-Aldrich, St. Louis, MI, USA), di-potassium hydrogen phosphate trihydrate (K_2HPO_4 ; $\geq 99\%$, Merck, Darmstadt, Germany), polyvinyl alcohol (PVA; M = 25 kDa, 88 mol% hydrolysis, Polysciences, Warrington, UK), phosphoric acid (H_3PO_4 ; C = 75% w/w, Latvijas ķīmija, Riga, Latvia), dichloromethane (DCM; $\geq 99.8\%$, Merck, Darmstadt, Germany), methanol ($\geq 99.9\%$, Sigma-Aldrich, St. Louis, MI, USA), phosphate-buffered saline tablet (PBS, Sigma-Aldrich, St. Louis, MI, USA), Lugol solution (Deltalab Eurotubo[®], Barcelona, Spain).

2.2. Blood Collection and Separation of PRF

Blood of 10 healthy volunteers was collected in 10 mL i-PRF+ tubes and immediately placed in the centrifuge ("PRF Duo Quattro"). A medical nurse drew the blood with a clinically approved butterfly blood collection method ("BC-12, 21 G \times 3/4"). The centrifugation time was 3 min and the rotor radius was 100 mm, 700 rpm. After the centrifugation, the upper layer of liquid PRF (1 mL) from each tube was transferred into a 24-well cell culture plate for further use.

Written consent from all of the volunteers for use of their samples in the research studies was obtained. All donors were free of any infectious disease and did not have any abnormal consumption of nicotine or alcohol. None of the subjects used any drugs for anticoagulation. Permission No. 6-2/10/53 of the Research Ethics Committee of Riga Stradins University has been received for the research.

2.3. Preparation of VANKA Carriers

2.3.1. Preparation of Liposomes

Liposomes composed of DSPC and cholesterol in a molar ratio of 2:1 were synthesized using a thin film hydration method and three dehydration–rehydration cycles [14,15]. To obtain a thin film, DSPC and cholesterol were dissolved in chloroform. The sample was then dried in a stream of nitrogen gas until dry lipid film formation on the vessel walls was observed. To dry completely, sample was placed at -400 mbar vacuum for 6 h. Hydration was carried out gradually by adding 1 mL of deionized water to the sample and treating the sample in an ultrasonic bath to reduce liposome size and agglomeration. Hydration was complete when 5 mL of deionized water were added to the sample. Hydrated liposomes were frozen and lyophilized. Three dehydration–rehydration cycles were performed to reduce liposome size.

VANKA-containing liposomes were synthesized according to the method described above. The concentration of VANKA in hydration solution was 250 $\mu\text{g}/\text{mL}$. Hydrated sample contained 6.25% VANKA from the total sample mass. During the second and third dehydration–rehydration cycles, VANKA-containing liposome samples were hydrated in 5 mL of deionized water.

2.3.2. Preparation of Microcapsules

For the preparation of microcapsules, the water–oil–water method was used. VANKA was dissolved in deionized water (10 mg/mL). This solution was added to the organic phase solution that consists of a PLGA polymer (1 g) dissolved in DCM (5 mL). Both solutions were stirred vigorously to yield a water-in-oil emulsion. Afterwards, the water-in-oil primary emulsion was added to 100 mL PVA aqueous solution (4 wt %) and further mixing was carried out for 30 to 60 s at a rate of 600 rpm [28]. The resulting emulsion was transferred to 2.5 L deionized water and stirred for 1 h. The suspension was centrifuged and frozen in liquid N_2 , then lyophilized for 72 h to obtain a dry microcapsule powder.

2.4. Incorporation of VANKA Carriers in PRF

The VANKA carriers were added to the PRF by suspending them in PRF with an automatic pipette before the clot formed. As control samples, PRF without VANKA carriers were prepared using the same procedure. The mixing procedures were carried out in sterile 24-well cell culture plates.

Nine different samples with corresponding abbreviations were prepared—see Table 1 below:

Table 1. Abbreviations of prepared samples.

Abbreviation	Sample
Blank liposomes	Liposomes without VANKA
VANKA liposomes	Liposomes with encapsulated VANKA
PLGA_μC_Blank	PLGA microcapsules without VANKA
PLGA_μC_VANKA	VANKA loaded PLGA microcapsules
PRF	Platelet-rich fibrin
PRF/VANKA liposomes	PRF with VANKA loaded liposomes
PRF/VANKA	PRF with VANKA- added as free drug powder, non-encapsulated
PRF/PLGA_μC_Blank	PRF without VANKA loaded PLGA microcapsules
PRF/PLGA_μC_VANKA	PRF with VANKA loaded PLGA microcapsules

2.5. Characterization of VANKA Carriers and PRF Scaffold

2.5.1. Drug Load and Encapsulation Efficiency

The drug load (DL) in liposomes and VANKA encapsulation efficiency was determined indirectly by measuring free VANKA in the liposome suspension. The sample preparation included liposome suspension centrifugation at 3000 rpm for 15 min (“Biosan LMC-3000”). To prepare the sample for VANKA determination, 1 mL of solution was filtered through 0.22 μm nylon membrane filter and then analyzed using ultra-performance liquid chromatography (see Section 2.6).

VANKA encapsulation efficiency was calculated using the equation below [13].

$$EE_L = \frac{W_{total} - W_{free}}{W_{total}} \cdot 100\%, \quad (1)$$

where W_{total} is the amount of drug (VANKA) added in liposomes and W_{free} is the detected amount of VANKA in the solution. The drug load (%) in liposomes was calculated according to Equation (2), where w_{lipid} is the amount of lipids added in the system:

$$DL_L = \frac{W_{total} - W_{free}}{W_{lipid}} \cdot 100\%, \quad (2)$$

To determine the total drug load (DL) in microcapsules, nitrogen content microanalysis (apparatus—Vario MACRO CHNS, Hanau, Germany) was used. Calculations were carried out according to Equation (3):

$$DL_{MK} = \frac{N_{el}}{N_{tot}} \cdot 100\%, \quad (3)$$

where N_{el} is the nitrogen content found using microanalysis and N_{tot} is the calculated nitrogen content in VANKA. The encapsulation efficiency (EE) was calculated according to Equation (4):

$$EE_{MK} = \frac{DL \cdot w_{microcapsules}}{W_{totalVANKA}} \cdot 100\%, \quad (4)$$

where $w_{microcapsules}$ is the number of microcapsules obtained and $w_{totalVANKA}$ is the amount of VANKA added in the microcapsule preparation process.

2.5.2. Particle Size

The average liposome size and particle size distribution was determined using a dynamic light scattering (DLS) analyzer and BIC Particle Sizing Software version 4.03. Measuring temperature 20 °C, angle 90°, 2 min per measurement, refractive index 1.45.

The average microcapsule size and particle size distribution was determined using a laser particle size analyzer (ANALYSETTE 22, measuring range from 0.01 to 1000 µm, laser wavelength 650 nm).

Each sample was measured in triplicate.

2.5.3. Morphology

The morphology of hydrated liposomes and as prepared PRF with and without carriers was determined by light microscope “Leica DFC320, DMLP”. The morphology and size of the negatively stained liposomes was characterized with a transmission electron microscope (TEM) “JEOL JEM1230”. We used SEM/energy dispersive spectroscopy (EDS) for semi-quantitative chemical analysis of the lyophilized liposomes, microcapsules, and PRF samples. The samples were analyzed with an Oxford X-Max^N Silicon Drift Detector (150 mm²) attached to Tescan Mira³ LMU SEM. Five randomly selected areas of at least 100 × 100 µm were analyzed on the surface of each sample at an accelerating voltage of 15 kV, working distance of 27 mm, and a counting time of 60 s.

2.5.4. Chemical Structure and Phase Composition

The obtained carriers and lyophilized PRF chemical structures were determined by Fourier-transform infrared spectroscopy (FTIR). FTIR (“Varian 800 FT-IR”, Scimitar Series, Randolph, MA 02368, USA) spectra were recorded in the attenuated total reflectance (ATR, “GladiATR™”, Pike Technologies, Madison, WI 53719, USA) mode. Spectra were obtained at 4 cm⁻¹ resolution co-adding 50 scans over a range of wavenumbers from 400 cm⁻¹ to 4000 cm⁻¹. Before every measurement, a background spectrum was taken and deducted from the sample spectrum.

2.5.5. Micro-Computed Tomography Analysis

To visualize 3D PRF samples, high-resolution micro-computed tomography (µCT50, Scanco Medical AG, Bruttisellen, Switzerland) was used. Samples were stained with a common soft tissue staining procedure that increases the contrast in non-mineralized biological tissues [35]. Staining was carried out with 0.3% Lugol’s solution [36] to see the drug delivery systems within the PRF samples. PRF sample with/without drug delivery systems was placed in 0.3% Lugol’s solution for 1 min, then rinsed with water. The following scanning parameters were used: 55 kVp voltage, 109 µA current, 7.4 µm voxel size, 0.1 mm Al filter, frame averaging = 6, and 360° rotation. The scanning time for each sample was 6 h and 40 min. Reconstruction of 3D datasets from microCT projection data, including beam hardening correction, was performed automatically after completion of each cone beam image stack. The visualization module performs sophisticated 3D rendering of large data sets using high-quality ray-tracing algorithms.

2.6. Assessment of VANKA Release Kinetics

Assessment of VANKA concentration and release kinetics was analyzed using ultra-performance liquid chromatography. The chromatographic method was transferred to the previously described method on active form VANKA detection on HPLC. “Waters Acquity UPLC H-class” with UV/VIS detector “Waters Acquity TUV” set at 210 nm and the chromatography column “Waters Acquity UPLC BEH C18, 1.7 µm, 2.1 × 50 mm” was used. The mobile phase consisted of two phases: A—0.05 M K₂HPO₄ × 3H₂O buffer (pH = 3.2): acetonitrile: methanol in ratio (v/v) 91:5:4, respectively; and B—0.05M K₂HPO₄ × 3H₂O buffer (pH = 3.2): acetonitrile: methanol in ratio (v/v) 84:8:8, respectively [22]. Separation of the active VANKA form was obtained using the following gradient (Figure 1) conditions at a flow rate of 0.3 mL/min: 100% A for 0.67 min, change to 100% B in 3.0 min, hold B

for 4.66 min, change to 100% A in 1.67 min and hold for 2 min. The total run time for one sample was 12 min. The column temperature was maintained at $30\text{ }^{\circ}\text{C} \pm 5\text{ }^{\circ}\text{C}$ and sample temperature at $10\text{ }^{\circ}\text{C} \pm 5\text{ }^{\circ}\text{C}$.

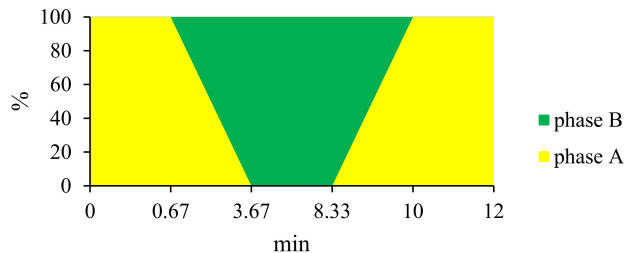


Figure 1. Gradient curve of mobile phase composition for VANKA quantification method.

Samples for the evaluation of in vitro VANKA release from the liposomes were immersed in 10 mL PBS, using dialyze membrane, and incubated at $37\text{ }^{\circ}\text{C} \pm 0.5\text{ }^{\circ}\text{C}$ and 50 rpm (Environmental Shaker—incubator ES-20, Biosan, Riga, Latvia). A total of 250 μL aliquots of the solution were taken directly from the vessels after 1 h, 2 h, 3 h, 5 h, 24 h, 48 h, 72 h, 96 h, and 168 h. The volume taken was replaced with 250 μL of fresh PBS, keeping the total dissolution medium volume constant.

PLGA- μC -VANKA and PRF/VANKA carriers were immersed in 10 mL deionized water and incubated at $37\text{ }^{\circ}\text{C} \pm 0.5\text{ }^{\circ}\text{C}$ and 50 rpm (Environmental Shaker—incubator ES-20, Biosan, Riga, Latvia). One milliliter aliquots of the solution were taken directly from the vessels after 1 h, 2 h, 4 h, 6 h, 24 h, 48 h, 72 h, 146 h, 217 h, and 239 h. The volume taken was replaced with 1 mL of deionized water, keeping the total dissolution medium volume constant. The cumulative fraction of the release rate was calculated from the following equation [15]:

$$\text{Release rate} = \frac{c_n v_0 + \sum_{i=0}^{n-1} c_i v_i}{c_0 v_0} \cdot 100\%, \quad (5)$$

where c_n is the VANKA concentration in the release medium of each time interval, v_0 is the total volume of the release medium, v_i is the volume of the withdrawn medium, c_i is the drug concentration in the release medium at time, and c_0 is the total VANKA concentration in the system.

2.7. Preparation of Bacterial Suspension and Inoculum for Antibacterial Tests

Antibacterial properties were tested via the disk diffusion test, also known as the Kirby-Bauer disk diffusion method, which is a standardized method used in microbiology laboratories in order to determine bacterial susceptibility against antibiotic substances. Bacterial suspension of *Staphylococcus aureus* (ATCC 25923) reference culture was prepared according to EUCAST (European Committee on Antimicrobial Susceptibility Testing) standards in optic density of 0.5 according to McFarland standard with McFarland optic densitometer (Biosan, Riga, Latvia). Bacterial suspension was inoculated onto a sterile Mueller–Hinton (MH) agar (Oxoid, Altrincham, UK) with a sterile cotton swab.

2.8. Determination of VANKA Loaded PRF Antibacterial Properties

After bacterial inoculation, samples were placed onto MH agar with sterile forceps, and MH agar with samples was incubated in the thermostat for 24 h at $37\text{ }^{\circ}\text{C}$ degrees. After 24 h, the antibacterial properties of the samples were analyzed by measuring the sterile area (diameter) around the samples. After the measurements, a new bacterial suspension was prepared and inoculated onto a new sterile MH agar, and the samples were transferred from the old to the new MH agar and incubated for another 24 h at $37\text{ }^{\circ}\text{C}$. These actions

were repeated every 24 h until no trace of antibacterial characteristics or sterile area around the samples was found for two days in a row.

2.9. Determination of Antibacterial Properties of Sample Incubation Medium

The samples were immersed in the medium and incubated at $37\text{ }^{\circ}\text{C} \pm 0.5\text{ }^{\circ}\text{C}$ and 50 rpm. One milliliter aliquots of the solution were taken directly from the vessels after 1 h, 2 h, 4 h, 18 h, 24 h, 48 h, 70 h, 90 h, 146 h, 217 h, and 239 h. The volume taken was replaced with 1 mL of deionized water, keeping the total dissolution medium volume constant. After bacterial inoculation, the nitrocellulose disks were placed on MH agar and impregnated with 20 μL of incubation solutions. Three nitrocellulose disks from one series were used. MH agar were incubated in the thermostat for 24 h in $37\text{ }^{\circ}\text{C}$ degrees. After 24 h, antibacterial properties were analyzed by measuring the sterile area (diameter) around the disks.

2.10. Statistical Evaluation

All results were expressed as the mean value \pm standard deviation (SD) of at least three independent samples. The significance of the results was evaluated using an unpaired Student's *t*-test with the significance level set at $p < 0.05$. One- and two-way analyses of variance (ANOVAs) were performed to evaluate the differences between the results.

3. Results

3.1. Evaluation of VANKA Carriers

3.1.1. Particle Size Distribution and Morphology

In order to develop a controlled VANKA delivery system based on PRF, VANKA was encapsulated in two carrying systems—liposomes and microcapsules, respectively. Conventional methods for preparation of liposomes and microcapsules were chosen to establish the difference between the VANKA carrying materials within the PRF scaffolds. Nevertheless, VANKA is hydrophilic drug and according to the previous studies, the encapsulation efficiency in both liposomal and microcapsule systems is low [15].

Blank liposomes were prepared to evaluate the baseline of the particle characteristics. The obtained sizes and polydispersity indexes of the liposomes are summarized in Table 2.

Table 2. Size and polydispersity index of liposomes.

	Blank Liposomes	VANKA Liposomes
Average effective diameter, nm	1354.8 ± 100.6	932.7 ± 114.2
Polydispersity index	0.17	0.24

VANKA binds to liposome with a millimolar affinity. The larger the size of the liposomes, the stronger the binding of VANKA and liposomes. VANKA associates with liposome through its interaction with the head group of the lipids. The previous studies state that it is unlikely for the VANKA to penetrate deep into the lipids bilayer this means that VANKA does not interact and bind to lipid tails [37,38].

Liposomal sizes were verified by Transmission electron microscopy (TEM) (Figure 2). TEM analysis shows that prepared liposomes have a heterogeneous population in which it is possible to observe a close presence of two-layer structures. Also, Figure 2. shows that the majority of liposomes are spherical particles.

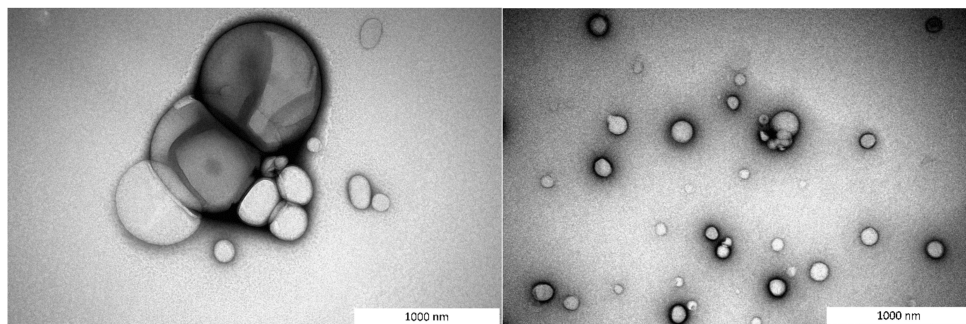


Figure 2. TEM pictures of VANKA loaded liposomes.

The sizes of the microcapsules prepared in this study ranged from 3 μm to 46 μm (Figure 3). The mean size according to the granulometric analysis of blank PLGA microcapsules is $15.17 \pm 0.11 \mu\text{m}$, while the encapsulation of the VANKA resulted in a decrease in the particle size (mean size $12.60 \pm 0.09 \mu\text{m}$) (Table 3). According to the ANOVA test, the p values between the different groups range from 0.00001 to 0.00012. We assume that the decrease is observed due to the VANKA's high solubility in water; it draws the water into the polymer membrane, thus accelerating the hydrolytic process [39].

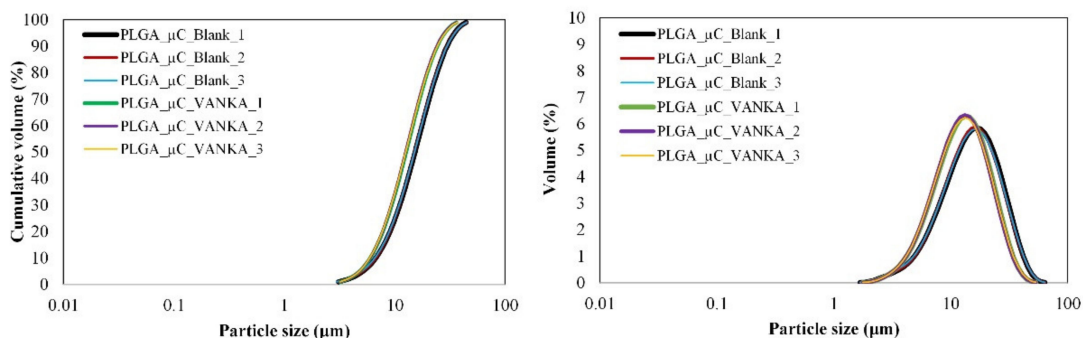


Figure 3. Particle size distribution of blank PLGA microcapsules and VANKA-loaded PLGA microcapsules.

Table 3. Particle size distribution of VANKA-loaded PLGA microcapsules prepared via w/o/w technique.

Microcapsules	Particle Size \pm SD, μm		
	d_{10}	d_{50}	d_{90}
PLGA_μC_Blank	6.69 ± 0.08	15.17 ± 0.11	29.51 ± 0.44
PLGA_μC_VANKA	5.96 ± 0.03	12.60 ± 0.09	24.26 ± 0.18

SEM images of the microcapsules with and without VANKA are shown in Figure 4. SEM photographs exhibited spherical particles with smooth surfaces, which indicated the absence of any drug crystal on the surface and confirmed the even distribution of the drug in the polymeric matrix (Figure 4B).

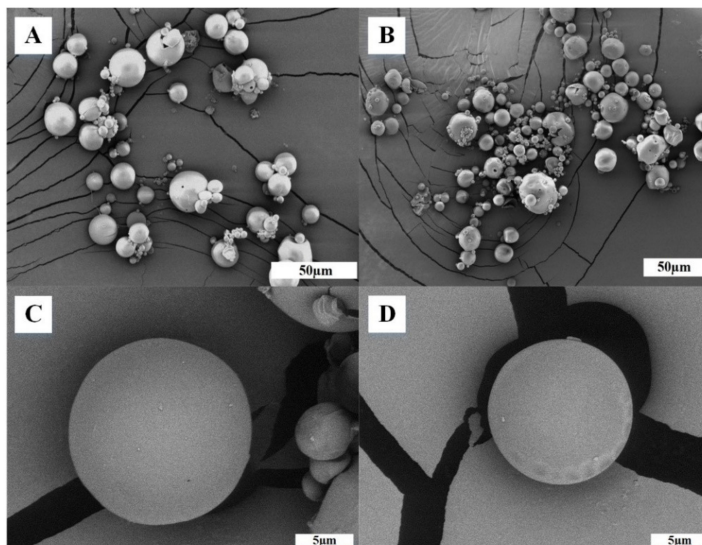


Figure 4. SEM pictures of surface of PLGA microcapsules (A,C) without and (B,D) with VANKA.

3.1.2. Drug Load and Encapsulation Efficiency

The drug load and encapsulation efficiency are important parameters to evaluate the properties of microcapsules and liposomes (Table 4). The results of loading efficiency indicated that 56.44% of the initially used drug were encapsulated within liposomes and 12.30% were encapsulated within microcapsules. Their drug load resulted in $2.61 \pm 0.01\%$ for liposomes and $1.77 \pm 0.03\%$ for microcapsules. Although the results show that the loading of the drug into liposomes and microcapsules was very low, the MIC concentration can be reached by administering a certain amount of drug carriers to the PRF sample: 20 mg of liposomes and 50 mg of microcapsules, respectively. As the MIC value is negligible, it is not necessary to administer high concentrations of liposomes and microcapsules to the PRF. In the literature, the highest reported efficiency of drug encapsulation in liposomes is $35.58 \pm 2.66\%$, drug load $2.55 \pm 0.065\%$ [15], which is lower than that achieved in our study, but in microcapsules, the drug encapsulation efficiency can reach 80 to 97% and drug load $>54.6\%$ when using PLGA 90:10, where the ratio of polymer to drug is superior [39]. A number of researchers have documented that highly hydrophilic drugs face the problems associated with low affinity for the polymer, resulting in unsatisfactory loading efficiency [40]. With a poor interaction between drug and polymer, the drug will tend to diffuse from the organic phase into the external aqueous environment during the spontaneous emulsification of the polymer. Although VANKA was completely dissolved in the organic phase, the drug could leak out during diffusion of the remaining dichloromethane from droplets of the organic phase into the aqueous dispersion medium [41]. The microcapsules used in this study with PLGA composition 50:50 have a faster (~ 20 days) degradation time, compared to PLGA 90:10 and PLGA 70:30 [29], and are more appropriate for the release of antibiotic agents with an optimal therapy time up to 14 days.

Table 4. Drug loading and encapsulation efficiency of liposomes and microcapsules.

	VANKA Liposomes	PLGA_μC_VANKA
Drug load, %	2.61 ± 0.01	1.77 ± 0.03
Encapsulation efficiency, %	56.44 ± 0.02	12.30 ± 0.05

3.1.3. Chemical Structure of VANKA Carriers

The FTIR spectrum of liposomes is shown in Figure 5A. The VANKA molecule is characterized by oscillations of O-H and N-H₂ bonds, the absorption observed is in the range of 3000 to 3600 cm⁻¹, as well as fluctuations of C=O bonds, the absorption that occurs at 1670 cm⁻¹.

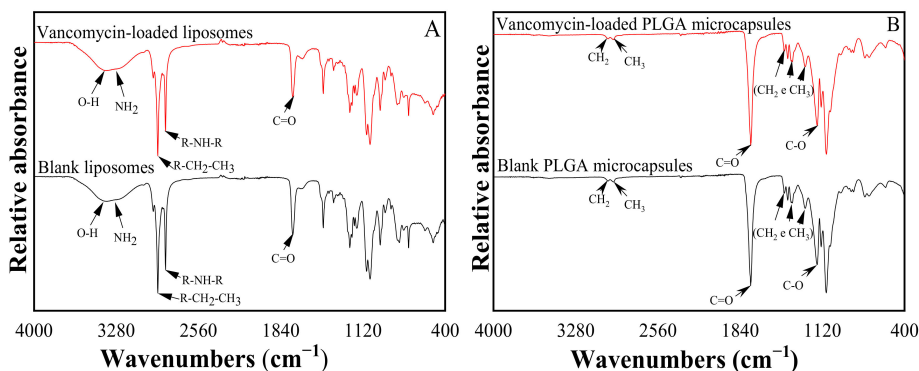


Figure 5. FTIR spectrum of (A) liposomes and (B) microcapsules.

The FTIR spectrum of the synthesized PLGA samples is shown in Figure 5B. In the PLGA microcapsule sample spectrum, it is possible to observe a thick band in the range between 1750 cm⁻¹ and 1740 cm⁻¹, a characteristic range of carbonyl (C=O), present in the two monomers. Grouping band (C-O), between 1300 cm⁻¹ and 1150 cm⁻¹ can be observed, which is characteristic of ester groups. The absence of absorption bands between 3600 and 3400 cm⁻¹ in Figure 5B, characteristic bands of the hydroxyl group, indicates that the PLGA copolymers are anhydrous.

No specific binding of VANKA with carrier materials, lipids (Figure 5A), or PLGA (Figure 5B) accordingly, were observed.

3.2. Characterization of Modified PRF Scaffold

SEM images of PRF samples after lyophilization are shown in Figure 6. The surface morphology of PRF (Figure 6) shows a fibrous nature. PRF scaffolds without VANKA carriers and free drug show spaces between fibrin fibers that have been formed by thrombin (Figure 6A). In the literature, it has been found that greater the increase of thrombin concentration, the denser and thicker the fibers are [33]. All the prepared scaffolds contained fibrin networks and fibrin layers that interweave with the blank and VANKA-loaded microcapsules (Figure 6B,C). In turn, the PRF scaffolds with VANKA (Figure 6D) but without drug carriers exhibit a smooth surface, which indicates the absence of drug crystals on the surface. SEM-EDX analysis (see Figure 7) confirms the uniform distribution of the drug in the PRF scaffolds; the chloride distribution is attributed to the VANKA; the drug is in hydrochloride form.

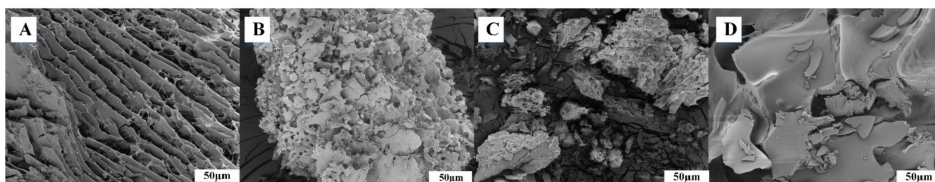


Figure 6. SEM pictures of PRF scaffolds: (A)—PRF; (B)—PRF/PLGA_μC_Blank; (C)—PRF/PLGA_μC_VANKA; (D)—PRF/VANKA.

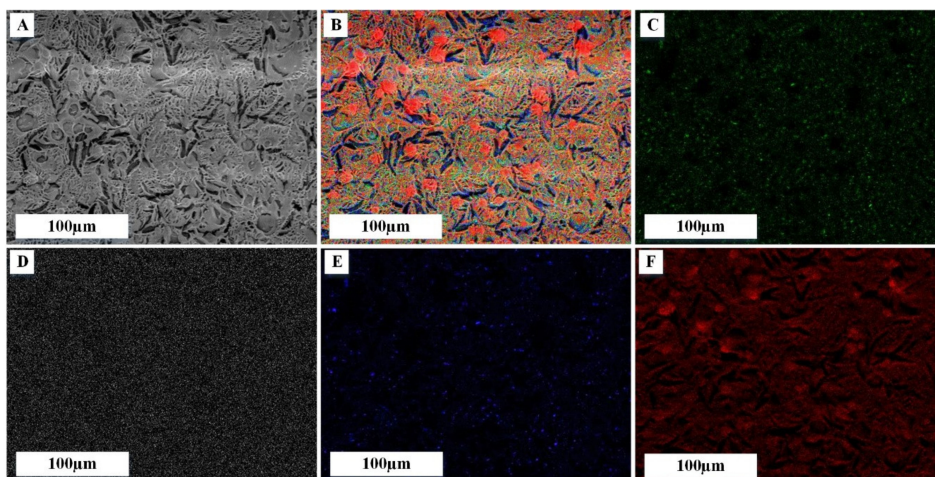


Figure 7. EDX mapping analysis on PRF/VANKA scaffold; (A) SEM image; (B) overall mapping elements on the same spot, corresponding to: (C) chloride, (D) potassium, (E) sodium and (F) oxygen mapping.

The FTIR spectra of the samples (Figure 8) show the absorption bands characteristic of the fibrin phase in Figure 8: maximum at 1644 cm^{-1} —amide I (C = O), maximum at 1531 cm^{-1} —amide II (N-H), and maximum at 1259 cm^{-1} —amide III (C-N). It can be seen that deformations of fibrin clots (either elongation or compression) have caused a marked rearrangement of the secondary structure of the proteins, which is reflected in the characteristic changes in the FTIR spectra. At the qualitative level, these changes could be described as a redistribution of the absorption intensity from higher to lower wavenumbers. This shift was confirmed by the differences in spectral peak positions observed in the different vibration modes of the peptides: amide I (decrease at $1649\text{--}1651\text{ cm}^{-1}$ and increase at $1620\text{--}1630\text{ cm}^{-1}$), amide II (decrease at $1540\text{--}1550\text{ cm}^{-1}$ and increase at $1530\text{--}1540\text{ cm}^{-1}$) and amide III (decrease at $1290\text{--}1320\text{ cm}^{-1}$ and increase at $1220\text{--}1240\text{ cm}^{-1}$). As found in the literature, the absorption of different proteins at higher wavenumbers ($1649\text{--}1651\text{ cm}^{-1}$, $1540\text{--}1550\text{ cm}^{-1}$, and $1290\text{--}1320\text{ cm}^{-1}$) is mainly due to α -helical structures, whereas the lower wavenumbers ($1620\text{--}1630\text{ cm}^{-1}$, $1530\text{--}1540\text{ cm}^{-1}$, and $1220\text{--}1240\text{ cm}^{-1}$) are mostly characteristic of β structures [42]. It can be concluded that the structure of β is more pronounced in the studied sample.

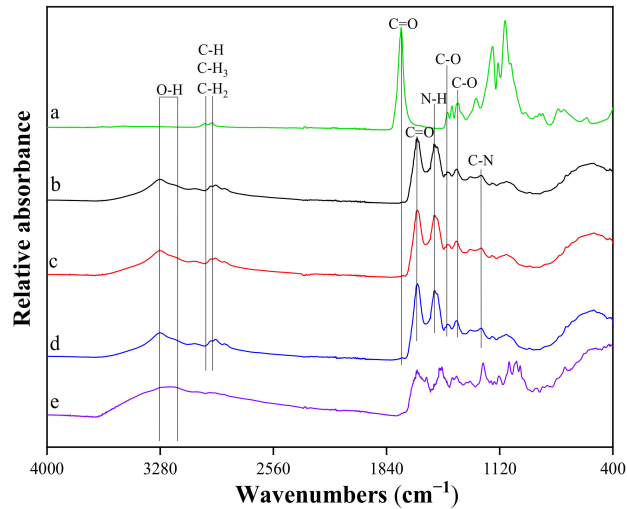


Figure 8. FTIR spectra of: (a) PLGA_μC_Blank; (b) PRF scaffold; (c) PRF/ PLGA_μC_Blank scaffold; (d) PRF/ PLGA_μC_VANKA scaffold; (e) VANKA.

The FTIR analysis of PRF scaffolds with VANKA carriers showed a pronounced absorption maximum at 3304 cm^{-1} , which indicates the presence of an OH group in the structure of the samples, which is characteristic of OH groups in the fibrin structure. In turn, the absence of this peak in the PLGA spectrum indicates that PLGA copolymers are anhydrous [43]. Absorption peaks at 1415 cm^{-1} (group C-O) and 1371 cm^{-1} (group C-O) correspond to the PLGA phase from the PLGA microcapsules added to the sample [44]. Absorption maxima at 2948 cm^{-1} and 2995 cm^{-1} are related to stretching vibrations of PLGA C-H, C-H₃, and C-H₂ functional groups [45].

The maximum at 1215 cm^{-1} indicates the presence of the hydroxyl group of the phenol in the structure of the samples, which is characteristic of the structure of VANKA [46]. From the FTIR spectra, it can be concluded that there is no specific binding of VANKA to PRF scaffold.

3.3. 3D Structure of Modified PRF Scaffolds

Micro-CT images of three types of freshly made PRF samples after staining are shown in Figure 9. Micro-CT analysis of stained samples confirmed that VANKA carriers are encapsulated within the scaffolds during the preparation of the PRF scaffolds. In addition, the data shows the distribution of the medium according to the volume of the PRF framework. The upper portion seen in 3D micro-CT reconstruction images and cross-sectional images (colored white) is likely a PRF crust formed by coagulation of the sample. As seen in the images, VANKA liposomes are distributed directly in the PRF cortex. It is possible that a large amount of VANKA is released during the decomposition of the PRF crust. This is also supported by the release kinetics data (Figure 10). In turn, in the case of PRF/PLGA_μC_VANKA, it can be seen that the PLGA_μC_VANKA particles are scattered throughout the sample. Thus, as the sample degrades, only a portion of the encapsulated VANKA in the crust is rapidly released. The remainder of VANKA is released gradually and evenly (Figure 11).

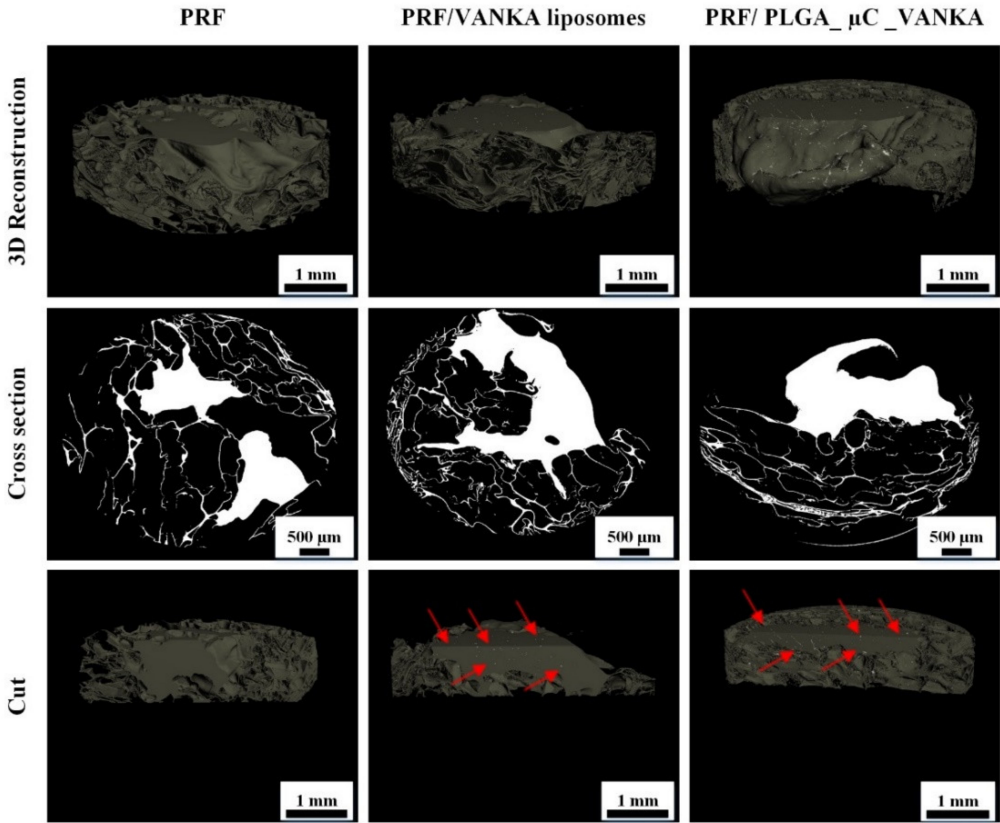


Figure 9. Micro-CT images of the PRF samples with VANKA liposomes (PRF/VANKA liposomes) and with VANKA microcapsules (PRF/PLGA_μC_VANKA) and the control samples without drug delivery systems (PRF); red arrows indicate the existence of delivery systems in the PRF samples.

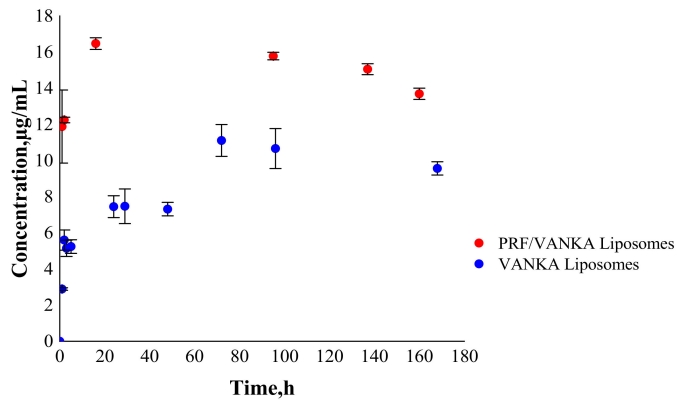


Figure 10. Drug release from PRF/VANKA liposomes and VANKA liposomes.

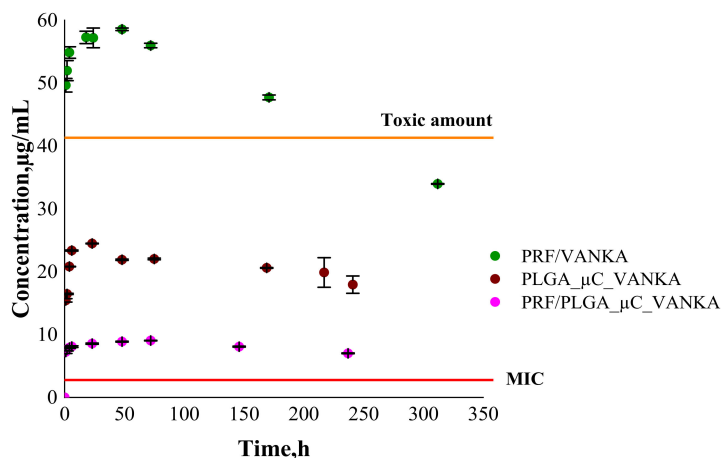


Figure 11. Drug release from PRF/VANKA scaffolds; PLGA_μC_VANKA and PRF/PLGA_μC_VANKA scaffolds.

3.4. VANKA Release Kinetics

Over time, VANKA degrades into CDP-1; thus, the concentration of the active form of VANKA decreases [20,21]. Consequently, an appropriate drug concentration quantification method has been developed. Therefore, instead of cumulative release, we indicate concentrations of free VANKA form at each measured time point.

The release kinetics of VANKA from PRF/VANKA liposomes is higher than from VANKA liposomes (Figure 10). The increased concentration of VANKA can possibly be explained by the fact that the Ca^{2+} ions in fibrin form a shell around the lipids, compressing them and thus destroying the liposomes [47,48]. Based on the results, it can be concluded that Ca^{2+} ions adversely affect the liposomes; thus, VANKA is released faster and in higher concentrations.

Based on the VANKA release studies from PLGA microcapsules (Figure 11), the kinetics of VANKA release from PRF/PLGA_μC_VANKA scaffolds are reduced fivefold compared to PRF/VANKA samples, ensuring controlled VANKA release and preventing burst release. These differences are also confirmed by the ANOVA test, which at $p < 0.05$ indicates a statistically significant difference. In contrast, comparing PLGA_μC_VANKA with PRF/PLGA_μC_VANKA scaffolds, it can be observed that the VANKA release concentration is reduced twofold. This suggests that the PRF scaffold inhibits the rapid release of VANKA. It was observed that with the release of VANKA from PRF /PLGA_μC_VANKA scaffolds, the highest VANKA concentrations are observed in the first hours, which is actually required to prevent possible postoperative infections. Results of VANKA release kinetics from PRF/VANKA samples exceeds the toxic amounts of VANKA during the first 24 h. As mentioned above, the therapeutic effect occurs at 20–40 μg/mL, but here, the concentration is above 49 μg/mL. It can be concluded that the introduction of VANKA in PRF scaffolds without VANKA carriers does not ensure a controlled delivery of the drug that is necessary for the therapeutic effect.

3.5. Antibacterial Properties of VANKA Containing PRF Scaffolds

PRF/VANKA liposome samples were not included in further experiments because, as demonstrated by the micro-CT images, liposomes cannot be homogeneously mixed into the PRF matrix and, as the PRF crust in which the liposomes are incorporated degrades more rapidly, rapid VANKA release is observed. The undesirable effect of Ca^{2+} ions on the structure of liposomes, which promotes the destruction of liposomes and results in faster VANKA release, cannot be excluded either.

The maximum duration of antibacterial effect for VANKA-containing samples was observed for 48 h. For the first 24 h, the mean diameter of the sterile area around the samples is 30 mm. For the next 24 h, the diameter of the sterile area was reduced by 50% (Figure 12). No antibacterial properties were observed for samples without VANKA. The decrease of the sterile area after 48 h can be explained by the experimental method, as the sample dries out during the incubation period and the diffusion of drugs from the sample is limited. To overcome this issue, we tested the antibacterial properties of the incubation medium of the sample rather than the sample itself (see Section 3.6).

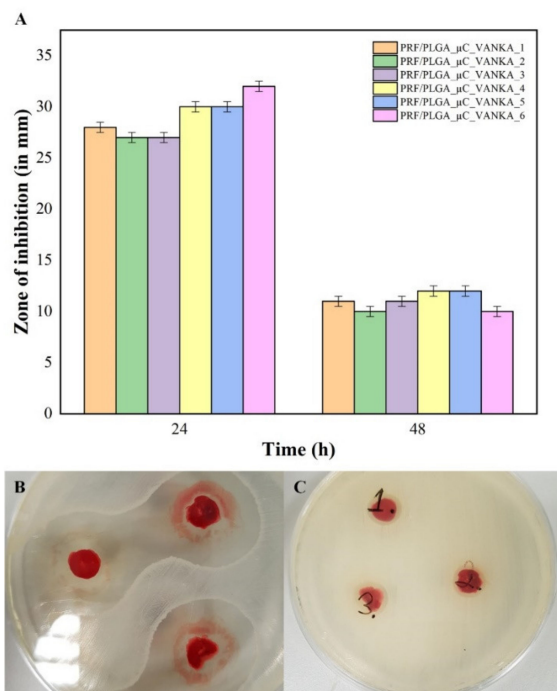


Figure 12. Antibacterial properties of PRF/PLGA_μC_VANKA samples: (A) inhibition zones in mm; (B) sterile areas around the PRF/PLGA_μC_VANKA samples after 24 h incubation; (C) sterile areas around the PRF/PLGA_μC_VANKA samples after 48 h incubation. The diameter of the petri dishes is 8.5 cm.

3.6. Antibacterial Activity of Sample Incubation Medium

The release of VANKA from the samples in the incubation medium was observed at all time points in the study (see Figure 13A). Concentrations of released VANKA from PRF/PLGA_μC_VANKA were 70% lower than PRF/VANKA samples. Due to the excretion of VANKA, antibacterial properties (sterile areas around the impregnated nitrocellulose disks) were not observed in PRF/PLGA_μC_VANKA samples at 24- and 48-h intervals. Significant differences in concentration between different types of samples gave proportionally higher antibacterial effects—the mean diameter of the sterile zone at 1-h intervals is 11 mm for PRF/VANKA incubation medium, but 8 mm for PRF/PLGA_μC_VANKA incubation medium. Differences in concentrations between samples of the same type were negligibly low and did not impact different antibacterial parameters, and the diameter of the sterile zones were maintained without significant differences.

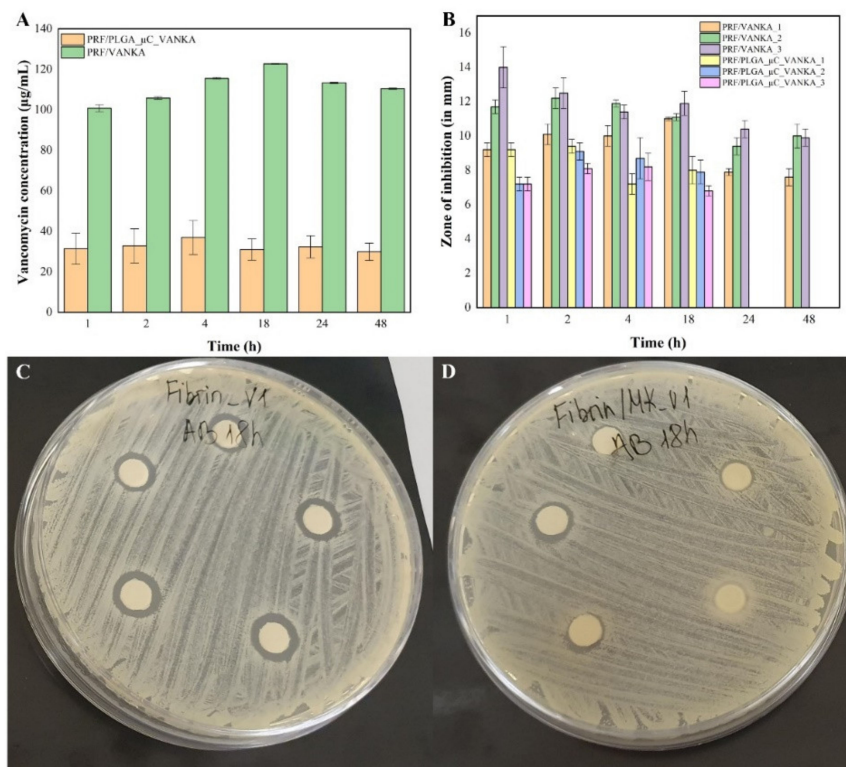


Figure 13. Antibacterial properties of sample incubation medium at different time points: (A) detected VANKA concentrations at sample incubation medium at different time points; (B) inhibition zones of disks impregnated with sample incubation medium at different time points; (C) sterile areas around the disks that were impregnated with PRF/VANKA sample incubation medium at 18-h time point; (D) sterile areas around the disks that were impregnated with PRF/PLGA_µC_VANKA sample incubation medium at 18-h time point. The diameter of the petri dishes is 8.5 cm.

4. Conclusions

According to the obtained results, we can conclude that the introduction of VANKA in PRF scaffolds without a carrier system does not ensure controlled delivery of active VANKA form at the therapeutic effect level and there is no specific binding of VANKA to PRF scaffold. This study confirms that the use of a carrier system can ensure controlled VANKA release for 6 to 10 days. A complete antibacterial effect lasts for 48 h, but with a rapid drop of effectiveness after the first 24 h. The methodology of antibacterial tests needs to be modified to ensure full VANKA release in the testing system.

Staining of the samples for micro-CT analysis is mandatory to distinguish the PRF scaffold from the encapsulated particles, thus showing the contrast between drug delivery systems and PRF. During 3D reconstruction of the samples, we observed that the liposomes are located at the upper layer of the sample, but the microcapsules are dispersed throughout the sample. These findings reinforce the observations of the VANKA release kinetics in this study and thus approve that micro-CT can be a tool for predicting the properties of drug delivery systems based on PRF.

Author Contributions: Conceptualization, writing—original draft preparation and review, supervision and funding acquisition, A.D.; methodology, validation, and writing—original draft preparation, K.E.; methodology, writing and formal analysis, M.S.-M.; methodology and writing, I.S. (Ingus Skadins); resources on DLS analysis and review, J.R.; methodology, review and editing, I.S. (Ilze Salma). All authors have read and agreed to the published version of the manuscript.

Funding: This research was funded by the European Union’s Horizon 2020 research and innovation programme under the grant agreement No 857287 and the Latvian Council of Science research project No. Izp-2020/1-0054 “Development of antibacterial autologous fibrin matrices in maxillofacial surgery (MATRI-X)”.

Institutional Review Board Statement: The study was conducted according to the guidelines of the Declaration of Helsinki, and approved by the Research Ethics Committee at Riga Stradins University, Latvia, Permission No. 6-2/10/53, 28 November 2019.

Informed Consent Statement: Written consent from all of the volunteers for use of their samples in the research studies was obtained.

Data Availability Statement: The data presented in this study are openly available in Zenodo at [10.5281/zenodo.5082110](https://doi.org/10.5281/zenodo.5082110) (accessed on 7 July 2021).

Acknowledgments: The authors thank biol. Juris Jansons for his help with TEM images and Latvian Biomedical Research and Study Centre for the opportunity to use their TEM infrastructure. The authors also thank Mohammed Inayathullah, Advanced Drug Delivery and Regenerative Biomaterials Laboratory of Cardiovascular Institute, Stanford University School of Medicine, for his help with DLS analysis.

Conflicts of Interest: The authors declare no conflict of interest.

References

1. Miron, R.J.; Zhang, Y. Autologous liquid platelet rich fibrin: A novel drug delivery system. *Acta Biomater.* **2018**, *75*, 35–51. [[CrossRef](#)]
2. Anitua, E.; Nurden, P.; Prado, R.; Nurden, A.T.; Padilla, S. Autologous fibrin scaffolds: When platelet- and plasma-derived biomolecules meet fibrin. *Biomaterials* **2019**, *192*, 440–460. [[CrossRef](#)]
3. Thorn, J.J.; Sørensen, H.; Weis-Fogh, U.; Andersen, M. Autologous fibrin glue with growth factors in reconstructive maxillofacial surgery. *Int. J. Oral Maxillofac. Surg.* **2004**, *33*, 95–100. [[CrossRef](#)] [[PubMed](#)]
4. Choukroun, J.; Ghanaati, S. Reduction of relative centrifugation force within injectable platelet-rich-fibrin (PRF) concentrates advances patients’ own inflammatory cells, platelets and growth factors: The first introduction to the low speed centrifugation concept. *Eur. J. Trauma Emerg. Surg.* **2018**, *44*, 87–95. [[CrossRef](#)]
5. Bennardo, F.; Liborio, F.; Barone, S.; Antonelli, A.; Buffone, C.; Fortunato, L.; Giudice, A. Efficacy of platelet-rich fibrin compared with triamcinolone acetonide as injective therapy in the treatment of symptomatic oral lichen planus: A pilot study. *Clin. Oral Investig.* **2021**, *25*, 3747–3755. [[CrossRef](#)] [[PubMed](#)]
6. Giudice, A.; Antonelli, A.; Muraca, D.; Fortunato, L. Usefulness of advanced-platelet rich fibrin (A-PRF) and injectable-platelet rich fibrin (i-PRF) in the management of a massive medication-related osteonecrosis of the jaw (MRONJ): A 5-years follow-up case report. *Indian J. Dent. Res.* **2020**, *31*, 813. [[CrossRef](#)]
7. Shah, R.; Gowda, T.M.; Thomas, R.; Kumar, T.; Mehta, D.S. Biological activation of bone grafts using injectable platelet-rich fibrin. *J. Prosthet. Dent.* **2019**, *121*, 391–393. [[CrossRef](#)]
8. Kemmochi, M.; Sasaki, S.; Takahashi, M.; Nishimura, T.; Aizawa, C.; Kikuchi, J. The use of platelet-rich fibrin with platelet-rich plasma support meniscal repair surgery. *J. Orthop.* **2018**, *15*, 711–720. [[CrossRef](#)] [[PubMed](#)]
9. Kapse, S.; Surana, S.; Satish, M.; Hussain, S.E.; Vyas, S.; Thakur, D. Autologous platelet-rich fibrin: Can it secure a better healing? *Oral Surg. Oral Med. Oral Pathol. Oral Radiol.* **2019**, *127*, 8–18. [[CrossRef](#)]
10. Brancaccio, Y.; Antonelli, A.; Barone, S.; Bennardo, F.; Fortunato, L.; Giudice, A. Evaluation of local hemostatic efficacy after dental extractions in patients taking antiplatelet drugs: A randomized clinical trial. *Clin. Oral Investig.* **2021**, *25*, 1159–1167. [[CrossRef](#)]
11. Safari, J.; Zarnegar, Z. Advanced drug delivery systems: Nanotechnology of health design A review. *J. Saudi Chem. Soc.* **2014**, *18*, 85–99. [[CrossRef](#)]
12. Li, J.; Wang, X.; Zhang, T.; Wang, C.; Huang, Z. A review on phospholipids and their main applications in drug delivery systems. *Asian J. Pharm. Sci.* **2015**, *10*, 81–98. [[CrossRef](#)]
13. Yang, Z.; Liu, J.; Gao, J.; Chen, S.; Huang, G. Chitosan coated vancomycin hydrochloride liposomes: Characterizations and evaluation. *Int. J. Pharm.* **2015**, *495*, 508–515. [[CrossRef](#)] [[PubMed](#)]
14. Pumerantz, A.; Muppidi, K.; Agnihotri, S.; Guerra, C.; Venketaraman, V.; Wang, J.; Betageri, G. Preparation of liposomal vancomycin and intracellular killing of methicillin-resistant *Staphylococcus aureus* (MRSA). *Int. J. Antimicrob. Agents* **2011**, *37*, 140–144. [[CrossRef](#)] [[PubMed](#)]

15. Liu, J.; Wang, Z.; Li, F.; Gao, J.; Wang, L.; Huang, G. Liposomes for systematic delivery of vancomycin hydrochloride to decrease nephrotoxicity: Characterization and evaluation. *Asian J. Pharm. Sci.* **2015**, *10*, 212–222. [[CrossRef](#)]
16. Rybak, M.J. The Pharmacokinetic and Pharmacodynamic Properties of Vancomycin. *Clin. Infect. Dis.* **2006**, *42*, S35–S39. [[CrossRef](#)]
17. Lodise, T.P.; Graves, J.; Evans, A.; Graffunder, E.; Helmecke, M.; Lomaestro, B.M.; Stellrecht, K. Relationship between Vancomycin MIC and Failure among Patients with Methicillin-Resistant Staphylococcus aureus Bacteremia Treated with Vancomycin. *Antimicrob. Agents Chemother.* **2008**, *52*, 3315–3320. [[CrossRef](#)]
18. Kshetry, A.O.; Pant, N.D.; Bhandari, R.; Khatri, S.; Shrestha, K.L. Minimum inhibitory concentration of vancomycin to methicillin resistant Staphylococcus aureus isolated from different clinical samples at a tertiary care hospital in Nepal. *Antimicrob. Resist. Infect. Control.* **2016**, *4*–9. [[CrossRef](#)]
19. Adani, S.; Bhowmick, T.; Weinstein, M.P.; Narayanan, N. Impact of Vancomycin MIC on Clinical Outcomes of Patients with Methicillin-Resistant Staphylococcus aureus Bacteremia Treated with Vancomycin at an Institution with Suppressed MIC Reporting. *Antimicrob. Agents Chemother.* **2018**, *62*, 1–6. [[CrossRef](#)]
20. Suchy, T.; Supova, M.; Klapkova, E.; Horny, L.; Ryglova, S.; Zaloudkova, M.; Braun, M.; Sucharda, Z.; Ballay, R.; Vesely, J.; et al. The Sustainable Release of Vancomycin and Its Degradation Products from Nanostructured Collagen / Hydroxyapatite Composite Layers. *J. Pharm. Sci.* **2016**, *105*, 1288–1294. [[CrossRef](#)]
21. Melicherik, P.; Klapkova, E.; Landor, I.; Judl, T.; Sibek, M.; Jahoda, D. The effect of Vancomycin degradation products in the topical treatment of osteomyelitis. *Bratisl. Med. J.* **2014**, *115*, 796–799. [[CrossRef](#)]
22. Backes, D.W.; Aboleneen, H.I.; Simpson, J.A. Quantitation of vancomycin and its crystalline degradation product (CDP-1) in human serum by high performance liquid chromatography. *J. Pharm. Biomed. Anal.* **1998**, *16*, 1281–1287. [[CrossRef](#)]
23. Thassu, D.; Deleers, M.; Pathak, Y. Nanoparticulate drug delivery systems. *Chem. Biodivers.* **2007**, *166*, 1829–1841. [[CrossRef](#)]
24. Kavrakovski, Z.; Popovska, O.; Simonovska, J.; Kavrakovski, Z.; Rafajlovská, V. An Overview: Methods for Preparation and Characterization of Liposomes as Drug Delivery Systems. *Int. J. Pharm. Phytopharm. Res.* **2013**, *3*, 13–20.
25. Singh, R.P.; Gangadharappa, H.V.; Mruthunjaya, K. Phospholipids: Unique carriers for drug delivery systems. *J. Drug Deliv. Sci. Technol.* **2017**, *39*, 166–179. [[CrossRef](#)]
26. Kohli, A.G.; Kierstead, P.H.; Venditto, V.J.; Walsh, C.L.; Szoka, F.C. Designer lipids for drug delivery: From heads to tails. *J. Control. Release* **2014**, *190*, 274–287. [[CrossRef](#)] [[PubMed](#)]
27. Pei, Y.; Mohamed, M.F.; Seleem, M.N.; Yeo, Y. Particle engineering for intracellular delivery of vancomycin to methicillin-resistant Staphylococcus aureus (MRSA)-infected macrophages. *J. Control. Release* **2017**, *267*, 133–143. [[CrossRef](#)] [[PubMed](#)]
28. Gonzalez Gomez, A.; Syed, S.; Marshall, K.; Hosseinidoust, Z. Liposomal nanovesicles for efficient encapsulation of staphylococcal antibiotics. *Am. Chem. Soc. Omega* **2019**, *4*, 10866–10876. [[CrossRef](#)]
29. Hirenkumar, M.; Steven, S. Poly Lactic-co-Glycolic Acid (PLGA) as Biodegradable Controlled Drug Delivery Carrier. *Polymers* **2012**, *3*, 1–19. [[CrossRef](#)]
30. Wang, S.S.; Yang, M.C.; Chung, T.W. Liposomes/chitosan scaffold/human fibrin gel composite systems for delivering hydrophilic drugs—Release behaviors of Tirofiban In Vitro. *Drug Deliv.* **2008**, *15*, 149–157. [[CrossRef](#)]
31. Faizullin, D.; Valiullina, Y.; Salnikov, V.; Zuev, Y. Direct interaction of fibrinogen with lipid microparticles modulates clotting kinetics and clot structure. *Nanomed. Nanotechnol. Biol. Med.* **2020**, *23*, 102098. [[CrossRef](#)] [[PubMed](#)]
32. Mu, Z.; Chen, K.; Yuan, S.; Li, Y.; Huang, Y.; Wang, C.; Zhang, Y.; Liu, W.; Luo, W.; Liang, P.; et al. Gelatin Nanoparticle-Injectable Platelet-Rich Fibrin Double Network Hydrogels with Local Adaptability and Bioactivity for Enhanced Osteogenesis. *Adv. Healthc. Mater.* **2020**, *9*, 1–16. [[CrossRef](#)] [[PubMed](#)]
33. Le Nihouannen, D.; Le Guehennec, L.; Rouillon, T.; Pilet, P.; Bilban, M.; Layrolle, P.; Daculsi, G. Micro-architecture of calcium phosphate granules and fibrin glue composites for bone tissue engineering. *Biomaterials* **2006**, *27*, 2716–2722. [[CrossRef](#)] [[PubMed](#)]
34. Al-Maawi, S.; Herrera-Vizcaino, C.; Orłowska, A.; Willershausen, I.; Sader, R.; Miron, R.J.; Choukroun, J.; Ghanaati, S. Biologization of collagen-based biomaterials using liquid-platelet-rich fibrin: New insights into clinically applicable tissue engineering. *Materials* **2019**, *12*, 3993. [[CrossRef](#)]
35. Juliana, J.M.; Zanelle, I.; Noël, P.B.; Cardoso, M.B.; Kimm, M.A.; Pfeiffer, F. Three-dimensional non-destructive soft-tissue visualization with X-ray staining micro-tomography. *Sci. Rep.* **2015**, *5*, 1–7. [[CrossRef](#)]
36. Heimel, P.; Swiadek, N.V.; Slezak, P.; Kerbl, M.; Schneider, C.; Nürnberger, S.; Redl, H.; Teuschl, A.H.; Hercher, D. Iodine-Enhanced Micro-CT Imaging of Soft Tissue on the Example of Peripheral Nerve Regeneration. *Contrast Media Mol. Imaging* **2019**, *2019*. [[CrossRef](#)]
37. Hu, X.; Tam, K.Y. Association of vancomycin with lipid vesicles. *ADMET DMPK* **2017**, *5*, 182–191. [[CrossRef](#)]
38. Jia, Z.; O'Mara, M.L.; Zuegg, J.; Cooper, M.A.; Mark, A.E. The effect of environment on the recognition and binding of vancomycin to native and resistant forms of lipid II. *Biophys. J.* **2011**, *101*, 2684–2692. [[CrossRef](#)]
39. Özalp, Y.; Özdemir, N.; Kocagöz, S.; Hasirci, V. Controlled release of vancomycin from biodegradable microcapsules. *J. Microencapsul.* **2001**, *18*, 89–110. [[CrossRef](#)]
40. Uchida, T.; Nagareya, N.; Sakakibara, S.; Konishi, Y.; Nakai, A.; Nishikata, M.; Matsuyama, K.; Yoshida, K. Preparation and characterization of poly(lactic acid) microspheres containing bovine insulin by a w/o/w emulsion solvent evaporation method. *Chem. Pharm. Bull.* **1997**, *45*, 1539–1543. [[CrossRef](#)]
41. Barichello, J.M.; Morishita, M.; Nagai, T. Encapsulation of Hydrophilic and Lipophilic Drugs in PLGA Nanoparticles by the Nanoprecipitation Method. *Drug Dev. Ind. Pharm.* **1999**, *25*, 471–476. [[CrossRef](#)]

42. Litvinov, R.I.; Faizullin, D.A.; Zuev, Y.F.; Weisel, J.W. The α -Helix to β -Sheet Transition in Stretched and Compressed Hydrated Fibrin Clots. *Biophys. J.* **2012**, *103*, 1020–1027. [[CrossRef](#)] [[PubMed](#)]
43. Erbetta, C.D.C.; Alves, R.J.; Resende, J.M.; Freitas, R.F.S.; Sousa, R.G. Synthesis and Characterization of Poly (D,L-lactide-co-glycolide) Copolymer. *J. Biomater. Nanobiotechnol.* **2012**, *3*, 208–225. [[CrossRef](#)]
44. Silva, A.; Cardoso, B.; Silva, M.; Freitas, R.; Sousa, R. Synthesis, Characterization, and Study of PLGA Copolymer In Vitro Degradation. *J. Biomater. Nanobiotechnol.* **2015**, *6*, 8–19. [[CrossRef](#)]
45. Singh, R.; Kesharwani, P.; Mehra, N.K.; Singh, S.; Banerjee, S.; Jain, N.K. Development and characterization of folate anchored Saquinavir entrapped PLGA nanoparticles for anti-tumor activity. *Drug Dev. Ind. Pharm.* **2015**, *41*, 1888–1901. [[CrossRef](#)] [[PubMed](#)]
46. Ain, Q.; Munir, H.; Jelani, F.; Anjum, F.; Bilal, M. Antibacterial potential of biomaterial derived nanoparticles for drug delivery application. *Mater. Res. Express* **2019**, *6*. [[CrossRef](#)]
47. Hinch, D.K. Effects of calcium-induced aggregation on the physical stability of liposomes containing plant glycolipids. *Biochim. Biophys. Acta Biomembr.* **2003**, *1611*, 180–186. [[CrossRef](#)]
48. Melcrová, A.; Pokorna, S.; Pullanchery, S.; Kohagen, M.; Jurkiewicz, P.; Hof, M.; Jungwirth, P.; Cremer, P.S.; Cwiklik, L. The complex nature of calcium cation interactions with phospholipid bilayers. *Sci.Rep.* **2016**, *6*, 1–12. [[CrossRef](#)]

**Fucoidan/Chitosan Hydrogels as Carrier for Sustained Delivery of Platelet-Rich Fibrin
Containing Bioactive Molecules**

Karina Egle, Eva Dohle, Verena Hoffmann, Ilze Salma, Sarah Al-Maawi, Shahram Ghanaati and
Arita Dubnika.

Int. J. Biol. Macromol. **2024**, 262 (1), 129651.



Contents lists available at ScienceDirect

International Journal of Biological Macromolecules

journal homepage: www.elsevier.com/locate/ijbiomac

Fucoidan/chitosan hydrogels as carrier for sustained delivery of platelet-rich fibrin containing bioactive molecules

Karina Egle^{a,b,*}, Eva Dohle^c, Verena Hoffmann^c, Ilze Salma^{b,d}, Sarah Al-Maawi^c, Shahram Ghanaati^{c,*1}, Arita Dubnika^{a,b,**,1}

^a Institute of Biomaterials and Bioengineering, Faculty of Natural Science and Technology, Riga Technical University, LV-1048 Riga, Latvia

^b Baltic Biomaterials Centre of Excellence, Headquarters at Riga Technical University, LV-1048 Riga, Latvia

^c FORM, Frankfurt Oral Regenerative Medicine, Clinic for Maxillofacial and Plastic Surgery, Johann Wolfgang Goethe University, 60590 Frankfurt am Main, Germany

^d Institute of Stomatology, Riga Stradins University, LV-1007 Riga, Latvia

ARTICLE INFO

Keywords:

Fucoidan
Chitosan
Hydrogels
Platelet-rich fibrin
Growth factors
Marine polysaccharide

ABSTRACT

Platelet-rich fibrin (PRF), derived from human blood, rich in wound healing components, has drawbacks in direct injections, such as rapid matrix degradation and growth factor release. Marine polysaccharides, mimicking the human extracellular matrix, show promising potential in tissue engineering. In this study, we impregnated the self-assembled fucoidan/chitosan (FU_CS) hydrogels with PRF obtaining PRF/FU_CS hydrogels. Our objective was to analyze the properties of a hydrogel and the sustained release of growth factors from the hydrogel that incorporates PRF. The results of SEM and BET-BJH demonstrated the relatively porous nature of the FU_CS hydrogels. ELISA data showed that combining FU_CS hydrogel with PRF led to a gradual 7-day sustained release of growth factors (VEGF, EGF, IL-8, PDGF-BB, TGF- β 1), compared to pure PRF. Histology confirmed ELISA data, demonstrating uniform PRF fibrin network distribution within the FU_CS hydrogel matrix. Furthermore, the FU_CS hydrogels revealed excellent cell viability. The results revealed that the PRF/FU_CS hydrogel has the potential to promote wound healing and tissue regeneration. This would be the first step in the search for improved growth factor release.

1. Introduction

Regenerative medicine has great potential to improve treatment outcomes, and advances in bioengineering have fueled its growth in recent decades. Tissue engineering techniques and functional construct assembly for regenerating tissues and organs have profoundly influenced medicine and healthcare. Techniques for combining biomimetic materials, cells, and bioactive molecules are essential to promote the regeneration of damaged tissues or as therapeutic systems [1]. Biomaterials for tissue engineering need precise surface chemistry, porosity, and biodegradability to enhance cell interactions and matrix deposition [2].

Molecules with protein binding sites that are involved in disease-related protein-protein interactions are promising candidates for therapeutic intervention [3]. In recent decades, controlled drug delivery

systems have enhanced wound healing and tissue regeneration by efficiently delivering cytokines and growth factors. Fibrin, better known as a natural hydrogel, is the end product of the physiological clotting cascade that is naturally involved in wound healing. In addition to its essential role in hemostasis, it acts as a local reservoir of growth factors and cytokines and a temporary matrix for cells to enhance the regenerative process. On the other hand, the properties of fibrin cannot be used entirely, which increases the need to modify its chemical and physical properties [4]. This might be beneficial to enable the combination of PRF with additional growth factors and cytokines to ensure their timely release. The most common way to ensure the delivery of bioactive molecules is the development of polymeric microspheres, nanospheres, lipid nanoparticles, and hydrogels [5–8]. Various compositions of these delivery systems have demonstrated their potential in treatment, particularly in wound healing and tissue regeneration.

* Corresponding author.

** Correspondence to: A. Dubnika, Institute of Biomaterials and Bioengineering, Faculty of Natural Science and Technology, Riga Technical University, LV-1048 Riga, Latvia.

E-mail addresses: karina.egle@rtu.lv (K. Egle), shahram.ghanaati@kgu.de (S. Ghanaati), arita.dubnika@rtu.lv (A. Dubnika).

¹ Shahram Ghanaati and Arita Dubnika contributed equally to this work.

<https://doi.org/10.1016/j.ijbiomac.2024.129651>

Received 23 August 2023; Received in revised form 17 January 2024; Accepted 18 January 2024

Available online 25 January 2024

0141-8130/© 2024 The Authors. Published by Elsevier B.V. This is an open access article under the CC BY-NC-ND license (<http://creativecommons.org/licenses/by-nc-nd/4.0/>).

Different effects of cytokines and growth factors on wound healing using various biomaterials have been investigated in numerous studies. Wong et al. research data suggests that PRF treatment can accelerate Achilles tendon healing and serve as a cytokine delivery vehicle to promote cell viability, proliferation, and differentiation in vitro [9]. The combination of PRF properties, including the leukocytes and platelets, growth factors, and cytokines embedded in the three-dimensional fibrin matrix, seem to work synergistically to promote rapid and robust growth of tissue regeneration [10]. Growth factors are a heterogeneous group of proteins secreted by leukocytes and platelets with a short biological half-life rapidly eliminated from the bloodstream; they act mainly locally. Platelets are involved in hemostasis and store growth factors in alpha granules, which are activated to release these factors at the injury site. Among others, platelets store and transport several essential growth factors such as beta-transforming growth factor (TGF- β), platelet-derived growth factor (PDGF), insulin-like growth factor (IGF), vascular endothelial growth factor (VEGF), and basic fibroblast growth factor (bFGF) [11]. Especially, TGF- β is an important growth factor in tissue regeneration since its primary role in tissue repair is the promotion of fibrosis [12].

Controlled drug release is considered to be the key to improving the effects of drug-related tissue engineering. Various hydrogels have been developed for the controlled release of loaded or covalently immobilized proteins [13–15]. In particular, many strategies have been developed to influence changes in charge [16], pore size [17], and release of loaded proteins that electrostatically interact with scaffolds, including multi-layer hydrogels [18]. Hydrogels have a wide range of functions in the field of tissue engineering. According to Khandan et al., hydrogel scaffolds provide a physical surface for the adsorption of biomolecules and the immobilization of proteins, growth factors, and other biologically active biomaterials [19]. In recent years, various methods, such as drying, lyophilization, ion/chemical gelation, 3D printing, etc., have been available to develop scaffolds. Thus, scaffolds with different structures and tailored properties are prepared to obtain the required tissue regeneration. Freeze-drying is one of the most common methodologies for obtaining 3D porous materials [20]. In addition, bioactive molecules can be released from hydrogel scaffolds for a variety of applications, including promotion of angiogenesis and secretory cell encapsulation [21].

Cell encapsulation is another attractive alternative for long-term controlled, sustained drug delivery [21]. Currently, most enzyme and hormonal deficiencies are treated by oral administration or injection of the missing substance. Cell encapsulation offers a method by which a substance can be released over an extended time. There are studies describing the encapsulation of various primary cells, including pancreatic islets [22–25], hepatocytes [22], and adrenocortical cells [22]. Studies using hydrogels as cell reservoirs [26,27] to express specific enzymes and growth factors have also been described.

In this study, we developed a hydrogel composed of fucoidan (FU) and chitosan (CS) matrices due to their biocompatibility and ability to form polyelectrolyte complexes via self-assembly [28]. Recently, several FU-based composites have been established for bone tissue engineering purposes because FU increased the proliferation capacity of osteoblast-like cells and enhanced osteoblast-mediated mineral deposition [29]. FU's similarity to the human extracellular matrix and impressive qualities, like high biocompatibility and renewability, have recently intrigued researchers. It shows promise in developing regenerative medicine materials, particularly for wound treatment [30]. FU, a heparin-like molecule, enhances growth factor effects on cell proliferation, osteogenic differentiation, and mesenchymal stem cell activity [31]. Several studies [32,33] have reported that FU can interact with growth factors (such as bFGF and TGF- β) to control their release and activity by binding and regulating signaling pathways. These are highly important in autologous PRF samples to support the release of growth factors from the matrices. In general, the structure and properties of chitosan are similar to glycosaminoglycan (GAG), a natural

polysaccharide and the main component of the extracellular matrix (ECM) [34]. Chitosan, a natural cationic copolymer, has generated significant interest for its potential in hydrogel formations. This polymer's hydrophilic nature allows it to degrade using human enzymes, ensuring biocompatibility and biodegradability, two crucial properties for biological devices. Chitosan-based hydrogels could serve as scaffolds for tissue repair success [35]. Chitosan accelerates wound healing by activating and modulating inflammatory cells and promoting granulation tissue formation. Its ability to bind negatively charged red blood cells enhances clotting, making it a crucial component in wound dressings [36].

Thus, previous studies [37,38] have only investigated the amount of proteins in hydrogels that were combined with PRP or PRF during synthesis. To our knowledge, no studies have reported the impregnation of FU_CS hydrogels with PRF, investigating the release of growth factors. This would allow surgeons to use hydrogels during surgery combined with the required amount of PRF according to the site to be treated. Accordingly, the present study aimed to develop PRF/FU_CS hydrogels for sustained various growth factors release from incorporated PRF compared to pure PRF. To achieve the goal, we fabricated FU_CS hydrogels and filled them with PRF. First, hydrogels were characterized by swelling and gel fraction properties, morphology, and cytotoxicity. After the addition of PRF to the FU_CS hydrogels, the growth factor release capacity was investigated, testing its ability to apply over a long period of time. Finally, histological and immuno-histological characteristics were analyzed, allowing to evaluate the penetration of PRF into the hydrogel structure.

2. Materials and methods

2.1. Materials

Chitosan sourced from shrimp shells (CS, 50,000–190,000 Da, low viscosity, 75–85 % deacetylated) acquired from Sigma-Aldrich (USA), fucoidan FucoMax (FU, extracted from *Undaria pinnatifida*, *Laminaria saccharina*, *Cladosiphon okamuranus*; 100,000 MW, fucose content 12 %, Organic SO_4^- content is circa 10 %, Specification No. (A4)000) provided by BGG Europe SA, Switzerland were used to create fucoidan/chitosan hydrogels. Sodium hydroxide (NaOH) and hydrochloric acid (HCl, 37 %) from Sigma-Aldrich (USA) were also employed. For histology, ethanol from Carl Roth GmbH + Co. KG (Germany), xylene from VWR International (Germany), 2-propanol from Sigma-Aldrich (USA), Mayer's Hematoxylin solution from Panreac AppliChem, and 2 % eosin from Morphisto GmbH (Frankfurt am Main) were utilized. ELISA and cell experiments were conducted using various materials. These included Dulbecco's Modified Eagle's Medium/Nutrient Mixture F-12 Ham (DMEM/F-12) from Gibco Thermo Fisher Scientific, Fetal Bovine Serum (FBS) from Biocrom AG, alpha modification of Minimum Essential Medium Eagle (α -MEM) from Gibco, Corning® Fetal Bovine Serum (FBS) of Regular quality sourced from South American Origin, Penicillin/Streptomycin (P/S) from Gibco (USA), 10 \times trypsin-EDTA from Gibco (UK). Sodium bicarbonate (NaHCO_3), fibroblast growth factor (FGF-2), dimethyl sulfoxide (DMSO), and phosphate-buffered saline (PBS) were supplied from Sigma Aldrich (USA).

2.2. Preparation of hydrogels

The hydrogel preparation is shown in Fig. 1. CS was dissolved in 1.5 M hydrochloric acid to obtain a 2 % solution. 0.25 % FU/water solution was added to the CS solution in a ratio 1:1 (v/v). Samples were prepared in a 24-cell plate and shaken at 500 rpm for 4 h. Samples were frozen in the plate at -26°C and lyophilized (Martin Christ BETA 2–8 LSCplus, Osterode am Harz, Germany) at -80°C under 1 mbar for 72 h. Obtained hydrogels were neutralized with 1.5 M NaOH and rinsed with water until pH of 7 was obtained. The samples were then lyophilized again for 72 h.

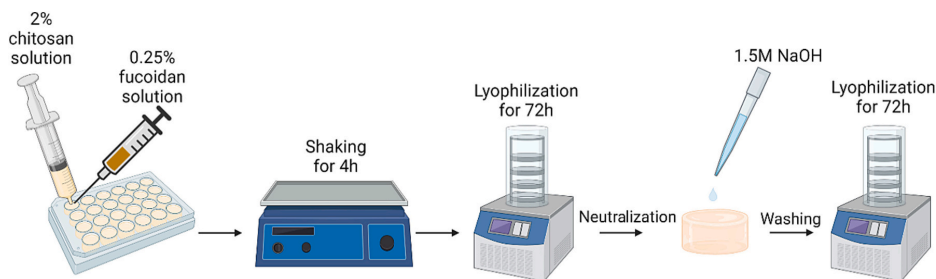


Fig. 1. FU_CS hydrogels preparation.
Fig. created with Biorender.com.

2.3. Blood collection and PRF preparation

Blood from the peripheral vein of 6 healthy donors was collected in 10 mL sterile plastic S–P tubes (Process for PRF, Nice, France) and immediately placed in a centrifuge (Duo centrifuge, Process for PRF, Nice, France) with a fixed angle rotor with a radius of 110 mm. Low RCF protocol (600 rpm, 44 g for 8 min) was used for centrifugation, with parameters based on previous studies [39,40]. After centrifugation, liquid PRF was collected from all S–P tubes and quickly transferred to a 50 mL tube. The obtained PRF was divided for further studies according to the defined volumes specified in Sections 2.4–2.7. Written consent from all of the volunteers for the use of their samples in the research studies was obtained. All donors were free of any infectious diseases and were not consuming alcohol or nicotine. Permission No. 6–2/10/53 of the Research Ethics Committee of Riga Stradins University has been received and was in accordance with the principle of informed consent. Research also received approval from the responsible Ethics Commission of the state Hessen, Germany (No. 265/17).

2.4. Addition of PRF to hydrogels

200 μ L liquid PRF was applied directly to the center of the hydrogel with an automatic pipette before it could coagulate. As control samples, PRF without hydrogels were prepared. Preparation procedures were performed in sterile 24-well cell culture plates.

Three different samples were prepared with their respective abbreviations - see Table 1 below:

2.5. Characterization of prepared samples

2.5.1. Swelling ratio

The swelling test of FU_CS hydrogels was conducted in H₂O, PBS, and DMEM/F-12 (pH 7.4) [41–44]. Dry hydrogels were placed in a vessel containing 20 mL of H₂O, PBS, or DMEM/F-12 and kept in an incubator at 37 °C with constant shaking (50 rpm). The swollen hydrogels were periodically removed (after 1 h, 2 h, 3 h, 4 h, 5 h, 6 h, 1d, 2d, 3d, 6d, 7d) and immediately weighted by eliminating excess water with a wet paper. The swelling degree of the hydrogels was calculated from the following (Eq. (1)):

$$\text{Swelling degree (\%)} = \frac{M_1 - M_0}{M_0} \cdot 100, \quad (1)$$

where, M_0 - the initial weight of dried sample, g; M_1 - weight of swollen sample, g.

2.5.2. Gel fraction

The gel fraction represents the insoluble part of the matrix, describing which part of the prepared matrix is cross-linked. The FU_CS hydrogels, pure PRF, and PRF/FU_CS hydrogels were first lyophilized 72 h before the gel fraction was determined. All samples were weighed and placed in 200 mL of deionized water at room temperature and left for 48 h. The samples were then removed, re-frozen, lyophilized, and weighed. The gel fraction was determined as follows [45] (Eq. (2)).

$$\text{Gel fraction (\%)} = \frac{M_1}{M_0} \cdot 100, \quad (2)$$

where M_0 - the initial weight of the lyophilized sample, g;

M_1 - weight of the lyophilized sample after water extraction, g

2.5.3. Biodegradation properties

Degradation of PRF, PRF/FU_CS hydrogel, and FU_CS hydrogel samples were evaluated according to the EN ISO 10999-4:2017 and ISO 10999-14:2001 for 2 weeks at 37 °C in an extreme solution (citric acid buffer, pH 3) and in a simulation solution (tris (hydroxymethyl) aminomethane/hydrochloric acid (TRIS-HCl) buffer, pH 7.4 \pm 0.2). Finally, the degradation degree of samples was calculated using Eq. (3).

$$\text{Degradation degree (\%)} = \frac{M_0 - M_1}{M_0} \cdot 100, \quad (3)$$

where M_0 - hydrogel weight before immersing in TRIS-HCl or citric acid, g;

M_1 - hydrogel weight after immersing in TRIS-HCl or citric acid, g

2.5.4. Rheological properties

Discovery series HR20 rheometer from TA Instruments, United States, was used to analyze samples' rheological and mechanical properties. Prior to measurements, each lyophilized sample was saturated with 200 μ L of either water or PRF (with the quantity determined based on swelling data), and pure PRF was used as a control. The amplitude sweep test was executed in oscillation mode at 37 °C, utilizing 20 mm plate geometry, shear strain ranging from 0.01 to 1000 %, and a constant frequency of 1 Hz. Following this, a frequency sweep test was carried out in oscillation mode at 37 °C, employing a 20 mm plate geometry and a frequency ranging from 0.01 to 100 Hz at a 0.2 % strain. Each data point was sustained at each strain/frequency until the instrument yielded a stable reading, and all measurements were repeated

Table 1
Abbreviations of prepared samples.

Abbreviation	Sample
PRF	Pure platelet-rich fibrin
FU_CS hydrogels	Fucoidan/chitosan hydrogels
PRF/FU_CS hydrogels	Platelet-rich fibrin with fucoidan/chitosan hydrogels

three times for reproducibility.

2.5.5. Morphology and chemical structure

The morphology of the lyophilized pure PRF, FU_CS hydrogel, and PRF/FU_CS hydrogel was determined using Tescan Mira/LMU (Tescan, Brno, Czech Republic) scanning electron microscope (SEM). Before analysis, the samples were coated with a thin layer of gold at 25 mA for 3 min using Emitech K550X (Quorum Technologies, Ashford, Kent, United Kingdom) and scanned at 5 kV, using secondary electrons.

The chemical structures of the obtained samples were determined using Fourier transform infrared spectroscopy (FTIR). FTIR spectrums (Thermo Fisher Scientific Nicolet iS50, Waltham, Massachusetts, US) were recorded in the attenuated total reflection mode (ATR). Spectra were acquired at 4 cm⁻¹ resolution by adding 64 scans in the wave-number range from 400 cm⁻¹ to 4000 cm⁻¹. Before each measurement, the background spectrum was recorded and subtracted from the sample spectrum.

2.5.6. BET-BJH method

The surface area, pore size, and porosity for lyophilized FU_CS hydrogels were determined using the Brunauer–Emmett–Teller (BET)/Barrett–Joyner–Halenda (BJH) method. The surface area, pore volume, specific surface area of pores, and average pore diameter were analyzed by the Autosorb Degasser Model AD-9 (Quantachrome Instruments, Boynton Beach, FL, USA) and gas sorption system Quadrasorb evo (Quanta Tec. Inc., Boynton Beach, FL, USA). Samples were degassed for 24 h hours at room temperature using 9 mm large bulb sample cells to remove surface moisture and impurities. The gas sorption system Quadrasorb evo analyzed specific surface area through low-temperature (77 K) nitrogen physical absorption-desorption isotherms.

2.6. Amount of growth factors and cytokines

200 µL of PRF was added to the prepared hydrogels in a 24-well plate, pure PRF matrix was also designed for comparison of the release kinetics. After the addition of PRF, 1 mL of DMEM/F-12 medium supplemented with 10 % FBS and 1 % P/S was added to each cell well and further incubated at 37 °C. FU_CS hydrogels placed in the same cell medium as PRF samples were used as a blank control. 1 mL of culture supernatants from different experimental groups were collected after 6 h, 1d, 2d, 3d, 6d, and 7d of cultivation and replaced with 1 mL of fresh cell culture medium. After collection, supernatants were frozen at -80 °C and stored until growth factor analysis. The protein concentrations of transforming growth factor (TGF-β1, kit#: DY240-05), human interleukin-8 (IL-8, kit#: DY208-05), human platelet-derived growth factor BB (PDGF-BB, kit# DY220-15), epidermal growth factor (EGF, kit#: DY236-05) and vascular endothelial growth factor (VEGF, kit# DY293-05) were quantified using sandwich enzyme-linked immunosorbent assay (ELISA) kits (Quantikine® ELISA, R&D Systems, Minneapolis, USA). In order to accurately determine the concentration of growth factors, the sample supernatants were diluted (Table 2) during preparation with the same Reagent Diluent used for standard preparation. At 450 nm, the optical density of the samples was determined using a microplate reader (Tecan Infinite M Nano, Switzerland), and cumulative release values were calculated. The experiments were performed in duplicate for each blood donor and preparation protocol.

Table 2

Parameters used to determine different growth factors.

Growth factor/cytokine	Detection range	Dilution
TGF-β1	31.3–2000 pg/mL	1:10
IL-8	31.3–2000 pg/mL	1:20
EGF	3.9–250 pg/mL	1:7
VEGF	31.3–2000 pg/mL	Non diluted
PDGF-BB	31.3–2000 pg/mL	Non diluted

2.7. Histology and immunohistology

The samples were prepared in the same way as mentioned in Section 2.6 by placing them in 1 mL of full cell medium. After 3 and 7 days of incubation in cell culture media (DMEM/F-12 + 10 % FBS + 1 % P/S), the medium was removed. Referring to Ghanaati et al. [46–48], the samples were fixed in 4 % formaldehyde (ROTI®Histofix 4 %, Carl Roth GmbH + Co. KG) for 24 h, removed from 24 well plate. The samples were then dehydrated in an ascending ethanol and xylene series using a tissue processor (Leica TP1020, Wetzlar, Germany) and embedded in paraffin blocks. Initially, sections of blocks of the thickness of 2 µm were sliced using a rotary microtome (Leica RM2255, Wetzlar, Germany). For immunohistology, sections of samples were deparaffinized, rehydrated, and finally sonicated in citrate buffer at 96 °C for 20 min. The sections were stained with anti-human CD31 marker (Leukocytes, 1: 40, Clone JC70A, Dako) and CD61 marker (platelets, 1:50, Dako) by autostainer (Lab vision Autostainer 360, Thermo Fisher Scientific). From each sample, one slide was used for hematoxylin and eosin (H&E) staining. The morphology of all prepared samples was determined by light microscope “Leica DFC320, DMLP”.

2.8. Cell culture and cell viability

Single primary cells were chosen to analyze cytotoxicity in this study. Human mesenchymal stem cells (hMSCs, AO Research Institute Davos, Switzerland) derived from bone marrow were cultured in α-MEM supplemented with 10 % FBS, 1 % P/S, and 50 µg/mL bFGF.

Cells were pre-seeded in 96-well plates in a density of 5 × 10³ cells/100 µL in each well and incubated (Memmert, CO2 Incubator, INCO108, Schwabach, Germany) for 24 h to allow them to attach. Then, the medium was replaced with 100 µL of FU_CS hydrogel extract dilutions. The extract dilutions – 1:4, 1:8, 1:16, 1:32, and 1:100 – were chosen for this experiment based on those used in the publication [49,50]. As positive control, untreated cells were used. The negative control was the corresponding extraction medium with 10 % dimethyl sulfoxide (DMSO, Sigma-Aldrich). After incubating the cells in a humidified atmosphere with 5 % CO₂, 90 % humidity at 37 °C for 24 h, 48 h, and 72 h, all medium in the 96-well plates were replaced with 120 µL CellTiter Blue (CTB) prepared in media (α-MEM + 10 % FBS + 1 % P/S) to each well. The plates were put back into the cell incubator for 2 h before optical density was measured by a microplate reader (Infinite M Plex, Tecan, Switzerland) at 590 nm.

2.9. Statistical evaluation

All results were expressed as the mean ± standard deviation (SD) of at least three independent samples. The reliability of the results was assessed using the unpaired Student's t-test with a significance level of *p* < 0.05. One - and two-way analysis of variance (ANOVA) was performed to determine the differences between the results.

3. Results

3.1. Evaluation of samples

3.1.1. Stability, deformation and flow behavior of materials

One of the determining factors in this study was the hydrogel swelling degree, which indicates its ability to absorb solution. Fig. 2 illustrates the swelling behavior of hydrogels in 3 different solutions (H₂O, PBS, and DMEM/F-12). DMEM/F-12 was chosen as one of the solutions as this cell medium is used for further histology and growth factor experiments. Thus mimicking the stability of prepared samples in this environment.

It can be seen that for incubation with H₂O and PBS, the swelling process could be observed for up to 2 h, followed by equilibrium. There is no statistically significant difference between the swelling data in

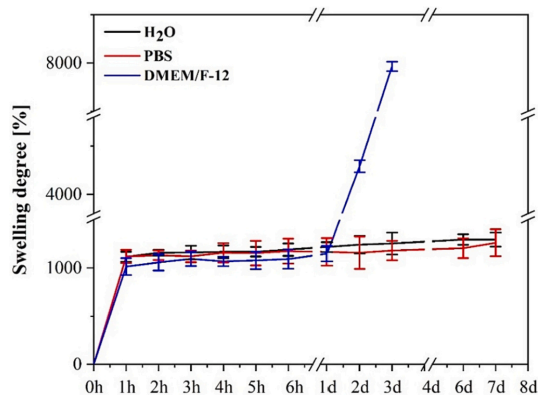


Fig. 2. Swelling degree of FU_CS hydrogels in 3 different solutions (H₂O, PBS, and DMEM/F-12).

these two solutions. On the other hand, for hydrogels placed in DMEM/F-12, the swelling was observed in the first 2 h, followed by the rapid increase of swelling after 2 to 3 days. On the 4th day samples began to degrade, and swelling could not further be detected. In our case, the hydrogels have a neutral environment, while the DMEM/F-12 medium has a pH between 6.9 and 7.3. Thus, on day 4, the dissolution of the sample was observed. The obtained data helped to determine the amount of PRF to be added for further experiments.

To obtain evidence of cross-linking of two marine polysaccharides with/without PRF and PRF alone, gel fraction analysis was performed. The gel fraction of all synthesized samples is shown in Fig. 3.

Looking at the gel fractions of the hydrogels with/without PRF and PRF alone, the *t*-test showed a statistically significant difference between the three types of hydrogels. Comparing the FU_CS hydrogels with/without PRF, it can be seen that the addition of PRF reduces the cross-linking of the samples. As shown by the FTIR analysis (Section 3.2), after adding PRF to the hydrogel, the C—O bond of the hydrogel is broken (at 1024 cm⁻¹), thus weakening the mutual interaction between FU and CS. It can also be seen that the amide I bond decreases in the PRF/FU_CS hydrogel sample, indicating a weakening of the carboxyl group. From this, it can be concluded that PRF is the dominant factor affecting the degree of insoluble part of the hydrogel after its addition.

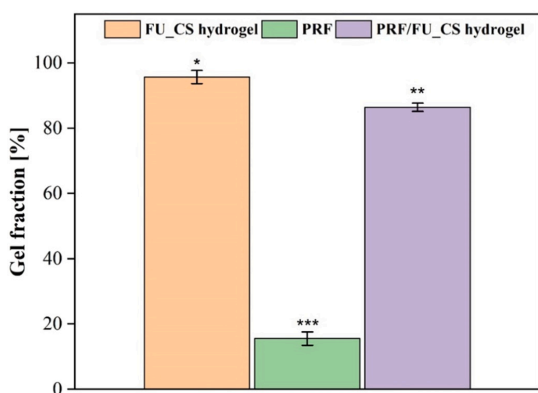


Fig. 3. Gel fraction of synthesized hydrogels with/without PRF and PRF alone ($n = 3$, $*p > 0.05$, $**p < 0.05$, and $***p < 0.01$); average 3 donor gel fractions for PRF, PRF/FU_CS hydrogel samples.

The lowest gel fraction was observed for the PRF matrix, indicating that within 48 h, the matrix had started to degrade and the crosslinks weakened. DMEM/F-12 contains a large variety of components that may interact with PRF, weakening bonds and allowing for faster degradation. In our case, the gel fraction was determined in water, which is probably why the degradation of the sample is observed starting from the 2nd day.

The degradation of FU_CS hydrogels with/without PRF and pure PRF during 2 weeks in TRIS-HCl and citric acid was determined and it is illustrated in Fig. S1. Based on the results, the addition of PRF to FU_CS hydrogels slowed down the degradation rates of both PRF and FU_CS hydrogels. Statistical analysis reveals no significant difference in media between FU_CS and PRF/FU_CS hydrogel samples. There is a notable gap in PRF degradation, with 87 % in TRIS-HCl and 96 % in citric acid within 14 days.

Rheological experiments were used to explore the deformation and flow behaviors of PRF, FU_CS and PRF/FU_CS hydrogels. All samples exhibited characteristic gel-like behavior, with the storage modulus (G') substantially exceeding the loss modulus (G'') (Fig. 4). The amplitude sweep test identified a consistent linear viscoelastic region (LVER) down to $e \approx 2.5$ % for all samples (marked with a black line in Fig. S2A), and $G'-G''$ crossing point were observed at $e \approx 14$ % for FU_CS hydrogel, $e \approx 28$ % for PRF/FU_CS hydrogel, and at $e \approx 55$ % for PRF (marked with colored lines). In all frequency ranges, G' remained constant for all samples (Fig. 4B), indicating a solid-like and stable internal structure.

3.1.2. Structural changes

SEM images of all prepared samples after lyophilization are shown in Fig. 4. From the structure of the hydrogel, it can be seen that it has a rough, corrugated surface. A similar observation has been described by Rodriguez-Jasso [51], noting that the structure of polysaccharides resembles a rough flat with many cavities. BJH/BET test results showed that FU_CS hydrogels have a porosity of 86.51 ± 8.35 %, a pore size of 3.136 ± 0.074 nm and a surface area of 19.95 ± 3.14 m²/g (Fig. S2). The PRF surface morphology shows a porous, fibrous nature. For PRF/FU_CS hydrogel, the added PRF fills the pores of the hydrogel and forms a network (Fig. 5).

In order to get insights into the interaction of the two marine polysaccharides in the production of hydrogels and the presence of PRF in the samples, FTIR analysis was done (Fig. 6).

The peaks appearing at 1652 cm⁻¹ and 1575 cm⁻¹ in the CS spectrum were attributed to the secondary amide carbonyl (C=O) stretching and N—H (acetylated residues) bending vibrations, respectively. The CS spectrum also revealed asymmetric C—O—C stretching and C—O skeletal vibration at 1147 cm⁻¹ and 1024 cm⁻¹ [52]. For the FTIR spectrum of FU, the absorption band at 1251 cm⁻¹ was attributed to the stretching of the S—O asymmetric sulfate groups. The characteristic C—O—S stretching peak at 835 cm⁻¹ was also attributed to the extent to which two-O and three-O sulfate groups influence FU [53]. The FTIR spectrum of the FU_CS hydrogel and PRF/FU_CS hydrogel contained the characteristic absorption peaks attributed to CS and FU. However, there is a shift in the C=O group, which may be caused by a different environment around this group [54,55]. After combining this CS-specific band with other species, intermolecular interactions are added, causing a shift in the spectrum, due to hydrogen bonds and electrostatic interactions, which explains the changes in the described functional groups in the environment [56]. FTIR analysis shows that no covalent interaction was found between the two polysaccharides; thus, the hydrogels were formed based on the electrostatic interaction between the positively charged CS (amino group) and the negatively charged FU (sulfate group) according to the preparation method [57]. The spectrum of the FU_CS hydrogel indicates that the C—O band has increased after combining FU and CS, thereby gelation of the sample. On the other hand, the band at 1251 cm⁻¹ belonging to the group of FU sulfates, which is also involved in the gelling process, has also been absent [58].

The FTIR spectra of PRF, PRF/FU_CS hydrogel show absorption

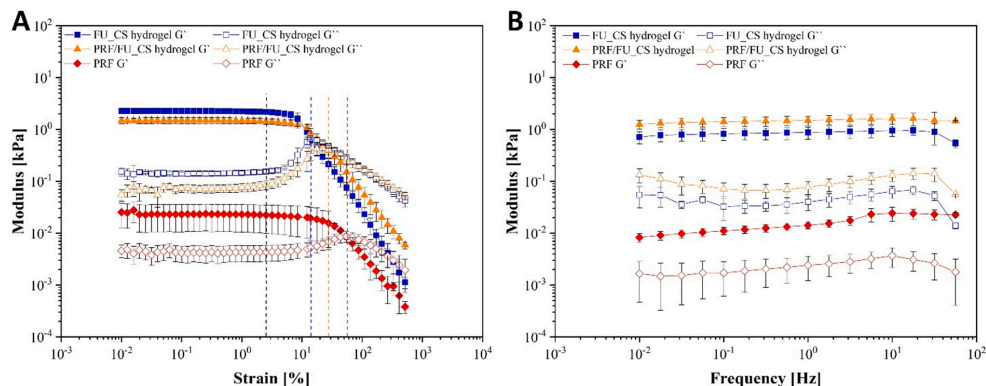


Fig. 4. Mechanical properties of scaffolds. (A) Amplitude sweep test of hydrogels with/without PRF obtained at 1 Hz frequency; (B) frequency sweep test of FU_CS hydrogels with/without PRF obtained at 0.2 % strain. All data is represented as average \pm SD ($n = 3$).

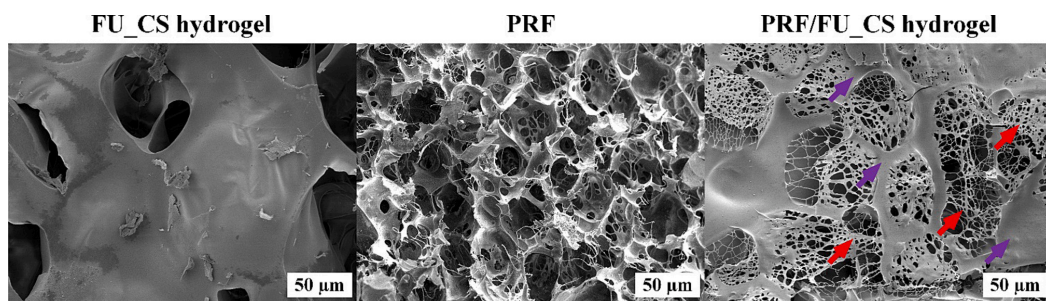


Fig. 5. SEM images of samples; violet arrows show the presence of hydrogel, and red arrows- the presence of PRF in the samples. (For interpretation of the references to color in this figure legend, the reader is referred to the web version of this article.)

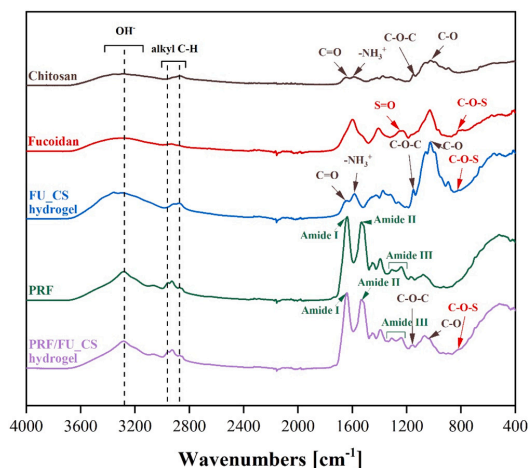


Fig. 6. FTIR spectra of used substances and prepared samples.

bands typical of the fibrin phase: peak at 1639 cm^{-1} – amide I (C = O), peak at 1533 cm^{-1} – amide II (N–H) and amide III (C–N) (decreases at 1307 cm^{-1} and increases at 1241 cm^{-1}) [59]. The amide I band at 1639

cm^{-1} in both samples (PRF and PRF/FU_CS hydrogel) indicates a secondary structure, mainly in the α -helix [60]. After combining PRF with FU_CS hydrogel, the wavenumbers of fibrin bands are almost the same as those of pure PRF. This may indicate that the secondary structure of fibrin was not affected. Although a significant increase in the N–H band (amide II band) was not observed, a decrease in the intensity of amide I indicates a more covalently cross-linked structure and a weakened carboxyl group linked by the formation of a new bond. The OH-band vibrations are present in all samples in approximately 3285 cm^{-1} , including modified hydrogels.

Comparing the FU_CS hydrogel with the PRF/FU_CS hydrogel, it was observed that the addition of PRF had cleaved the C–O bond of the hydrogel (at 1024 cm^{-1}), which increased slightly during crosslinking of the hydrogel. This explains the gel fraction data (Fig. 3).

3.2. Growth factor and cytokine release

Release kinetics of five growth factors were analyzed for PRF and PRF/FU_CS hydrogels: VEGF, TGF- β 1, EGF, IL-6, and PDGF-BB. Concentrations of growth factors and cytokines in supernatants are shown as cumulative release over 7 days (Fig. 7).

The cumulative release of TGF- β 1 shows a steady increase over 7 days. On day 7, the cumulative amount of TGF- β 1 released from PRF ($7304.33 \pm 887.39\text{ pg/mL}$) was nearly twice compared to PRF/FU_CS hydrogel ($4714.89 \pm 418.35\text{ pg/mL}$) matrices release. After 6 h, an increase in TGF- β 1 release from PRF was observed compared to PRF/FU_CS hydrogel matrices, showing sustained TGF- β 1 release over 7 days

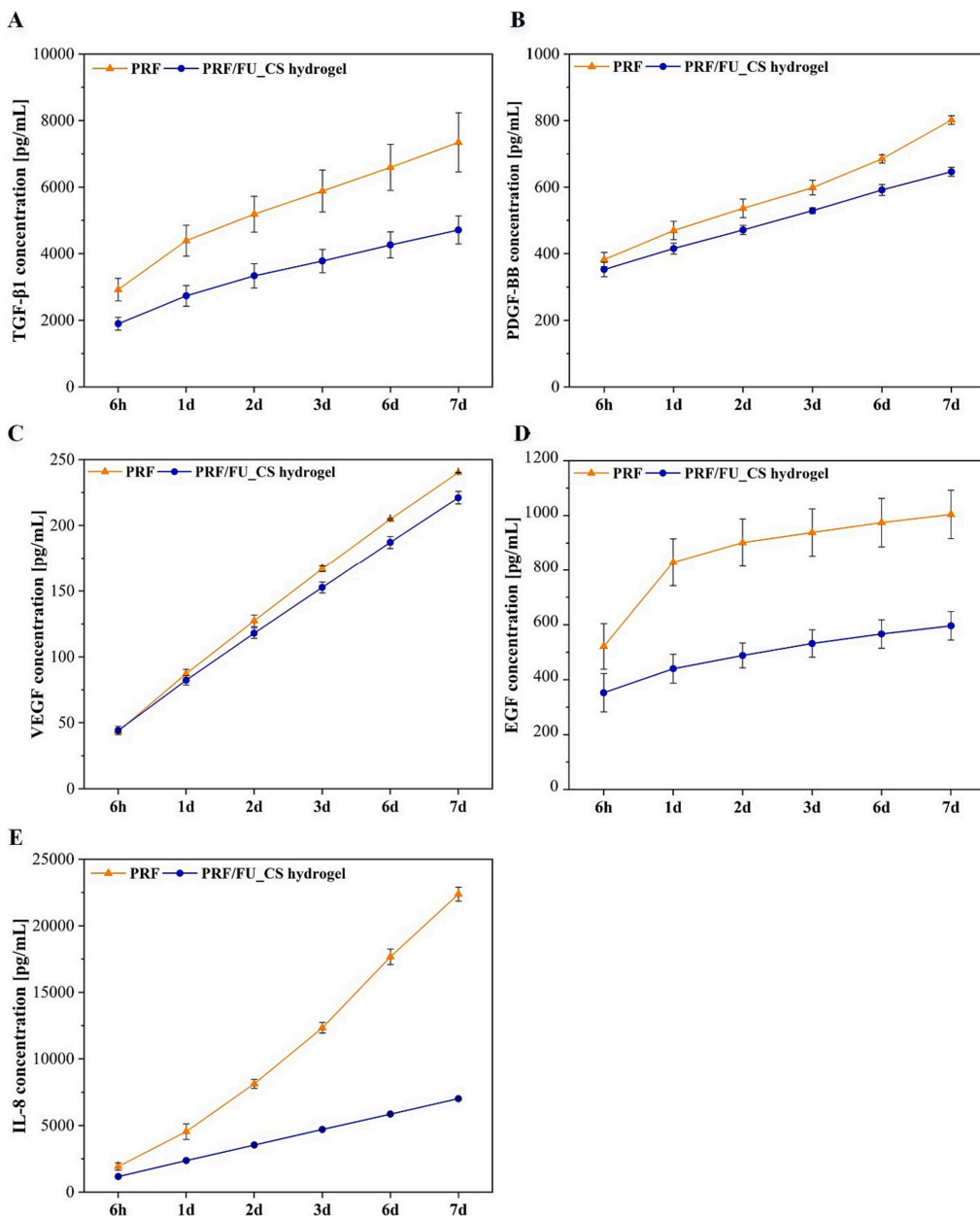


Fig. 7. Cumulative release of growth factors and cytokines. The concentrations of released growth factors and cytokines in the solution were measured by ELISA at 6 h, 1d, 2d, 3d, 6d, and 7 days after PRF incorporation into the FU_CS hydrogel and PRF alone. A-E shows growth factor and cytokines release at each time point for TGF-1, PDGF-BB, VEGF, EGF, and IL-8, respectively.

(Fig. 7A). Cumulative PDGF-BB release showed continuous and increasing values over 7 days in all evaluated groups. After 6 h, a minor but different strap release from PRF and PRF/FU_CS hydrogel matrices was again observed. The difference increased during the course of cultivation, with a peak on day 7 with significantly more PDGF-BB released from PRF (801.47 ± 12.91 pg/mL) compared to the release

from PRF/FU_CS hydrogel matrices (646.37 ± 13.64 pg/mL) (Fig. 7B).

Cumulative VEGF release in the period from 6 h and 1st day shows no differences between the two analyzed groups (pure PRF and PRF/FU_CS hydrogel matrices). On the other hand, from day 2 to day 7, an increase in VEGF release concentration was observed from pure PRF (240.16 ± 0.23 pg/mL) compared to PRF/FU_CS hydrogel (221.13 ± 4.64 pg/mL)

matrices (Fig. 7C). The cumulative release of EGF shows a rapid increase from pure PRF within 6 h to 1d compared to PRF/FU_CS hydrogel matrices. After 1 day, a steady release of EGF can be observed in the supernatants of both analyzed groups. On day 7, the cumulative release of EGF from pure PRF (1004.35 ± 87.85 pg/mL) is 1.5-fold higher compared to PRF/FU_CS hydrogel (596.30 ± 51.98 pg/mL) matrices (Fig. 7D). IL-8 release increased during the cultivation period in all evaluated groups. On day 7, the accumulated IL-8 release was significantly higher in pure PRF ($22,382.32 \pm 527.79$ pg/mL) compared to PRF/FU_CS hydrogel matrices (7023.16 ± 23.51 pg/mL) (Fig. 7E).

For all analyzed growth factors and cytokines, a general trend of higher released concentrations from pure PRF matrices than from PRF/FU_CS hydrogel matrices was observed. The release kinetics fit the Higuchi modulus (Figs. S3–S7).

3.3. Histological and immunohistological evaluation of PRF/hydrogel matrices

Histological and immunohistological analysis of PRF, PRF/FU_CS

hydrogel samples was performed to evaluate/estimate the incorporation of PRF within the pores of the hydrogel. The distribution of leukocytes and platelets in the hydrogel matrix and the arrangement and saturation of the fibrin network were also investigated. The obtained data can be seen in Figs. 8 and 9. The liquid PRF had penetrated the whole hydrogel matrix, entrapped the hydrogel fibers, compared to the FU_CS hydrogel alone. Hematoxylin and eosin staining images visualize the architecture of the fibrin network (Fig. 8), in which fibrin fibers are light pink, while red blood cells and leukocytes are intensely red and dark blue, respectively. The images also show platelets (well seen in the case of pure PRF), which are also dark blue; however, they are much smaller in size compared to leukocytes.

Comparison of PRF samples after 3 and 7 days shows a decrease in the number of cells in the PRF matrix. In addition, histology data show that PRF is still incorporated into the FU_CS hydrogel structure after 7 days.

Fig. 9 shows that leukocytes and platelets had reached the central region of the hydrogel matrix and were relatively evenly distributed within the matrix.

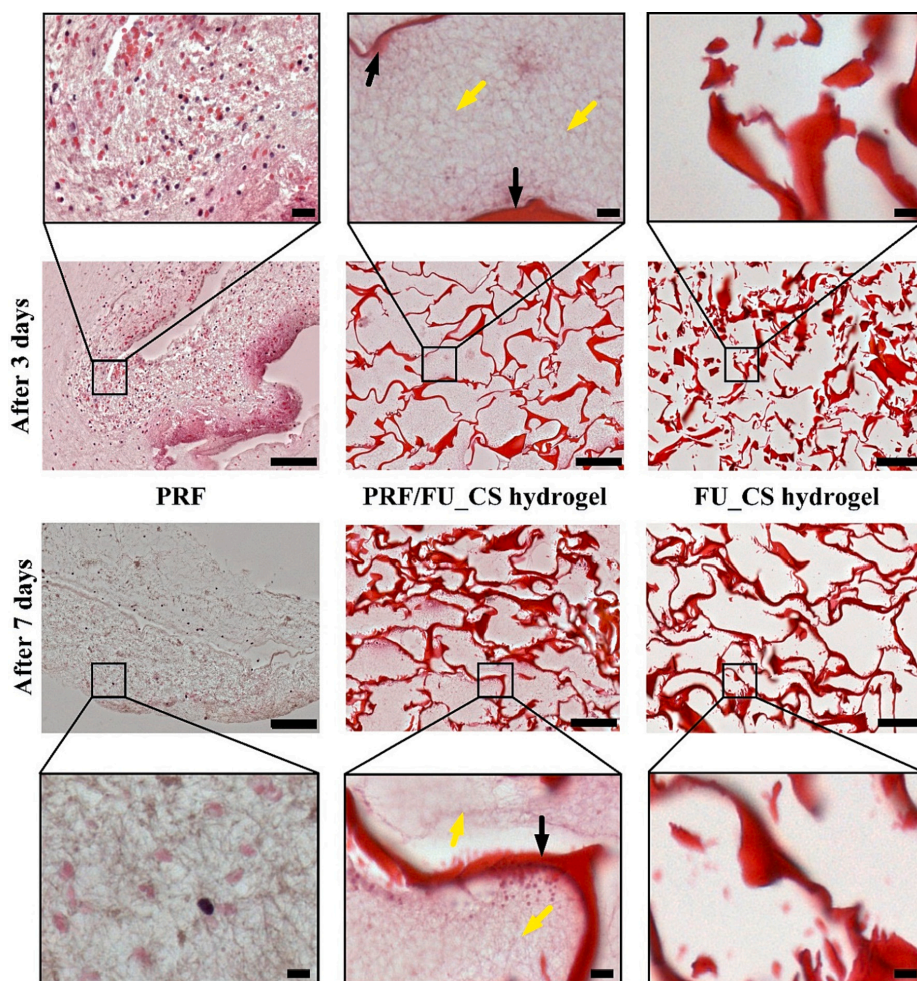


Fig. 8. Fibrin morphology after 3 and 7 days of incubation. (Scale bar: 100 μ m, increases have scale bar = 20 μ m; yellow arrows show the presence of PRF and black arrows- the presence of hydrogel). (For interpretation of the references to color in this figure legend, the reader is referred to the web version of this article.)

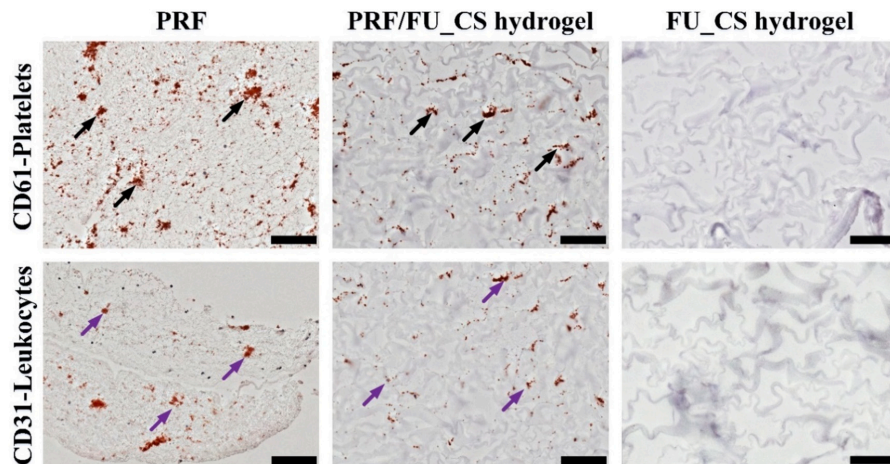


Fig. 9. Immunohistological analysis of PRF in the composition of different samples; black arrows indicate the presence of platelets, and violet arrows- the presence of leukocytes in the samples (Scale bar: 100 μ m). (For interpretation of the references to color in this figure legend, the reader is referred to the web version of this article.)

3.4. Cell viability

The evaluation of cell viability in response to CTB for FU_CS hydrogels are shown in Fig. 10. Mesenchymal stem cells are used for materials testing because of their ability to self-renew and differentiate into various mesenchymal tissues, especially bone, cartilage, and adipose tissue [61]. Data shows that >100 % cell viability was obtained with a 12.5 % (1:8) hydrogel-extracted medium. And cell viability increases every day, which indicates cell proliferation. More than 70 % of cells were viable in a 25 % (1:4) hydrogel extracted medium. Two controls were used in the experiment: untreated cells (positive control) and cells treated with 10 % DMSO (negative control).

4. Discussion

In this study, FU_CS hydrogels were prepared and characterized to test their potential for use as a PRF storage material. Release kinetics of various bioactive molecules from PRF and PRF/FU_CS hydrogels were

determined and analyzed. To our knowledge, this is the first study investigating the interaction between PRF and FU_CS hydrogels as well as the ability of a hydrogel to sustain the release kinetics of PRF-containing growth factors and cytokines. Related research in existing literature explores the combination of PRP or PRF with chitosan/fucoidan complex or gelatin/chitosan hydrogel accordingly [37,38]. In these studies, both types of platelet concentrates are blended with a chitosan solution, and the quantity of proteins released is assessed for the resulting materials. Implementation of the described methodologies would complicate medical procedures involving multiple development steps. Before studying the release of growth factors, it was necessary to know the ability of the hydrogel to take up PRF.

Swelling data for FU_CS hydrogels show that, the maximum swelling in H₂O and PBS solutions is between 1115 % - 1119 %, which, according to the calculations, ensures the absorption of 200 μ L PRF (Fig. 2). On the other hand, the absorption experiment in DMEM/F-12 medium showed rapid swelling at 2 time points (after 2 h and after 2 days) and dissolution after 3 days (Fig. 2). This could be explained by the fact that the DMEM/F-12 medium contains a higher diversity of components than other cell media. Its composition contains 2 times higher concentration of amino acids and 4 times more elevated amount of vitamins compared to α -MEM [62]. Developed hydrogels contain chitosan, which binds to amino acids when it enters the DMEM/F-12 environment, and thus a conjugation reaction is performed on the free amino groups of chitosan, forming amide bonds [63,64]. This process was likely observed in the period from 1 to 3 days. Likewise, the interaction of chitosan with amino acids increases the solubility of chitosan, especially in the range of neutral and alkaline pH values [63,64]. The swelling of the hydrogels can also be attributed to hydration of the hydrophilic groups in both chitosan and fucoidan. Amino groups in chitosan and sulfate groups in fucoidan can play a major role in swelling [44].

The gel fraction data (Fig. 3) show that PRF has a very low degree of cross-linking, indicating its ability to degrade rapidly. Fibrin degradation can reach up to 60 % during the first day, allowing for the potential maximum release of growth factors from fibrin until its complete breakdown, which is no longer than 96 h [42]. Our results show that it is possible to determine the release kinetics of growth factors up to 168 h placing of PRF samples in DMEM/F-12 medium. On the other hand, to ensure longer-term growth factor release, fibrin should be combined with materials that reduce its degradation, allowing longer release

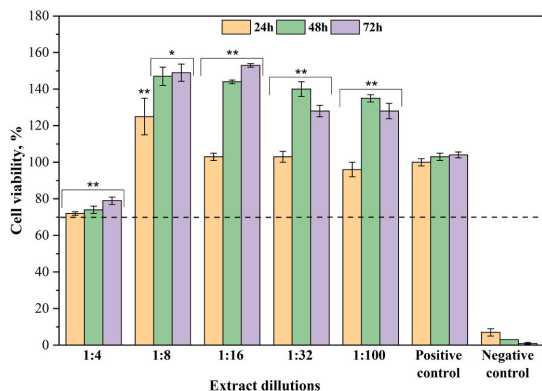


Fig. 10. Determination of cell viability of hMSC treated with FU_CS hydrogel extract dilutions at different time points (24 h, 48 h, and 72 h); $n = 3$, * $p > 0.05$, ** $p < 0.05$.

kinetics. Rheology and degradation tests (Fig. 4) show that the addition of PRF to FU_CS hydrogels improves their mechanical properties. The degradation of PRF/FU_CS hydrogels reduced to 62 % in TRIS-HCl (compared to the prior 87 % PRF degradation in 14 days) and to 70 % in a citric acid solution (compared to the earlier 96 % PRF degradation in 14 days). Accordingly to rheology data, the addition of PRF to FU_CS hydrogels improved their strength almost 2 times compared to FU_CS hydrogels. For example, addition of PRF powder to PEG microspheres can extend their degradation time (>30 days) compared to pure PEG microspheres (8 days), while liquid PRF degrades in 3 days [65]. On the other hand, addition of PRF to polycaprolactone/chitosan (PCL/CS) scaffolds can increase not only their degradation rate but also tensile strength of PCL/CS-PRF core-shell nanofibrous scaffolds [66]. In addition, it was essential to investigate the chemical structure of the samples, making sure of the cross-linking of the hydrogel.

The increase in the C—O bond during the mixing of CS and FU (Fig. 6) indicates cross-linking and hydrogel formation. In the presence of PRF, the interaction between FU and CS decreases as the CO bond is cleaved. Thus, cross-links are reduced, which is well demonstrated by the gel fraction data (Fig. 3) comparing pure FU_CS hydrogel with PRF/FU_CS hydrogel. It is also observed that the amide I bond in the PRF/FU_CS hydrogel sample decreases, indicating the weakening of the carboxyl group. All of the above could indicate that PRF is incorporated into the hydrogel structure and released after the weakening of the two mentioned bonds.

Growth factors play an important role in tissue regeneration and wound healing. This study illustrates the cumulative release of growth factors from PRF and PRF/FU_CS hydrogels over 7 days, with the highest concentration being shown for PRF. The first 7 days of PRFs' cell and GF release is the most important to burst and activate the body's own immune reaction to induce and improve regeneration, especially during the first phase/activation of wound healing [67]. The obtained data allows to conclude that the developed hydrogels, formed through electrostatic interaction, facilitate the encapsulation of growth factors present in PRF, ensuring their gradual release. The results obtained for the PRF matrix were observed to show a constant and gradual increase in the release of growth factors. This indicates that the FU_CS hydrogel can effectively maintain the release of bioactive molecules and encloses them within the hydrogel matrix, ensuring their sustained availability for tissue engineering purposes. The formation of polyelectrolyte complexes between oppositely charged groups of chitosan and fucoidan makes the incorporation of factors possible due to electrostatic interactions [68]. TGF- β 1, known as a regulator of inflammation, is the most potent inducer of fibrosis among all cytokines and can induce massive synthesis of collagen and fibronectin [69]. Previous studies have indicated [70–72] that growth factors (TGF- β 1, PDGF-AB, VEGF, and thrombospondin-1) released from PRF have a positive effect on tissue healing by stimulating collagen production. According to the scientific literature, PDGF is one of the first growth factors found at the injury site. It is released from platelets and is able to support the migration, proliferation, and survival of mesenchymal cells [73]. In turn, EGF released by platelets promotes angiogenesis and shortens healing time [74]. It also increases the secretion of cytokines in epithelial and mesenchymal cells [75]. VEGF is known to be released by activated platelets and macrophages after tissue injury. It plays a central role in angiogenesis-related processes and endothelial cell proliferation, migration, and survival [76,77]. PDGF and EGF can significantly increase VEGF secretion [78]. Finally, the IL-8 cytokine has potentially positive effects on healing and immunomodulation, as it is able to stimulate re-epithelialization and recruit neutrophils to the site of injury [79]. On the other hand, neutrophils destroy contaminating bacteria at the wound site [80]. The higher amount of growth factors in PRF may be related to the fibrin gel structure and molecular structure of cytokines [81]. This could also be attributed to a stronger fibrin architecture that trapped more leukocytes in the fibrin matrix, thus allowing relatively slow release of growth factor from the fibrin matrix [82]. However, a

better result of growth factor release was achieved by including PRF inside the hydrogel matrix - an even slower release kinetics was obtained compared to PRF. In a comprehensive exploration of scaffold modifications, FD-functionalized scaffolds (FD-SDGC and FD-SDGCG) exhibited a notably slower BMP-2 release over 14 days compared to their unmodified counterparts (SDGC and SDGCG), suggesting an enhancement in binding [83]. Another study found an initial release of 5 % BMP-2 from fucoidan/poly-L-lysine microdroplets, followed by sustained in vitro BMP-2 release over a remarkable period of 60 days [84]. Adding to the spectrum of scaffold variations, the incorporation of heparin into chitosan scaffolds extended the release of BMP-2 for at least 28 days, in contrast to the uncoated chitosan scaffold [85]. This diversity in scaffold modifications underscores the nuanced control achievable in BMP-2 release for various biomedical applications.

In a multifaceted exploration of biomaterial performance, various studies have illuminated distinctive release patterns of growth factors. Bone grafts (β -TCP) prepared with PRF demonstrated a swift release of PDGF [86]. Embedded in bone cement compositions, sustained TGF- β and VEGF release patterns were revealed over a 28-day period in bone cement/PRF and bone cement/gelatin/PRF samples [87]. Moving on to the release of growth factors from PRF alone and in combination with penicillin, reported on the dynamic release profiles of IGF-1, PDGF, FGF-2, and TGF- β 1 [88]. Expanding the scope to wound dressings, Gelatin/sodium tripolyphosphate/carrageenan/PRF (Gel-STPP/Carr-PRF) demonstrated a sustainable release of growth factors (PDGF-AB and VEGF) over 7 days, showcasing its potential for extended therapeutic applications [89]. A study was conducted to determine the release kinetics of 5 growth factors (VEGF, EGF, TGF- β 1, PDGF-BB, and MMP-9) from liquid and solid PRF, looking at release kinetics up to 10 days. For VEGF, TGF- β 1, and PDGF-BB factors, which were also considered in our study, the highest concentrations were reached on day 7 with a further decrease until the day 10. Meanwhile, for EGF, highest concentration was observed already after 7 h for both types of matrices, and there was a significant decrease between days 7 and 10 [90]. The release of PDGF-AB, TGF- β 1, VEGF, EGF, and IGF from the PRF membrane was also evaluated, but not compared to other platelet concentrations or combinations of PRF with any of the materials [91]. In the same year, osteoblasts and fibroblasts cultured with PRF or PRF showed differential expression of various growth factors [92]. The PDGF release trend similar to our study has been reported before. The study indicated that it was sustained from fucoidan-containing hydrogels combined with PRF than pure PRF gel [93]. The release kinetics of PDGF-AA, PDGF-AB, EGF, IGF-1, TGF- β 1, and VEGF in liquid PRF (I-PRF) over 10 days were investigated. I-PRF has shown significant long-term increases in PDGF-AA, PDGF-AB, EGF, and IGF-1 [94]. In another study an increased release of growth factors was observed in the first 7 days, peaking at day 14, but seeing a further decline until day 28. This indicates that PRF can accelerate soft and hard tissue healing and progressive resorption [73].

The release of growth factors depends on the structure of the fibrin network obtained after platelet polymerization and leukocyte concentration [82]. The PRF fibrin matrix is known to slowly release platelet cytokine, accelerating the process of fibrin network integration at the regenerative site, promoting endothelial cell migration, and aiding in the neoangiogenesis process, thus creating a perpetual healing process [95]. The scientific literature suggests that as the fibrin matrix resorbs, platelets release cytokines that promote healing [96]. It is also mentioned that the incorporation of cytokines into the fibrin network allows them to be gradually released over time (7–10 days) as the fibrin network breaks down [97]. But the inclusion of the fibrin network in the hydrogel could extend the release time, which would be longer than 10 days. As reported in several studies, FU is a heparin-like molecule that can interact with growth factors to control their release and activity [32,33]. The addition of heparin or a heparin-like molecule to fibrin protects the growth factors. Thus, sequestration in the matrix retards diffusion and delays the release of growth factors [4]. It is also mentioned that the growth factor release kinetics can be altered by

adjusting the scaffold degradation rate.

Our study presented the histological and immunohistological analysis of the combination of autologous liquid-PRF and FU_CS hydrogel. This study was the first to analyze the interaction pattern between PRF and FU_CS hydrogels to understand the ability and suitability of biomaterials for PRF incorporation. The effect of platelets and leukocytes on the fibrin mesh, observed in the fibrin region, may mean that various blood cells are able to stay in PRF for a long time, releasing cytokines and thereby promoting tissue regeneration. Leukocytes and cytokines, which can be found in high concentrations in PRF fibrin networks can play an essential role in the control of inflammatory and infectious processes [96]. Cytokines released from platelets also modulate platelet activation and leukocyte proliferation and differentiation, which play an essential role in immunology [98]. Platelets are a reservoir of growth factors that induce various processes such as collagen synthesis, cell division, cell differentiation, and migration of other cells to the injured/treated site [99]. Platelets can theoretically be entrapped en masse in a strong fibrin network and retain growth factors within a given PRF network, followed by a slow and gradual release of growth factors over time from platelet alpha granules [10,96]. This explains the increase in the amount of growth factors on the 7th day, because platelets and leukocytes are responsible for maintaining growth factors in the PRF network (Fig. 8). This indicates the possibility of studying growth factor release kinetics beyond 7 days in the future studies. The results of this study are potentially useful for translation into specific clinical indications with improved regenerative potential.

To ensure that the obtained FU_CS hydrogels can be used for medical purposes, in vitro cell viability tests were carried out. According to ISO 10993-5:2009, a decrease in cell viability of >30 % is considered a cytotoxic effect [100]. In our study, the highest cell viability was observed for 48–72 h dilutions, exceeding 120 % for most samples (Fig. 10). The increase in viability indicates that FU in hydrogels increases cell proliferation. FU can modulate the action of various growth factors on cell proliferation, promoting osteogenic differentiation and increasing the bioactivity of mesenchymal stem cells [31]. The ability of FU and heparin to increase cell growth was tested and both were found to inhibit the proliferation of vascular smooth muscle cells in the presence of serum [101]. In another study, FU was shown to be a more potent inhibitor of smooth muscle cell proliferation than heparin [102]. It is known that fucoidan can bind TGF- β 1 and protect it from proteolytic degradation [103]. Thus indicating that combining FU_CS hydrogels with PRF will not only increase cell proliferation, but also prolong the persistence of TGF- β 1. Incorporation of PRF into PCL/CS nanofibrous core-shell scaffolds as a growth factor carrier enhances the osteogenic differentiation of MSCs [66].

5. Conclusions

In this study, the combination of autologous liquid PRF as a growth factor system with marine polysaccharide hydrogels was analyzed, focusing on growth factor release kinetics and histological-immunohistological analysis. The present study shows that incorporating PRF into the FU_CS hydrogel matrix sustains the release of growth factors, ensuring a longer delivery. As the data indicate, 65 % of TGF- β 1, 92 % of VEGF, 32 % of IL-8, 80 % of PDGF-BB, and 66 % of EGF growth factor have been released from the PRF/FU_CS hydrogel within 7 days of the total amount of released PRF. Thus implying that residual amounts of growth factors could be observed after 7 days. Overall, the FU/CS-based hydrogel can serve as a controlled release system for the sequential delivery of multiple growth factors and cytokines to accelerate tissue repair and regeneration. Histological and immunohistological studies have also shown that PRF penetrates the FU_CS hydrogel matrix, enabling the release of growth factors. Cell viability increased in the presence of FU_CS hydrogels, indicating fucoidan's capacity to influence cell proliferation. The results are the first step towards finding alternative solutions to enhance the release of growth factors from PRF

for more prolonged lasting wound healing and tissue regeneration. Further clinical studies involving larger patient groups are essential to implement this method and to enhance postoperative tissue regeneration. PRF use has low clinical risks, such as mild inflammation, temporary discomfort, and a low chance of allergic reactions. These risks are generally minor and transient, making PRF a safe treatment option in various clinical scenarios. The next step of this study would be the development of PRF/FU_CS hydrogels with added antibiotics, reducing the possibility of the risk of postoperative infections and the need for oral drugs. This would be followed by combining PRF/FU_CS hydrogels with cells, offering cell therapy, which, when combined with drugs, will significantly enhance tissue regeneration and wound healing.

Ethical approval

The study was conducted according to the guidelines of the Declaration of Helsinki and approved by the Research Ethics Committee at Riga Stradins University, Latvia, Permission No. 6-2/10/53, 28.11.2019, and was in accordance with the principle of informed consent. Research also received approval from the responsible Ethics Commission of the state Hessen, Germany (No. 265/17).

Funding

Part of this research activities were funded by the project "Rising competitiveness of early stage researchers and research management in Latvia (RISEus2)" [grant No. 952347]. The authors acknowledge financial support for granting Open Access from the European Union's Horizon 2020 research and innovation programme under the grant agreement No. 857287 (BBCE – Baltic Biomaterials Centre of Excellence).

CRediT authorship contribution statement

Karina Egle: Writing – review & editing, Writing – original draft, Validation, Methodology, Investigation, Formal analysis. **Eva Dohle:** Writing – review & editing, Supervision, Resources, Methodology, Formal analysis. **Verena Hoffmann:** Validation, Methodology, Formal analysis. **Ilze Salma:** Writing – review & editing, Methodology. **Sarah Al-Maawi:** Writing – review & editing, Supervision, Methodology. **Shahram Ghanaati:** Writing – review & editing. **Arita Dubnika:** Writing – review & editing, Supervision, Resources, Project administration, Funding acquisition, Conceptualization.

Declaration of competing interest

The authors declare that they have no known competing financial interests or personal relationships that could have appeared to influence the work reported in this paper.

Acknowledgments

The authors acknowledge financial support from the European Union's Horizon 2020 research and innovation programme under grant agreement No. 952347 (RISEus2) and Latvian Council of Science research project No. lzp-2020/1-0054 "Development of antibacterial autologous fibrin matrices in maxillofacial surgery (MATRI-X)." The authors also acknowledge the access to the infrastructure and expertise of the BBCE – Baltic Biomaterials Centre of Excellence (European Union's Horizon 2020 research and innovation programme under grant agreement No. 857287), especially the AO Research Institute in Davos, Switzerland, for help with the cell experiment. The authors thank BGG Europe SA company for providing fucoidan for the experiments. They would also like to thank Valentina Stepanova and Anna Rubina for their excellent support in BET and rheology analyses.

- [91] C.Y. Su, Y.P. Kuo, Y.H. Tseng, C.-H. Su, T. Burnouf, In vitro release of growth factors from platelet-rich fibrin (PRF): a proposal to optimize the clinical applications of PRF, *Oral Surgery, Oral Med, Oral Pathol. Oral Radiol. Endodontology*. 108 (2009) 56–61, <https://doi.org/10.1016/j.tripleo.2009.02.004>.
- [92] V.L.W. Gabling, Y. Açil, I.N. Springer, N. Hubert, J. Wiltfang, Platelet-rich plasma and platelet-rich fibrin in human cell culture, *Oral Surgery, Oral Med, Oral Pathol. Oral Radiol. Endodontology*. 108 (2009) 48–55, <https://doi.org/10.1016/j.tripleo.2009.02.007>.
- [93] Chang Lu, Tsai, Chen, Chen, Mi, Development of injectable fucoidan and biological macromolecules hybrid hydrogels for intra-articular delivery of platelet-rich plasma, *Mar. Drugs* 17 (2019) 236, <https://doi.org/10.3390/md17040236>.
- [94] R.J. Miron, M. Fujioka-Kobayashi, M. Hernandez, U. Kandalam, Y. Zhang, S. Ghanaati, J. Choukroun, Injectable platelet rich fibrin (i-PRF): opportunities in regenerative dentistry? *Clin. Oral Investig.* 21 (2017) 2619–2627, <https://doi.org/10.1007/s00784-017-2063-9>.
- [95] S. Yajamanya, A. Chatterjee, A. Hussain, A. Coutinho, S. Das, S. Subbaiah, Bioactive glass versus autologous platelet-rich fibrin for treating periodontal intrabony defects: a comparative clinical study, *J. Indian Soc. Periodontol.* 21 (2017) 32–36, <https://doi.org/10.4103/0972-124X.201628>.
- [96] C. Aricioglu, D. Dolanmaz, A. Esen, K. Isik, M.C. Avunduk, Histological evaluation of effectiveness of platelet-rich fibrin on healing of sinus membrane perforations: a preclinical animal study, *J. Cranio-Maxillofacial Surg.* 45 (2017) 1150–1157, <https://doi.org/10.1016/j.jcms.2017.05.005>.
- [97] A. Kathuria, S. Chaudhry, S. Talwar, M. Verma, Endodontic management of single rooted immature mandibular second molar with single canal using MTA and platelet-rich fibrin membrane barrier: a case report, *J Clin Exp Dent* (2011) e487–e490, <https://doi.org/10.4317/jced.3.e487>.
- [98] V. Gupta, V.K. Bains, G.P. Singh, A. Mathur, R. Bains, Regenerative potential of platelet rich fibrin in dentistry: literature review, *Asian J. Oral Heal. Allied Sci.* 1 (2011) 23.
- [99] R. Dahiya, A. Blaggana, V. Panwar, S. Kumar, A. Kathuria, S. Malik, Clinical and histological comparison of platelet-rich fibrin versus non-eugenol periodontal dressing in the treatment of gingival hyperpigmentation, *J. Indian Soc. Periodontol.* 23 (2019) 345–350, <https://doi.org/10.4103/jisp.jisp.688.18>.
- [100] S.R. Mardashev, A. Nikolaev Ya, N.N. Sokolov, Isolation and properties of a homogenous L asparaginase preparation from *Pseudomonas fluorescens* AG (Russian), *Biokhimiya* 40 (1975) 984–989.
- [101] J.-L. Giroux, S. Matou, A. Bros, J. Tapon-Bretaudière, D. Letourneur, A.-M. Fischer, Modulation of human endothelial cell proliferation and migration by fucoidan and heparin, *Eur. J. Cell Biol.* 77 (1998) 352–359, [https://doi.org/10.1016/S0171-9335\(98\)80094-0](https://doi.org/10.1016/S0171-9335(98)80094-0).
- [102] P. Religa, M. Kazi, J. Thyberg, Z. Gaciong, J. Swedenborg, U. Hedin, Fucoidan inhibits smooth muscle cell proliferation and reduces mitogen-activated protein kinase activity, *Eur. J. Vasc. Endovasc. Surg.* 20 (2000) 419–426, <https://doi.org/10.1053/ejvs.2000.1220>.
- [103] R. O'Leary, M. Rerek, E.J. Wood, Fucoidan modulates the effect of transforming growth factor (TGF)-BETA.1 on fibroblast proliferation and wound repopulation in vitro models of dermal wound repair, *Biol. Pharm. Bull.* 27 (2004) 266–270, <https://doi.org/10.1248/bpb.27.266>.



Karina Egle dzimusi 1995. gadā Daugavpilī. Rīgas Tehniskajā universitātē (RTU) ieguvusi inženierzinātņu bakalaura (2018) un inženierzinātņu maģistra (2020) grādu ķīmijas tehnoloģijā. Kopš 2018. gada strādā RTU. Patlaban ir RTU Dabaszinātņu un tehnoloģiju fakultātes Biomateriālu un bioinženierijas institūta pētniece.

Zinātniskās intereses saistītas ar trombocītiem bagātināta fibrīna pētījumiem to lietojumam mutes, sejas un žokļu ķirurģijā. Piedalās zinātnisko projektu rakstīšanā un izstrādē.

Karina Egle was born in 1995 in Daugavpils. In 2018 she graduated from Riga Technical University with a Bachelor`s degree in Engineering Sciences in Chemical Engineering. In 2020, she received a Master`s degree in Engineering Sciences in Chemical Engineering. She has worked at Riga Technical University since 2018. She is currently a Researcher at the Institute of Biomaterials and Bioengineering of the RTU Faculty of Natural Sciences and Technology.

Her research interests include studies on platelet-rich fibrin for use in maxillofacial surgery. Karina Egle participates in the writing and implementation of scientific projects.